Year : 2018

Bacteriophages and other mobile genetic elements in microbial host adaptation, physiopathology and potential therapy

Oechslin Frank

Oechslin Frank, 2018, Bacteriophages and other mobile genetic elements in microbial host adaptation, physiopathology and potential therapy

Originally published at : Thesis, University of Lausanne

Posted at the University of Lausanne Open Archive http://serval.unil.ch
Document URN : urn:nbn:ch:serval-BIB_6BED226727FF5

UNIL | Université de Lausanne
Faculté de biologie et de médecine

Département de Microbiologie Fondamentale

Bacteriophages and other mobile genetic elements in microbial host adaptation, physiopathology and potential therapy

Thèse de doctorat ès sciences de la vie (PhD)

présentée à la

Faculté de biologie et de médecine

de l'Université de Lausanne par

Frank Oechslin

Master de l'Université de Lausanne

Jury

Prof. Marc Robinson-Rechavi, Président
Prof. Philippe Moreillon, Directeur de thèse
Prof. Jodi Lindsay, Expert
Prof. Aidan Coffey, Expert

Lausanne 2018

UNIL | Université de Lausanne
Faculté de biologie
et de médecine

Ecole Doctorale

Doctorat ès sciences de la vie

Imprimatur

Vu le rapport présenté par le jury d'examen, composé de

Président· e	Monsieur	Prof. Marc **Robinson-Rechavi**
Directeur· rice de thèse	Monsieur	Prof. Philippe **Moreillon**
Experts· es	Monsieur	Prof. Aidan **Coffey**
	Madame	Prof. Jodi A **Lindsay**

le Conseil de Faculté autorise l'impression de la thèse de

Monsieur Frank Oechslin

Master en sciences moléculaires du vivant Université de Lausanne

intitulée

Bacteriophages and other mobile genetic elements in microbial host adaptation, physiopathology and potential therapy

Lausanne, le 2 mars 2018

pour le Doyen
de la Faculté de biologie et de médecine

Prof. Marc Robinson-Rechavi

« Ceux qui rêvent le jour auront toujours un avantage sur ceux qui rêvent la nuit»

Edgar Allan Poe

Remerciements

Je tiens à remercier en premier lieu mon directeur de thèse, le professeur Philippe Moreillon pour sa générosité, la liberté qu'il a accordé à mes travaux de recherche et son ouverture d'esprit.

Mes remerciements s'adressent aussi à José Entenza pour sa gentillesse et ses conseils avisés.

Sans oublié Marlyse, Carmen, Théodora, Philippe, Shawna, Stefano et Grérory avec qui j'ai eu la chance de travailler et d'accomplir tous ces projets de recherche.

Mes remerciements vont aussi à mes collègues de travail les plus chères, Nadim, Vitali, Glib, Andrea et Davide pour leur joie de vivre ainsi que pour toutes les soirées passées ensemble.

A mes ancien professeurs Bernard Genier et Anne-José Frey qui m'ont enseigné l'art de la dissertation et de la photographie.

Des remerciements à mes parents qui m'ont toujours soutenu.

Et ma très chère et plus belle épouse Cenour.

Table of contents

Résumé

La présente thèse comprend trois chapitres qui étudient la manière dont les éléments génétiques mobiles (EGMs), y compris les bactériophages (phages), peuvent être impliqués dans (i) l'adaptation des bactéries à différents mammifères, (ii) le parasitage des bactéries (par les phages) tout en préservant l'hôte bactérien, et (iii) le détournement des phages à des fins thérapeutiques (phagothérapie) pour traiter les infections bactériennes.

Le premier chapitre s'intéresse au récent saut d'espèces de la souche humaine de *Staphylococcus aureus* du Complexe Clonal 8 (CC8) aux bovins, chez qui elle est responsable de mastites. Nous démontrons que le premier événement responsable de ce saut est l'acquisition d'une cassette chromosomique staphylococcique appelée SCC*bov*. SCC*bov* est un EGM codant pour une nouvelle protéine de surface appelée « Adherence-Like Bovine protein » (ADLB) impliquée dans la pathogenèse des mastites. En effet, les souches de CC8 bovines envahissent et tuent les cellules mammaires bovines en culture. Au contraire, l'excision de SCC*bov* ou l'inactivation d'ADLB diminuent la virulence dans ces conditions. Le second événement du saut est la perte d'un phage inséré dans le chromosome (ou prophage) qui interrompt le gène de la lipase. La restauration de l'activité lipase est susceptible de faciliter la croissance des staphylocoques dans le milieu riche en lipides du lait. Le troisième événement est la perte d'un prophage interrompant le gène de la β-hémolysine. La restauration de la β-hémolysine promeut la colonisation épithéliale. Enfin, nous avons construit des souches isogéniques de CC8 comportant différentes combinaisons de ces EGMs, permettant d'étudier le saut d'espèce dans une approche « d'évolution inverse ». En conclusion, c'est ce trafic d'EGMs qui est à l'origine du saut des CC8 humains aux bovins.

Le second chapitre étudie la relation structure-fonction et la régulation de l'activité de la lysine du phage PlySK1249 de *Streptococcus dysgalactiae*. Les phages produisent des lysines en fin de réplication pour lyser les bactéries hôtes et libérer leur progéniture. Cependant, libérer les lysines dans l'environnement risque de lyser des bactéries voisines qui portent le même phage, ou des bactéries constituant de nouvelles proies. PlySK1249 a une structure multi-modulaire intrigante, constituée d'un domaine central de liaison à la paroi bactérienne, encadré par un domaine amidase (bactériolytique) et domaine endopeptidase (CHAP; non-bactériolytique). Nous démontrons que cette multi-modularité remplit trois fonctions. (A) la combinaison des deux domaines enzymatiques et du domaine de liaison est hautement synergique en termes de dégradation de la paroi et de lyse bactérienne. (B) le domaine de liaison prévient la diffusion de la lysine en la gardant liée aux débris de paroi cellulaire après la lyse bactérienne. (C) en présence de paroi bactérienne PlySK1249 est progressivement clivée et par une protéase de la paroi bactérienne (encore non-identifiée), qui désamorce son activité bactéricide. En résumé, la structure multi-modulaire de PlySK1249 implique une régulation inter-domaines sophistiquée, permettant de circonscrire la lyse à la cellule infectée afin de ne pas compromettre l'intégrité des cellules avoisinantes.

Le troisième chapitre est une preuve de concept de la phagothérapie, utilisant un cocktail de 12 phages anti-*Pseudomonas aeruginosa* et un modèle d'endocardite expérimentale (EE) chez le rat. Les phages se sont révélés hautement bactéricides *in vitro* (perte de >6 logs CFU/ml en 6 h), mais sélectionnaient des pseudomonas résistants. Les phages étaient aussi bactéricides *in vivo* (perte de >2 logs CFU/g de végétations en 6 h), mais ne sélectionnaient pas de résistance chez les animaux. L'absence de résistance *in vivo* était due au coût d'adaptation chez l'animal, car elle affectait la synthèse des pili et du LPS, deux facteurs de virulence critiques de pseudomonas. Enfin, la combinaison de phages et d'antibiotiques (dans ce cas la ciprofloxacine) s'est révélée hautement synergique, prévenant la résistance *in vitro*, et démontrant une fréquence de stérilisation des végétations cardiaques (>50% en 6 h) sans précédent dans l'EE à *P. aeruginosa*. En conclusion, la phagothérapie combinée ou non aux antibiotiques ouvre des promesses nouvelles pour le traitement des infections bactériennes systémiques sévères.

Summary

The present thesis comes in three chapters studying how mobile genetic elements (MGEs), including bacterial viruses called bacteriophages (phages), may be involved in (i) adaptation of bacteria to different mammalian hosts, (ii) parasiting bacteria (in the case of prophages) while preserving their bacterial hosts, and (iii) new therapeutic applications.

The first chapter studied the recent human-to-bovine host jump of typical human *Staphylococcus aureus* Clonal Complex 8 (CC8) to cowherds, where it causes invasive mastitis. We show that the first event driving the human-to-bovine jump was the acquisition, by human CC8 strains, of a new "staphylococcal cassette chromosome" called SCC*bov*. SCC*bov* is a new MGE encoding for a new bacterial surface protein called Adherence-Like Bovine protein (or ADLB), which is implicated in mastitis pathogenesis. Indeed, while parent bovine CC8 readily invaded mammary cells lines, then escaped endosomes, and eventually lysed cultured cells, excision of SCC*bov* or knocking out ADLB decreased invasiveness and mammary cell death. We then show that the second event of the host-jump was the loss of a phage inserted in the bacterial chromosome (called a prophage), which interrupted the lipase-encoding gene. The loss of this prophage restored *S. aureus* lipase activity, which is likely to facilitate staphylococcal growth in the lipid-rich milk milieu. The third event was the loss of a β-hemolysin-interrupting prophage, restoring β-hemolysin activity, which was shown to promote epithelial colonization. Finally, we constructed isogenic bovine CC8 strains carrying these MGEs in various combinations, which will help determine the host-jump dynamics in a "reverse evolution" approach. Thus, MGE trafficking was the driving force behind the adaptation of human CC8 staphylococci to cows.

The second chapter dissected the molecular structure-function activity and regulation of phage lysin PlySK1249 from *Streptococcus dysgalactiae*. Phages produce lysins at the end of their replication cycle to lyse host bacteria and release their progeny. However, uncontrolled diffusion of lysins in the surrounding might also lyse neighboring bacteria carrying sibling phages or potential new bacterial hosts. PlySK1249 has an intriguing multimodular structure with a central cell wall-binding domain (CWBD) bracketed by a bacteriolytic amidase domain and a non-bacteriolytic endopeptidase (CHAP) domain. We show that this multi-modularity serves a triple purpose. On the one hand, combining the two enzymatic and the CWBD domains led to a synergistic activity in cell wall degradation and bacterial lysis. On other hand, the CWBD prevented lysin diffusion after bacterial lysis by keeping lysin attached to cell wall debris. Finally, we found that in the presence (but not in the absence) of cell wall protein extract, PlySK1249 was subject to proteolytic cleavage by an as yet unknown bacterial wall protease, further introducing posttranscriptional modification in order to control its lytic activity. Thus, the multimodular structure of PlySK1249 implicates sophisticated inter-domain interactions promoting synergistic – yet cell-restricted – lysis, in order to release the phage progeny without jeopardizing neighboring host cells.

The third chapter was a proof of concept study of phage therapy, using a cocktail of 12 phages directed against *Pseudomonas aeruginosa* and a model of *P. aeruginosa* experimental endocarditis (EE). Phages were highly bactericidal *in vitro* (loss of >6 logs CFU/ml in 6 h), but selected for phage resistance. Phages were also bactericidal *in vivo* (loss of >2 logs CFU/g of vegetations in 6 h), but did not select for resistance in animals. The absence of *in vivo* resistance selection was due to the fitness cost of resistance, which affected synthesis of bacterial pilus or LPS, two *P. aeruginosa* virulence factors that are critical for *in vivo* infection. Finally, combining phages with antibiotics (namely ciprofloxacin) was highly synergistic, prevented resistance selection *in vitro*, and cured notoriously difficult-to-treat EE due to *P. aeruginosa* at an unprecedented rate, healing >50% of the animals within 6 h of therapy. Thus, thoughtful utilization of phage therapy combined or not with antibiotics might become an alternative to treat severe systemic bacterial infections.

Executive summary

Bacteria are unicellular organism classified in the domain of Prokaryota since they lack membrane bound organelles like nucleus. Prokaryotes are further divided in Eubacteria (referred to as bacteria below), and Archea, which are closer to eukaryotes in terms of DNA and enzymology. With a size ranging from 1 to 10 uM bacteria can adopt a variety of shapes including spherical (cocci) and rod-shaped (Bacilli), spiral-shaped (spirochete) and comma-shaped (Vibrio). Also sexual reproduction is not observed, DNA transfer can occur horizontally via bacteriophage transduction, plasmid conjugation and transformation. As one of the first form of life on earth, bacteria colonized the major part of the environment including plants and animals. Bacteria colonizing animals, mainly in the gut and on the skin, outnumber the eukaryotic cells of the host. This microbiota is mainly composed of harmless or even beneficial bacteria having a positive impact on health by metabolising food compounds, training the immune system, synthetizing vitamins and providing direct protection against pathogens.

Although most of the bacteria are harmless or beneficial to humans or animals, a minority of them is considered as pathogenic and cause infections. One of these pathogens is *Staphylococcus aureus*, a Gram-positive commensal bacterium that is found in approximately 30 % of healthy people who carry it asymptomatically in the nose, and also in numerous animal species including cows. This opportunistic pathogen can produce a large variety of disease in human, including skin and soft tissue infections, as well as life-threatening infections such as pneumonia, osteoarthritis, sepsis or endocarditis. Likewise, it is notoriously known to produce mastitis in cows. However, while *S. aureus* are quite ubiquitous in terms of host species, different animals tend to harbour different staphylococcal lineages. Several

studies suggested that critical modulators of this apparent host specificity might be related to DNA transfer and acquisition of novel exogenous genes that might be beneficial in specific environments, referred to as mobile genetic elements or MGEs.

MGEs are DNA sequences that are or were able to mediate their own transfer from one genome to another. These elements include, bacteriophages (phages), pathogenicity islands, plasmids, transposons and staphylococcal cassette chromosome (SCC) in the case of staphylococci. Since these elements often harbour genes coding for virulence or resistance functions, their study can reveal how bacteria cause disease with important clinical implications.

The present thesis was dedicated to study the implication of MGEs (including phages) in host adaptation, physiopathology and therapy from three standpoints:

1. From the standpoint of the bacterium (in this case *Staphylococcus aureus*), which may acquire new genotypic and phenotypic properties via MGEs, and take advantage of these properties to jump from one host species to another. The question here was how MGEs have influenced the human-to-bovine host jump of the typical human *S. aureus* Clonal Complex 8 (CC8).
2. From the standpoint of peculiar MGEs, i.e. phages and their chromosomal-integrated “prophage” forms. Phages and prophages reunify bacterial-dependent and bacterial-independent lifestyles, along which they can act either as bacterial predators (or lytic), commensals or symbionts (when integrated in the bacterial chromosome as prophages and provide useful genes), or temperate phages, which can switch from one phenotype to the other depending on environmental conditions.

The question here was how bacteriophages sharing both lifestyles can optimize their lytic enzymes in order to allow extrusion of their progeny by lysing the host bacteria and yet preserve neighbouring bacteria carrying sibling prophages, or potential new bacterial prey from collateral lytic damages.

3. From the standpoint of therapy, purely predator (or lytic) phages have been used since a century to cure bacterial infections. While Eastern countries still use so called phage-therapy in their anti-infective arsenal, it was abandoned in Western countries to the benefit of antibiotics. However, the current threat of multiple antibiotic-resistant pathogens is reviving the interest in phage therapy as potential alternative strategy.

   The question here was whether phage therapy could demonstrate efficacy in the stringent model of experimental endocarditis due to Pseudomonas aeruginosa.

1. From the standpoint of the bacterium:

S. aureus in an important problem for human health and it can also produce different diseases in animals. This is particularly the case in Swiss dairy farms were a specific clonal complex is becoming epidemic in cowherds. These epidemic strains were found to belong to the Clonal Complex 8 (CC8), which is a typical human associated staphylococcal lineage. For this reason, these bovine-adapted strains were highly suspected to originate from human. The genetic makeup of collections of human and bovine CC8 strains was further compared using a comparative whole-genome sequencing approach in order to identify new factors that could correlate with the human to bovine jump. One of these factors could be a new SCC mobile element, called SCC*bov*, which was present in 38/39 of unrelated bovine CC8 isolates.

Interestingly, this SCC*bov* element, which was never found in human CC8 isolates, harbours a gene encoding a previously unknown LPXTG-protein (referred to as ADLB for Adherence-Like Bovine protein). The surface-attached nature of ADLB was confirmed by proteomic analysis of bovine CC8 *S. aureus* isolates as well as by cloning it and expressing it in *Lactococcus lactis*, followed by proteomic analysis, and by ELISA detection. Although present on the surface of recombinant lactococci, ADLB did not demonstrate adherence properties onto host matrix proteins such as collagen of fibronectin. Thus, it does not seem to be an adhesin. On the other hand, ADLB-positive lactococci adopted a striking star-like colony morphology on nutrient agar plates, confirming that there surface was altered.

In order to acquire more insights in the function of ADLB, we performed a pull-down experiment using the ADLB recombinant *L. lactis* and whole protein extracts from bovine udder tissue. Interestingly, ADLB *L. lactis* bound dynein 1 heavy chain, a golgin like protein implicated in intracellular vesicle trafficking, as well as type I cytokeratin from the udder extract. Interaction with these proteins could possibly interfere with intracellular trafficking of endocsomal vesicles after bacterial internalization into bovine mammary cells, which could fit with the known intracellular lifestyle of *S. aureus*.

In order to verify this hypothesis, two *S. aureus* CC8 bovine mutants were constructed and tested for internalization and survival in bovine mammary cell cultures (MAC-T cell line). The first mutant was inactivated in the gene coding for the ADLB protein, but still carried the SCC*bov* element. The second mutant was cured from the SCC element *in toto*. The results showed that the two inactivated mutants were less able to escape endosomal vesicles after internalization. This could possibly highlight a key aspect of this protein in the pathogenesis of these strains.

Finally, human and bovine CC8 strains were analysed for possible differences in integrated prophages. Interestingly, all bovine strains could be categorized in three different subgroups regarding both gene microarray and prophage composition. The first group was composed of strains that contained one β-hemolysin-converting prophage and one lipase-converting prophage. The second group was composed of strains which had only the β-hemolysin converting bacteriophage and the third group was devoid of prophages. Interestingly, the first two groups clustered with mixt human and bovine strains, which was not the case of the third one that was composed only by bovine ones. This could suggests an evolutionary scenario where the human-to-bovine jump necessitates first the acquisition of the SCC*bov* element, second the loss of the lipase-converting prophage, thus restoring lipase activity, and third the loss of the β-hemolysin-converting prophage, thus restoring the β-hemolysin function. In this scenario, SCC*bov* could provide staphylococci with advantages in cow colonization and virulence with the ADLB protein, restoration of lipase activity could provide a nutritional advantage in the milk-rich milieu, and restoring β-hemolysin could help colonize mammary epithelia, invade mammary cells or and/or escape professional macrophage attack.

2. From the standpoint phages and prophages:

In order to release their progeny, phages use phage-encoded lysins to lyse their host bacteria. However, the concurrent release of lysins in the milieu could be counterproductive in that it could unwillingly lyse neighbouring bacteria carrying prophage siblings, of lyse potential new bacterial preys. This is peculiarly true in Gram-positive bacteria, which are devoid of an outer-membrane and can be lysed directly from the outside by soluble lysins.

Here we delved on the mechanism of action a new *Streptococcus dysgalactiae* phage lysin active that we described previously (Oechslin et al. Antimicrob. Agents Chemother. 2013; 57:6276-83). The lysin had an unusual multidomain architecture composed of one amidase (Ami) and one endopeptidase (CHAP) peptidoglycan-hydrolase, as well as one cell-wall binding domain (CWBD). It was highly lytic against a large panel of streptococci and kept its antimicrobial activity in a mouse model of septicaemia.

However, several fundamental questions remained open regarding the lysin's architecture in the phage biology. For instance, what is the purpose of multi-modularity? Indeed, precedents in the literature suggest that multi-modular lysins always carry one silent catalytic site. Is the putative silent domain an evolutionary by product on the way to be lost? How are the domains regulated in order to prevent untoward lysis of neighbouring bacteria?

We first observed, by overexpressing each separate domains individually, that the amidase and CHAP domains synergized for lysing whole bacteria, in spite of the fact that CHAP alone was not active in term of bacterial lysis. However, optical and electron microscopy demonstrated that although CHAP did not lyse bacteria, it induced de-chaining of streptococcal cell chains as well as detectable minimal alterations of the cell surfaces. Analysis of peptidoglycan degradation products by HPLC and LC-MS confirmed that all domains synergized for full enzymatic activity even though CHAP domain was not directly lytic. Peptide sequencing further highlighted that while the CHAP domain was able to resolve the stem peptides crosslinks from heptamers or tetramers to dimers, it was not able to resolve them to monomers, which is indispensable for total wall solubilisation. Indeed, dimers are enough to maintain a loose glycan-peptide meshwork that can prevent lysis.

The CWBD was also studied by ELISA and diffusion essay and was shown not to confer bacterial species specificity, as usually presumed, but rather retained the lysin to the wall and wall debris. Hence, the CWBD had a dual action, promoting lysis on one hand and preventing extracellular diffusion of lysin on the other hand, thus protection neighbouring bacteria from untoward lysis.

Finally, the PlySK1249 lysin was also observed to be proteolysed in a very specific manner in presence of cell wall protein extract or trypsin.

3. **From the standpoint of phage therapy**:

Phages can be implicated in key aspect of pathogenesis by introducing virulence factors or modulation their expression via type specific integration switch off/on as prophage. However, since these viruses are also notoriously known as bacterial predators, their use as an alternative to antibiotics has generated hope for the development of new antimicrobial strategies. Indeed, since the foundation of the modern antibiotic era by Ehrlich and Fleming in the beginning of the twentieth century, the overuse and misuse of antibiotics have been responsible for the constant selection of new antibiotic-resistant microorganisms. For this reason, new therapy and research in this field is needed. The use of bacteriophage as antibiotics, although not new, was recently revived in Europe with the European research and development project Phagoburn (http://www.phagoburn.eu). This study aimed at evaluating phage therapy for the treatment of burned patients using a cocktail composed of twelve different anti-pseudomonas phages.

In this third part of this thesis project, we aimed at evaluating the phage cocktail produced by the company Pherecydes Pharma for the Phagoburn clinical trial in a rat model of experimental endocarditis due to *Pseudomonas aeruginosa*. Although rare,

pseudomonas endocarditis is an archetype of highly lethal valve infection in human and thus a good model to test new therapies. We used both *in vitro* and *in vivo* models mimicking valve infection (fibrin clots and rats with catheter-induced aortic vegetations, respectively) to study the efficacy of an anti-pseudomonas Pherecydes Pharma phage cocktail and ciprofloxacin administered alone or in combination. In fibrin clots, the phage cocktail decreased bacterial density but regrowth due to phage resistance was observed after 24h. This regrowth could be prevented by the addition of ciprofloxacin. In rats, phage therapy alone decreased vegetation bacterial density as efficiently as ciprofloxacin, which is the gold standard for pseudomonas antibiotherapy. Moreover, combining phages with ciprofloxacin appeared highly synergistic. Phage-induced killing was also observed to correlate with *in situ* phage multiplication and cytokines production compared to antibiotherapy alone. The use of phage therapy also raised the question of the emergence of phage-resistant bacteria, as for antibiotics. Interestingly, we could detect phage resistant bacteria *in vitro* but not *in vivo*, which was most likely due to altered fitness. Indeed, phage-resistant clones isolated *in vitro* were significantly less infective than the phage-susceptible parent in rats with experimental endocarditis. This infectivity decrease correlated with modification of surface receptor that impaired either motility (in one mutant) or LPS production (in another mutant). These results were published (Oechclin et al. J. Infect. Dis. 2017; 215:703-12) and demonstrated that phage therapy alone or combined with antibiotics represents a promising alternative in the treatment of severe *P. aeruginosa* infections and maybe more importantly that phage resistance might not a limitation of their use in therapy.

Conclusion and perspectives

This thesis highlights a fascinating journey through horizontal interactions between life kingdoms. Originally interested in understanding the mechanisms of interaction between microbial surface components and the host, in the case of ADLB and the human-to-bovine host jump of *S. aureus* CC8, as well as phage lysin mechanisms of action and potential antimicrobial therapy, in the case of the multidomain phage lysin of *S. dysgalactiae*, it dragged us in much more fundamental questions regarding the comprehension of virus-bacteria-eukaryote interactions.

For instance, the *S. aureus* jump from human to cows was associated with an array of factors. Although the ADLB surface protein appeared as central (no human strains possess it), it relied on parallel changes such as the loss of the lipase- and the β-hemolysin-converting phages.

This highlighted the central role of phage biology in the whole process, which was conceptually not new, but enriched knowledge on the system and provides now the tools to reconstruct the determinant steps of the host-jump by phage manipulation and *in vitro* reverse evolutionary experiments. Beyond academic interest, this could help track problematic germ evolution in cattle and the dairy industry.

Likewise, studying the biology of phage lysins revealed a sophisticated intrinsic regulation aimed at protecting neighbouring bacterial cells, and thus preventing untoward bacterial lysis and abortion of potentially prophage siblings. This is different from the massive lysis and killing that is sought in the development of phage lysins as alternative anti Gram-positive therapy. Clearly, phage-bacteria co-evolution is more sophisticated than that. However, such understanding will be critical in designing efficient therapeutic lysins in R&D, for instance by taking into account the diffusion limiting action of the cell-wall binding domain.

Eventually, the translational experiments on phage therapy highlight the link between bacterial resistance to phages and the *in vivo* loss of bacterial fitness and infectivity. This of course does not solve the whole issue of phage resistance in therapy, as other resistance mechanisms than bacterial surface alterations do exist. But it provides hints toward alternative approaches in case of bacterial intracellular-related resistance mechanisms (e.g. restriction enzymes, CRISP), such as combination therapy or synthetic phage development.

Thus, taken together, all three sets of experiments presented herein contribute to both fundamental mechanistic understanding and potential translational developments.

Chapter I

Implication of mobile genetics element in the human-to-bovine host jump of Staphylococcus aureus clonal complex 8

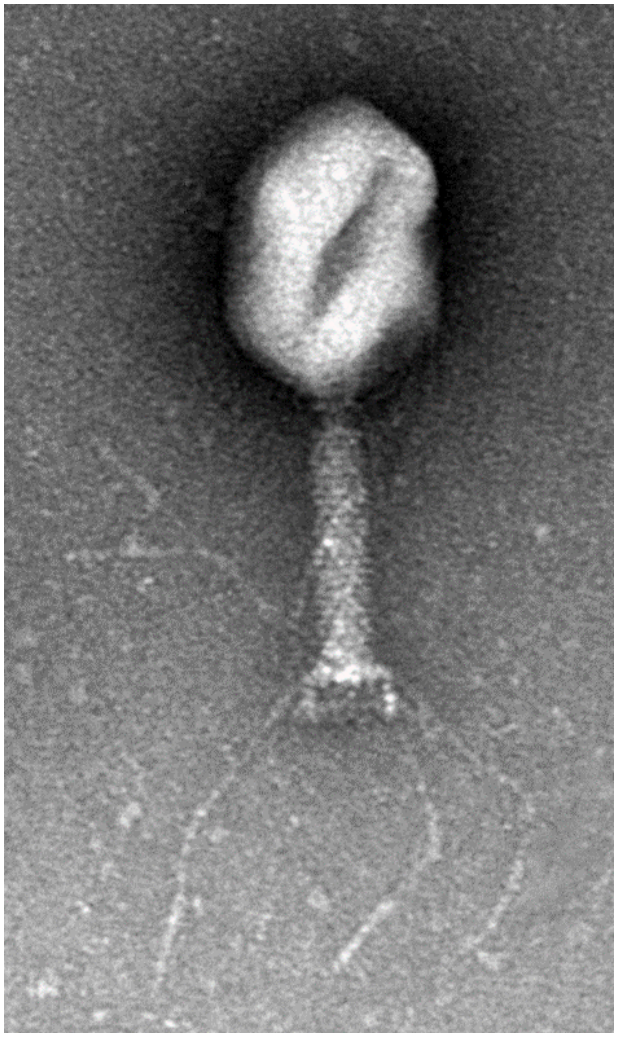

Myoviridae. Negative staining. 2016. F. Oechslin

F. Oechslin performed the experiments.

F. Oechslin, P. Moreillon and G. Resch designed the experiments and protocols.

F. Oechslin and G. Resch prepared the libraries for genomic sequencing.

G. Resch did the phylogenetic analysis.

T. Steiner run the FACS analysis and modified the *S. aureus* prophage content.

S. Mancini did the *adlb* knockout by site-specific insertion.

S. McCallin prepared sample for surface protein analysis by LC-MS.

P. Varidel did the LC-MS analysis.

F. Oechslin and P. Moreillon wrote the paper.

F. Oechslin supervised the research.

The following work was presented at:

- Sympostaph. 20-21.10.14, Lyon (France). Oral presentation
- SGM-SSM: 73rd Annual Assembly of the SSM, 28-29.05.15, Lugano (Switzerland). Oral presentation.
- ISSSI. 30.08.2016, Seoul (South Corea). Oral presentation
- Sympostaph. 26.10.2016, Lyon (France). Oral presentation

Abstract

Staphylococcus aureus isolates of human clonal complex 8 (CC8) recently emerged as a bovine mastitis pathogen. Studies suggested that human CC8 had adapted to cows and acquired of a novel staphylococcal chromosome cassette (SCC*bov*) carrying a novel LPXTG-surface protein gene named *adlb*, for Adhesin-Like Bovine protein. Here we confirm the human-to-bovine directional jump using whole-genome sequencing and core-gene comparison of 45 (8 human and 37 bovine) CC8 isolates. Moreover, we show that the jump was accompanied by sequential acquisition of SCC*bov* followed by successive losses of lipase- and β-hemolysin-converting prophages.

SCC*bov*-mediated phenotype was studied using SCC*bov* excisants, *adlb*-inactivated mutants, and heterologous *adlb*-expression in *Lactococcus lactis*. ADLB was present on both bovine isolates and recombinant lactococci. It did not bind host matrix proteins or promote biofilm formation. However, when exposed to udder protein extracts, ADLB retrieved cytoplasmic molecules implicated in vesicle trafficking, including Dynein 1 heavy chain, Golgin like protein and Keratin type I cytoskeletal protein. The role of ADLB in intracellular *S. aureus* trafficking was supported in mammary cell cultures. Parent strains were more prone than SCC*bov* or *adlb* mutants to escape endosomes and lyse host cells. Finally, we constructed isogenic bovine strains carrying SCC*bov* plus two prophages, one prophage or no prophages, allowing studying the host-jump in reverse evolution.

Altogether, the present results highlight the MGE trafficking and some salient virulence mechanisms associated with the host-jump. Moreover, they suggest potential mastitis prevention strategies, such as vaccine blocking ADLB, and maybe lipase and β-hemolysin, which are uniquely restored in bovine isolates.

Introduction

Agriculture was developed around 11.500 years ago and is considered as the main factor that led to the Neolithic revolution. However, while agriculture was a source of food, it also generated unexpected problems including the transmission of zoonotic pathogens, which account for >60% of all known human virulent microorganisms including viruses, fungi, and bacteria [1]. One of these important bacteria is *Staphylococcus aureus*, which is an opportunistic pathogen for both humans and animals. In humans, the major reservoir of *S. aureus* is healthy carriers. They account for up to 30% of the population, and harbour the microorganism on their skin and mucosa, typically in the nose [2].

Although most healthy carriers never experience staphylococcal disease, *S. aureus* is the causative agent of a broad range of clinical syndromes extending from local disease to more severe systemic infections such as bacteremia, pneumonia or endocarditis [3]. It also has the capacity to acquire antibiotic resistance, as illustrated by methicillin-resistant *S. aureus* (referred to as MRSA). Currently *S. aureus* in general and MRSA in particular are among the most common causes of community- and hospital-acquired infections [4].

S. aureus carriage has also been reported in numerous animal species including dogs, cats, horses, pigs, and poultry [5]. It has become the most frequent etiological agent of bovine mastitis in modern farming. Bovine mastitis is an inflammation of the mammary glands that affects lactating cattle and is one of the main sources of economic loss for the dairy industry [6]. Infection starts by ascending colonization of the teat canal with bacteria coming from teat cup liners or milker's hands or milking machines. After gaining access to the milk duct, bacteria adhere to the ductal and glandular epithelium

where they trigger macrophage and neutrophil migration and activation. This results in epithelial cell damage and in increased somatic cell counts (SCC) in the milk.

However, while *S. aureus* is quite ubiquitous in terms of host species, different animals tend to harbour different lineages (i.e. clonal complexes, or CC for short). The evolution of *S. aureus* lineages is driven by genetic changes such as point mutations or importation of foreign DNA, which may confer novel phenotypic properties. The fittest mutants in specific conditions are privileged by the selective pressure of the environment, such as, for instance, host defences and antibiotics in humans and livestock.

These genetic changes have a major impact on the architecture of the *S. aureus* genome, which is composed of three components: (i) a core genome with single nucleotide polymorphisms (SNPs), (ii) a variable core that changes according to lineages, and (iii) mobiles genetic elements (MGEs) that are acquired by horizontal gene transfer (reviewed in [7]). In *S. aureus* MGEs account for 10% to 20% of the genome. Moreover, individual MGEs can either be widely distributed among unrelated lineages, which suggests convergent selection stability, or poorly distributed with no sign of correlation with particular lineages, which suggests a seminal event responding to a new environmental pressure, or serendipitous evolutionary accident.

Staphylococcal MGEs generally have a G+C content that is close to that of the host genome, suggesting that they were acquired by horizontal transfer from other staphylococci or related gram-positive bacteria, rather than from more remote organisms with different G+C contents, such as Proteobacteria. This permits escaping the restriction system that blocks DNA transfer between species.

Three main types of MGEs have been described so far in staphylococci, namely bacteriophages (phages), Pathogenicity Islands and staphylococcal cassette chromosome (SCC) [8]. Phages are between 20 and 40 Kb in size and are present as latent prophages integrated in the genome with short flanking inverted repeats (*attL* and *attR*) that match a short sequence at a specific insertion site of the chromosome (*attP*), and are recognized by an integrase, which triggers site specific integration. For example, β-hemolysin-converting phages have a specific insertion site in the gene coding for the β-hemolysin toxin, referred to as Hlb. Even if the lytic action of phages is potentially harmful, bacteria can take advantage of phages that carry virulence factors or toxin genes by inserting them as prophages and disseminate them via their own replication or via general transduction.

S. aureus Pathogenicity Islands (SaPIs) are around 15Kb DNA sequences and depend on helper bacteriophages for their transfer. Like phages, SaPIs integrate into the genome at specific sites using integrases and provide the recipient with virulence factors such as toxins, super-antigens and immune suppressing factors [9].

Like SaPIs, SCC mobile genetic elements are also discrete genetic sequences ranging in size from 3Kb to 60Kb. All SCCs have common elements including recombinase genes (*ccrA/ccrB* and / or *C*), a specific insertion site that is in the *orfX* gene, and flanking direct repeats for recombination. The mechanism by which SCC are transferred to different hosts is currently not elucidated, but could implicate general transduction. There are at least eleven described SCC types that convey resistance to methicillin (SCC*mec*), named Type I to XI. Ten of them carry the classic *mecA* gene (referred to as SCC*mec*) and one carrying the *mecA*$_{LGA251}$ variant (Type XI). The *mecA* gene confers resistance to methicillin and is associated with both healthcare- and community-acquired MRSA [10]. The *mecA*$_{LGA251}$ variant was originally described in

livestock MRSA and was missed by molecular tests aimed at detecting *mecA*, because of its sequence variation [11]. MRSA positive for *mecA*$_{LGA251}$ were found in humans, but seem less implicated then *mecA* in large human epidemics of MRSA.

The aptitude of *S. aureus* to infect different animal species, including humans, raises the question as to whether different strains are able to infect an array of different host species or whether they are rather adapted to a single host. Population genetics studies comparing bovine mastitis isolates to strains isolated from humans tend to indicate that mastitis is due to a small number of bovine-adapted *S. aureus* clones with lineages that are rarely found in human [12-17]. Although these studies suggest the existence of host range barriers, a small number of cross-species jumps have been documented including human to animal (anthroponotic switch), animal to human, and bidirectional jumps [18-21].

Interestingly, a previous study described that some bovine-adapted *S. aureus* strains showed a close genetic relationship to strains of the human clonal complex 8 (CC8) [22]. In this study, the genetic relatedness of 500 *S. aureus* mastitis isolates was compared to that of nasal carriage isolates from a population of farmers who were in direct contact with cows, as well as with carriage isolates from a population of non-farmers healthy volunteers. Regarding the genotypic composition, farmers and non-farmers were colonized by a variety of isolates that belonged to a series of shared CCs. In contrast, mastitis isolates were quite distinct from the human isolates, and particularly from the farmers' isolates, in spite of close proximity with their cowherds. However, one-third of the bovine mastitis isolates belonged to the CC8 complex, which is typically associated with human infection and includes notoriously known strain USA300, which is the predominant clone responsible for community-associated MRSA

in the United States of America [23]. The authors concluded on a possible host jump between human and cows with the emergence of new bovine adapted strains.

A more recent study investigated the possible genetic determinants associated in this presumed host shift [24]. By using total chromosome microarrays, CC8 isolated in the previous study from cow mastitis were compared to typical bovine non-CC8 mastitis isolates as well as to CC8 isolated from colonized or infected human patients. Clustering analysis revealed three CC8 subgroups, named Ia, Ib and Ic, respectively. Two of these subgroups (Ia and Ib) contained a mix of human and bovine strains, whereas the third subgroup (Ic) contained only bovine isolates. Strikingly, irrespective to the three subgroups, all bovine strains harboured a non-*mecA* SCC element (referred to as SCC*bov* in the following), which carried a gene coding for a LPXTG surface-like protein. In addition, the bovine-only subgroup (Ic) had lost the β-hemolysin converting prophage.

In parallel, veterinary epidemiologic studies revealed a peculiarly invasive bovine mastitis clone referred to as genotype B (GTB) based on 16S-23S ribosomal spacer PCR-typing [25]. Moreover, recent genomic analyses indicated bovine mastitis clone GTB was similar to human complex CC8 [26]. Finally, the GTB (or bovine CC8) strains also contained a gene encoding unique new LPXTG surface protein that was similar to the LPXTG described above [24] and was tentatively named *adlb*, for “Adhesin-Like Bovine” protein [27]. Thus, veterinary epidemiologic studies converged to the same host-jump conclusion than human studies regarding to CC8 *S. aureus* [22] [24].

In this present project we aimed at both confirming the presumed adaptation direction from human-to-bovine host, and understanding the molecular and pathogenic mechanisms behind it. To this end, robust phylogeny analysis based on core genome genes was combined to molecular biology. Beyond genetic and molecular mechanistic

comprehension, the ultimate goal was to construct the system for testing a “reverse like” evolution model, by adding or removing the genetic determinants that are supposed to be relevant for host adaptation (i.e. prophages, SCC, and the hypothetical surface protein). The different strains were then tested and compared for infectivity regarding internalization on bovine cell cultured epithelium.

Materials and methods

Bacterial strains, media and growth conditions. Bacterial strains and plasmids used in this study are listed in supplementary Table 1. *Escherichia coli* was cultivated in Luria-Bertani (LB) medium (Becton Dickinson, Sparks, MD) supplemented with 100 mg/L ampicillin (AppliChem, Darmstadt, Germany) at 37°C. *S. aureus* strains were grown with aeration in trypticase soy broth (TSB) (Difco Laboratories, Detroit, MI) at 180 rpm 37°C. If required, tetracycline and erythromycin (AppliChem) were added at a final concentration of 10 mg/L for plasmid propagation and 5 mg/L for flow cytometry analysis. Oxacillin was commercially purchased and used at the sub-MIC concentration of 4 mg/L for methicillin-resistant staphylococci. Mitomycin C (Sigma-Aldrich Chemie GmbH, Steinheim, Germany) was used at a final concentration of 1 mg/L.

PCR and DNA manipulations. For polymerase chain reaction (PCR) GoTaq DNA polymerase (Promega Corp.) was used for colony PCR screening analysis. KAPA HiFi DNA Polymerase (KAPA Biosystems, Cape Town, South Africa) was used to amplify fragments required for cloning. All reactions were carried out according to manufacturers' specifications. The primers used in this study are listed in supplementary Table 1. For *S. aureus*, genomic DNA was extracted using a protocol described previously in [28]. For *E. coli*, plasmids were isolated using the QIAprep Spin Miniprep Kit (QIAGEN, Hilden, Germany). For *S. aureus*, an additional lysostaphin treatment (final concentration 0.5 µg/ml) was performed before the lysis step. Digestions with restriction enzymes (Promega Corp.) were carried out according to the manufacturer's specifications. PCR fragments were purified using the "QIAquick PCR

Purification Kit" (Qiagen Inc.) and gel bands were purified using "QIAquick Gel Extraction Kit" (Qiagen Inc.) according to manufacturer's protocols. Ligations were performed using 1 µl of T4 ligase (Promega Corp.) according to the manufacturer's specifications.

Genome sequencing, assembly and annotation. Genomic DNA from 45 *S. aureus* CC8 strains (37 bovine strains and 8 human strains, listed in table 1) was purified using the Wizard Genomic DNA purification kit (Promega, Dübendorf, Switzerland). Genomic DNA libraries were prepared using 1µg of the purified genomic DNA and the TruSeq DNA LT Sample Preparation Kit according to the manufacturer's protocol (Illumina, San Diego, USA; Cat. No. FC-121-2001). The resulting libraries were pooled into a single library for 2x100-bp paired-end sequencing on the Illumina HiSeq 2500 sequencer using TruSeq PE Cluster Kit v3 (Cat. No. PE-401-3001) and TruSeq SBS Kit v3 (Cat. No. FC-401-3001). Data were processed using the Illumina Pipeline Software package v1.82 and aligned using Eland v2e. Assembly of paired-end reads was done with Edena [29]. Contigs were submitted to RAST v 2.0 for automated annotation [30]. The full genome sequence of *Staphylococcus epidermidis* strain ATCC 12228 was obtained from NCBI (Accession N°: NC_004461.1)

Phylogenetic analysis. Fasta files of Open Reading Frames (ORFs) (both nucleotide and amino-acids sequences) from each genome were downloaded from RAST and used by two in-house perl scripts (available upon request) to build a phylogenetic tree. Briefly, core proteins, i.e. proteins encoded on the genome of the *S. aureus* strains and *S. epidermidis ATCC 12228* were identified by blasting each single protein sequence

of a given strain to each single protein sequence of the other strains using BlastP with e-value threshold of 10^{-10}. Corresponding nucleotide sequences of genes coding for core proteins present in single copies in all genomes were further used to build a multiple alignment with MAFFT-7.187 [31]. Newick formula was obtained by submitting the MAFFT output file to FastTree-2.1.7 [32]. Finally, the Newick formula was uploaded in Njplot 2.3 [33] to visualize and root the corresponding phylogenetic tree using *S. epidermidis* ATCC 12228 as outgroup.

Heterologous expression of the new LPXTG (ADLB) protein in *Lactococcus lactis*. The gene (tentatively named *adlb*) coding for the LPXTG (ADLB) protein present in the SCC*bov* cassette of *S. aureus* strain M186 was cloned in the expression vector pORI23 (generating pORI23-ADLB^{M186}) in *L. lactis* following the system described in [34]. Briefly, the surface protein was PCR amplified using the sets of primer ADLB_SalI and ADLB_PstI and digested with their respective enzyme to be finally cloned in the pORI23 shuttle vector. After *E. coli* amplification and sequencing, the plasmid was finally transformed in *L. lactis* by electroporation. ADLB-expression was confirmed by western blotting and liquid-chromatography coupled to mass spectrometry (LC-MS), as described below. In addition, a mutated version of the ADLB protein was also produced by replacing the LPXTG signal of the protein by a 6-his-tag. The his-tag substitution was done by PCR amplification of the plasmid pORI23-ADLB^{M186} using the Q5 Site-Directed Mutagenesis Kit (New England Biolabs, Massachusetts, USA) and the set of primers Q5SDM_ADLB_F and Q5SDM_ADLB_R. The reaction product was then transformed into *E. coli* for amplification and sequencing and finally transformed in *L. lactis* as described before.

Surface protein analysis using western blotting, ELISA and LC-MS. Cell-wall associated proteins were extracted from *L. lactis* and *S. aureus* as described in [34]. Western blotting was performed as described before [35] and blots were incubated 1 h with a 1:1000 dilution of anti-ADLB antibody following by a 1 h incubation with a 1:2000 dilution of peroxidase-conjugated goat anti-rabbit secondary antibody. Bands were detected using ECL Western blotting detection reagent (Amersham Bioscience. Piscataway, NJ). The presence of the ADLB protein on the recombinant *L. lactis* was also tested by ELISA on overnight cultures or directly on colonies. To this end, overnight cultures were washed three-time with PBS and colonies were picked and directly resuspended in 500 μl of PBS. 100 μl of cell solution was then incubated in a 96 well plate for 1h at 37°C. After three PBS washes, the plate was blocked for 1 h with a solution of PBS-3%BSA. After a second three-time PBS wash, anti-ADLB antibodies were added at a dilution of 1/1000 and incubated for 1 h. After a third three time PBS wash, the plate was incubated 1h with a 1:2000 dilution of peroxidase-conjugated goat anti-rabbit secondary antibody. 150 μl of colorimetric substrate (TMB, Thermo Fisher Scientific, Massachusetts, USA) was added to the plate after six PBS washes. 150 ul of 2M H_2SO_4 was added after 30 min of incubation to stop the reaction and absorbance was recorded at 450_{nm}. The anti-ADLB was composed of an equimolar mix of two antibodies raised against two fragment of the protein corresponding to the amino acid position 73-87 and 602-616 (Eurogentec, Liège, Belgium).

For LC-MS analysis, cultures were adjust to $1x10^9$ CFU/ml in PBS and digested with 1 ug/ml trypsin (Promega Corp) for 1 hr at 37 ºC. The suspension was centrifuged, the supernatant filtered, and then dried ON in a speedvac. Samples were suspended in 100 mM ammonium bicarbonate, pH 8.5 (Sigma), to which 1,4-dithio-DL-threitol

(Fluka) was added to a final concentration of 4.5 mM and incubated 30 min at 60 ºC with shaking. After cooling, iodoacteamid was added to a concentration of 10 mM and samples were incubated 30 min at RT in the dark. A second digestion with trypsin was performed ON at 37 ºC. Samples were cleaned with Sep-Pak tC18 cartridges (Waters). LC_MS was performed at the protein analysis facility of the University of Lausanne (PAF, Center for Integrative genomic, University of Lausanne, Switzerland)

FACS analysis. For flow cytometry, cells were grown to OD 0.4 and kept on ice. 1 ml samples were then washed three time with ice cold PBS and transferred to a 5 ml Falcon tube. Flow cytometry was performed with a FACS-Aria (BD Biosciences, Erembodegem, Belgium). GFP fluorescence was recorded in the FL1 (525+15 nm channel). Cells were immediately plated on blood agar after sorting.

Excision of the SCC*bov* cassette and inactivation of the *adlb* (LPXTG-protein) gene in prototypic bovine strain M186. In order to study the phenotype conferred by the SCC*bov* cassette and the new ADLB surface protein in bovine CC8 staphylococci, it pas critical to generate isogenic mutants lacking these particular determinants. Prototype bovine strain M186, belonging to subgroup Ib, was used to this end.

First, to screen for spontaneous SSC*bov* excisants, bovine strain M186 was transformed with plasmid pPGFP, which expresses GPF under the promoter of the SCC recombinases *ccrA/ccrB* [28]. GFP-overexpressing cells were retrieved by FACS-sorting, grown into colonies, and screened for the loss of SCC*bov* by PCR. Loss of

SCC*bov* was confirmed by the concomitant loss of the surface ADLB protein western blot and by LC-MS.os

Second, bovine M186 mutants inactivated in *adlb* (M186 Ω *adlb*^{M186}) were generated using the TargeTron Gene Knockout System (Merck). This system is based on the activity of group II introns, which can insert themselves into a user-specified chromosomal gene via the activity of an RNA-protein complex (RNP) expressed from a single plasmid (pNL9164) [36]. First, the RNA portion of the RNP was mutated to re-target insertion into the desired gene. To do that, a computer algorithm (http://www.sigmaaldrich.com/life-science/functional-genomics-and-rnai/targetron.html) was used to identify group II intron target sites in the *adlb* gene. Among the primer sets that were output from the algorithm, the one comprising primers IBS, IBS1d and IBS2 was used to synthesize the DNA coding for the mutated intron RNA by PCR using pNL9164 (containing the RNA portion designed to target the *hsa* gene) as a template. The resulting 350 bp PCR product was then digested with HindIII and BsrGI and ligated into pNL9164, also digested with the same enzymes. The ligation reaction was transformed into *E. coli* DH5α cells. The presence of the RNA portion mutated to target the *adlb* gene was confirmed by sequencing. The construct was then electroporated into the *S. aureus* RN4220 restriction-defective strain and then in the *S. aureus* M186 cells. To induce the TargeTron system, cells were grown at 32°C in BHI medium containing 10 µg/ml erythromycin to the exponentially phase (OD = 0.5) and then induced with 10 µM $CdSO_4$ for 90 min. Cells were then plated on BHI plates containing 10 µg/ml erythromycin and incubated ON at 32°C. The day after colony PCRs were performed to screen for the presence of the intron within the *adlb* gene, using primers adlb_fw and Fw4200_adlb (supplementary Table 1). Colonies containing the *adlb* wild type gene generated a product of 2.246 Kp, whereas colonies

carrying Ω*adlb* generated a PCR product of approximate size of 3.3 Kb. The presence of the group II intron therein was verified by sequencing.

Pulling downs proteins from udder extracts using ADLB-expressing *L. Lactis*. Fresh udder tissues from lactating cows were obtained from the slaughterhouse, dissected and glandular tissues were grinded with a mortar-pistil after being frozen in liquid nitrogen. Homogenized tissues were then suspended in T-PER® Tissue Protein Extraction Reagent (Thermo Fisher Scientific, Massachusetts, USA) at 1g / 20 ml according the manufacturer's instructions. Protein extracts were dialyzed overnight (12-14 kDa membrane tubing, Spectra/Por®, Rancho Dominguez, CA, USA) at 4°C against PBS and then incubated for 1 h with either the parent *L. lactis*, *L. lactis* carrying the empty pORI2 vector, or *L. lactis* / pORI23-ADLB^{M186}, washed three time with PBS and processed for surface proteomics as described before. The same experiment was done with PBS instead of protein extracts as a negative control.

Adherence test and biofilm essay. Adherence to solid-phase human and bovine collagen and fibronectin (Sigma-Aldrich, Munich, Germany) using ADLB-expressing *L. Lactis*, M186 Δ SCC_bov and M186 Ω ADLB was measured a previously described [37]. Biofilm formation was tested as in [38].

Prophage excision and re-introduction. Prophage excision was done by UV induction as described in [7]. Briefly, 25 ml exponential phase cultures were washed one time with ice-cold NaCl and 12.5 ml was transferred in empty petri dishes. UV

induction was done for a total dose of 900 erg/mm/min. To screen for bacteria that had lost the β-hemolysin-converting prophage, irradiated cells were serially diluted, plated on blood agar, and screened colonies that had a restored hemolytic phenotype. The same protocol was used for bacteria that had lost the lipase-converting phage, except that irradiated bacteria were platted on TSB agar containing 2% tributyrin and screened was for colonies that had restored a clear halo around them. Excision was confirmed using the set of primers *hlb*-2 and *hlb*-527 (supplementary table 1) to generate a 526 bp fragment when excised from the genome.

In order to integrate prophages into the different *S. aureus* strains, prophage-excision was first induced by adding mitomycin C (1µg/ml) to exponentially growing culture (OD = 0.4). After ON incubation, cultures were centrifuged and the supernatant filtered through a 200 nm pore filter. Hundred microliter aliquots were then serially diluted and mixed with 4 ml of soft agar contain 200 µl overnight culture of the prophage recipient strain and incubated at 37°C for 24 h. Lytic plates were isolated by puncturing them with a micropipette tips and re-suspended in saline solution for serial dilution on blood agar plate. Integration was observed by phenotypic conversion and confirmed by multiplex PCR using the set of primers *lip2*_Fw, 366_Rv and *int*_Rv (supplementary Table 1).

Cell culture and bacterial internalization assay. MAC-T cells (kindely provided by Madame Olga Wellnitz, University of Bern, Switzerland) were cultured in growth medium consisting of Dulbecco's modified Eagle medium (DMEM) supplemented with 10% fetal bovine serum (FBS), penicillin and streptomycin (100 units penicillin and 0.1 mg streptomycin/mL final concentration, Sigma-Aldrich), and ITS liquid media supplement (Sigma-Aldrich). Cells were cryopreserved in DMEM / F12 (Sigma-Aldrich,

Munich, Germany) containing 20% FBS and 10% dimethyl sulfoxide (DMSO, Sigma-Aldrich), and stored in liquid nitrogen. For bacterial internalization test, cells were grown in BD FalconTM 6-well cell culture plates (BD Biosciences, San Jose, CA, USA) at 37°C and c.a.16 h prior to infection the culture medium was replaced by fresh medium without antibiotics. For infection, bacteria from ON cultures were washed 3 times with PBS, and re-suspended at various concentrations in culture medium without antibiotics before 1 ml aliquots were added to the cell culture wells. After 2 h of incubation, plates were washed and the antibiotic-free culture medium was replaced with fresh medium containing 100 mg of gentamicin. After different incubation periods the cell monolayers were examined by optical microscopy for visible cell damages, before being washed 3 times with sterile PBS and lysed by adding 1 ml of distilled water supplemented with 0.24% trypsin and 0.025% triton X. Cell lysates were serially diluted and plated for viable counts to quantify intracellular bacteria.

Results

Human and Bovine CC8 phylogeny based on core genome analysis. In order to determine the direction of host jump shift between human and bovine CC8 strains, a phylogeny study based on whole genome analysis was undertaken using a collection of 45 (8 human and 37 bovines) *S. aureus* CC8 independent isolates. This core genome is composed of ca. 2100 genes that are present in all 45 strains. After total genome sequencing by Illumina, genes present in the core were extracted and aligned using MAFFT. The output was analyzed by RAXML for the creation of a phylogenic tree. The tree (presented in Figure 1) shows that all the CC8 bovine isolates clustered together in a branch emerging from human strains, with the exception of SaMBk and SaMBc. This suggests that, at a certain point, one or more successful events of host adaptation have happened and led to a clonal spread of bovine-adapted CC8 strains. Interestingly, we could confirm that all the bovine strains present in the cluster harbored the non-*mecA* SCC*bov* element carrying the gene of a predicted new LPXTG surface protein (originally name *orf1* and recently renamed *adlb*) [24, 27], as well as the conserved *ccrA/ccrB* recombinases of SCC*mec*. Alignment of the SCC*bov* sequences present in the different strains did not highlight any differences regarding gene composition and synteny (result not shown). In addition, the SCC*bov* element was absent from the two bovine isolates SaMBk and SaMBc, which did not cluster with the rest of the bovine strains (Figure 1). These two isolates differed from the bovine cluster in several respects. First, strain SaMBk did not carry the SCC*bov* elements inserted at the OrfX location. Second strain SaMBc carried a type IV SCC*mec* cassette instead of SCC*bov* at this very location, and appeared to be a descendant of the human MRSA SaI2. Third they did not give raise to a bovine cluster similar to that of the SCC*bov*

containing strains. Thus, they were likely to represent accidental passage or accidental contamination rather than established bovine strains.

Regarding the prophage content of the different strains, three main observations could be made. First, the β-hemolysin-converting prophage was present in all human strains. This was however not the case for the bovine strains, as it was absent in 1/3 of the isolates. Second, the lipase converting phage was present in both types of isolates but was less represented than the β-hemolysin-converting one. Third, prophages were also observed to be integrated in other position in human strains but not in the bovine ones were c.a. half of the strains did not had prophages at all. Interestingly, strains having lost their prophage content tend to cluster well, like for example for M192, M160, M86, M283, MFU1. This was less the case for the *spa*-typing were micro clusters could still be observed.

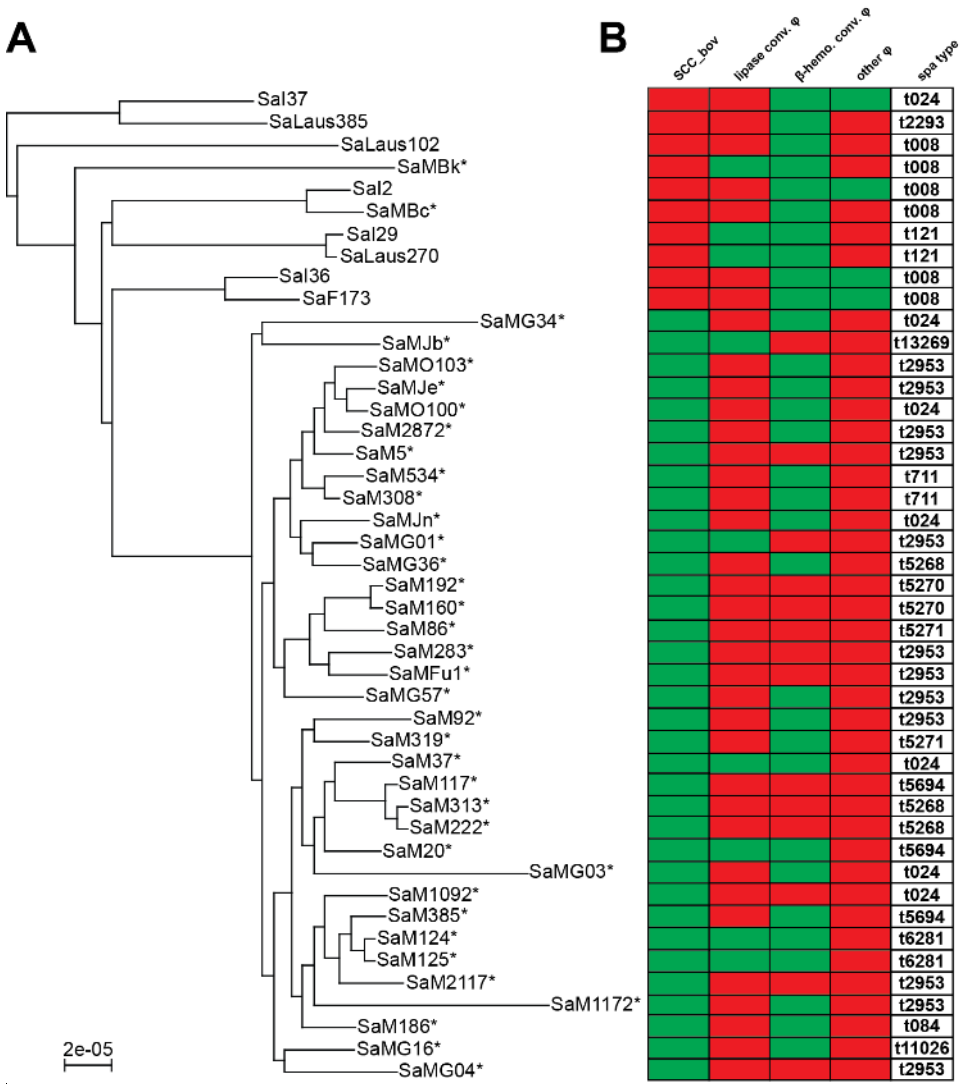

Figure. 1. A) Phylogeny of the 45 CC8 strains (8 of human and 37 of bovine origin) based on the core genome, which account for c.a. 2100 genes present in all 45 CC8 strains. Bovine strains are indicated by asterisks and SaI stands for strains isolated from infected patients, SaLaus for strains isolated from healthy carriers and SaM for strains isolated from bovine mastitis. The scale bar represents 10^{-5} mutations. The branch corresponding to the *S. epidermidis* ATCC 12228 outgroup was removed for convenience. B) The right side panel indicates the presence (green) or absence (red) of the SCC*bov* element, the lipase-converting prophage (lipase conv. Φ), the β-hemolysin-converting prophage (β-hemo. Conv. Φ) and other integrated prophage. In addition, the *spa*-type of the different strain is indicated.

Excision of the non-*mecA* SCC*bov* mobile element and inactivation the novel *adlb* surface protein gene. The results obtained with the phylogeny analysis revealed the possible importance of the non-*mecA* SCC*bov* element in the host jump. In order to study its implication in virulence, prototypic bovine strain M186 was used to both excise the SCC*bov* cassette *in toto* (referred to as M186 Δ SCC*bov*^{M186} in the following), and to interrupt its ADLB-encoding gene.

Excision of the SCC*bov* cassette was first attempted by the strategy developed by Katayama et al [39], consisting in transforming M186 with the plasmid pSR3-1 that constitutively expresses the *ccrA* and *ccrB* recombinases present in the type II SCC*mec* of MRSA N315. Recombinase overexpression was meant to promote SCC*bov* excision. Transformed cells were then screened of excisants by PCR. Although the SCC*mec* and SCC*bov*^{M186} shared the same *attB* and *attL* flanking region and the same *ccrA* and *ccrB* recombinases (with 99% coverage and 95% homology taking minus 200bp from start into account), no SCC*bov* excisants could be isolated using this method.

To achieve excision, we developed an alternative method, using flow cytometry to enrich in cells spontaneously expressing the *ccrA/ccrB* recombinases. To this end, strain M186 was transformed with the plasmid pPGFP-N315 [28], which expresses GFP under the control of the *ccrA/ccrB* promoter (Figure 2.A-D). Flow cytometry indicated that the proportion of cells spontaneously activating the *ccrA/ccrB* promoter was between 3% and 5%, which was comparable to the rate of spontaneous expression of *ccrA/ccrB* observed with MRSA N315 [28]. The population expressing GFP was then sorted and DNA from colonies was extracted and further analyzed by PCR (Figure 2.E). We observed that SCC*bov* had been excised in up to 50% of 40

randomly screened colonies. One colony was picked, purified and named M186 Δ SCC^{M186} for further analyses.

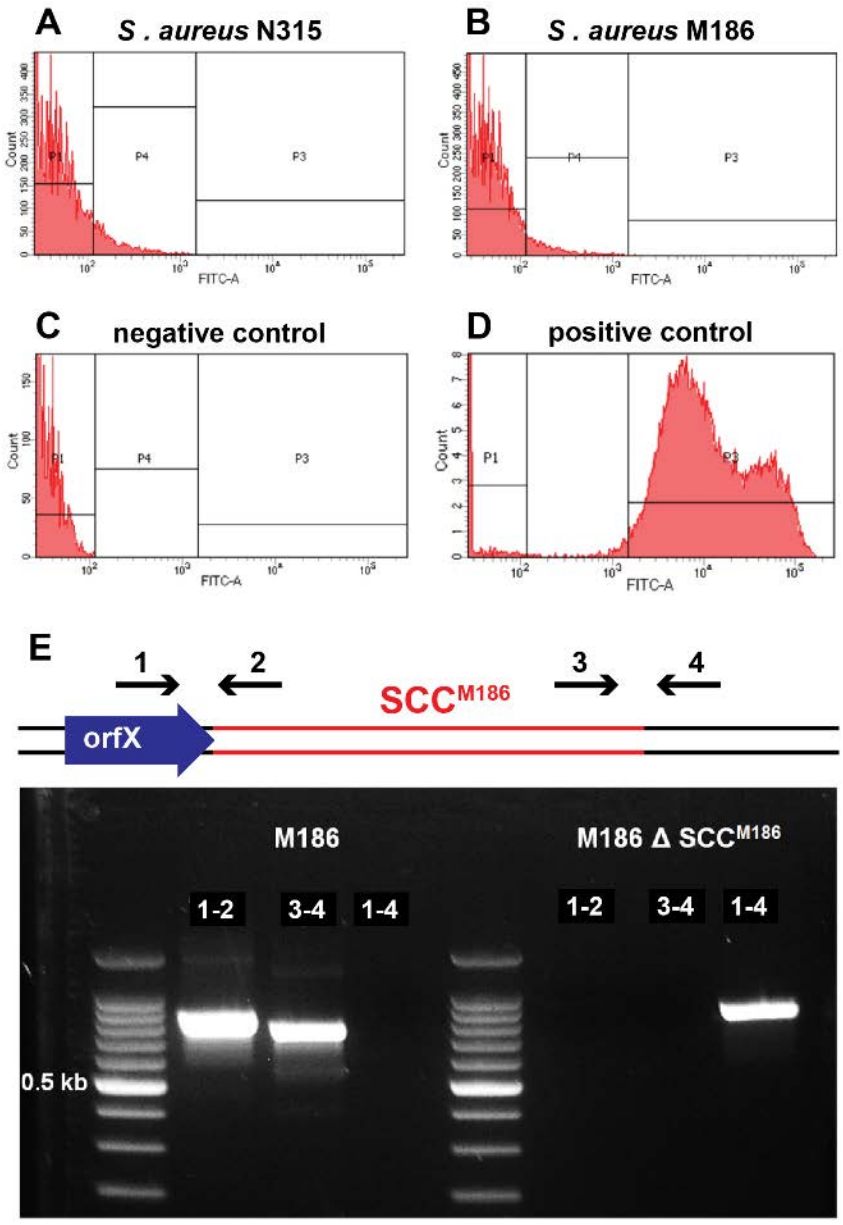

Figure. 2. Flow cytometry analysis of strain *S. aureus* N315 (A) and M186 (B) transformed with plasmid pPGFP-N315 expressing GFP under the control of the *ccr*A/*ccr*B promoter. Both strains showed similar levels of GFP expression in the population (c.a. 3 to 5 %). For each measurement, the subpopulation expressing GFP was determined with respect to negative (C) (strain N315 with an empty plasmid) and positive controls (D) (strain N315 with GPF under constitutive expression) as described by Stojanov *et*

al. and who made de pPGFP plasmid and control strains [28]. (E) Upper part: locations of the PCR primers allowing detecting the presence or the loss of the SCC*bov* cassette. Lower part: PCR products from the SCC*bov*-positive parent M186 (left part of the gel) and a SCC*bov*-excisant, named M186 Δ SCC*bov*^{M186} (right part of the gel) as indicated by the absence of amplification via primer sets 1-2 and 3-4 (as in the SCC*bov*-positive parent) and amplification via primer set 1-4.

In addition, an ADLB-defective mutant (M186 Ω ADLB) was produced by site-specific transposon insertion using the TargeTron gene knockout system (see supplementary Figure 1).

Expression and characterization of the new ADLB surface protein in bovine *S. aureus* and recombinant *L. lactis*. The SCC*bov* element, which was present in all the bovine strains, unanimously carried a gene with all the characteristics of a surface protein (Figure 3.A). Originally named *LPXTG-Bov*^{M186}, in reference to the C-terminal LPXTG sequence and the bovine *S. aureus* M186 in which it was observed, it was recently renamed ADLB, owing to its presence in all observed bovine CC8 isolates and its apparent resemblance to surface adhesins [27].

To confirm the presence of the ADLB protein on the surface of the bovine strain M186, intact bacteria were incubated with trypsin to cleave surface proteins. Figure 3.B shows that the expected ADLB peptides were released from the bacterial surface and detected by LC-MS analysis. Thus, ADLB was indeed present and well represented on the surface of the bacteria.

In a parallel experiments, we constructed *L. lactis* expressing ADLB heterogeneously through the expression plasmid pORI23-ADLB^{M186}. As a control, we also contructed a version of the ADLB protein in which the LPXTG domain was replaced with a 6-his-tag (pORI23-ADLB^{M186} Δ LPXTG). As for *S. aureus* M186, pORI23-ADLB^{M186} recombinant *L. lactis* expressed surface ADLB, which was detected by LC-MS (see Supplementary Figure 2). Moreover, the presence of ADLB on the surface of *S. aureus* M186 and recombinant lactococci was further confirmed by western blotting, using cell wall protein extracts and antibodies directed against two epitopes present in the N-terminal part or in the C-terminal G5 domain (Figure 3.B, lane 4).

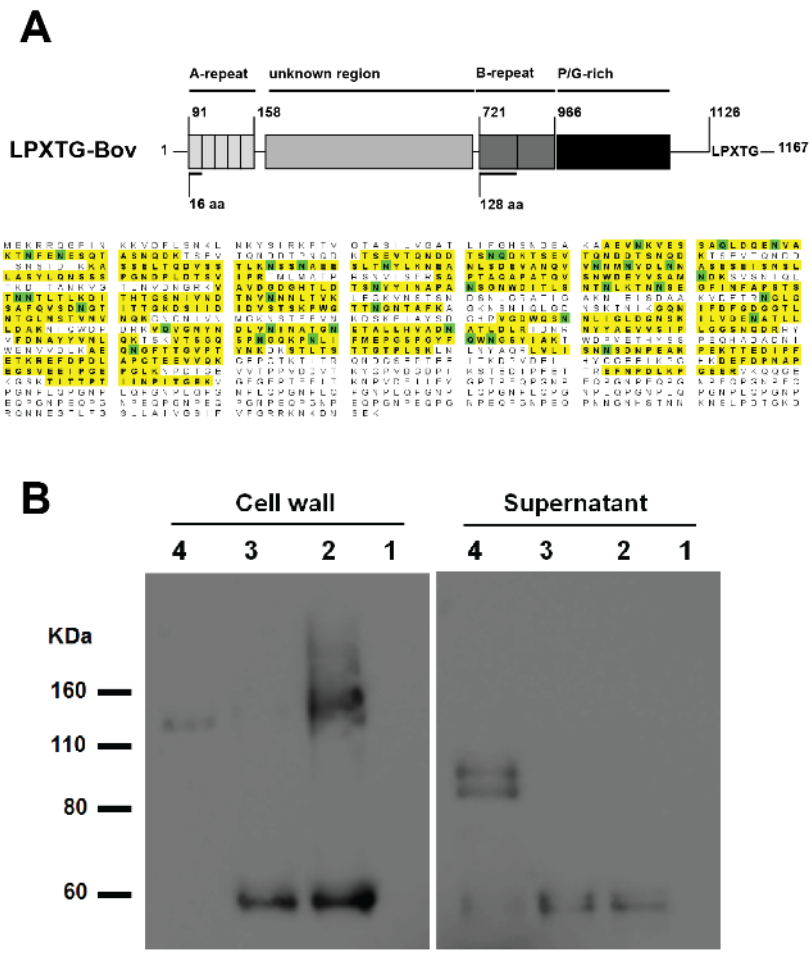

Figure 3. Detection of ADLB^{M186} on bacterial surfaces by LC-MS. (A) Structure of the putative surface protein present in the SCC*bov*^{M186} element named hereafter ADLB^{M186}. The protein possesses an N-terminal signal motif for secretion followed by 5 repeats of 16 amino acids. The C-terminal cell-wall sorting signal LPXTG motif is also present after a proline-glycine rich region that is composed of 25 PEQPGN repeats. The only partial homology obtained for the protein was for the B-repeat region that matched G5 like domains. Bacterial surface peptide digest of ADLB^{M186} confirmed its presence on the surface of strain M186. Amino acid sequences of the protein that matched with the peptides analyzed by LC-MS are highlighted in yellow. Methylated amino acids are highlighted in green. (B) The presence of ADLB^{M186} was also assessed by western blot on the surface and in the supernatant of *L. lactis* / pORI23 (lane 1), *L. lactis* / pORI23-ADLB^{M186} (lane 2), *L. lactis* / pORI23-ADLBM^{186} Δ LPXTG (lane 3), and *S. aureus* M186 (lane 4).

Size variations of *adlb* and its ADLB protein product in bovine CC8 *S. aureus*. The *adlb* gene was not only present and expressed in prototype strain M186, but also in all the other bovine adapted strains studied herein, with size variations ranging from c.a. 3.5 Kb to 6.5 Kb (Supplementary Figure 3.A). Size variations could not be directly localized by genomic sequencing since problems of missassemblies were always present in this specific gene. Therefore, the exact sequence of the *adlb*^{M186} gene was obtained by PCR walking and by adding DMSO to the reaction mixture, which is known to destabilize DNA secondary structures. By using PCR amplification directed on the repeat regions, size variation was observed to be located in specific region (Supplementary Figure 3.B).

Different CC8 strains showing *adlb* size variations were also analyzed by western blot (Supplementary Figure 4). In addition, we included the CC8 strain MBk that does not carry the SCC*bov* element harboring the ADLB protein gene. According to these results, the ADLB protein was present on the cell wall of all the CC8 bovine strains. Moreover, the variation in size of the *adlb* gene also correlated with the size of the proteins. On the other hand, the protein was absent for the SCC*bov*-negative strain MBk, used as a control.

Of note, in *S. aureus* extracts the ADLB protein generated several bands of different sizes. This suggests that the protein might be processed, as has been described for SasG [38] (see also Supplementary Figure 5). The pattern was also strain dependent and a correlation was observed between the number of bands and the size of the gene observed (Supplementary Figure 3.A et 4). On the other hand, ADLB was not processed when expressed in the *L. lactis* background (Figure 3.B).

Seeking a function for the ADLB^{M186} surface protein. Protein sequence analysis using InterPro could not predict any protein family membership, biological process or molecular function for this new surface protein. Searches using BLAST or HMMER showed homology with accumulation associated proteins for specific sites including the signal peptide, sorting signal and B repeats that matched with G5 domains (see also Supplementary Figure 5) [40].

In order to study the potential phenotype conferred by ADLB, we first used the recombinant *L. lactis* / pORI23-ADLB^{M186}, which expressed ADLB out of the potentially redundant *S. aureus* surface protein background (line 3 in Figure 3.B). Strikingly, Lactococcal colonies produced star-like irregular colonies when grown on blood agar (Figure 4 A). The phenotype was correlated with the presence of the protein by using ELISA directly on the colonies (Figure 4. B).

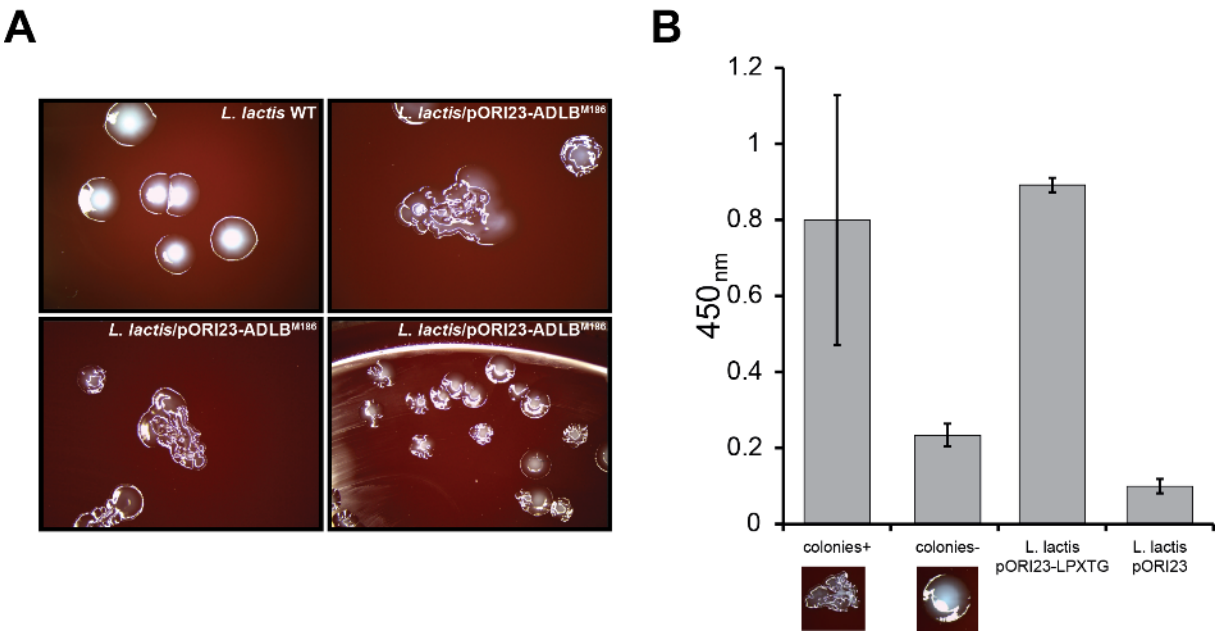

Figure 4. (A) Phenotypes observed for the *L. lactis* / pORI23-ADLB^{M186} after growth on antibiotic free blood agar. A certain number of colonies were growing with an irregular shape. (B) By using ELISA

directly on the colonies, the irregular shape phenotype was correlated with the presence of the ADLB^{M186} on the surface of the recombinant *L. lactis*. 10^9 log/ml of cultured bacteria was used as control.

However, no adherence-promoting activity to host matrix proteins (bovine collagen and bovine fibronectin) or milk was observed (results not shown) with lactococci. Moreover, we used the parent strain M186 and its M186 Ω *adlb* to test biofilm formation. Here again, no difference between the parent and the mutant was found. Thus ADLB might have a different function.

Finally, in order to gain more information on the potential function of the ADLB protein we performed a pull down assay using the *L. lactis* / pORI23-ADLB^{M186} recombinant and protein extracts from fresh udders of milking cows. Recombinant lactococci were incubated with the udder protein extracts, recovered by centrifugation, washed 3 times, and lactococcal surface proteomics was performed as described above. Negative controls included the *L. lactis* / pORI23 strain carrying an empty vector and the two test lactococcal strains incubated without udder extracts. Potential protein candidates were the ones observed only in the *L. lactis* / pORI23-ADLB^{M186} and absent in the negative controls (see Table 1). Interestingly, out of 9 proteins that were only recovered on the surface of the recombinant *L. lactis*, three could be involved in eukaryote intracellular vesicle trafficking, including Golgin like protein, a Dynein 1 heavy chain, and a Keratin type I cytoskeletal protein. Hence, ADLB could be involved in the intracellular staphylococcal lifestyle.

Identified Proteins	Molecular Weight	Fold Change (8416/8417)	*L. lactis* / pORI23-ADLB^{M186} + extract	*L. lactis* / pORI23 + extract	*L. lactis* / pORI23-ADLB^{M186}	*L. lactis* / pORI23
ADLB^{M186}	125 kDa	33.0	36	0	39	0
Golgin like protein	378 kDa	7.4	8	0	0	0
Dynein 1 heavy chain	532 kDa	4.6	5	0	0	0
Galactokinase	42 kDa	4.6	5	0	0	0
Alpha-enolase	47 kDa	4.6	5	0	0	0
Poly(rC)-binding protein	37 kDa	4.6	5	0	0	0
D-3-phosphoglycerate dehydrogenase	56 kDa	4.6	5	0	0	0
flavoprotein subunit beta	28 kDa	4.6	5	0	0	0
Keratin, type I cytoskeletal	49 kDa	1.0	4	0	0	0

Table 1. Proteins pulled down from udder extracts by *L. lactis* / pORI23-ADLB^{M186}

Cell culture internalization tests using MAC-T cell lines. As shown with the pull-down experiment, the ADLB^{M186} could potentially interact with proteins implicated in vesicle trafficking. Since internalization and phagosome escape is an important step in staphylococcal cell invasion, we tested this hypothesis using an internalization essay. To this end, a monolayer of MAC-T bovine mammary epithelial cell line was infected first by the M186 Ω ADLB^{M186} and then by M186 Δ SCC*bov*^{M186} to observe any difference in intracellular survival and cell morphology compared to the M186 wild type. Interestingly, excision of the SCC*bov* element or knockout of the *adlb* gene did not affect cell internalization at first. However, after engulfment the parent M186 strain

readily escaped endosomes and lysed the mammary cells. This resulted in a disintegration of the host cells and a decrease in bacterial viability ($\geq$ 2 log CFU after 24 h) due to their release in the gentamicin-containing medium (Figure 5.A). In contrast, excising the SCC*bov* cassette or knocking out the *adlb* gene resulted in more prolonged endosomal sequestration and increased intracellular survival. Indeed, the two knockout strains were observed in vesicles, which was not the case for the WT (Figure 5.B). Since mammary cells are not professional macrophages, they are not expected to readily kill bacteria after engulfment.

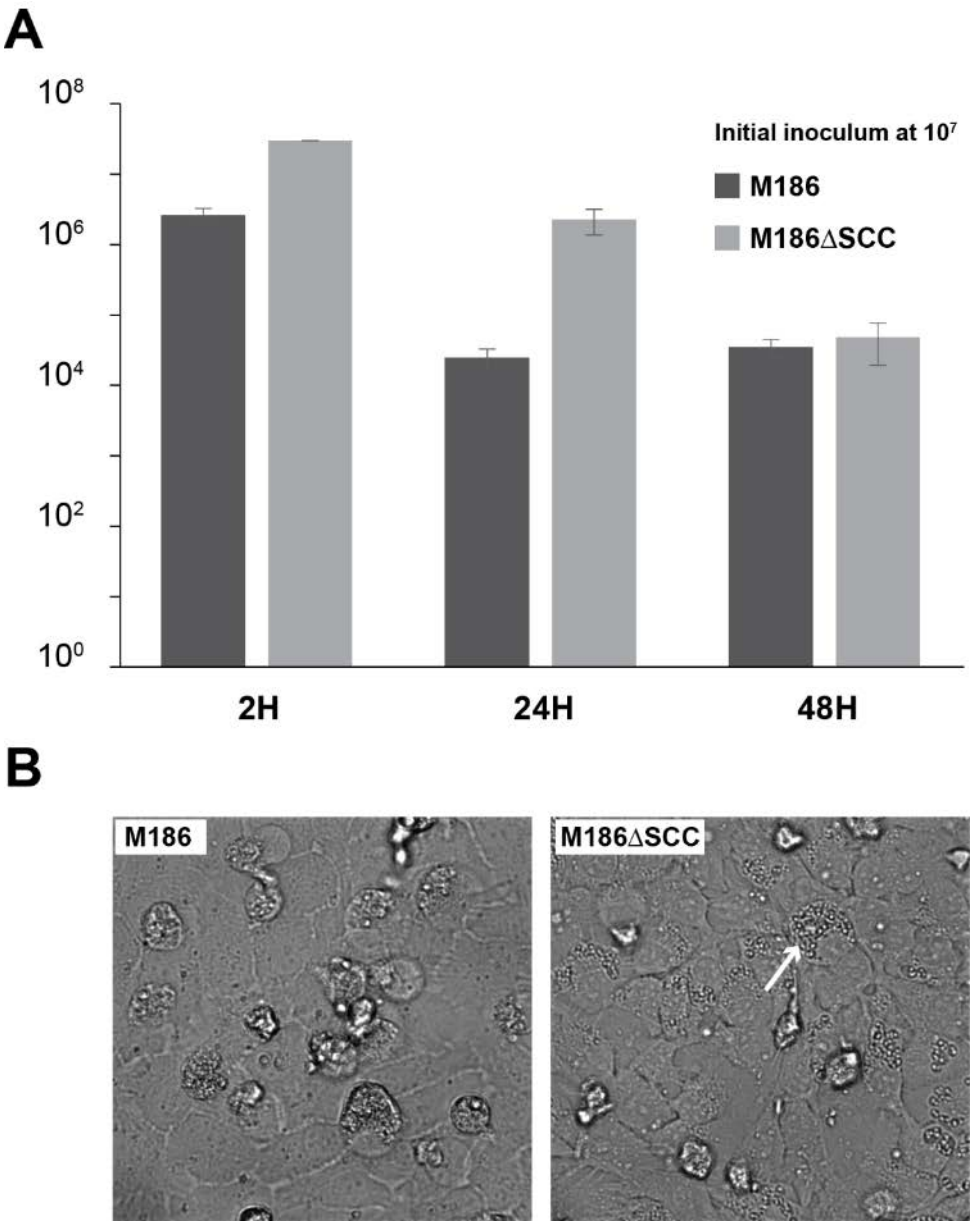

Figure 5. Cell culture internalization tests using MAC-T cell line. (A) Cells were infected by the M186 or M186 Ω ADLB^{M186} and M186 Δ SCC*bov*^{M186} at an initial inoculum of 10^7 CFU/ml. After different incubation time points, cell were washed, lysed and plated. (B) Light microscopy after 24h incubation of M186 or and M186 Δ SCC*bov*^{M18} strains.

Prophage content of human and bovine CC8 isolates. The genomes of the different human and bovine strains were also analyzed using the PHAge Search Tool (PHAST) in order to search for integrated prophages (Figure 7.A and 7.D). Based on phage content, we found that all isolates tended to cluster in three subgroups, which were similar to the three subgroups observed using microchips (Figure 6) [24].

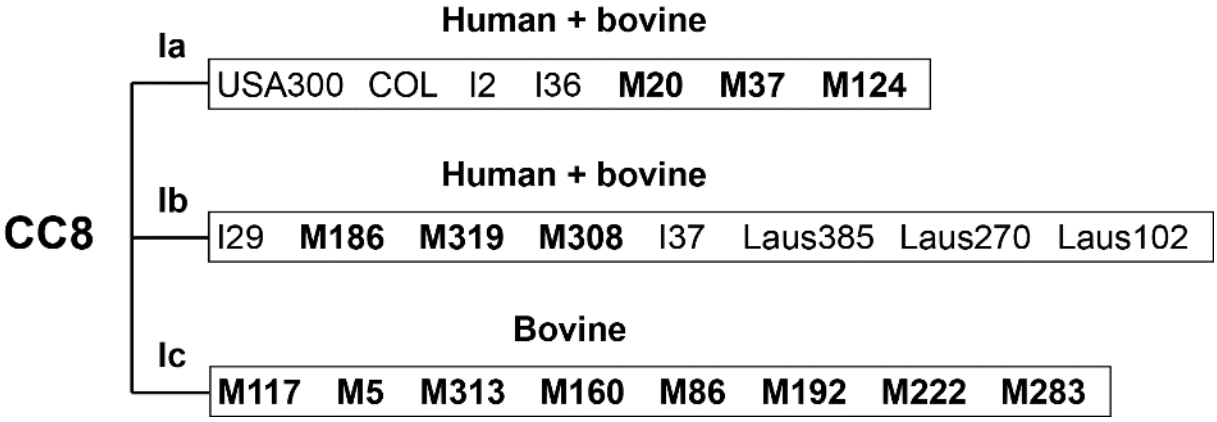

Figure 6. Microarray-based clustering of human and bovine CC8 isolates adapted from [24]. This clustering was confirmed by core genome gene phylogeny (Figure 1) and further associated to prophage content (see text for details). Bovine isolates are indicated in bold.

Interestingly, strains of mixed human-bovine subgroup Ia were observed to have two intact predicted prophages, one β-hemolysin converting prophage and one lipase converting prophage, respectively. Moreover, all strains from mixed human-bovine subgroup Ib had lost the lipase converting prophage but still contained the β-hemolysin converting prophage, whereas the strains of the bovine-only subgroup Ic were devoid of integrated prophages. Thus, in addition to the acquisition of SCC*bov*, which was

always present in bovine isolates, the loss of specific prophages seemed also to accompany the human-to-bovine host jump.

In addition, we also observed that bovine CC8 strains shared a similar GC content, with the same cumulative GC skew curve (supplementary Figure 6 A). An inversion in the cumulative GC skew between c.a. 993 and 995 kbp was present in all strains and corresponded to the integration site of an incomplete prophage (supplementary Figure 6 B). The other intact prophages had a GC content similar to the *S. aureus* genome, which suggests horizontal transfer.

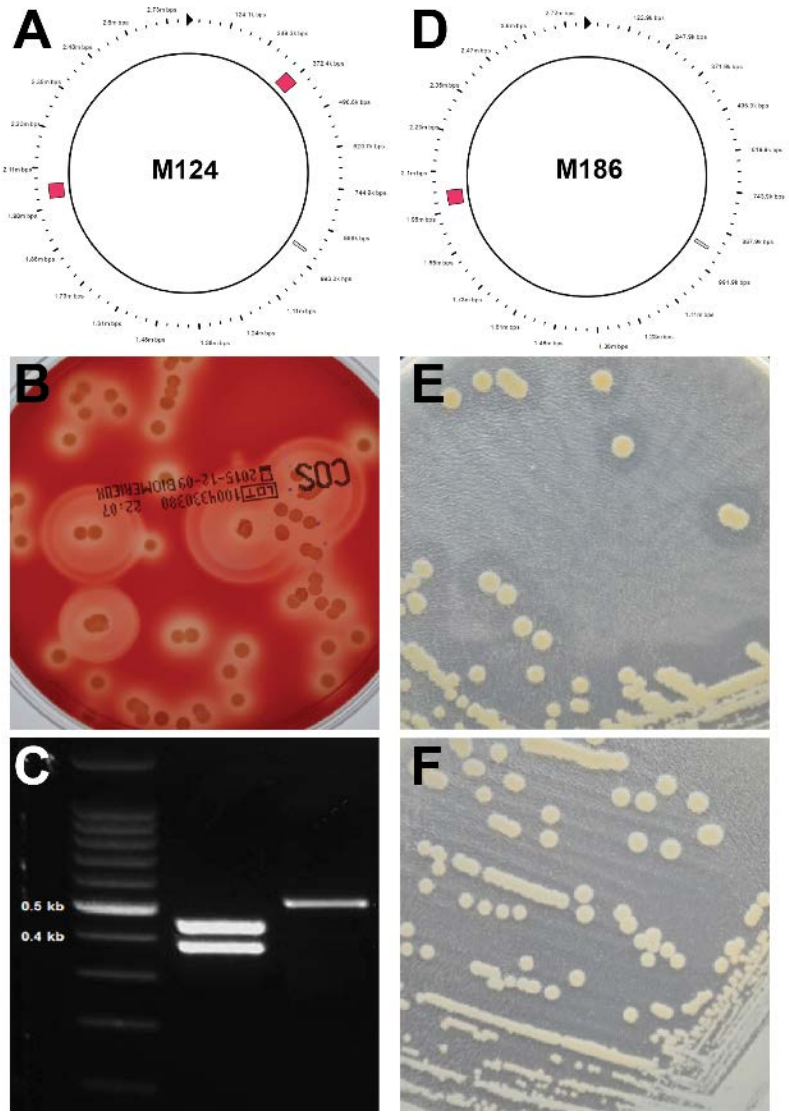

Figure 7. Analyses of prophages present in prototypic CC8 strains from subgroups Ia, Ib and I.c using PHAST (PHAge Search Tool). (A) Two prophages annotated as intact (red squares) were present in the strain M124, M20 and M37 (only M124 is shown in the Figure) that are part of the mixed human-bovine group Ia**.** The prophage present at c.a. 2m bps is a β-hemolysin converting bacteriophage**,** which is also present in strain M186 (red squares, D) and all associated ones from the mixed human-bovine group Ib (M319 and M308). The prophage present in strain M124 at c.a. 370K bp was also present in strains from group Ia but absent from subgroup Ic (result not shown). An incomplete prophage was also predicted at c.a. 993 Kbp in all CC8 bovine strains. (B) UV-induced excision of β-hemolysin-converting bacteriophages after UV exposition of strain M186, hemolysis was observed around certain colonies. This phenotype was due to the loss of the β-hemolysin-converting prophages that restore the hemolytic activity of the strain. Prophage excision was confirmed by multiplex PCR using primers for the amplification of the staphylokinase (sak) and the integrase present on the prophage or the β-hemolysin (*Hlb*). (C) The introduction of the lipase converting bacteriophage from strain M124 (subgroup Ia) into strain M186 was also achieved and phenotypic conversion regarding lipase activity was observed as presented in panels (E), parent strain M186 growing on tributyrin-containing plates and (F): strain M186 in which the lipase interrupting phage of strain M124 was introduced and grown on tributyrin-containing plates.

Prophage curing and reintroduction in bovine CC8 isolates. To further study the implication of prophages in the host-jump, we attempted to cure and reintroduce prophages in the prototypic strain M186 (which belongs to the human-bovine subgroup Ib and contains only the β-hemolysin prophage) in order to obtain a series of strains encompassing subgroups Ia (human-bovine, with 2 prophages) to Ic (bovine only with no prophages).

We first, succeeded in curing strain M186 (human-bovine subgroup Ib) form its β-hemolysin-converting prophage by exposing it to UV radiation. Indeed, UV light is known to generate stress by inducing DNA damage that induces prophage excision

(Figure 5.B and 5.C). Because phage-excision is supposed to restore the phage-interrupted β-hemolysin gene, it was possible to screen for colonies producing hemolysis on blood agar (Figure 5B and 5C). As a mirror experiment, the β-hemolysin-converting prophages could also be reintroduced in the bovine-only strain M117 (bovine-only subgroup Ic) by incubating it with mitomycin C induced supernatant from strain M186 and screening for the loss of hemolysis on blood agar (results not shown).

The same experiments were also performed with the lipase converting bacteriophage (Figure 5.E and 5.F). To this end strain M124, which contained two prophages (subgroup Ia) was induced by UV exposure as above. Then, strain M186 was exposed to the phage-containing supernatant and platted of tributyrin-containing agar to screen for colonies that had lost a lipolytic halo. All phage losses and acquisitions were confirmed by PCR.

Discussion and perspectives

The present study aimed at shedding a comprehensive light on the genealogy and mechanistic events involved in the putative human-to-bovine host jump of CC8 *S. aureus*. We first reconstructed the phylogeny of human and bovine isolates based on core genome genes. This refined genealogy confirmed previous assumptions of the human-to-bovine directional jump based on AFLP, MLST [22] and microarrays [24]. Indeed, while microarray analysis – which is restricted to the presence or absence of known genes – showed that 98% of the differences between human and bovine isolates were related to MGEs, the present results indicate that human and bovine CC8 isolates differed in even more intrinsic features that resided in their core genome genes. This highlights the depth of the divergent evolution of originally human-anchored CC8 strains, which at a certain point of time gave rise to a unique bovine branch. Moreover, while the present observations addressed the directional jump from the side of the human host, veterinary epidemiologic studies came to the same conclusion from the bovine side [26]. They independently disclosed that a recently described particularly invasive bovine mastitis *S. aureus*, referred to as genotype B (or GTB), was identical to human CC8 and was likely to be a descendant of this very human staphylococcal clonal complex. Even more, they propose that all bovine *S. aureus* have a human ancestor.

In the following we briefly discuss three aspects that we studies more deeply regarding the mechanism of this host jump, including its association with specific MGEs, the putative mechanisms mediated by these MGEs, and the possibility to study “reverse evolution” by reconstructing the dynamic of the MGE trafficking responsible for the host jump.

MGEs associated with the host jump. In addition to the global genealogy discussed above, the present analyses also underlined the dynamic of acquisition and loss of MGEs that happen along the human-to-bovine passage. Microarray analyses classified human and bovine CC8 in 3 subgroups (Ia, Ib and Ic) where the acquisition of SCC*bov*, found only in bovine strains, clearly discriminated between human and bovine isolates [24]. In this very study, the Ia and Ib subgroups contained mixt human and bovine isolates, all of which carried the β-hemolysin-converting prophage, while only bovine isolates carried the additional SCC*bov*. In contrast, the third subgroup (Ic) contained only bovine isolates, all of which had lost the β-hemolysin-converting prophage. This suggested a progressive passage from Ia to Ic, but without a clear clue explaining the difference between the mixt human-bovine subgroups Ia and Ib.

The present results confirmed these three subgroups from the core genomic point of view. Moreover, they added critical information regarding the passage from subgroup Ia to Ib. Indeed, bovine strains of subgroup Ia carried two prophages, i.e. one lipase-converting and one β-hemolysin-converting prophage, whereas bovine strains of subgroup Ib had lost the lipase-converting prophage. Finally, the bovine-only subgroup Ic has lost both prophages. Thus, although acquisition of SCC*bov* was a *sine qua none* condition for the host jump, as highlighted by core genome phylogeny, additional requirements such as reestablishment of lipase activity (by losing the lipase-converting prophage) and β-hemolysin activity (by losing the β-hemolysin-converting prophage) were likely to facilitate the establishment and stability of CC8 staphylococci in the bovine environment.

In counterpart, the loss of the β-hemolysin-converting prophage is also likely to hamper the jump-back of bovine CC8 (or GTB) strains to humans. This is suggested by the quasi absence of bovine CC8 (or GTB) in farm-workers in previous studies [22, 26],

and by the fact that when they loose the β-hemolysin-converting prophage, *S. aureus* also lose the prophage-associated immune evasion cluster (ICE) carrying the staphylokinase (*sak*), enterotoxin A (*sea*), chemotaxis inhibitor protein (*chips*) and staphylococcal complement inhibitor (*skin*) genes [41].

To further study the role of these MGEs in the host jump we first addressed the role of SCC*bov*, which was a prerequisite for the human-to-bovine passage.

Putative role of SCC*bov* in the human-to-bovine host jump. SCC*bov* carries several genes that might be beneficial in the agriculture milieu, such as arsenic and copper resistance genes, plus one intriguing gene encoding a putative peptidoglycan-anchored protein via the LPXTG-SortA system [24, 42]. This gene, tentatively named *adlb* (for Adhesin-Like Bovine protein) [27] is constituted of a central domain of unknown function, bracketed by a N-terminal and a C-terminal repeats domains, the latter showing homology with AAP proteins [24, 27, 40].

To understand the role of SCC*bov* and the putative ADLB protein it was critical to first assess its presence on the staphylococcal surface, then test the phenotype it could confer, and finally test whether excising SCC*bov in toto* or inactivating *adlb* would lead to phenotype modifications. The presence of ADLB on the bacterial staphylococcal was unambiguously demonstrated by LC-MS and western blot in several independent bovine CC8 isolates, as well after heterologous expression of *adlb* in *L. lactis*. Interestingly, we also observed strain-dependent variation in the length of the *adlb* gene, which translated in parallel length variation of the ADLB surface protein. These length variations occurred in the N-terminal and C-terminal AAP-like repeats, not in the central domain.

Since length variations of LPXTG proteins may be associated with clonality, as in the protein A gene (*spa*) that gave rise to *spa*-typing [43], we asked whether *adlb*-length

could correlate with *spa*-types, which correlated with clonality in GTB (or CC8) infected farms [26]. Unfortunately, the number of comparable isolates was to small to draw a conclusion on this matter.

Nevertheless, beyond molecular characterization is was also determinant to identify the putative phenotype conferred by ADLB. The first striking observation was that expressing ADLB in *L. lactis* (as confirmed by western blot) produced irregular star-shaped colonies. In contrast, colonies losing ADLB returned to natural smooth and round-shaped morphologies. Thus, we expected ADLB to confer some kind of surface-related phenotype, such as adherence to host matrix proteins or milk components, or to promote biofilm formation as does AAP [40]. However, these functional tests did not disclose differences between parent and mutant staphylococci or lactococci.

We next attempted to identify potential ADLB host ligands by pulling down proteins from extracts of lactating udders using ADLB-expressing lactococci as baits. These experiments did not yield additional host-matrix protein that had not been tested in the first screening experiments, but rather oriented us to the intracellular lifestyle of *S. aureus*. Indeed, 3 out of 9 udder proteins recovered by ADLB-positive lactococci were related to intracellular vesicle trafficking, namely Dynein 1 heavy chain, Golgin like protein and Keratin type I cytoskeletal protein. This prompted us to seek a role of ADLB in the setting of mammary gland cell cultures.

To this end, we generated isogenic bovine CC8 strains (using prototypic strain M186) from which the SCC*bov* cassette had been excised *in toto*, or in which the *adlb* gene had been inactivated. We also used the ADLB recombinant lactococci as a control. First, ADLB-recombinant lactococci did not show differences in mammary cell adhesion or internalization, indicating that ADLB was not involved in these initial steps of infection.

Second, parent and SCC*bov* excisants or *adlb*-interrupted mutants invaded cells similarly early after inoculation. Since ADLB alone did not mediate cell internalization on its own in the recombinant lactococci experiments, mammary cell uptake of *S. aureus* might have been prompted by other staphylococcal components, such as ubiquitous FnBPA, which mediates staphylococcal internalization in eukaryotic cells [44].

Third, upon more prolonged incubation, parent staphylococci escaped endosomes and lysed the host cells, as assessed by optical microscopy, whereas the SCC*bov* and *adlb* mutants respected both the vesicles and the cells. As a result, parent *S. aureus* were released into the gentamicin-contained medium and killed by the antibiotic. In contrast, mutants survived for prolonged periods of time in the non-professional phagocyte milieu of mammary cells.

Taken together, these experiments indicate that at least one effect of ADLB is vesicle escape and lysis of host cells. The exact mechanism by which this occurs is as yet unclear, but it is linked to the presence of ADLB, plus or minus other non-SCC*bov* proteins (FnBPs, β-hemolysin etc), since no difference was observed between SCC*bov* excisants and *adlb* mutants. Moreover, whether processing and release of ADLB by bovine CC8 staphylococci is important is a matter of speculation. Indeed, releasing polypeptides able to bind dynein-motor and cytoskeleton structures inside mammary host cells could contribute to paralyzing the natural vesicle addressing such as lysosome formation and thus promote intracellular staphylococcal survival.

The invasive phenotype associated with ADLB could potentially explain privileged bacterial multiplication of bovine CC8 (or GTB) strains in the bovine milieu, and thus non-specific (bulk-related) spread within cowherds. However, it does not explain its propensity to preferentially colonize lactating udders and milking apparatuses [26]. A

hint to this explanation could emerge from the trafficking of prophages, which is addressed next.

Potential role of prophage trafficking in the human-to-bovine host jump. Acquisition or loss of prophages and prophage-related genes play a well-known role in microbial adaptation and pathogenicity [45]. Salient examples regarding *S. aureus* include prophage-encoded Panton-Valentine leukocidin and exfoliative toxin A [46, 47]. Moreover, acquisition and loss of prophages were also associated with human-animal exchanges of *S. aureus*, as exemplified by human-poultry and human-porcine jumps [18, 48]. In these two examples, poultry- and porcine-adapted *S. aureus* lost the ICE-carrying β-hemolysin prophage typical of human strains, and poultry strains acquired a new prophage instead (Phage AVβ) encoding for proteases that might be important in the avian niche.

The present observation between human and bovine hosts implies the sequential loss of two prophages. The first, interrupting the lipase gene, has not yet been involved in human-animal host jumps, while the second, interrupting the β-hemolysin gene, was associated with the human-porcine jump [48]. To study the putative role of the loss of these two prophages we used prototypic strain M186 (from the mixt human-bovine subgroup Ib) containing only the β-hemolysin-converting prophage and generated two recombinants: one from which we excised the β-hemolysin-converting prophage, generating a bovine-only subgroup Ic prototype, and one in which we inserted the lipase converting prophage of subgroup Ia strain M127, generating a mixt human-bovine subgroup Ia prototype. This M186 triad, containing SCC*bov* and spanning the three Ia, Ib and Ic prophage subgroups is now being used to determine their role in lipid-rich milked environment, for the lipase converting prophage, and mammary cell

adherence, β-hemolysin was previously reported to facilitate epithelial colonization [49].

Conclusion and perspectives. Taken together, these present results highlight the sophisticated interplay between complementary actors involved in the CC8 (or GTB) human-to-bovine host jump. Although SCC*bov* cassette and ADLB were central to the host jump (no human strains possessed them), it relied on parallel losses of lipase- and β-hemolysin-converting prophages, which were present in human-only strains but totally absent from bovine-only strains. On this basis we propose the following scenario:

1. Restoring lipase activity (loss of lipase-interrupting prophage) could promote growth in lipid-rich lactating udder environment.
2. Restoring β-hemolysin (loss of β-hemolysin-converting prophage) might promote epithelial colonization as previously shown in animal models.
3. Fibronectin-binding protein, which is ubiquitous in *S. aureus*, promotes internalization into mammary cells, as previously demonstrated.
4. ADLB promotes endosomal escape and mammary cell lysis, allowing further spread and explaining the virulent phenotype of this peculiar clone.

While the role of the prophage trafficking is the purpose of current studies, these results suggest new approaches to enrich the preventive armamentarium against this particular organisms, first by proposing a new detection test to improve sanitation [27], and second by suggesting new vaccine targets for blocking antibodies against CC8 (or GTB) determinants, such as ADLB, lipase and β-hemolysin.

Supplementary Tables

Table 1: Bacterial strains and their origins, plasmids and nucleotides

Bacterial strains	Characteristics	Origin
E. coli		
DH5α/pORI23		[34]
DH5α/pORI23-ADLB^{M186}		This study
DH5α/pORI23-ADLB^{M186}ΔLPXTG		This study
DH5α/ pPGFP-N315		[28]
L. lactis		
L. lactis subsp. cremoris 1363		[50]
L. lactis pORI23-ADLB^{M186}		This study
L. lactis pORI23-ADLB^{M186}ΔLPXTG		This study
S. aureus		
RN4220	Restriction-deficient derivative of RN450; intermediate cloning host	[51]
N315	MRSA carrying type II SCCmec	[52]
M186ΩDALB	DALB inactivation by transposon insertion	This study
M186ΔSCC_bov	SCC_bov element excised form strain M186	This study

M186ΔφβhemB	Beta-hemolysin converting prophage excised from strain M186	This study
M186::φlipM124	Lipase converting prophage present in strain M124 introduced in strain M186	This study
I37	Human isolate	[22]
Laus385	Human isolate	[22]
Laus102	Human isolate	[22]
MBk	Isolated from milk sample	H. Graber
I2	Human isolate	[22]
MBc	Isolated from milk sample	H. Graber
I292	Human isolate	[22]
Laus270	Human isolate	[22]
I369	Human isolate	[22]
F173	Human isolate	H. Graber
MG34	Isolated from milk sample	H. Graber
MJb	Isolated from milk sample	H. Graber
MO103	Isolated from milk sample	H. Graber
Mje	Isolated from milk sample	H. Graber
MO100	Isolated from milk sample	H. Graber
M2872	Isolated from milk sample	H. Graber
M5	Isolated from milk sample	[22]
M534	Isolated from milk sample	[22]
M308	Isolated from milk sample	[22]
MJn	Isolated from milk sample	H. Graber

MG018	Isolated from milk sample	H. Graber
MG36	Isolated from milk sample	H. Graber
M192	Isolated from milk sample	[22]
M160	Isolated from milk sample	[22]
M86M	Isolated from milk sample	[22]
M283	Isolated from milk sample	[22]
MFU1	Isolated from milk sample	H. Graber
MG57	Isolated from milk sample	H. Graber
M92	Isolated from milk sample	[22]
M319	Isolated from milk sample	[22]
M37	Isolated from milk sample	[22]
M117	Isolated from milk sample	[22]
M313	Isolated from milk sample	[22]
M222	Isolated from milk sample	[22]
M20	Isolated from milk sample	[22]
MG03	Isolated from milk sample	H. Graber
M1092	Isolated from milk sample	H. Graber
M385	Isolated from milk sample	[22]
M124	Isolated from milk sample	[22]
M125	Isolated from milk sample	[22]
M2117	Isolated from milk sample	[22]
M1172	Isolated from milk sample	[22]
M186	Isolated from milk sample	[22]
MG16	Isolated from milk sample	[22]

MG04	Isolated from milk sample	H. Graber

Plasmids

pOri23	ermAM ori ColE1 P23	[34]
pORI23-ADLB^{M186}	DALB cloned into pORI23ermAM ori ColE1 P23	This study
pORI23-ADLB^{M186}	DALB with 6-his tag inserted into the LPXTG signal cloned into pORI23ermAM ori ColE1 P23	This study
pPGFP-N315p	ccrAB promoter fusion with GFP cloned in pCN36; tet(M)	[28]

Oligonucleotides

LPXTG_DALB_SalI	ACGCGTCGACTTATTGGGAGGTAATAATATG GAAAAAAG	This study
LPXTG_DALB_PstI	AAAACTGCAGTTATTTTTCACTATTATCCTTAT TTTTACG	This study
IBS	AAAAAAGCTTATAATTATCCTTAACTCTCAAT ACAGTGCGCCCAGATAGGGTG	This study
IBS1d	CAGATTGTACAAATGTGGTGATAACAGATAA GTCAATACAGGTAACTTACCTTTCTTTGT	This study
IBS2	TGAACGCAAGTTTCTAATTTCGATTAGAGTTC GATAGAGGAAAGTGTCT	This study
ADLB_fw	TTGGAAAAAAGAAGACAAGGCCC	This study
Fw4200_ADLB	GTTCCTGTAGTACTTGTC	This study
hlb-2	AGCTTCAAACTTAAATGTCA	This study
hlb-527	CCGAGTACAGGTGTTTGGTA	This study

13int-for	GCTTTGAAATCAGCCTGTAG	This study
sak-for	GTGCATCAAGTTCATTCGAC	This study
sak-rev	TAAGTTGAATCCAGGGTTTT	This study
lip2_Fw	GTTAGATGGCTCTGCAAAATTG	This study
Lip_366_Rv	CTTCACCAACACCGGTTGTTC	This study
Lip_int_Rv	CGAGAAGTACAAAGATCCATAC	This study
Q5SDM_ADLB_F	CACCACCACAAAGACCGTCAAAATAATGAAG	This study
Q5SDM_ADLB_R	ATGATGATGTGAATTCTTGTTGTTTGTTGAATG	This study

[a] Abbreviations: Cam[r], chloramphenicol resistance; Kan[r], kanamycin resistance [b] Centre hospitalier universitaire vaudois (CHUV, Switzerland) [c] Deutsche Sammlung von Mikroorganismen und Zellkulturen (DSMZ, Leibniz-Institut, Germany) [d] American type culture collection (ATCC, Manassas, Virginia, USA) [e] Restriction sites are underlined.

Supplementary Figures

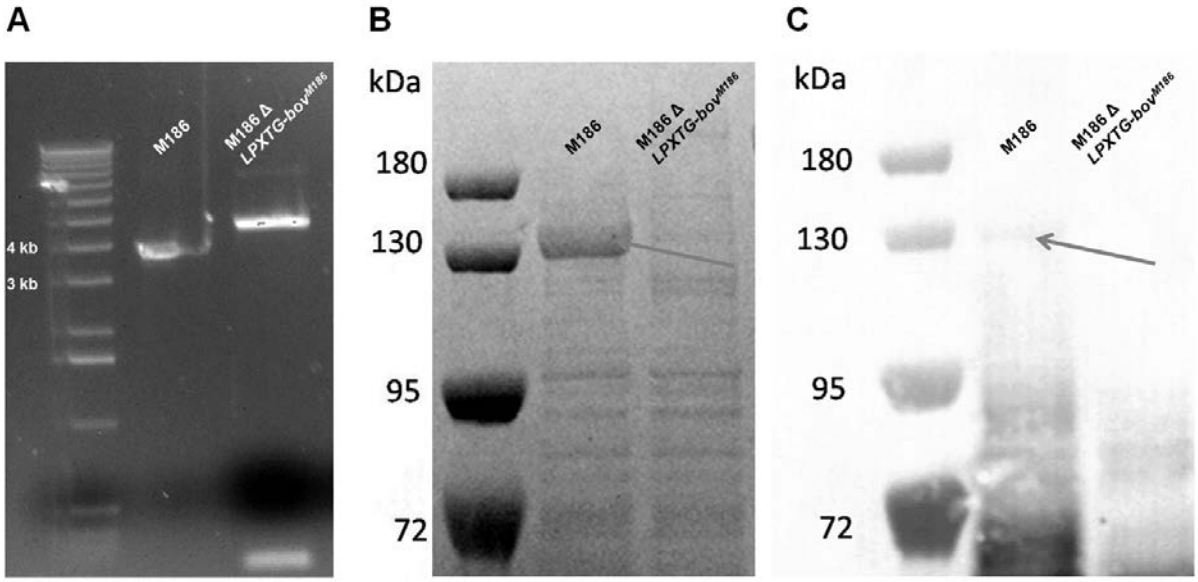

Supplementary Figure 1. Generation of a knockout construction for the *LPXTG-Bov* gene present in strain M186 using site-specific transposon insertion. (A) A shift in the *LPXTG-Bov* ^{M186} gene due to transposon insertion was observed after PCR amplification on the M186 WT and the M186 Δ *LPXTG-Bov* ^{M186} strains. (B) Absence of the protein on the surface was confirmed by gel electrophoresis (Coomassie blue staining) and (C) and western blotting. Arrows indicate the presence of the protein in the WT.

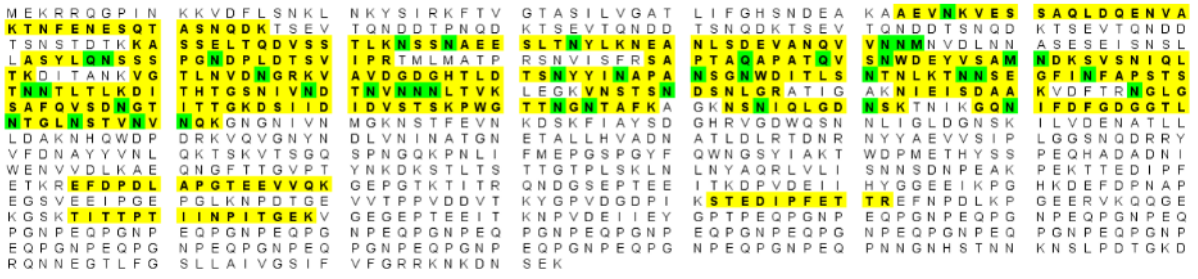

Supplementary Figure 2. Detection of ADLB^{M186} on *L. lactis* / pORI23-ADLB^{M186} surfaces by LC-MS/MS. Amino acid sequences of the protein that matched with the peptides analyzed by LC-MS/MS are highlighted in yellow or green (methylated animo acids).

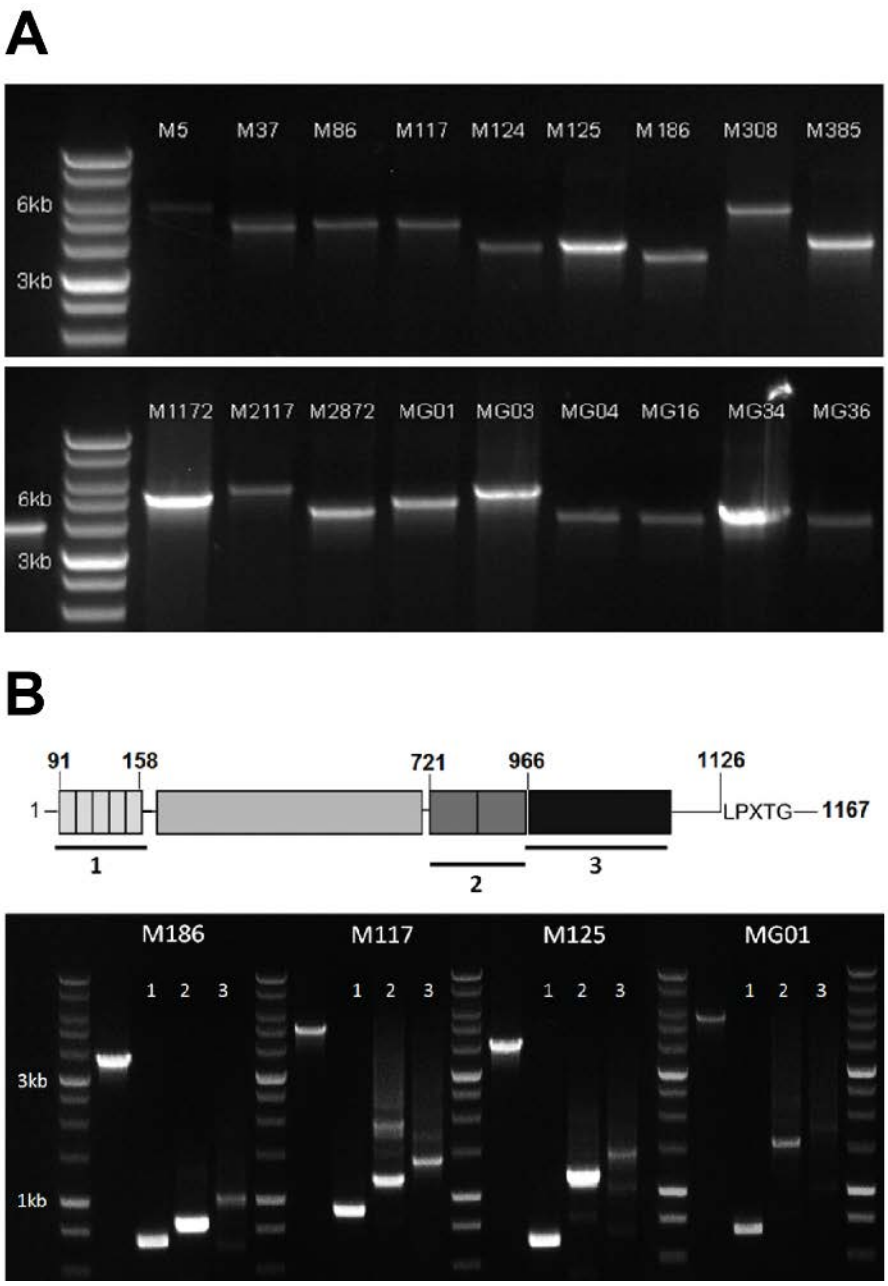

Supplementary Figure 3. (A) The same set of primers that were used to amplify the *adlb*^{M186} were used on other CC8 bovine strains. PCR products ranged from c.a. 3.5 Kb (M186) to 6.5 Kb (M2117) showing interspecies variation. (B) Different sets of primers were designed to amplify the regions containing repeats. Size variation observed in Figure A is due to size variation in the repeated region

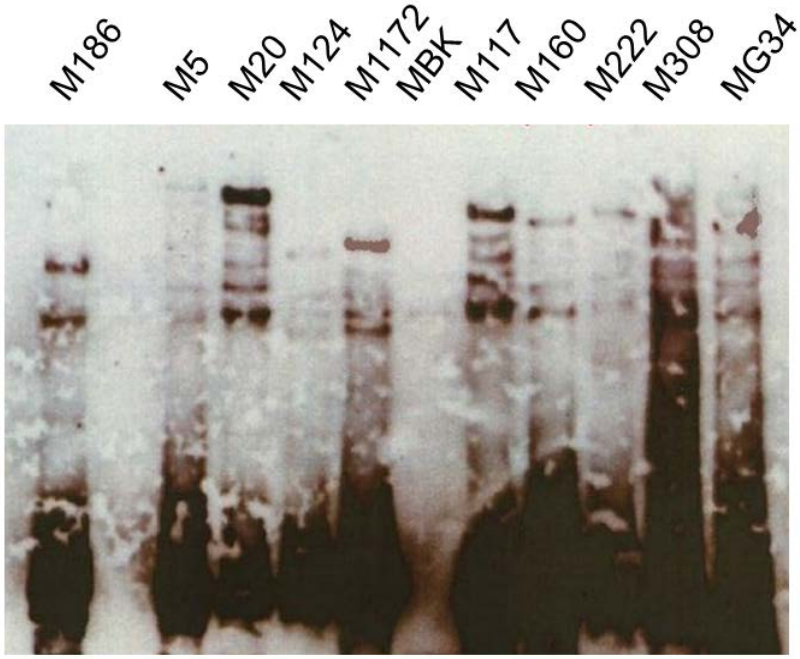

Supplementary Figure 4. A western blot with protein extracts present in the supernatant of CC8 strain M186, 5, 20, 124, 1172, 117, 160, 222, 308 and G34 that are *ADLB* positive and CC8 strain MBk that is *ADLB* negative was also prepared. All Protein extracts and Western blots were prepared as already described [34]. Image (A) was taken with a camera and image (B) with film after the first one get out of order.

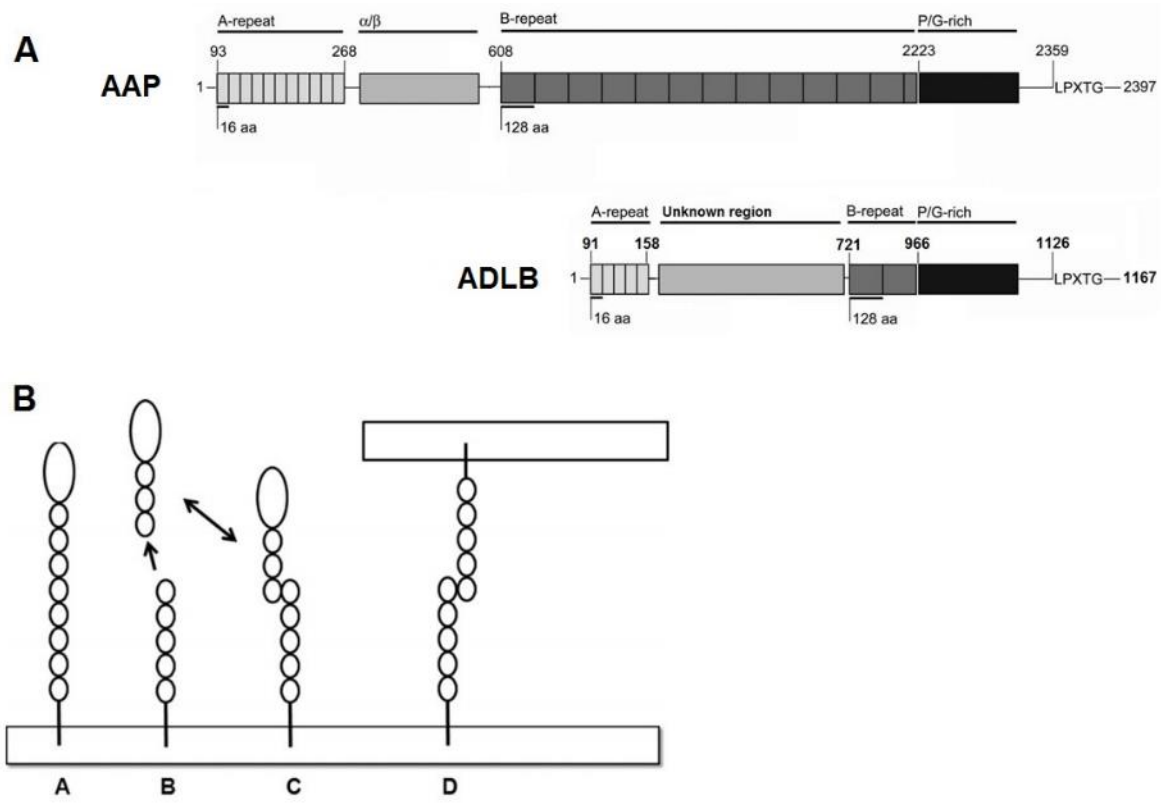

Supplementary Figure 5. (A) Structural similarities between the ADLB and Agglutination Associated Proteins (APP). AAP contains an N-terminal A-repeat region with degenerate 16-aa repeats, a globular domain (α/β), and a B-repeat region with a variable number (5 to 17) of nearly identical 128-aa G5 domains. (Adapted from reference [53]). (B) Proposed mechanism of action for AAP. The B-repeats will spontaneously cleave, which will trigger G5 domain polymerization and ultimately bacterial aggregation [38].

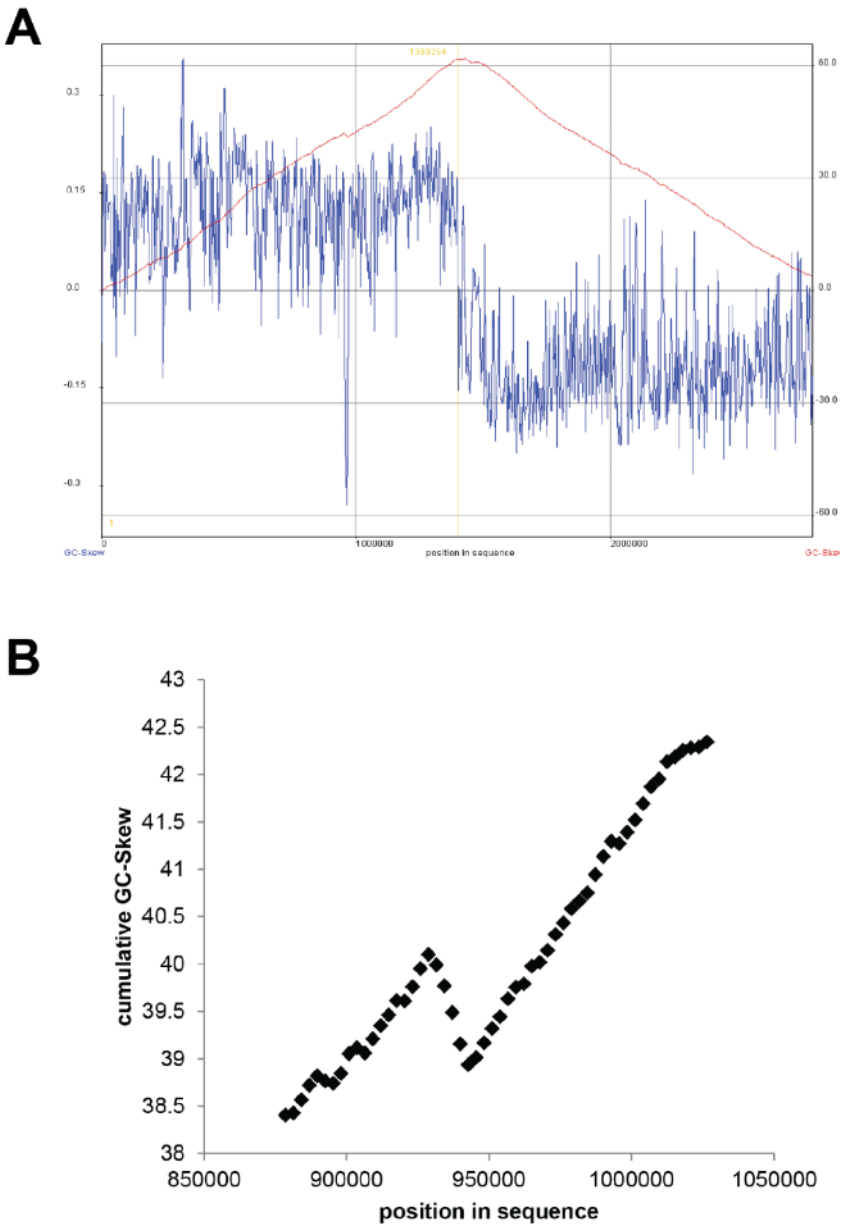

Supplementary Figure 6. Bovine CC8 strains shared a similar cumulative GC skew as the one presented in A. An inversion in the cumulative GC skew between c.a. 993 and 995 Kbp was always observed and correspond to the integration site of the incomplete prophage (B).

Chapter II

Intramolecular regulation of bacteriophage lysins explains complex multi-domain architecture and prevents untoward lysis of neighbouring bacterial cells

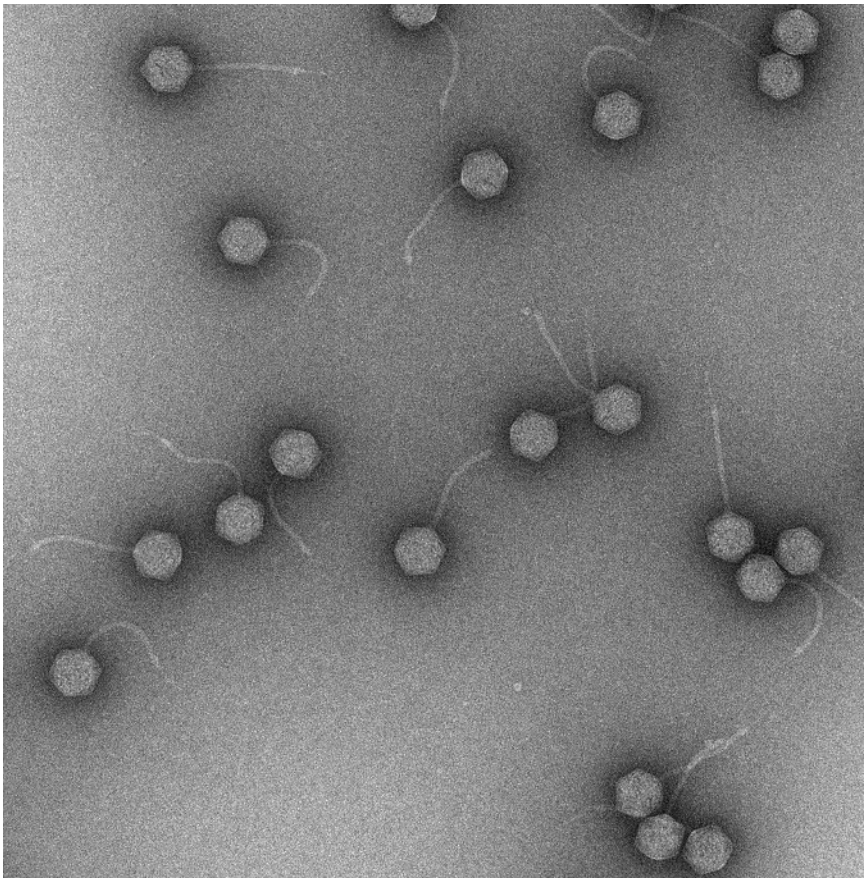

Siphoviridae. Negative staining. 2016. F. Oechslin

F. Oechslin did the experiments.

C. Menzi did the enzyme truncation characterization (host range and synergism), prepared the digestions for HPLC and LC-MS and did the ELISA.

Paul Majcherczyk ran the HPLC.

P. Varidel did the LC-MS analysis.

F. Oechslin and P. Moreillon wrote the paper.

S. Mitri and H. Brussow corrected the manuscript.

F. Oechslin conceived and supervised all the experiments.

General introduction.

Bacteriophages (phages) are bacterial viruses that can be found in extremely different environments [54] and are known to be the most diverse and abundant biological entities on earth [55]. They are currently classified in more than ten different families according to their morphology and nucleic acid composition [56]. Nevertheless, 95% of them belong to the order of *Caudovirales*, which is composed of tailed morphotypes with a double stranded linear DNA [56]. Since phages are obligate parasites that do not have an independent metabolism, they need to infect a bacterial host in order to replicate. It is during this infection process that phages, depending on their type, can follow a lysogenic or a lytic life cycle. In the lytic cycle, replication of phages is followed by the destruction of the host bacteria.

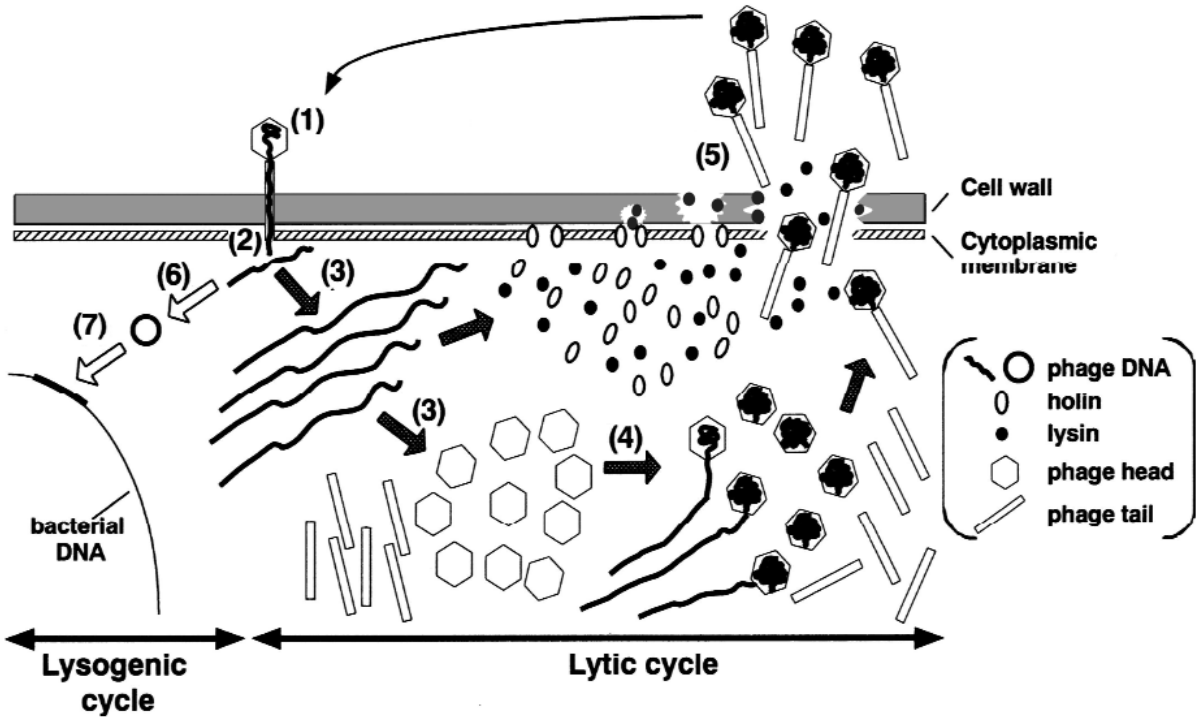

Figure 1. In the lytic cycle, phage replication pass through five main steps that are 1) the attachment of the phage to his host, 2) the injection of the viral DNA, 3) the hijacking of the cell molecular machinery

in order to replicate the DNA and synthesize structural components, 4) the assembly of the newly produced phages and 5) the release from the host by its lysis. In the lysogenic cycle, phage DNA is circularized after injection (6) and integrated into the host genome (7). Adapted from [57].

In the lysogenic cycle, the phage genome is first integrated into the host chromosome as a prophage and can stay integrated and replicates with the host chromosome until an induction event occurs. Events that induce prophage excision imply host cell damage, such UV light or chemicals, which are generally related to the bacterial SOS response.

Excised prophage genomes can then re-enter the lytic cycle, including DNA replication, protein synthesis and capsid assembly and eventually host cell lysis and release of the phage progeny. Bacterial lysis at the end of the replication cycle is due to the coordinated action of two phage proteins forming the holin/lysin system. In this two component system, holin is produced in order to form holes in the inner membrane so that the lysin, which is a peptidoglycan hydrolase enzyme, can attack the cell wall of the bacterial host and induce cell lysis [58].

It is only relatively recently that phage lysins were considered as potent antimicrobial agents and used to control gram-positive bacterial infection in different animal models [59, 60]. Since gram-positive bacteria are lacking an outer membrane (in contrast to their gram-negative counterparts), it is indeed possible to add lysins from the outside of the cell to disrupt the bacterial cell wall and kill the bacteria.

Gram-positive phage lysins usually have a modular structure, which includes one or more catalytic domains (CD) and cell wall binding domains (CBD) linked together by a short linker [61, 62]. Depending on which bonds of the bacterial peptidoglycan are hydrolysed, lysins can be categorized in four main groups including glucosaminidases,

muramidases, amidases and endopeptidases, respectively (see Figure 2). Interestingly, it was observed that different lysins sharing the same catalytic activities had higher homologies between their CDs than their CWBDs [63]. The CWBD domain can mediate high bacterial specificity and help the enzyme to get properly positioned in order to degrade its peptidoglycan substrate [64, 65]. This is specially the case for the Cpl-1 muramidase, which CWBD helps the orientation of the enzyme and confers a high specificity for *Streptococcus pneumoniae* via attachment of the CWBD to choline-containing teichoic acids in the peptidoglycan [62, 66].

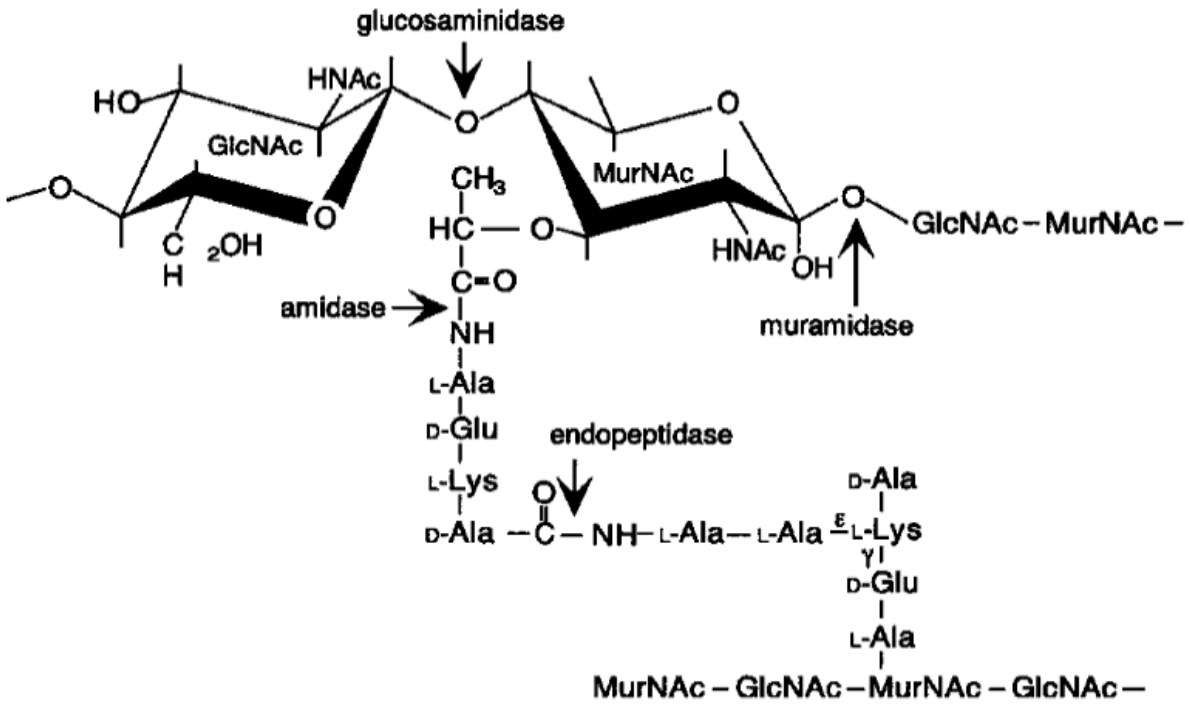

Figure 2. Lysins can be classified depending on the peptidoglycan subunits they hydrolyse. The muramidase (N-acetylmuramidases or lysozyme) and glucosaminidase (endo-β-N-acetylglucosaminidases) hydrolyze the glycosidic bonds of the glycan strand. The amidases (N-acetylmuramoyl-L-alanine amidases) are known to cleave the amide bond that link the MurNAc sugar

with the peptide strand and endopeptidases cleave inside the the peptide crosslink [67]. Adapted from [68].

Currently, a large number of phage lysins have been described for all major pathogens including *S. pneumoniae*, from which the Cpl-1 enzyme was isolated. Cpl-1 is one of the best-studied lysin since it was tested in different murine models and in combination with antibiotics and other lysins [69-74]. Other enzymes specific for streptococci include PlyC, B30, PlyGBS, LambdaSa1 and LambdaSa2, Ply30, PlySs2, LysSMP and PlySK1249 [68, 75-80]. The last one (PlySK1249), which is the purpose of the present chapter II, was isolated five years ago from a prophage carried by the bacterium *Streptococcus dysgalactiae* subsp. *equisimilis* SK1249. The lysin harboured a singular structure composed of a central binding domain (CWBD) surrounded by a N-terminal amidase domain and a C-terminal cysteine histidine-dependent amidohydrolase/peptidase (CHAP) domain [80]. The purified form of the enzyme was highly lytic both *in vitro* and also *in vivo* in a mouse sepsis model [80].

It is actually not uncommon for streptococci phages to have a modular architecture with more than one catalytic or binding domains. For example, this is the case for the B30 lysin that has two catalytic subunits, a CHAP domain with an endopeptidase activity and an acetylmuramidase domain (Acm) with a glycosidase activity [68]. Interestingly, inactivating mutations introduced in the CHAP domain demonstrated that CHAP was responsible for nearly all the lytic activity of the enzyme [81]. Similar observations were made with the PlyGBS lysin, which shares 99% identity with lysin B30 [82]. The LambdaSa2 and PlsS2 were also observed to have a similar structure

with two Cpl-7 binding domain in the central position and two flanking catalytic domains with one observed to be silent [77, 83].

Another example of even more complex architecture is the example of PlyC, which crystallographic analysis revealed an atypical multimeric structure. Indeed, the enzyme is composed of a single PlyCA catalytic subunits containing a CHAP domain with an amidase activity assembled with eight PlyCB molecules structured in an octameric ring having a CBD function [75] [65]. The two subunits were also observed to be transcribed from two distinct genes found in an operon like structure.

However, the purpose of multi-modularity is actually still not very clear since two or more domain organizations are dominant among gram-positive lysins, but usually not observed among gram-negative lysins, which lack the binding domain [84].

For instance, the benefit of a second catalytic domain is still open to debate since it is usually observed to be silent. Hence, it was hypothesized that it could act as a second binding domain or be on the way to get lost through evolution [85, 86]. Moreover, no clear consensus could emerge regarding the functional implication of the binding domain in either host specificity or as lysis helper, since different lysins were variously dependent on their CWBD for optimal activity [76, 81, 83, 87-91]. In addition, it was hypothesized by others that the CWBD could actually help to block diffusion of the lysin in order to prevent accidental lysis of neighbouring bacteria [92, 93]. Lysing neighbouring cells could result in abortion in sister bacteria carrying sibling prophages or destruction of phage-naive bacteria representing potential new preys.

Although never experimentally demonstrated, this hypothesis makes sense since biofilms are considered as the main form of bacterial life style in most of natural environments [94]. It is into this very dense environment that prophage genes were

also observed to be the most upregulated [95, 96]. As discussed in the first chapter of the present thesis, prophages contribute to bacterial genome diversification by introducing novel genes and also regulate host genes by acting as genetic switches as they can disrupt or restore gene expression during integration or excision. The prophage content of bacteria should probably not be seen as static situation, but rather as a more dynamic process with phages permanently escaping and reintegrating a subpopulation present in the biofilm. For this reasons, it is not impossible that post-lytic regulation mechanisms are existing in order to control and restrict diffusion of these highly lethal lytic enzymes.

It is already known that phage-induced bacterial lysis is a highly regulated event since it takes place only at the very late stage of phage infection. For this reason, a large and extended diversity of mechanisms impacting on endolysin activity can be observed for various phages at the transcriptional and posttranscriptional level. For example, in the case of the T4 phage it was shown that the transcription of the lytic genes started very early on, but that protein synthesis was delayed to the end of the replication cycle due to a hairpin structure adopted by the mRNA [97, 98]. Likewise, different regulation mechanisms exist at the posttranslational level, including regulation during translocation and inactivation of the lysin. Indeed, since the lysin has to pass through the plasma membrane, the timing can be controlled by oligomerization of the holin, which then permits passive diffusion of the lysin to the cell wall. Moreover, holin-independent regulation systems were also observed for in some phages, in which the lysin is translocated with the help of a N-terminal secretion signal sequence SAR (Signal-Arrested-Release) [99]. In addition, it was observed that the lysin has to lose its SAR sequence by proteolytic cleavage in the periplasmic space in order to become activated. Regulation by inactivation was also observed as some phages do export

they lysin in a holing-independent manner but still produce holins. In this case, the lysin remains inactive in the periplasmic space until depolarisation of the membrane occurs by the activity of the holin [100].

In the manuscript presented next (to be submitted for publication), we tried to clarify both the roles of the CDs and the CWBD in the recently described *S. dysgalactiae* phage lysin PlySK1249, as well as the mechanism(s) that regulate the enzyme activity at the level of the peptidoglycan cell wall.

In the first part, we tested different truncated versions of the PlySK1249 lysin – containing different active domains dissociated or linked together – against a panel of different gram-positive cocci. We could make three main observations regarding cell lysis:

- First the native enzyme was always more active that it's truncated versions.
- Second the amidase domain was more active in presence of the binding domain.
- Third the CHAP domain was not bacteriolytic *senso stricto* in bacterial cultures.

Although this third observation was similar to the silent domains described in the literature by others regarding multidomain lysins, a more detailed analysis of the macro and chemical structure of the cell wall revealed that CHAP was in fact active. Indeed, light and electron microscopy highlighted morphological changes of bacteria treated with CHAP alone, including a dechaining activity of the enzyme as well cell surface alterations with an irregular appearance. Moreover, we could observe that both amidase and CHAP domains synergized at lysing bacteria when mixed together in an equimolar concentration.

Importantly, all these observations could be confirmed at the molecular level using HPLC and LC-MS peptide sequencing. Although the amidase domain disconnects the glycan chains from the stem peptides, as expected, it could not resolve cross-linked stem peptides multimers to simpler structures. In sharp contrast, CHAP resolved cross-linked stem peptides but was unable to disconnect glycans from peptides. In addition, peptide sequencing of the degradation products revealed that the CHAP domain was able to hydrolyse the stem peptide multimers (from trimers to heptamers) down to dimers, but virtually never to monomers. These observations clearly explain why both domains can synergize and also why the CHAP domain does not directly lyse cells, since the glycan strands can still remain connected though dimer crosslinks.

In the second part we focused on the CWBD. In the context of this enzyme, the role of the CWBD was actually not to confer specificity regarding the bacterial host range, but rather to first position the enzyme for appropriate lysis, and then retain the lysin to the wall and wall debris in order to prevent its diffusion in the surrounding milieu. In other words, a dual lysis-promoting and lysis-preventing function with regard to its bacterial host and its bacterial neighbours, respectively.

Regarding the lysis-preventing function, we most interestingly observed that the lysin was subject to proteolytic cleavage by host proteases during the cell lysis process, which lead to two degradation products composed of an amidase-CWBD moiety and a CHAP moiety. Hydrolysis was observed to take place on both inter-domain linkers but was prevalent on the LysM-CHAP link in the presence of the peptidoglycan substrate. This led to an amidase-CWBD domain, which could digest the proper host wall, but could not diffuse because it remained attached to the wall debris (via the CWBD) and a CHAP domain, which was not bacteriolytic on its own even in the case of diffusion.

Taken together, we observed that both catalytic domains of the enzyme were active and acted coordinately with the CWBD to both ensure bacterial lysis of the host, thus helping the release of the phage progeny, and prevent further diffusion after host proteolytic cleavage, in order to restrict lysis to the lysing host bacterium and prevent collateral lytic damage of other cells.

Abstract

Lysins are peptidoglycan hydrolases produced at the end of the phage life cycle to lyse the host cell. However, this may also release lysins in the environment and detrimentally kill neighbouring cells carrying sibling prophages or potential new bacterial preys. This is particularly true for Gram-positive bacteria, which lack an outer-membrane protection. Here we show that the multi-domain architecture of Gram-positive *Streptococcus agalactiae* prophage lysin PlySK1249 prevents this phenomenon. PlySK1249 reunifies three functional domains, including two peptidoglycan-hydrolases – i.e. one amidase (Ami) and one endopeptidase (CHAP) – and one cell-wall binding domain (CWBD). Molecular dissection revealed that all three domains synergized for full bacterial lysis, in spite of the fact that CHAP was marginally active and CWBD only mediated binding of PlySK1249 to the wall. Moreover, while the CWBD helped position the lysin for optimal peptidoglycan digestion, also prevented its further diffusion by keeping it attached to wall debris after bacterial lysis. Finally, cell wall associated proteases promoted catalytic cleavage of PlySK1249 between Ami_CWBD and CHAP, thus inactivating the lytic Ami/CHAP synergism while retaining the Ami_CWBD moiety to wall debris. Thus, altogether the three domains acted coordinately to optimize bacterial lysis while curbing lysin diffusion and inactivating it after lysis completion. In addition, bacterial wall protease(s) contributed to restricting exuberant cell destruction by inactivating the lysin *in situ*.

Introduction

Phage lysins represent a fascinating family of peptidoglycan hydrolases that are indispensable for bacterial lysis and release of the phage progeny at the end of its replicating cycle [101]. They have gained recent interest in biomedical development as potential antibacterial agents [92, 102, 103]. The target of phage lysins is the bacterial peptidoglycan, an essential bacterial structure made of a complex meshwork of *N*-acetylglucosamine (GlcNAc) – *N*-acetylmuramic acid (MurNAc) glycan strands cross-linked by short stem peptides attached to MurNac residue (reviewed in [104, 105]). Phage lysins cut either between the sugars or peptide chains.

Lysins come in a variety of multi-modular forms that may have evolved in order to adapt to their bacterial hosts. They are usually composed of several functional domains including glucosaminidases, amidases and endopeptidases (referred to as catalytic domains or CDs) and cell wall-binding domains (referred to as CWBD), which are believed to help position the catalytic domains in the peptidoglycan [61]. However, several questions remain open regarding their function in the phage biology. For instance, what is the purpose of multi-modularity? What determines their bacterial specificity? How are they regulated in order to prevent accidental lysis of neighbouring bacteria, which could result in abortion in sister bacteria carrying sibling prophages or destruction of phage-naive bacteria representing potential new preys? This may be particularly relevant in Gram-positive bacteria, which lack an outer-membrane barrier and are thus more prone than their Gram-negative counterparts to lysin-induced lysis from outside. In this regard, there are indeed some structural differences between Gram-positive and Gram-negative phage lysins, which most of the time lack a CWBD domain [106].

In lysins from gram-positive bacteria the architecture and functions of CDs and CWBDs are quite variable. For instance, the well characterized staphylococcal lysins Lysk, Φ11 and MV-L, as well as the streptococcal lysins B30 and lSa2 contain two CDs and one CWBD [68, 77, 107-109]. However, when individually tested in truncated constructs only one of these CDs conferred bacterial lysis. This was exemplified by the Isa2 lysin, which possesses both an endopeptidase and a glucosaminidase domain, but where only the endopeptidase conferred bacterial lysis [86]. Similar observations were made with the unrelated streptococcal lysins B30 and PlyGBS, which are 99% identical, where bacterial lysis was solely due the amidase and not the glucosaminidase domain [81, 82]. Likewise, staphylococcal phage lysins LysK and Φ11 carry a lytic endopeptidase and a non-lytic amidase [87, 91, 110]. The reasons for conserving these non-lytic domains is currently unclear and hypotheses have been made regarding a possible loss through evolution or an implication in reinforcing cell wall binding.

CWBDs are thought important for addressing and positioning the CDs in the peptidoglycan [111-113], and conferring the lysin specificity to their target bacteria. CWBDs are commonly located at the N- or C-terminals of the lysins and rarely in the central region [64, 114]. However, CWBDs are not always necessary for bacterial lysis and deleting them even improved the lytic activity of some lysins, without a loss of specificity in the case of lysin B30 [76, 81, 83, 87-91]. Hence, CWBDs may have additional roles in the lysin physiology.

In this work we attempt to clarify the roles of the CDs and the CWBD in the recently described *Streptococcus dysgalactiae* phage lysin PlySK1249. This lysin is unusual in that its CWBD (called LysM for Lysin Motif) occupies a central position (see Figure 1A) and is bracketed by a predicted amidase domain at its N-terminal side and a predicted

“cysteine histidine-dependent amidohydrolase/peptidase” (CHAP) domain at its C-terminal side. Amidases (or *N*-acetylmuramoyl-L-alanine amidases) hydrolyze the amide bond between the *N*-acetylmuramoyl glycan moiety and the first L-Ala from the stem peptides, thus separating the glycan strands from the stem peptide network [115]. On the other hand, CHAP domains are primarily endopeptidases, sometimes with amidase activities [116]. Amidase and CHAP domains are often combined in bifunctional lysins [87, 117, 118].

We tested a variety of truncated PlySK1249 constructs and made several original observations regarding its structure-function relation and lysis regulation. First, in contrast to other reports [81, 82, 86, 87, 91, 110], we observed that the amidase and CHAP domains synergized for both lysing whole bacteria and digesting purified peptidoglycan to completion. This was the case even if the CHAP domain was observed to be “silent” regarding its lytic activity when overexpressed alone.

Second, the CWBD did not confer specificity of the lysin to peculiar bacterial species, as often believed, but rather retained the lysin to the wall and wall debris, simultaneously promoting lysis and preventing lysin diffusion and untoward lysis of neighbouring bacteria.

Third, while PlySK1249 was stable in buffer solution, it underwent proteolytic cleavage in the presence of bacteria and protein cell wall extract. Hydrolysis was observed to take place on both inter-domain linker but was prevalent on the LysM_CHAP link in presence of the substrate. This led to a degradation product composed of a lytic amidase_LysM part, which could possibly not diffuse because it remained attached to the wall debris (via the CWBD) and a CHAP domain, which was note bacteriolytic on its own even in the case of diffusion.

Thus, taken together, the two CDs and the CWBD of PlySK1249 act coordinately to first ensure bacterial lysis and then curb its activity and diffusion in order to restrict lysis to the lysing bacteria and prevent collateral lytic damage.

Methods

Cell culture and growth conditions. All bacterial strains used in this study are listed in Table 1. Gram-positive bacteria were grown at 37°C in Brain Heart Infusion (BHI, Becton Dickinson, New Jersey, USA) and plated on Mueller Hinton agar with 5% sheep blood (bioMérieux SA, Marcy l'Etoile, France). Broth cultures of streptococci and enterococci were grown without agitation. *Escherichia coli* were cultured at 37°C in Lysogeny Broth (LB) with agitation (220 rpm) or plated on Lysogeny Broth Agar (LA). The following compounds (at final concentrations) were added to the media when necessary: kanamycin sulfate (30 µg/ml), chloramphenicol (25 µg/ml for LA plates and 50 µg/ml for LB) or isopropyl β-D-1-thiogalactopyranoside (IPTG) (0.4 mM). Culture stocks were prepared from cells in the exponential growth phase in 20% glycerol (vol/vol) and stored at -80°C. All chemicals were reagent grade commercially available products.

Cloning and purifying of the different truncated version of the PlySK1249 enzyme. To clone truncated forms of the PlySk1249 lysin (Figure 1.A), the plasmid pPlySK124928a [80] was used as a template for PCR amplification using the specific primer pairs listed in Table 1 (Microsynth AG, Balgach, Switzerland). PCR products were digested using restriction enzymes NcoI and XhoI (Promega, Madison, WI, USA), and ligated into the expression vector pET28a. The different plasmids obtained, namely, pAmi^{28a}, pAmi_LysM^{28a}, pLysM_CHAP^{28a}, pLysM^{28a} (Supplementary Table 1), were transformed in One Shot BL21 (DE3)pLysS chemically competent *E. coli* cells (Life Technologies Europe B.V., Zug, Switzerland). Constructs were purified by affinity chromatography as described before [80] and loaded in NuPAGE 4-12% BisTris gels

(Invitrogen, Carlsbad, CA, USA), in order to assess their purity and correct molecular weight. All constructs were validated by DNA sequencing using universal T7 primers.

Assessment of lysin-induced bacterial lysis. Lysin-induced bacterial lysis was determined for the parent PlySK1249 lysin and its various truncated constructs by following the decrease in turbidity of a bacterial suspension as described in [80]. In order to assess a potential synergism between Ami_LysM and LysM_CHAP or Ami and LysM_CHAP, the two truncated enzymes were mixed together in different molar ratios ranging from 1:1 to 1:100. *In vitro* time-kill essays were performed as described in [80].

Light and Electron microscopy. *S. dysgalactiae* cells were incubated with the different lysin constructs at a concentration of 3.5 µM during 7 min for the PlySK1249 and Ami_LysM constructs and after 1 h for the control and the CHAP domain. For light microscopy, cells were immobilized on 1% agarose pads and phase contrast microscopy images were taken with a Plan-Apochromat 100X/1.45 oil Ph3 objective on an AxioImager M1 microscope (Zeiss). For EM microscopy, glutarldehyde was then added (25% final concentration), incubation for 1 h at RT and washed with PBS. The same procedure was applied for metaperiodate (1% final concentration, 15 min incubation) and osmium tetroxide plus hexacyanoferate (1% and 1.5%, respectively. 1 h incubation). Cells were then centrifuged and the pellets were spun down in microcentrifuge tubes containing melted agar. After solidification of the agar, pellets were embedded in epon for ultra-thin sections preparation as described [119]. Micrographs were taken with a transmission electron microscope FEI CM100 (FEI,

Eindhoven, the Netherlands) at an acceleration voltage of 80 kV with a TVIPS TemCam-F416 digital camera (TVIPS GmbH, Gauting, Germany).

Purification and digestion of peptidoglycan. Peptidoglycan of *S. dysgalactiae* SK1249 was purified as previously described [120]. Briefly, 10 ml of an ON culture was added to 1 l of fresh BHI medium. The cells were grown until an OD_{600nm} of 0.4-0.5 and then quickly chilled down in an ice bath for 5-10 min. The culture was centrifuged at 4°C and resuspended in PBS to reach a total volume of 40 ml. The bacterial suspension was poured dropwise into 40 ml of boiling SDS (8%) and boiled with agitation for 15 min to inactivate intrinsic autolytic enzymes. The cells were centrifuged at 20°C to avoid SDS precipitation, washed twice with NaCl 1M, and 5 times with dH_2O. After the final washing step, the bacteria were resuspended in 2 ml dH_2O and stored at -20°C ON. The next day, the cells were broken in the FastPrep (Thermo Savant FastPrep FP120 Homogenizer) 3 times for 45 sec and 6.5 m/sec with a cooling step of 5 min in between each agitation. The supernatant was transferred into a Falcon® tube and centrifuged for 5 min at 4°C and then again for 20 min at 4°C. The pellet was resuspended in 3 ml Tris (0.1 M), pH = 7.5 and 0.3 ml NaN_3 (0.5%). After the addition of 0.3 ml $MgSO_4$ (200 mM), 60 µl DNAse (500 µg/ml) and 60 µl RNAse (2500 µg/ml), the mixture was incubated for 2 h at 37°C with agitation and then ON after having added 0.3 ml $CaCl_2$ (100 mM) and 0.3 ml trypsin (100 µg/ml). For the last steps, SDS (1% final concentration) was added to the preparation, which was then heated for 15 min at 75°C to extract peptides from protease digestion. After centrifugation for 20 min at 20°C, the pellet was washed once with dH_2O, resuspended in 20 ml LiCl (8M) and incubated at 37°C with agitation for 15 min. The mixture was again centrifuged at 4°C for 20 min, resuspended in 20 ml EDTA (0.1 M) and incubated another time to remove

material bound by ionic interactions. At last, the bacterial peptidoglycan was re-centrifuged, washed twice and resuspended in 2 ml dH_2O. Aliquots of 1 ml were transferred into pre-weighed Eppendorf tubes and dried ON by rotary evaporation (UniEquip UNIVAPO 150 ECH). The dried bacterial peptidoglycan was then resuspended to reach a concentration of 10 mg/ml. For enzymatic digestion, 100 µl of the purified cell wall was mixed with 900 µl of the previously purified lysin constructs (3 µM). The mixture was incubated ON at 37°C with agitation. The next day, the solution was heated for 3 min at 100°C to inactivate the enzyme, centrifuged at 13'500 rpm for 10 min and the supernatant containing the solubilized walls was transferred into a new tube.

Biochemical analysis of peptidoglycan hydrolysis sites. Cell wall digestion were performed as described before. A modified Park-Johnson essay was used for reducing sugar analysis, and quantification of free amimo acids was done with a modified Ghuysen procedure with 1-fluoro-2.4-dinitrobenzene as described [121]. Undigested cell wall was used as a blank and calibration curves of glucose or L-Alanine were used for calculations. All experiments were performed in triplicate.

Analysis of the digested peptidoglycan using reverse phase (RP) HPLC. The digested peptidoglycan was put at -80°C for 5 min and then dried ON by rotary evaporation. After the addition of 0.5 ml acetone, the tube was sonicated to re-suspend the pellet and 1 ml of acetone was added to remove any contaminating endotoxin. The tube was left at room temperature (RT) for 30 min and was then centrifuged for 10 min. The supernatant was decanted and again dried by rotary evaporation for 10 min. Two-

hundred µl of dH_2O was added, the preparation was sonicated and put 5 min at -80°C and was then dried by rotary evaporation for 2 hours. The quantity of a solution (25% 2-propanol, 25% acetonitrile, 50% dH_2O and 10% TFA) necessary to obtain a final concentration of about 2 mg/ml was added to the sample in order to separate the glycan chains from the peptides by differential precipitation. The tube was vortexed, sonicated and put on ice for 15 min. After centrifugation at 13'500 rpm for 15 min at 4°C, the supernatant, containing the stem peptides and peptide bridges, was transferred into a new tube and frozen at -80°C until further analysis. The frozen peptides were dried by rotary evaporation ON and resuspended in 500 µl dH_2O. To separate the peptides, a HPLC system (Hitachi Instruments, Ichige, Hitachinaka, Japan) consisting of a L-7200 autosampler, a L-7100 gradient pump, and a L-7400 UV detector, was used as described previously [120]. Aliquots of 100 µl were injected into a C18 reverse phase column (SuperPac Sephasil C18, 5 µm, 4 x 250-mm column, Amersham Pharmacia Biotech), which temperature was maintained at 25°C using a pelcooler (Lab-Source, Reinach, Switzerland). A linear gradient of 0-15% acetonitrile in 0.1% of trifluoroacetic acid at a flow rate of 0.5 ml/min over 100 min allowed the separation of the peptides, which were detected at 210 nm. The results were analysed with the D-7000 HPLC System Manager program (Hitachi).

Mass spectrometry analyses of digested peptidoglycan. Cell wall digestion was performed as described before. At the end of digestion, samples were boiled at 100°C to stop enzymatic reaction, filtered through a 5000 MW cut-off column (REF) and desalted using C18 cartridge (REF). Peptidoglycan fragments were eluted with an 80% MeCN + 0.1% TFA solution and dried with a SpeedVac, before being redissolved in a loading buffer (2% MeCN + 0.1% TFA). Samples were injected on a Dionex RSLC

3000 nanoHPLC system (Dionex, Sunnyvale, CA, USA) interfaced via a nanospray source to a high-resolution mass spectrometer QExactive Plus (Thermo Fisher, Bremen, Germany). Peptidoglycan fragments were loaded onto a trapping microcolumn Acclaim PepMap100 C18 (20 mm x 100 µm ID, 5 µm, Dionex) before separation on a C18 reversed-phase analytical nanocolumn at a flowrate of 0.25 µl/min.Q-Exactive Plus instrument was interfaced with an Easy Spray C18 PepMap nanocolumn (50cm x 75µm ID, 2µm, 100Å, Dionex) using a 37 min gradient from 4 to 76 % acetonitrile in 0.1 % formic acid for separation (total time: 65min). Full MS survey scans were performed at 70,000 resolution. In data-dependent acquisition controlled by Xcalibur software 3.1 (Thermo Fisher), the 10 most intense multiply charged precursor ions detected in the full MS survey scan (250-2000 m/z window) were selected for higher energy collision-induced dissociation (HCD, normalized collision energy NCE=27 %) and analysis in the orbitrap at 35’000 resolution. The window for precursor isolation was of 1.5 m/z units around the precursor and selected fragments were excluded for 10s from further analysis. MS raw files were processed with PEAKS software (version 8.0, Bioinformatics Solutions Inc., Waterloo, Canada) for peptide identification by de novo sequencing and database search. The set of *Streptococcus dysgalactiae* subsp. *equisimilis* SK1249 proteome sequences downloaded from UniProt database (February 2016 version, 2’309 sequences) was used for database search of sample contamination by proteins from *S. dysgalactiae*, while peptidoglycan peptides were identified by de novo sequencing. Database search and de novo sequencing parameters were: no enzyme used as the enzyme definition, N-terminal acetylation of protein and oxidation of methionine as variable modifications, parent ion tolerance of 10 ppm and a fragment ion mass tolerance of 0.02 Da.

Enzyme-linked Immunosorbent Assay (ELISA). The adherence of lysin constructs to bacterial cells was assessed by ELISA. Cultures of *S. dysgalactiae* SK1249 were grown to an OD_{600nm} of 0.5-0.6, washed once by centrifugation in PBS and resuspended in the same buffer. The suspensions were diluted tenfold in order to obtain approximately 10^8 bacterial cells per ml. Two-hundred microliters of the bacterial suspensions were adsorbed to the wells of a 96-well plates (Nunc™) and the plates were stored ON at 4°C. Controls were performed by adsorbing the lysin constructs in binding buffer at different concentrations. The wells were washed 3 times with PBS and blocked with 200 µl of BSA-PBS (3%) for 2 h at RT. Plates were further washed 3 times with PBS before 200 µl of various concentrations of the lysin constructs (diluted in PBS) were added to the wells. Plates were then incubated on ice for 2 h. Unbound lysins were removed by washing with PBS and plates were incubated with primary 6X-His Tag antibodies diluted 1:1000 in BSA-PBS 3% (100 µl per well) for 1 h on ice. The wells were washed with PBS and plates were incubated with polyclonal goat anti-rabbit immunoglobulin/HRP diluted 1:2000 in BSA-PBS (3%) (100 µl per well) for 1 h on ice. The plates were then washed 6 times with PBS before 100 µl of substrate (TMB substrate kit, Thermo Scientific, Pierce Biotechnology, IL, USA) were added to each well. The reaction was stopped after 15 min by the addition of 100 µl of H_2SO_4 and the signal was detected with a microplate reader at 450 nm (Tecan, Microplate Reader, Infinite 200 PRO, Männedorf, Switzerland).

Lysin diffusion assay. This assay was designed to assess the implication of the CWBD in the diffusion of the lysins through bacteria embedded in soft agar. First, ON cultures of *S. dysgalactiae* were washed by centrifugation (in saline) and resuspended in 0.25 vol of PBS. Granulated agar (7.5 g/L) was added to the cell suspensions and

autoclaved 15 min at 120°C. 1 ml of solution was finally poured in 6 well plates that were stored at 4°C. For the assay, 4 mm diameter wells were punched in the center of the agar surfaces and 10 ul of enzyme at different concentrations were added into the pits. Diffusion was assessed by measure the diameter of the lysis halo formed after ON incubation at 37°C.

PlySk1249 proteolysis characterization. Cell wall protein extract was prepare as described elsewhere [34]. The native enzyme and its different truncated version (40 µM) were then digested ON by mixing them with half of the extract. The native enzyme and its different truncated version (40 µM) were also digested ON or for different time point by adding trypsin at 1 µM/ml. If required, purified cell wall was added to the reaction at a final concentration of 100 µg/ml. Reaction were stopped by incubating the mix with loading buffer and beta-mercaptoethanol during 15 min at 80°C. The reaction products were loaded on a NuPAGE 4-12% BisTris gel. Bands of interest were cut from the gel and amino acid sequence was identified by nanoLC-MS/MS at the at the protein analysis facility of the University of Lausanne (PAF, Center for Integrative genomic, University of Lausanne, Switzerland). Western blotting was performed as described before [35] and blots were incubated 1 h with a 1:1000 dilution of 6X-His Tag rabbit antibody (Thermo Fisher Scientific, Massachusetts, USA) following by a 1 h incubation with a 1:3000 dilution of peroxidase-conjugated goat anti-rabbit secondary antibody (Thermo Fisher Scientific). Bands were detected using ECL Western blotting detection reagent (Amersham Bioscience. Piscataway, NJ).

For fractionation of the cell wall protein extract, ammonium sulphate was used at different concentration ranging from 15% to 100%. For each fractionation steps, ammonium sulphate that was finely grinded was directly added to 10ml of cell wall

extract and let steered for 15 min at 4°C. The protein fractions were then collected using 4000 rpm centrifugation for 30 min. Pellets were re-suspended in 100 µl of PBS and mixed with 100 µl of the LysM_CHAP construct for ON incubation. Proteolytic activity of the different fraction was assessed by western blotting as described before. A second fractionation step was done by loading a 55% to 80% ammonium sulfate fraction on a size exclusion column (Superdex® 200 Increase 10/300 GL, GE Healthcare, Little Chalfont, United Kingdom) equilibrated with PBS. The protein content was then eluted in 0.5-ml fractions with 1 column volume of the same buffer. Fraction were tested for proteolytic activity using the LysM_CHAP construct as described before.

Results

Molecular dissection of the phage lysin PlySK1249. To assess the specific role of each of the predicted domains of PlySK1249, different truncated forms of the enzyme were cloned in *E. coli*, overexpressed and purified via 6X-His Tag affinity (Figure 1.A and 1.B). In this series, the amidase domain (Ami) could be overexpressed alone or in conjunction with the LysM CWBD, generating Ami_LysM, whereas the CHAP domain could never be obtained alone and needed the continuity with LysM to be produced (Figure 1.A). Therefore, CHAP could not be tested alone. All the other domain combinations were sucessfully produced. The puritiy and correct molecular weight following expression and affinity purification was verified on 4-12% BisTris gels (Figure 1.B). Bands were present at the expected molecular weights (~54 kDa for PlySK1249, ~19 kDA for Ami, ~37 kDA for Ami_LysM, ~26 kDA for LysM_CHAP and ~13 kDa for the CWBD LysM).

Lytic effect on whole bacterial cells. The relative contribution of the two CDs and the CWBD to bacterial lysis was compared to that of the parent enzyme. The constructs were first tested against an array of different Gram-positive bacteria (Figure 1.C). The decrease in turbidity of bacterial suspensions was measured after 30 min using equimolar concentrations (1 µM) of each construct. The parent enzyme had greater lytic activity against *Streptococcus* spp. than against more distantly related species such as enterococci. Moreover, the truncated forms were always less lytic than the parent enzyme and demonstrated a progressive decrease in lysis from Ami_LysM to Ami, followed by LysM_CHAP, which was not lytic at all even after 2 h of incubation (results not shown). Similar results were observed with purified cell wall (see Supplementary Figure 1).

We further tested possible synergistic effects between the Amidase and CHAP domains when applied separately or together on *S. dysgalactiae* cultures. Figure 1.D confirms the decrease in intrinsic lytic activity of the different subdomains observed in Figure 1 C. While the parent lysin inflicted a rapid 50% drop in turbidity in 5 minutes, Ami_LysM showed intermediate lysis (50% turbidity drop in 1 h) and LysM_CHAP was not lytic at all. However, adding equimolar amounts of non-lytic LysM_CHAP to Ami_LysM increased lysis substantially and adding 100 times more LysM_CHAP restored lysis almost completely after 60 minutes compared to Ami_LysM alone. In addition, these results correlated with a parallel drop in viable counts as depicted in Figure 1.E. Thus, although CHAP had no intrinsic lytic activity, it clearly contributed to cell lysis by Ami_LysM to mimic the parent enzyme. This was also corroborated by combining LysM_CHAP with the Ami construct (Supplementary Figure 2).

A closer look at LysM_CHAP effects by optical and electron microscopy also revealed more subtle non-lytic effects (Figure 2). First, adding LysM_CHAP to *S. dysgalactiae* cultures composed of 90% chains of 7 to 37 cells resulted in chain disruption after 1h (60% of cells were composed of 2 subunits) (Figure 2.A). Second, light and EM pictures of cells treated with LysM_CHAP revealed cell swelling and surface alteration, without genuine lysis (Figure 2.B). Thus, although non-lytic, LysM_CHAP did have a sub-lytic effect resulting in morphological alterations.

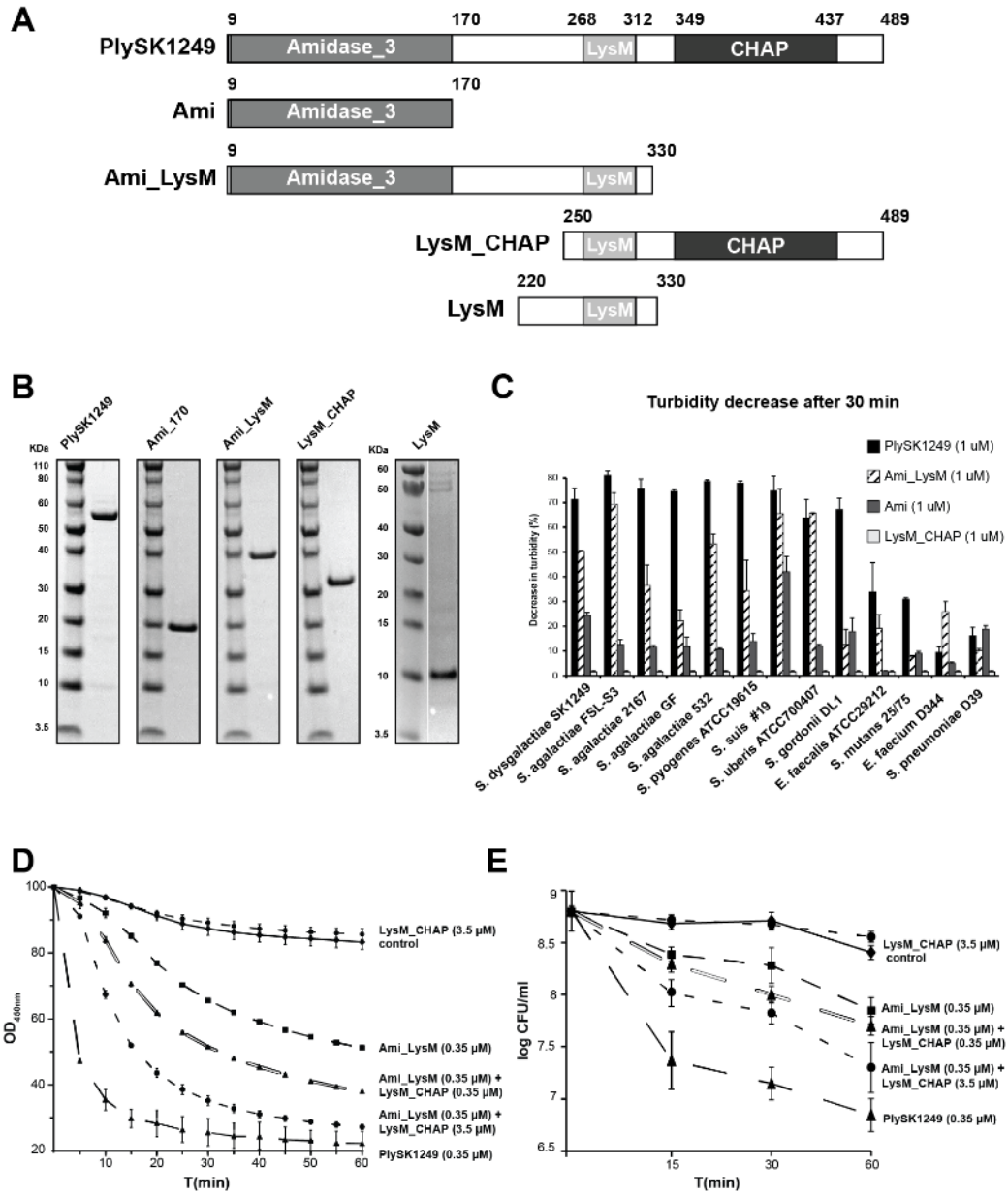

Figure 1. Lytic activity characterization of the PlySK1249 lysin and its different truncated forms.

A) Parent PlySK1249 (full enzyme, aa 1-489); Ami (N-terminal amidase, aa 1-170); Ami_LysM (N-terminal amidase + LysM, aa 1-330); LysM_CHAP (LysM + C-terminal CHAP domain, aa 250-489); LysM (central CWBD, aa 220-330). B) SDS-PAGE gel showing PlySK1249 and its different truncated constructions. The purified lysin constructions were loaded (2 mg/ml) on NuPAGE 4-12% BisTris and stained with Coomassie blue. Molecular mass was determined with a pre-stained protein standard. C) Cells of different bacterial species in the exponential growth phase were exposed to 1 µM of parent PlySK149 or its different truncated forms. Decrease in cultures' turbidity was measured at 600 nm after

30 min. No decrease in turbidity was observed in the absence of enzyme (not shown) or in the presence of LysM_CHAP. D) *S. dysgalactiae* cells in the exponential growth were also exposed to 1 µM of Ami_LysM or LysM_CHAP constructs alone or in combination the decrease in turbidity (at 600 nm) was followed over for 1 h. E) Viable counts in experiment D) were assessed by plating serial dilutions on nutrient agar. The experiments were repeated twice in triplicate and means ± standard deviations are shown.

Hydrolytic effect on purified cell walls. We first determined the glycosidase or peptidase nature of the PlySK1249 enzyme on purified *S. dysgalactiae* cell wall (see Supplementary Table 2). As predicted by bioinformatic analysis, no glycosidase activity was revealed by the Park-Johnson assay run with either the parent enzyme or its different constructs. In contrast, glycosidase activity was indeed present in the control experiment with the muramidase mutanolysin.

On the other hand, amidase or endopeptidase activities were detected in all the constructs by measuring concentrations of free amino groups after peptidoglycan hydrolysis using a modified Ghuysen assay. Although control mutanolysin produced a low level of free amino groups (around 0.1 mM), the PlySK1249 and its different catalytic domains produced 50 to 100 times more (between 5.7 and 11.4 mM). Thus, PlySK1249 carried purely amidase or peptidase activities, including when its non-bacteriolytic CHAP domain was used alone (see Supplementary Table 2).

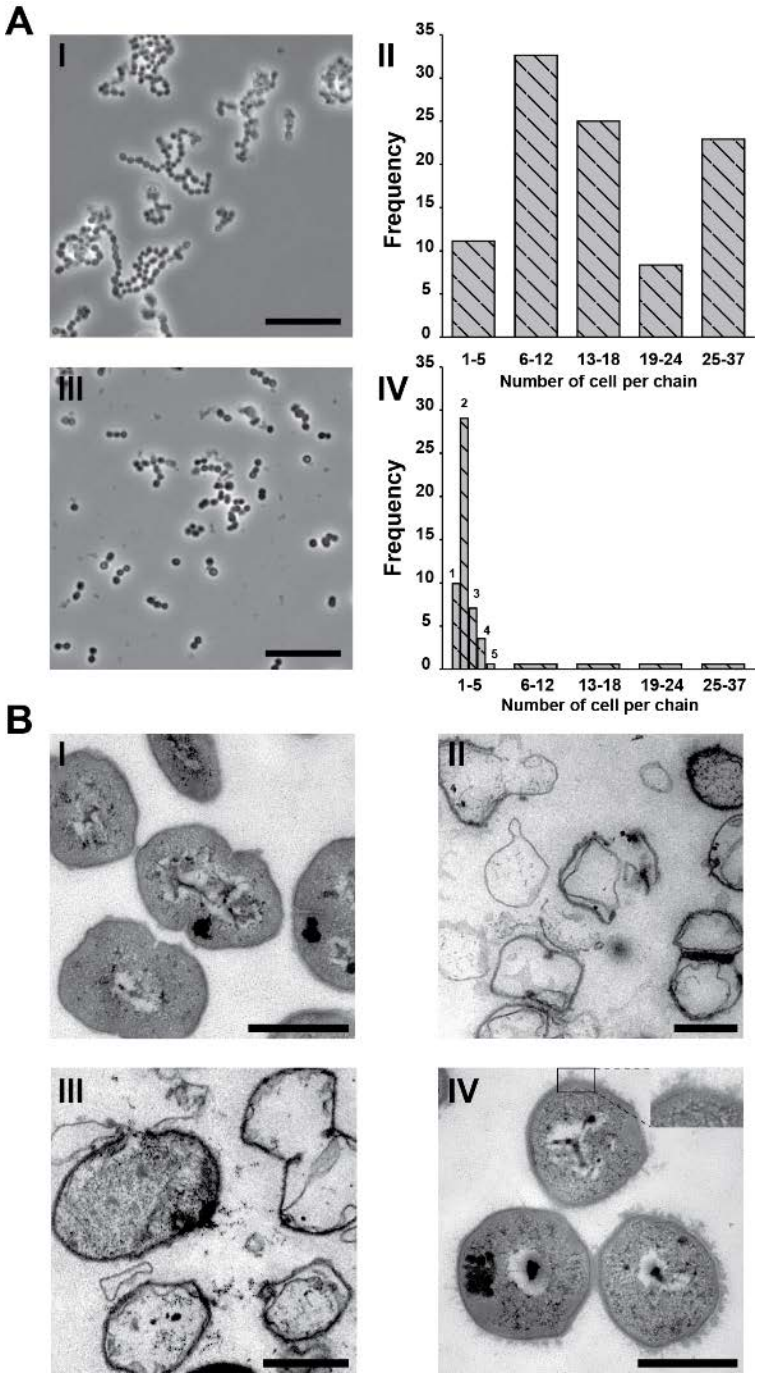

Figure 2. Morphological aspect of cells lysed by the PlySK1249 lysin and its different truncated forms. A) *S. dysgalactiae* in the exponential growth phase were observed after one hour using phosphate buffer as a control (A.I) or LysM_CHAP at a final concentration of 3.5 µM (A.III). Although the CHAP domain did not impact directly on cell lysis, an effect on chain disruption was observed. The control population was composed at 90% of chains of 7 to 37 cells for the control (144 cells observed in total, A.II) compared to the 60% of chains composed of two cells for the LysM_CHAP treatment (1044

cells observed in total, A.VI). B) Transmission electron microscopy of *S. dysgalactiae* cells treated with the native PlySK1249 lysin or its different truncated versions**.** *S. dysgalactiae* cells in the exponential growth phase were treated with (B.I) phosphate buffer for 1 h as a control, (B.II) Plysk1249 for 15 min, (B.III) Ami_LysM for 15 min, or (B.IV) LysM_CHAP for 1 h. Cells were then post-fixed using glutaraldehyde and embedded in epoxy for ultrathin sectioning. Scale bar represent 500 nm. The inset in figure (B.IV) highlights the non-lytic wall nibbling by the CHAP endopeptidase.

Dissection of the amidase and endopeptidase activities. To discriminate between the activities of the Ami and CHAP domains, purified wall-peptidoglycan was digested with each of the constructs and the released peptides were fractionated by RP-HPLC, before structural analysis by LC-MS (see next section). If amidase activity was present, glycan chains are expected to be cleaved from the peptides, which could be analysed by RP-HPLC. If only endopeptidase activity was present, the peptides are expected to remain attached to the glycan part and be lost during the step of sequential precipitation (see Methods section and Figure 3.A). In addition, a strong correlation between peak retention times and the chemical structure of the muropetides exists which can give information on their structure; low molecular weight monomeric muropeptide tend to elute first and high molecular weight muropetide like trimers to pentamers elute last [122].

After digestion with the parent enzyme, which contains both amidase and peptidase (CHAP) predicted domains, the released peptides revealed two major peaks with relatively short retention times (ca. 35 and 40 min, Figure 3.B). This presumably represented simple stem peptides, such as monomers and dimers, resulting from a dual amidase and endopeptidase peptidoglycan digestion.

After digestion with Ami or Ami_LysM alone, the two major peaks became marginal and were replaced by an array of smaller peaks appearing later (ca. 55 min, Figure

3.C and 3.D). Because of their longer retention time, they were likely to represent peptides of higher complexities resulting from pure amidase digestion, which disconnects the glycans without further fragmenting stem peptide polymers. Of note, the identical profiles obtained for Ami and Ami_LysM also tend to invalidate the hypothesis that the CWBD could be directly implicated in the hydrolytic activity of the enzyme.

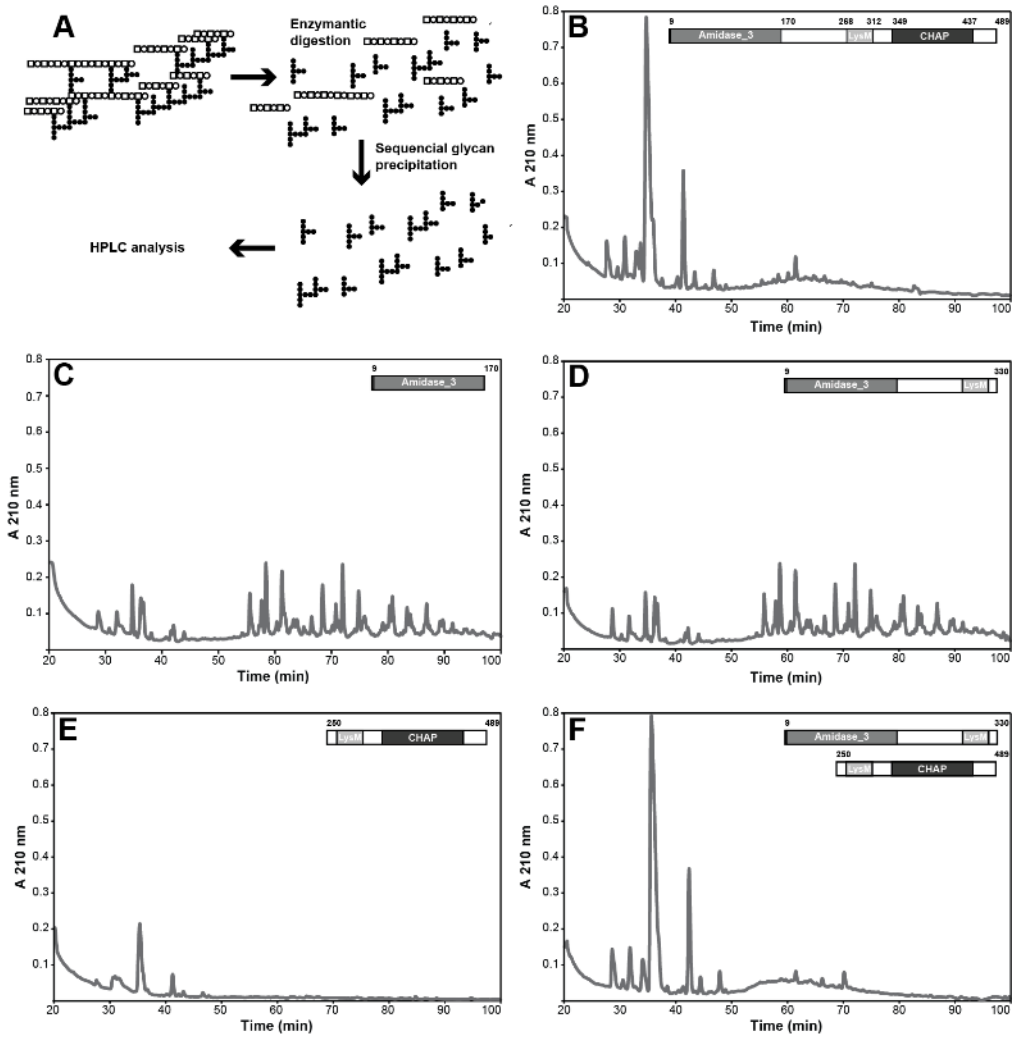

Figure 3. RP-HPLC chromatogram of *S. dysgalactiae* peptidoglycan digested with PlySK1249 or its truncated catalytic domains. A) Purified wall-peptidoglycan was digested ON and glycans were sequentially precipitated before chromatography on a C18 Sephasil column. Equimolar concentrations

(3.5 µM) of B) PlySK1249, C) Ami, D) Ami_LysM, E) LysM_CHAP and F) both Ami_LysM and LysM_CHAP were used and analyses were repeated three times with the same results.

After digestion with LysM_CHAP alone, no peptide peaks appeared in the chromatogram (Figure 3.E). According to the positive result of the Ghuysen test that clearly demonstrate peptidase activity for the CHAP domain (see Supplementary Table 2), the absence of peaks can be attributed to an endopeptidase. Indeed, the hydrolysis of the peptide cross bridge resulted in peptides that are still attached to the glycan fraction, which is lost during the sequential glycan precipitation. In addition, the synergism observed with cell lysis when Ami_LysM and LysM_CHAP were mixed in equimolar concentrations was also confirmed on purified cell wall with digestion patterns similar to the native enzyme (Figure 3.B and 3.F). Thus, even though LysM_CHAP was not able to solubilize the cell wall on its own, it did substantially contribute to complete digestion, most likely by trimming the peptide polymers generated by Ami_LysM, just as it potentiated the lytic activity of Ami_LysM in bacterial cell lysis assays (see Figure 1.D).

LC-MS analysis of peptide fragments. The endopeptidase hydrolytic activity of the CHAP domain could be demonstrated, but it still not explained why the domain was not directly lytic on its own since many lysin with endopeptidase activity are known to lyse bacteria efficiently. To this end, we further characterized the structures and hydrolysis sites of the peptides generated by cell wall digestion with either the parent enzyme or the Ami-LysM construct using LC-MS (Figure 4). For better comparisons, samples were analysed in the same injection batch and with a smooth elution gradient to separate potential isobaric precursors. The presence of precursor masses

containing the stem peptide motif AQKAAA and polymers of it was then assessed in both samples. *De novo* peptide sequencing of the observed masses allowed deducing their structures.

Potential monomers, dimers, trimers, quadrimers and heptamers were detected, but with great quantitative variability between the parent enzyme and its Ami_LysM construct (Figure 4.A and 4.B and Supplementary Figure 3). Indeed, digestion with the bifunctional parent lysin surprisingly not resulted in the production of monomers (4.8%) but principally in dimers (90.2%). In comparison, digestion with Ami_LysM generated an array of more complex peptides dominated by trimers and tetramers (48.3% and 34.3%, respectively), with a minority of dimers and heptamers (11.5% and 5.6%, respectively).

Taken together, these results suggest a N-acetylmuramoyl-L-alanine amidase activity for the Amidase domain and a L-Ala-D-Ala endopeptidase activity for the CHAP domain (Figure 4.C). More importantly, the PlySK1249 lysin was not observed to produce monomer peptide but mostly dimer, which signifies that the CHAP domain cannot resolve dimeric structure but rather more complex ones like trimers to heptamers. This also explains why the CHAP domain is not directly lytic, since the glycan strands can still remain connected though dimer crosslinks, which is sufficient maintain a polymer structure and prevent bacterial lysis.

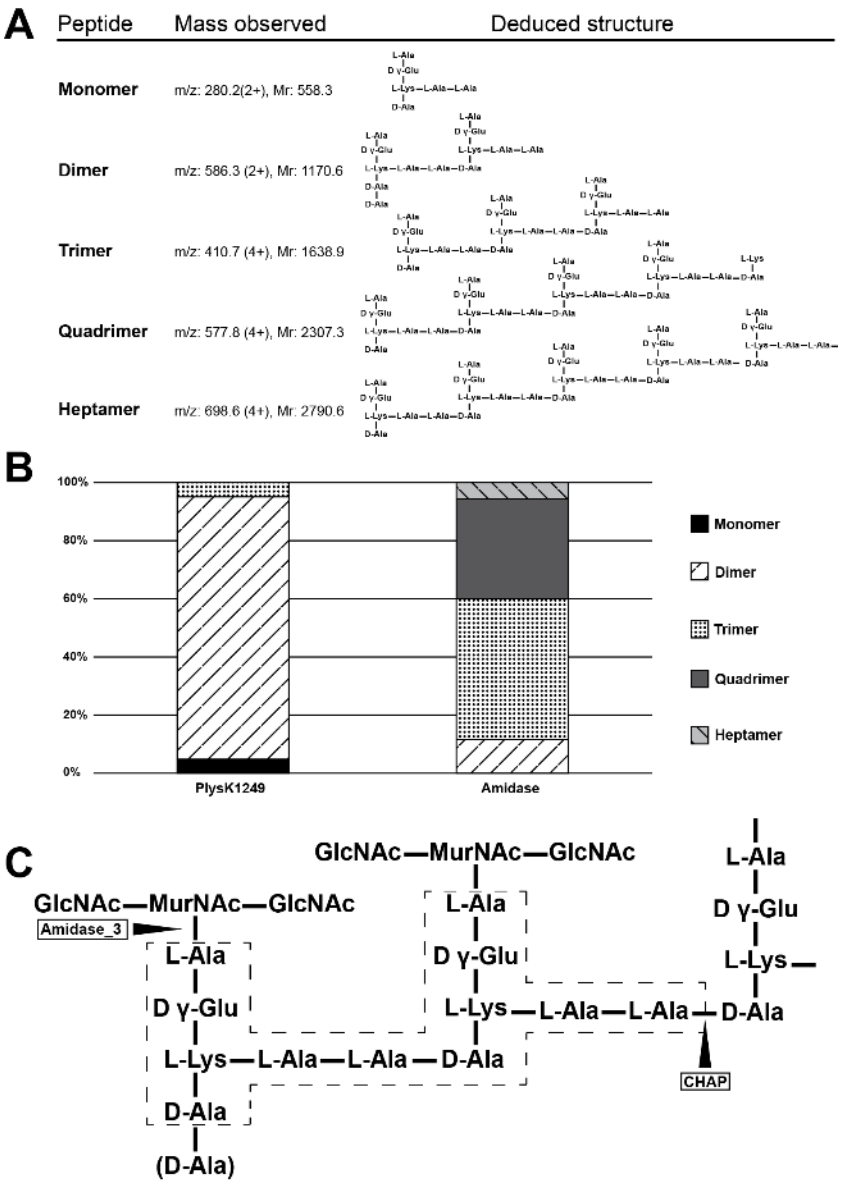

Figure 4. LC-MS analysis of *S. dysgalactiae* wall-peptidoglycan digested with PlysSK1249 or Ami_LysM. A) The digestion products of the native enzyme and its truncated Ami domain were analysed by LC-MS after a 5 kDa filtration. Precursor masses corresponding to dimer, trimer, quadrimer and heptamer of the AAAQKA monomer block were detected. All of them, at the exception of the heptamers, which were only present in the amidase digestion, were detected in both samples. Polymer structures could be deduced from masses after de novo peptide sequencing. B) Relative abundance of the different polymers observed in the native enzyme and amidase domain digestion. C) Representation of *S. dysgalactiae* peptidoglycan according to the masses and sequences observed. Arrows indicate the cleavage sites for the respective catalytic domains of the enzyme. The dotted line framed area corresponds to the dimer block.

Role of the LysM CWBD. Many lysins carry CWBDs, which are believed to position the CDs in the cell wall and to determine the enzymes' strain specificity. To investigate the contribution of LysM to the binding of PlySK1249 to bacterial cells, an ELISA was performed with its different constructs using the C-terminal 6X-His Tag of the constructs as an epitope.

The binding capacities of the parent enzyme and the truncated constructs were concentration dependent (Figure 5A and Supplementary Figure 4). Moreover, comparing binding-affinities of Ami_LysM and Ami indicated that the presence of LysM conferred greater binding capacity than amidase catalytic site alone thus confirming the assumption that CWBDs are important for cell binding.

Nonetheless, further measurements of the Ami and LysM binding affinities indicated that the amidase domain alone also had intrinsic binding capacities. Indeed, LysM was less prone to bind bacterial cells on its own (Figure 5.B). Moreover, when tested on different bacterial strains, LysM alone displayed a monotonous low level of binding, whereas Ami showed greater binding as well as strain specificity. Hence, Ami and LysM cooperate for cell binding, Ami ensuring strain specificity and LysM increasing overall binding but only in the presence of Ami.

Finally, the binding capacity of the LysM_CHAP was 1000 time lower than that of Ami_LysM (Supplementary Figure 4B), reinforcing the Ami and LysM functional relationship.

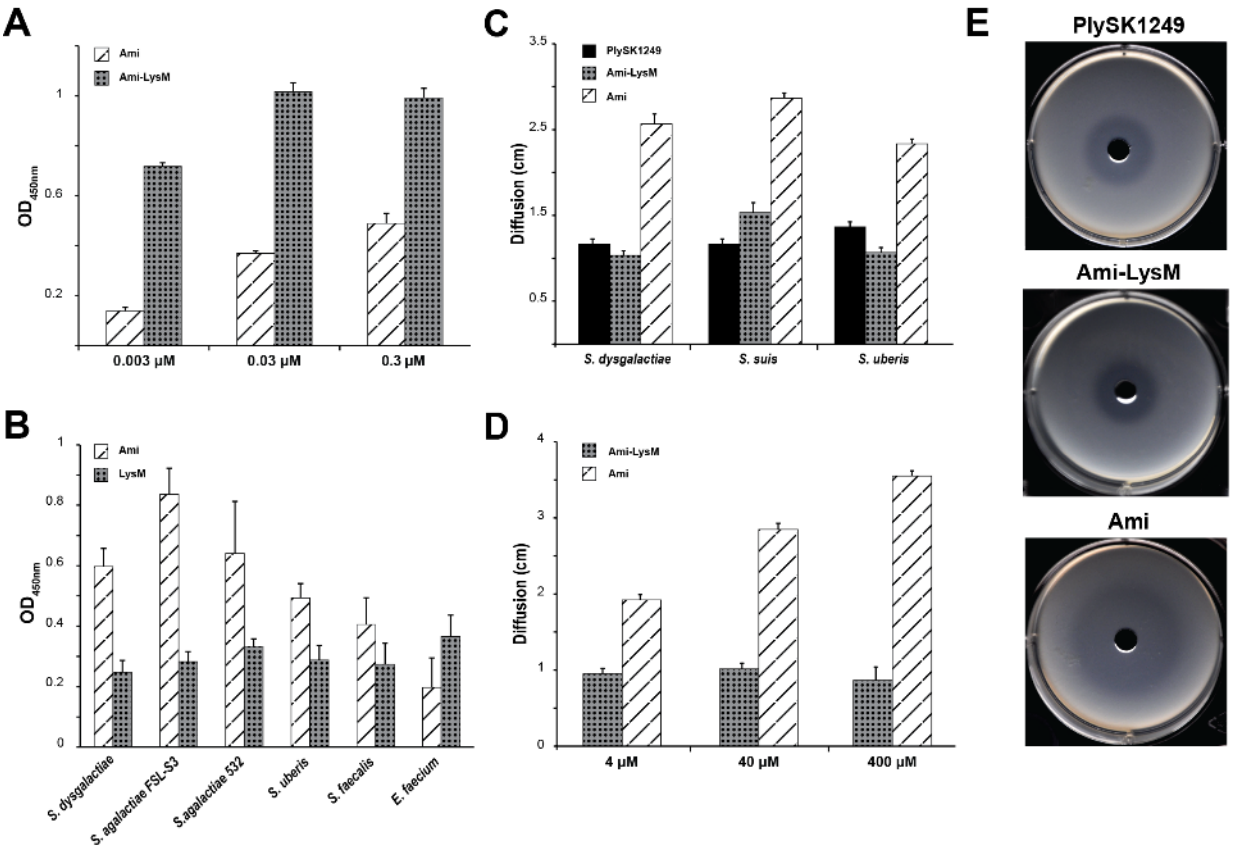

Figure 5. Cell binding capacity and diffusion of PlySK1249 and its amidase and CWBD domains.

A) Bacterial cells in the exponential growth phase were diluted to 10^8 cells per ml, adsorbed to a 96-well plate and exposed to different concentrations of Ami or Ami_LysM. The capacity of the enzyme to bind to coated-wells was assessed by adding an anti-His antibody that was coupled to peroxidase. The signal was read at 450 nm and the control measure was performed on adsorbed bacteria without the addition of enzyme. B) Different streptococcal species were used in the same way to test the affinity of either the Ami or LysM domains at 3 µM. C) Diffusion of the amidase domain in bacteria embedded in agar compared to the Ami_LysM construct and the native enzyme using a concentration of 40 µM and different streptococcal species. D) Diffusion of the Ami and Ami_LysM constructs regarding different concentration. E) Example of diffusion halos observed with *S. dysgalactiae* at 40 µM. All experiment was repeated three times. Means ± standard deviations are shown.

Interference of cell binding with extracellular spread of lysins. Although LysM increased wall binding and enhanced bacterial lysis, the cell wall-binding property does not exclude other functions, such as lysis regulation. In the following experiments, we tested the possibility that the binding domain could prevent the diffusion of the enzyme,, as previously suggested [92, 93], possibly to protect neighbouring cells from "lysis-from-the-outside" and preserve already infected cells from prophage abortion, or not yet-infected cells from new rounds of phage infection. To test this hypothesis, we measured the diffusion of the amidase domain (Ami) with and without the LysM CWBD across bacteria packed in soft agar. Because of the lytic activity of the amidase domain, it was possible to quantify diffusion by measuring the diameter of the clear halo produced by bacterial lysis (Figure 5.C to 5.E). Figure 5.C shows that the presence of the LysM CWBD clearly prevented diffusion of the Ami-induced lysis in agar containing susceptible strains (diameter decrease 2.5 cm to c.a. 1cm) compared to the Ami alone. Moreover, the lower diffusion of Ami_LysM was similar to that of the parent enzyme, indicating that the phenomenon was valid for the natural version of the lysin as well, and not related to the protein size. In the same vein, Figure 5.D shows that diffusion of the Ami domain was concentration dependent, whereas the presence of LysM prevented diffusion over a >100 times concentration range (Figure 6.D). Thus, the CWBD strongly prevented diffusion of the enzyme and potentially protected surrounding bacteria.

Proteolytic cleavage of PlySK1249 in the presence of cell wall protein extract and trypsin. In addition to hampering enzyme diffusion via bacterial wall binding, the enzyme was also observed to be degraded when incubated ON with cell wall protein extract (Figure 6.AI). Due to the large amount of proteins in the protein cell wall extract,

visualization of the degradation products was not directly possible on a SDS gel and for this reason western blotting with 6X-His Tag antibody was used. After ON incubation, two bands at c.a. 30 and 20 KDa were generated, which were absent in the control with the lysin only. No degradation product was observed when Ami_lysM was tested alone. In contrast, digestion of LysM_CHAP produced one specific band at 20 KDa (Figure 6.AII and 6.AIII). It is to note that degradation was first observed with lysed bacteria, but due to the few signal obtained after prolonged exposition of the blot it was decides to use cell wall protein extract (results not shown).

In order to study the proteolytic degradation in a more controlled environment, we also used trypsin and mixed it with the native PlySK1249 enzyme in the presence of purified cell wall. Figure 6 shows that the trypsin cleavage generated two main products (bands 1 and 2 in Figure 6B), which were confirmed by amino acid sequencing. Band 1, with the higher molecular weight, corresponded to the amino acid sequence ranging from aa 1 to 317, which encompassed the amidase catalytic domain plus LysM. Band 2 corresponded to the CHAP catalytic domain (aa 317 to 489). Western blot using a 6X-His Tag antibody also confirmed the presence of the C-terminal part of the enzyme (CHAP domain, Figure 6.C).

In addition, the native enzyme and its different truncated version were also digested with trypsin during different time points with or without purified cell wall (Figure 7). Interestingly, the presence of the substrate was shown to have an impact, with modification in the trypsin degradation patterns. Indeed, in absence of peptidoglycan substrate, the digestion pattern was different from the one observed in figure 6.B with the production of only one band at a size of c.a. 20 KDa (Figure 7.A). This actually suggested that the c.a. 40 KDa band corresponding to the Ami_LysM domain was less stable in absence of substrate. The hypothesis was confirmed in Figure 7.B, which

shows that the Ami_LysM construct is resistant to proteolysis in presence of purified cell. In addition, the LyM_CHAP domain was proteolysed with a similar pattern in presence or absence of substrate (Figure 7.C) and the Ami domain was not observed to be proteolytically degraded in this conditions (Figure 7.C). This highlight the fact that the protein is composed of different proteolytic resistant cores that correspond to the CD and CWBD domains and that the linker connecting the Ami CD to the LysM CWBD is more resistant to degradation when the enzyme is in contact with its peptidoglycan substrate. Of note, the trypsin western blot profiles were also similar to the one observed with cell wall protein extract for the LysM_CHAP and Ami_LysM constructs (Figure 6.AII, 6.AIII compared to Figure 8B, 8C, respectively). However, for the PlySK1249 a second band at 30 KDa was not present in the ON trypsin digestion compared to cell wall protein digestion (Figure 6.A compared to 6.C). The pattern was more similar to one observed with trypsin after 1 to 10 minutes, which could suggest imperfect digestion when using cell wall extract for the native enzyme.

In order to identify to protease responsible for the PlySK1249 degradation, we finally performed fractionation of the protein content present in the cell wall of the *S. dysgalactiae* strain. Ammonium sulphate was used to make a first sorting and fractions were tested on the LysM_CHAP construct with a higher proteolytic activity observed for 60% to 75% concentrations (Figure 9.A). A second purification step was performed by size exclusion chromatography using a 55% to 80% ammonium sulphate fraction and the output was again tested for proteolytic activity on the LysM_CHAP construct (Figure 9.BI and 9.BII). Fractions B9 will now be used for proteomic content analysis in order to observe protease enrichment compared to fraction B5 were no activity was present.

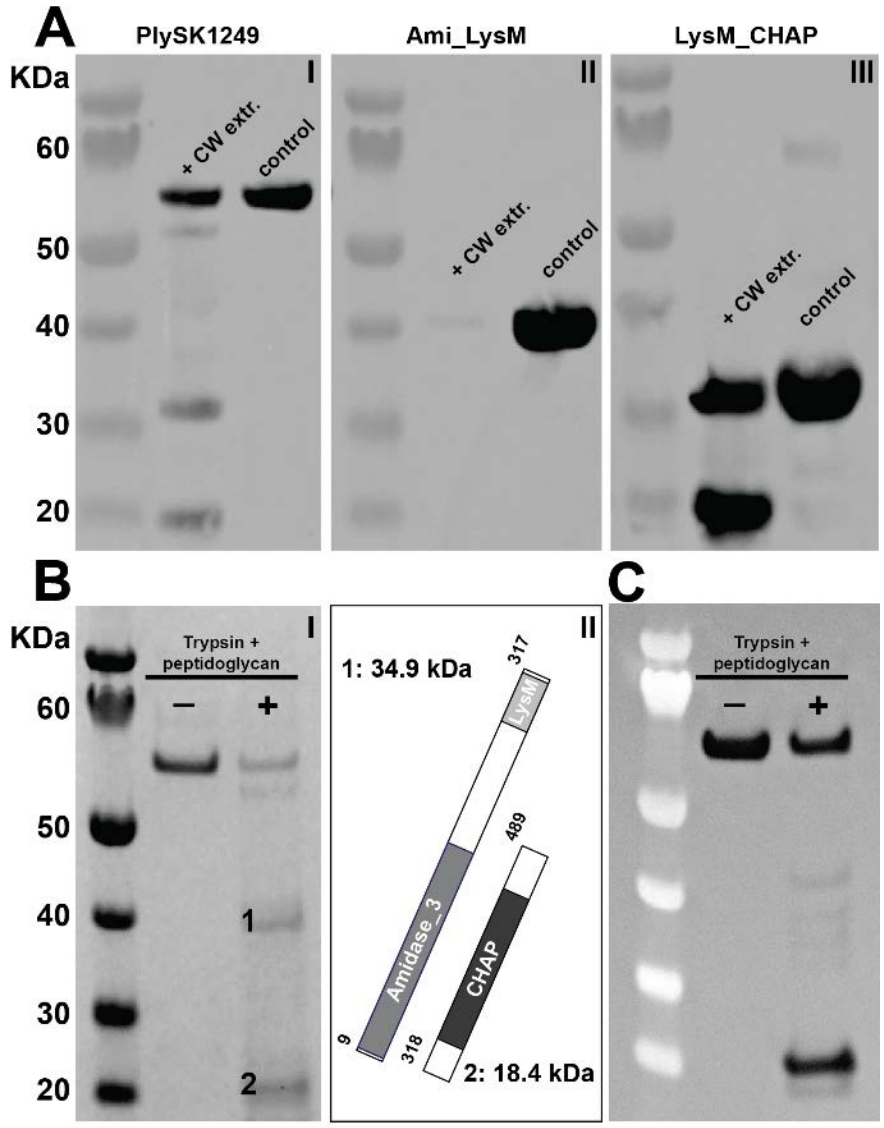

Figure 6. PlySK1259 and its truncated forms proteolysis in presence of protein cell wall extract. A) 40 µM of the parent enzyme (I), Ami_lysM (II) or LysM_CHAP (III) were incubated overnight with cell wall protein extract form S. dysgalactiae. Samples were migrated on NuPAGE 4-12% BisTris and degradation was confirmed by western blotting using the 6-his tag. B) 40 µM of the parent enzyme was incubated ON with 0.1 uM/ml of trypsin and 100 ug/ml of purified *S. dysglactiae* cell wall ON. Sample were migrated on NuPAGE 4-12% BisTris and stained with Coomassie blue. Protein degradation was observed in the presence of the substrate and bands 1 and 2 were sequenced. The N-terminal part of the protein encompassing the amidase domain plus LysM CWBD was detected in band 1 and the C-terminal with the CHAP domain part in band 2. C) Degradation was also confirmed by western blotting using the 6-His tag.

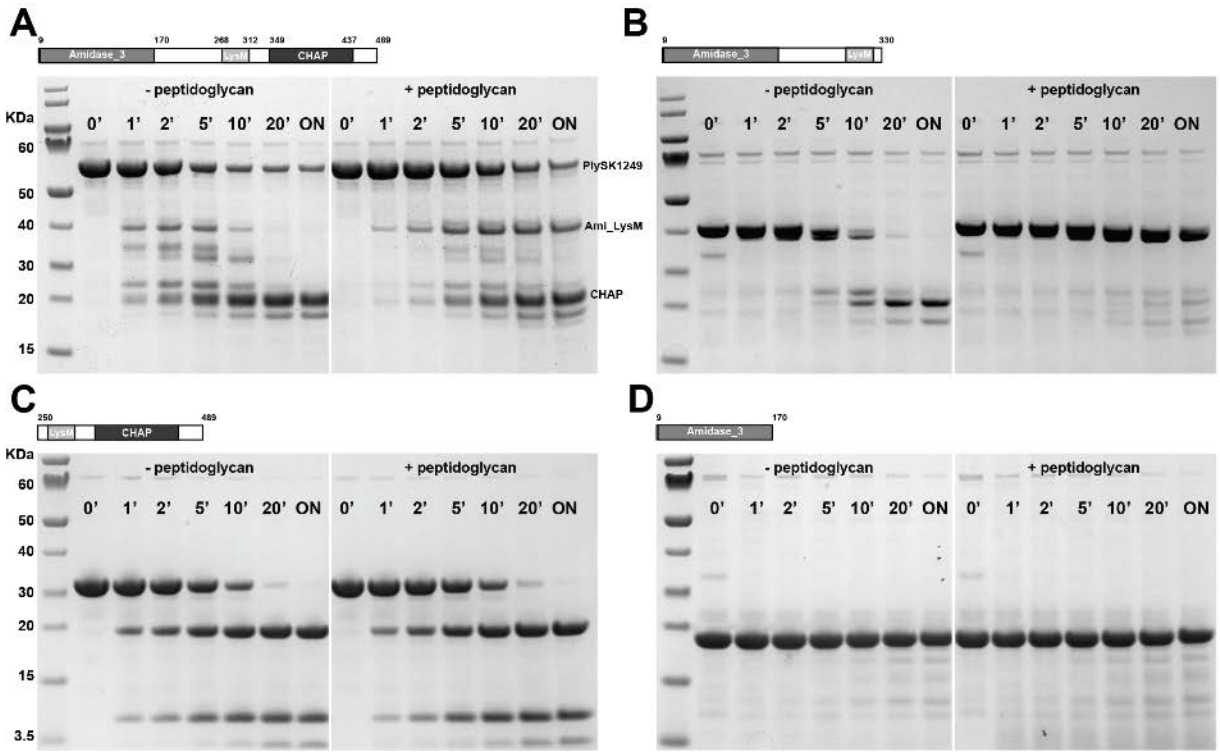

Figure 7. PlySK1259 and its truncated forms proteolysis in presence of Trypsin. A) 40 µM of the parent enzyme (I), Ami_lysM (II), LysM_CHAP (III) or Ami (IV) were incubated during different time points with 1 µM/ml of trypsin and with or without 100 µg/ml of purified S. dysgalactiae cell wall. Sample were migrated on NuPAGE 4-12% BisTris and stained with Coomassie blue.

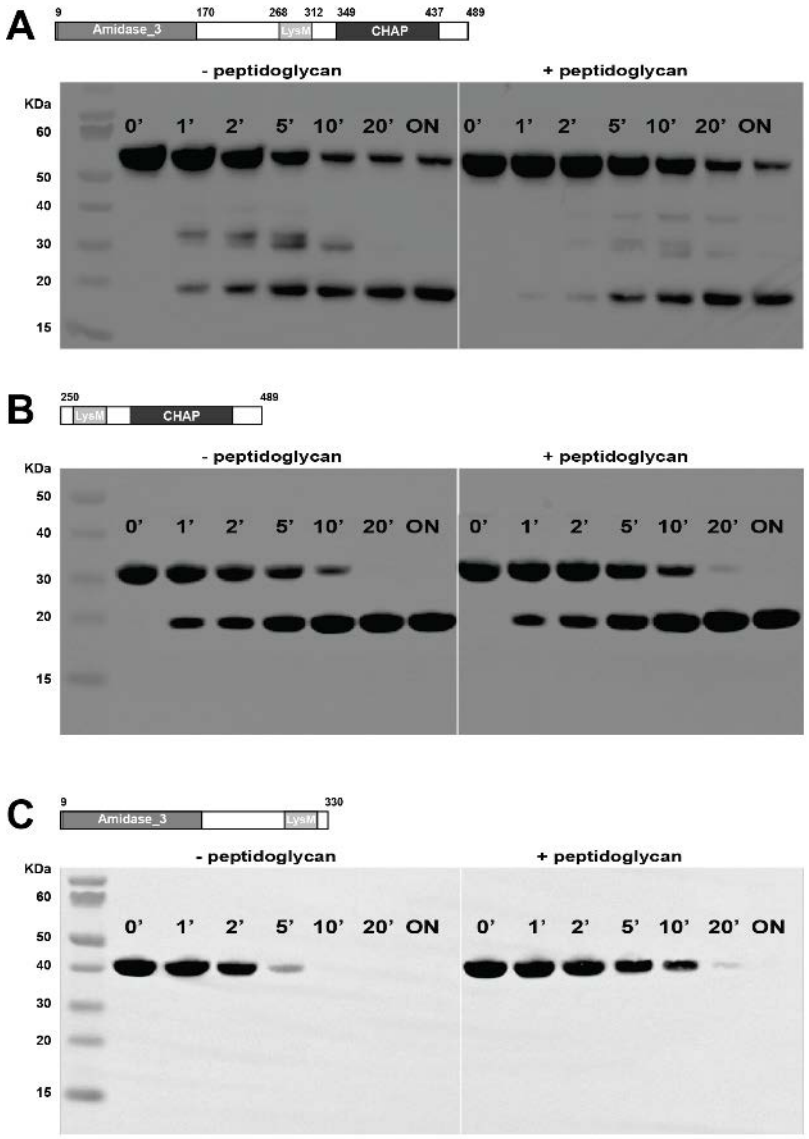

Figure 8. Western blot of PlySK1259 and its truncated forms proteolysed in presence of protein cell wall extracts. 40 µM of the parent enzyme (A), LysM_CHAP (B) or Ami_lysM (C), were incubated during different time points with I µM/ml of trypsin and with or without 100 µg/ml of purified S. dysgalactiae cell wall as in figure 7. Samples were migrated on NuPAGE 4-12% BisTris and degradation was confirmed by western blotting using the 6-his tag.

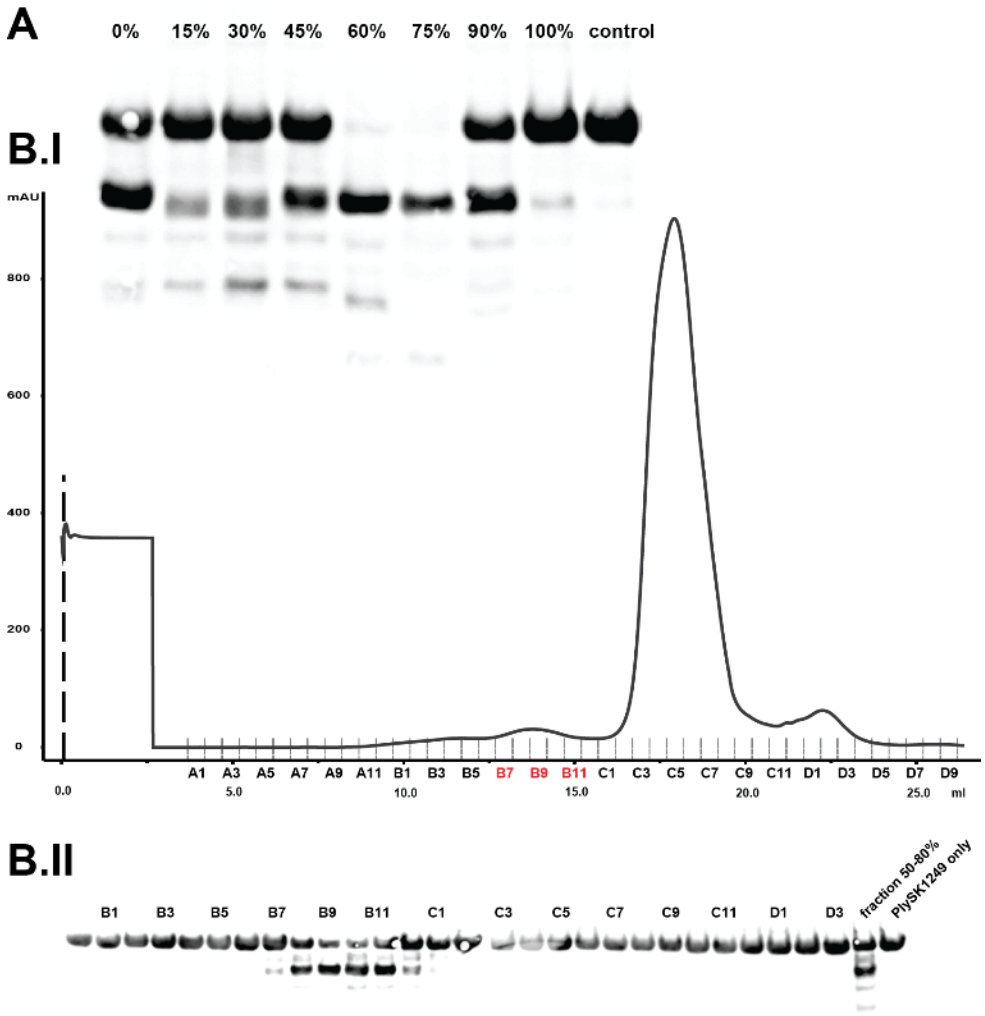

Figure 9. Protein content fractionation of *S. dysgalactiae* SK1249 total cell wall extract using ammonium sulphate precipitation and size exclusion chromatography. A) Proteins present in the total cell wall extract were serially precipitated by increasing steps of sulphate ammonium. Between each step, proteins were collected by centrifugation and the mixed with 40 µM of the LysM_CHAP construct and incubated ON. Samples were then migrated on a NuPAGE 4-12% BisTris and degradation was confirmed by western blotting using the 6-his tag. B.I) The 55% to 80% ammonium sulphate precipitation fraction was further separated using size exclusion chromatography. B.II) 500 yl fraction were tested for activity as described before.

Discussion and perspectives

Phage lysins are ubiquitous and prone to be dispersed in relatively large quantities in the microbial environment. Much has been learned about the timing of phage-mediated cell lysis and its complex control, with regulation taking place at lysin/holin expression, lysin translocation and lysin activation (for review, see [101, 123, 124]). However, less is known about their structure-activity relationship, their regulation during cell wall hydrolysis, and their fate once liberated in the surrounding.

Here we addressed the issues of lysin multi-modularity, bacterial specificity, and prevention of accidental lysis of neighbouring bacteria in the *S. dysgalactiae* prophage lysin PlySK1249. We first asked whether PlySK1249 needed all its three domains (two CDs and one CWBD) for effective lysis of its natural host bacterium. Using the parent enzyme and a variety of truncated constructs, we found that all three domains cooperated to increase the overall lytic activity of the parent enzyme, independently of their own intrinsic lytic activities. For instance, while CHAP_LysM was non-lytic, it synergized with amidase toward restoring the lytic activity of the parent enzyme. Likewise, the non-enzymatic CWBD LysM enhanced amidase-induced lysis, most likely by positioning the amidase appropriately in the cell wall, as proposed elsewhere [112]. Thus, although CHAP and LysM were not intrinsically bacteriolytic, they did have an effect when combined in the context of the multi-modular parent enzyme. In particular, the CHAP-amidase inter-domain synergism is a new observation. Moreover, although CHAP was not macroscopically lytic on whole bacteria, it had observable effects by optical and electronic microscopy. CHAP could resolve *S. dysgalactiae* chains to individual cells and nibble walls from the outside generating notched surfaces, although bacteria did not lyse or die.

To better understand the roles of amidase and CHAP in this synergism we investigated their individual hydrolytic activities during peptidoglycan digestion. Both amidase and CHAP yielded free amino groups compatible with their predicted amidase and endopeptidase activities. In contrast, no glycosidase activity was detected for either the whole enzyme or its truncated constructs.

We then studied their contribution to cell wall solubilisation by analysing the cut-out patterns of stem peptides during peptidoglycan digestion. We found that the ability of the parent enzyme to solubilize purified walls and digest their stem peptides resulted from the addition of its two catalytic domains: i.e. amidase disconnected glycan chains from the stem peptides but could not resolve peptide crosslinks, whereas CHAP resolved cross-linked stem peptides but was unable to disconnect glycans from peptides. Hence, as in cell lysis, the cooperation between the two domains was apparent. However, the endopeptidase activity measured for the CHAP catalytic site was still in conflict with its apparent inability to solubilize the walls on its own or lyse whole cells.

Cell lysis results from peptidoglycan digestion that must be extensive enough to allow the intracellular turgor pressure to burst the cell. In the present case, the CHAP of PlySK1249 did not resolve the stem peptides to monomers, but mainly to dimers, which are likely enough to maintain a loose glycan-peptide meshwork that can prevent total wall solubilisation and thus cell lysis. Interestingly, similar observations were made with the Lc-p75 and Msp1 *Lactobacillus* autolysins, which endopeptidase activities were observed to have a preference for tetrapeptide over tripeptide [125, 126].

Thus, although silent in terms of cell lysis *senso stricto*, CHAP was a genuine endopeptidase companion of amidase, and thus was not an inactive evolutionary

byproduct on the way to be lost, as sometimes suggested [85, 86]. The whole enzyme profited of these interactions.

Second, we asked whether LysM was a determinant of bacterial host specificity, in addition to promote lytic synergism between amidase and CHAP. But this was not the case. CWBD bound the walls of an array of streptococcal and other Gram-positive species with similar affinities, whereas it was the amidase domain that determined species specificity.

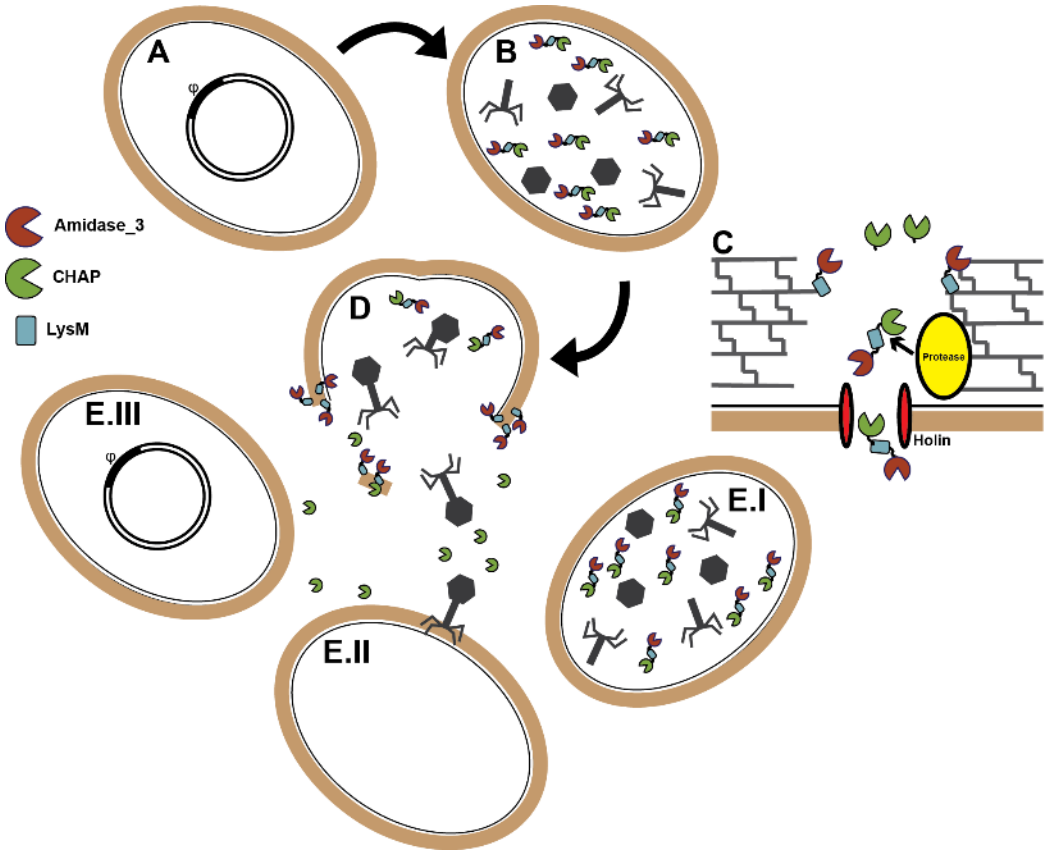

Figure 10 Proposed model for post-lysis lysin regulation. After induction of the integrated prophage (A), the lysin is produced during the replicative cycle (B). Cell lysis is controlled by the production of holin at the end of the replicative cycle, which permits the diffusion of the enzyme through the plasma

membrane to its peptidoglycan substrate (C). After cell wall degradation, the lysin get proteolysed by cell wall associated proteases and the diffusion of the active amidase domain is prevented by the CWBD (C, D). The second catalytic domain is released but has no direct impact on the surrounding cells, which can be in a different phase of its replicative cycle (E.I), new pray (E.II) or where the prophage can be still integrated (E.III).

We next asked whether wall attachment of lysins could have other roles, such as contributing to retaining the enzyme around the bacterium after cell lysis, and thus preventing uncontrolled diffusion and lysis-from-the-outside of neighbouring bacteria, as suggested [92, 93]. We identified such a role using a diffusion assay. While amidase alone could readily diffuse and lyse cells at a distance, the LysM-containing parent PlySK1249 and Ami_LysM enzymes could not diffuse, as they were retained around lysing cells by the LysM domain. This CWBD-related wall-retention persisted over 100-time concentration titrations, whereas such a titration drastically increased the diffusion of the amidase domain alone, thus experimentally supporting the hypothesis of *in situ* lysin blockage [92, 93].

If lysin control is as important, then it should be as thorough as possible. To this end we investigated the fate of the enzyme during peptidoglycan digestion. Most strikingly, we observed that, in the process of wall digestion, PlySK1249 underwent proteolytic cleavage. The cleavage site, either by cell wall protein extract or trypsin, was observed to be very specific and generated in the case of trypsin an Ami_LysM and CHAP moiety. Interestingly, it was already observed that the main autolysins AtlA for *E. faecalis* and AcmA in *Lactococcus lactis* were also degraded by extracellular proteases [127-129]. Both enzymes process also LysM domain and cleavage was observed to take place in the linkers that connect them by the HtrA serine protease in the case of *L. lactis*. A Truncated version of the AcmA that does not have its lysM domain was also

observed to be less active and thus it was hypothesize that proteolytic cleavage could play a role in controlling cell wall degradation during cell division. According to our preliminary results, which have to be proofed *in vivo*, we would make the hypothesis that the PlySk1249 proteolytic cleavage observed is the key aspect that can reunify the apparent contradiction of having a non-lytic domain. Indeed, proteolysis would simply stop the intramolecular synergism of both CD and create a still lytic Ami_LysM domain that remains avidly bound to digested walls debris, discouraging the enzyme from diffusion (see diffusion experiment above), while non-lytic CHAP that is supposedly harmless for neighbouring bacteria.

However, while binding the wall curbs Ami_LysM, CHAP might not be a useless bystander. The CHAP de-chaining activity is reminiscent of cell wall maturation by autolysins in *Bacillus subtilis*, which are also acting as de-chaining enzymes, as well as the Cse autolysin of *Streptococcus thermophilus* that is composed of a LysM and CHAP domain that promote cell separation [130, 131]. If CHAP is a de-chaining enzyme, one might speculate that it could help separate intact cells from the ones undergoing lysis, thus removing them from the risk of lysis-from-without and adding another level of protection.

In summary, the present observations provide logical explanations for the multi-modular architecture of PlySK1249 and the functionality of its various domains. Although all domains cooperate for lysis of host bacteria, they have specific roles that are summarized in the model proposed in Figure 10. First, amidase is the main lytic domain responsible for both bacterial lysis and host cell specificity. Second, LysM mediates PlySK1249 attachment and positioning in the wall, but also impairs diffusion of the enzyme that may be detrimental to surrounding bacteria. Finally, cleavage of the lysin during peptidoglycan digestion by serine protease present in the periplasmic

space or in the cell wall completes the intrinsic lytic regulation aimed at protecting closely related neighbouring cells from lysis-from-without. While the model complies with the observations reported herein, it also opens new areas to understand the subtle intra-molecular functioning of phage lysins. Moreover, it raises questions about the ideal architecture of therapeutic antibacterial lysins, where the presence of CWBDs might be detrimental for the diffusion of the enzymes within infected sites.

Supplementary data

Supplementary table 1: Bacterial strains and their origins, plasmids and nucleotides

Bacterial strains	Characteristics	Origin
E. coli		
BL21(DE3)pLysS	F^- *ompT hsdSB* (r_B^- m_B^-) *dcm*$^+$*gal* (DE3) pLysS (Cam^r)	Stratagene
BL21/pPlySK1249[28a]	*E. coli* BL21 (DE3) (pLysS) transformed with pPlySK1249[28a]	[80]
BL21/pAmi[28a]	*E. coli* BL21 (DE3) (pLysS) transformed with pAmi[28a]	This study
BL21/pAmi_LysM[28a]	*E. coli* BL21 (DE3) (pLysS) transformed with pAmi_LysM[28a]	This study
BL21/pLysM_CHAP[28a]	*E. coli* BL21 (DE3) (pLysS) transformed with pLysM_CHAP[28a]	This study
BL21/pLysM[28a]	*E. coli* BL21 (DE3) (pLysS) transformed with pLysM[28a]	This study
Streptococci		
S. dysgalactiae SK1249	Human, haemoculture	K. Mogens
S. agalactiae FLS-S3-026	Bovine	M. Stanhope
S. agalactiae 17-2167	Human, endocarditis	CHUV[b]

S. agalactiae 532	Human	G. Jordan
S. agalactiae GF	Human, haemoculture	F. Gilliand
S. pyogenes ATCC 19615	Human, sore throat	R.G. Wittler
S. gordonii DL1	Human	H.F. Jenkinson
S. mutans ATCC 25175	Human, carious dentine	DSMZ[c]
S. suis #19	Porcine	M. Haenni
S. uberis ATCC 700704	Bovine	ATCC[d]
S. pneumonia D39	Human	J. McCuller
Enterococci		
E. faecalis ATCC 29212	Human, urine	Micro-Media Systems, Inc
E. faecium D344	Human	J. Entenza

Plasmids	**Characteristics[a]**	**Origin**
pET-28a	Expression vector; Kan^r	Novagen
pPlySK1249^{28a}	pET-28a carrying *PlySK1249*	[80]
pAmi^{28a}	pET-28a carrying *Ami*	This study
pAmi_LysM^{28a}	pET-28a carrying *Ami_LysM*	This study

pLysM_CHAP[28a]	pET-28a carrying *LysM_CHAP*	This study
pLysM[28a]	pET-28a carrying *LysM*	This study

Oligonucleotides	**Sequence 5' → 3', restriction enzyme[e]**	**Origin**
plySK28aNcoIFw	GCATGCCATGGGAAAACATCTAGTGATT	Microsynth
	TGTGGACATGGGCAAGGACG	Microsynth
plySK28aXhoIRv	GCCGCTCGAGTGAAATTCTAAACCAACC TACAACTTTTCCAAGTTTAACTGTTCCAG	Microsynth
Ami28aXhoIRv	GCCGCTCGAGTGTTATTGCGGACACAAG ACCTTTCG	
Ami_LysM28aXhoIRv	GCCGCTCGAGCACACGGCTTGCAACACT GGTTGG	
	GCATGCCATGGAATCATGGGTGCTGGAG CAGGATGTAGAAGGAAC	
LysMCHAP28aNcoIF w		
LysM28aNcoIFW	GCATGCCATGGTCAAGGGGCGCACCTA	Microsynth
	CAAAATCCTCCAAGAA	
LysM28aXhoIRv	GCCGCTCGAGCACACGGCTTGCAACACT	Microsynth
	GGTTGGAATAGCGG	
T7	TAATACGACTCACTATAGGG	Novagen
T7 terminator	GCTAGTTATTGCTCAGCGG	Novagen

[a] Abbreviations: Cam^r, chloramphenicol resistance; Kan^r, kanamycin resistance [b] Centre hospitalier universitaire vaudois (CHUV, Switzerland) [c] Deutsche Sammlung von Mikroorganismen und Zellkulturen (DSMZ, Leibniz-Institut, Germany) [d] American type culture collection (ATCC, Manassas, Virginia, USA) [e] Restriction sites are underlined.

Supplementary table 2. Park Johnson and Ghuysen assays for differentiation of glycosidase and amidase/endopeptidase activity of different PGHs against purified *S. aureus* cell walls

	reducing activity [a] [µg glucose]	**Free NH_2 groups [b] [mM]**
PlySK1249	1.9 ± 25.9	8.1 ± 2.7
Ami	13.3 ± 8.0	11.4 ± 0.3
Ami_LysM	3.0 ± 26.0	3.0 ± 1.2
CHAP	6.3 ± 25.0	5.7 ± 2.6
Mutanolysin	438.4 ± 111.1	0.1 ± 0.2

[a] Quantification of reducing groups was performed using the Park-Johnson assay. Reducing activity is expressed as µg glucose equivalents released in the incubation mixture.

[b] The concentration of free amino groups was determined with the Ghuysen assay.

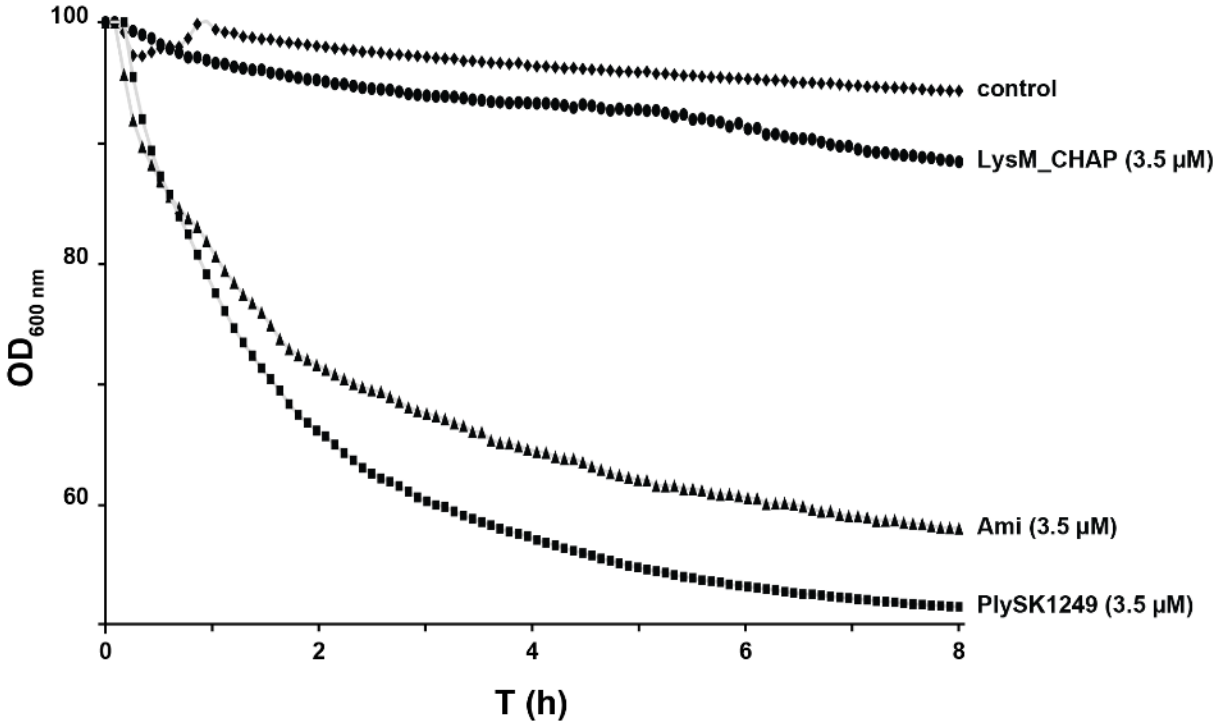

Supplementary Figure 1. Lytic activity of the PlySK1249 lysin and its different catalytic domains on purified cell wall. Decrease in turbidity was measured at 600 nm for 8 h using purified cell wall at a final concentration of 1 µg/ml.

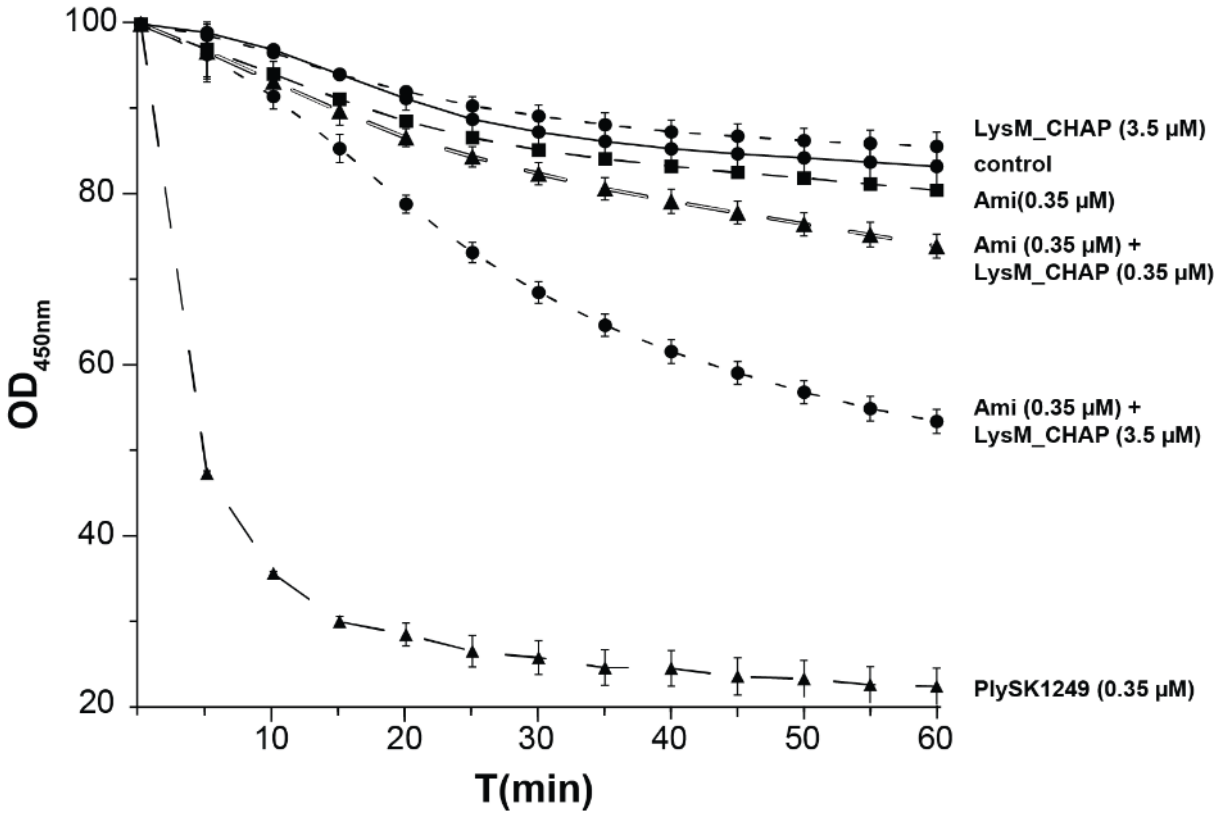

Supplementary Figure 2. Synergistic activity between the Ami and LysM_CHAP constructs. *S. dysgalactiae* cells in the exponential growth were treated with the native enzyme or the Ami and LysM_CHAP constructs alone or in combination. The decrease in turbidity was measured at 600 nm for 1 h. The experiments were repeated twice in triplicate and means ± standard deviation are shown.

A

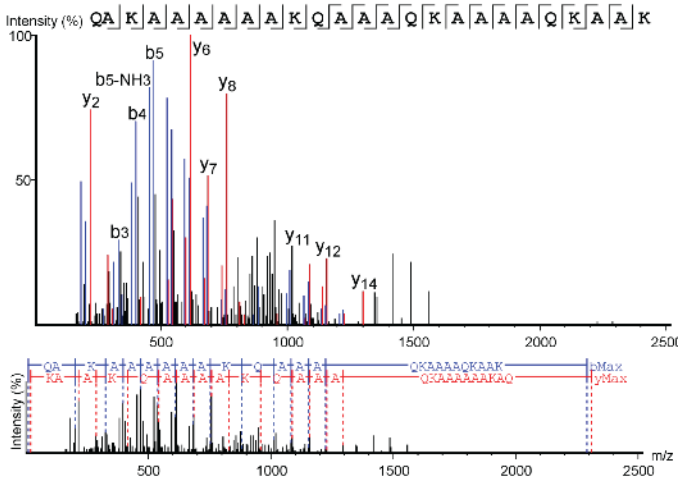

B

#	b	b-H2O	b-NH3	a	b (2+)	Seq	y	y-H2O	y-NH3	y (2+)	#
1	129.07	111.06	112.04	101.07	65.03	Q					25
2	200.10	182.09	183.08	172.11	100.55	A	2180.26	2162.25	2163.23	1090.63	24
3	328.20	310.19	311.17	300.20	164.60	K	2109.22	2091.21	2092.20	1055.11	23
4	399.24	381.23	382.21	371.24	200.10	A	1981.13	1963.12	1964.10	991.07	22
5	470.27	452.26	453.25	442.28	235.64	A	1910.09	1892.08	1893.07	955.55	21
6	541.31	523.30	524.28	513.31	271.14	A	1839.06	1821.05	1822.03	920.03	20
7	612.35	594.34	595.32	584.35	306.67	A	1768.02	1750.01	1750.99	884.51	19
8	683.38	665.37	666.36	655.39	342.18	A	1696.98	1678.97	1679.95	848.99	18
9	754.42	736.41	737.40	726.43	377.71	A	1625.94	1607.93	1608.92	813.47	17
10	882.51	864.51	865.49	854.52	441.76	K	1554.91	1536.90	1537.88	777.95	16
11	1010.57	992.56	993.55	982.58	505.79	Q	1426.81	1408.80	1409.79	713.91	15
12	1081.61	1063.60	1064.59	1053.62	541.31	A	1298.77	1280.74	1281.73	649.88	14
13	1152.65	1134.64	1135.62	1124.65	576.82	A	1227.72	1209.71	1210.69	614.36	13
14	1223.69	1205.68	1206.66	1195.69	612.35	A	1156.68	1138.67	1139.66	578.84	12
15	1351.74	1333.73	1334.72	1323.75	676.37	Q	1085.64	1067.63	1068.62	543.32	11
16	1479.84	1461.83	1462.81	1451.84	740.42	K	957.58	939.57	940.56	479.29	10
17	1550.88	1532.87	1533.85	1522.88	775.94	A	829.49	811.48	812.46	415.24	9
18	1621.91	1603.90	1604.89	1593.92	811.46	A	758.45	740.45	741.43	379.73	8
19	1692.95	1674.94	1675.92	1664.96	846.98	A	687.42	669.41	670.39	344.21	7
20	1763.99	1745.98	1746.96	1735.99	882.49	A	616.38	598.37	599.35	308.69	6
21	1892.05	1874.04	1875.02	1864.05	946.52	Q	545.34	527.33	528.32	273.17	5
22	2020.14	2002.13	2003.11	1992.15	1010.57	K	417.28	399.27	400.25	209.14	4
23	2091.18	2073.17	2074.15	2063.18	1046.09	A	289.19	271.18	272.16	145.09	3
24	2162.22	2144.21	2145.19	2134.22	1081.61	A	218.15	200.14	201.12	109.57	2
25						K	147.11	129.10	130.09	74.06	1

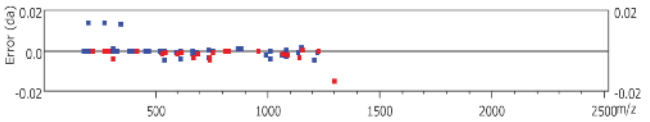

Supplementary Figure 3. Example for the quatrimeric peptide structure sequencing. Annotated MS/MS spectrum (A) and fragment table (B) of peptidoglycan peptide Mr 2307.313 (m/z 577.836). They were obtained by *de novo* sequencing using PEAKS 8.0. Matched b and y fragments ions are displayed in blue and red respectively in the MS/MS spectrum and the table. Residue local confidence calculated by PEAKS is shown by sequence color: blue > 60%, purple > 80%, red > 90%. The difference between the theoretical and the experimental peptide mass was 1.0 ppm.

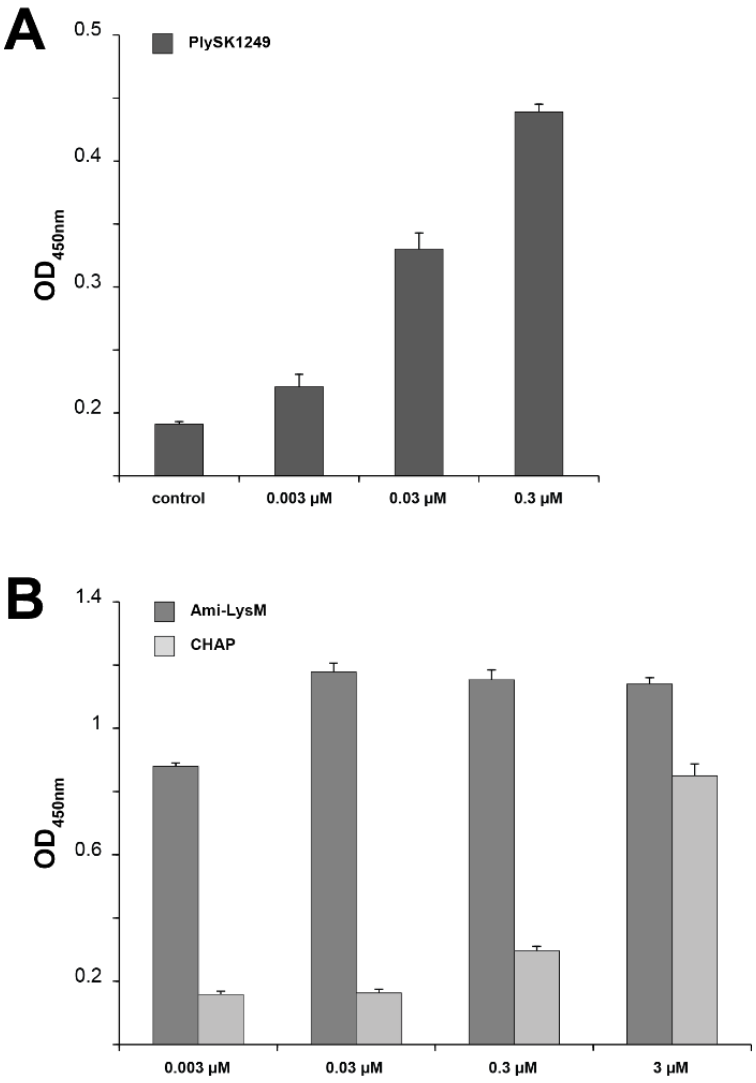

Supplementary Figure 4. Cell binding capacity the PlySK1249 native enzyme and the Ami_LysM vs LysM_CHAP constructs. Bacterial cells in the exponential growth phase were diluted to 10^8 cells per ml, adsorbed to a 96-well plate and exposed to different concentrations of PlySK1249, Ami_LysM or LysM_CHAP. Binding capacity of the enzyme to the wells was assessed by adding an anti-His antibody that was coupled to peroxidase. The signal was read at 450 nm and the control measure was performed on adsorbed bacteria without the addition of enzyme. The experiment was repeated three times. Means ± standard deviation are shown.

CHAPTER III

The prospect of phage therapy: an example in experimental endocarditis due to *Pseudomonas aeruginosa*

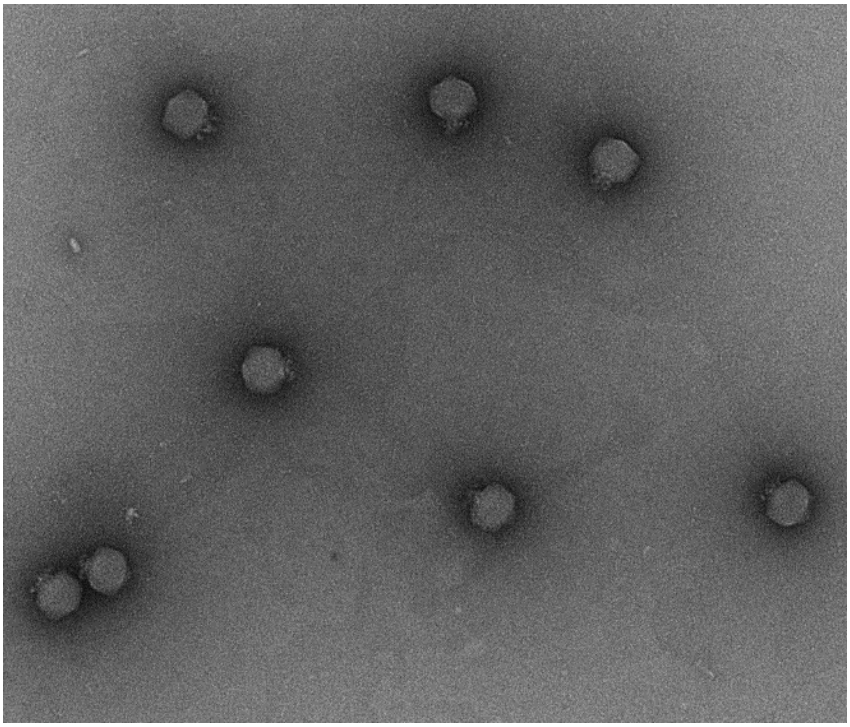

Podoviridae. Negative staining. 2016. F. Oechslin

F. Oechslin did the experiments.

F. Oechslin, J. Entenza, P. Moreillon, G. Resch and Y-A. Que conceived the experiments.

F. Oechslin, J. Entenza and S. Mancini did the animal model.

F. Oechslin and P. Piccardi did the fibrin clot model.

M. Parkan did the hierarchical clustering analysis.

G. Mazepa helped with the sequencing analysis of the phage resistant mutants.

Gilles Willemen did the cytokine quantification.

F. Oechslin and P. Moreillon wrote the paper.

J. Entenza, S. Mitri, S. Mancini, G. Resch and Y-A. Que corrected the manuscript.

F. Oechslin supervised all the experiments.

General introduction

Pseudomonas aeruginosa is an ubiquitous microorganism colonizing soil, plants and animals. In human it is an opportunistic pathogen that can cause a variety of severe opportunistic infections and is highly associated with antibiotic resistance and nosocomial infections. In the hospital environment, *P. aeruginosa* is specially known for colonizing water systems like tap water and showers, as well as medical apparatuses such as respiratory equipment. The variety of infections that are associated with this bacterium is largely due to its virulence factor repertoire, which includes different proteases that can be injected by type three secretion systems. These enzymes have dramatic effects on epithelial barrier and wound healing (for review on the topic see [132]). Its ability to rapidly proliferate in damaged tissues makes it a primary etiologic agent in burn wound infections, resulting in high rates of mortality and morbidity [133, 134]. In addition, both intrinsic and acquired resistances of the bacterium to several classes of antibiotics make these infections often untreatable by conventional antibacterial agents [135]. For these reasons, the development of new antimicrobial strategies to control pseudomonas infections is highly warranted.

An alternative – or complementary – strategy to antibiotherapy is the use of bacteriophages (phages) as new therapeutic agents. Indeed, their ability to kill their bacterial host by lysing them at the end of their life cycle makes them a weapon of choice for microbial control.

Felix d'Hérelle co-discovered phages hundred years ago (1917) and demonstrated their potential for therapeutic application by successfully treating dysentery [136]. However, with the advent of antibiotics and antibiotic research in the 1940s, the use of phages quickly decreased in the Western countries. It is only in some Eastern European countries like Georgia that phages are still used and commercially produced

[137]. Recently, and along with the development of multidrug resistant bacteria, phage therapy was re-evaluated by the Western scientific community. Originally limited to research in different animal models, the evaluation process underwent a breakthrough in 2015 with the first human multicenter randomized phase 1-2 clinical trial Phagoburn (NCT02116010, http://www.phagoburn.eu) [138]. The study aimed at evaluating the efficacy of phage therapy in burn wounds infected by *P. aeruginosa*. To this end, a cocktail composed of twelve different anti-pseudomonas phages was manufactured by the Phercydes Pharma company for the clinical trial and was tested in 11 health care burn units located in France, Belgium and Switzerland with the Centre Hospitalier Universitaire Vaudois (CHUV) (http://www.phagoburn.eu).

Taking advantage, on the one hand, of our involvement in the project and, on the other hand, on the long-lasting experience of our laboratory in microbial pathogenesis and new antibacterial therapy in animal models, we tested the Phagoburn phage cocktail in experimental endocarditis due to *P. aeruginosa*.

Endocarditis is an inflammation of the endocardium, which is the inner layer of the heart. It usually involves prior sterile heart valve lesions known as vegetations, which are composed of fibrin-platelet meshworks prone to be infected by circulating bacteria [139]. Also uncommon, *P. aeruginosa* infective endocarditis is associated with a high mortality and mortality which make it an archetype of highly lethal valve infection and thus a good model to test new therapies [140, 141]. Although phage therapy has been evaluated in specific rodent infection models (mainly sepsis, pneumonia and one time in meningitis) [142-144], experimental endocarditis is unique in reunifying a several important features that could predict the human situation. First, animal endocarditis mimics endocarditis in humans in that bacteria are embedded in fibrin-platelet vegetations devoid of cellular host defences. Second, eradiation of bacteria in this

therapeutic sanctuary strictly depends on the intrinsic bactericidal activity of antimicrobial agent, not on additional immune specificities that may vary between animal species. Third, drug penetration into vegetation can be readily determined (i.e. much more easily than in organ sub-compartments), thus facilitating pharmacokinetic/pharmacodynamic (PK/PD) studies. Fourth, drug plasma kinetics mimicking those in human can be readily achieved.

In the manuscript presented next, published in the *Journal of Infectious Disease* at the end of 2016, we studied phage therapy against *P. aeruginosa* experimental endocarditis. We report on a very substantial set of experiments both in an *in vitro* clot model mimicking cardiac vegetations and in rats with experimental aortic endocarditis. These include the whole continuum from susceptibility testing, resistance screening (as well as understanding resistance mechanisms and prevention), PK/PD profiles in animals (including phage penetration in infected tissues), and therapeutic assays including phage/drug combination therapy. Some salient findings of this work include the fact that although phage monotherapy was highly bactericidal, combining phages with antibiotics was highly synergistic both *in vitro* and *in vivo*. This was exemplified by an unprecedented rate of valve sterilization within 6 hours of combined-therapy in animals. Moreover, while phage-resistant bacterial mutants did arise in batch cultures *in vitro*, they were undetectable in the *in vivo* milieu. By investigating the mechanism of resistance, we found a tradeoff between resistance to the phage and virulence in the rat model, i.e. mutants that were resistant to the phage lost their infectivity.

We believe that this report addresses a major societal challenge in healthcare, i.e. antibiotic resistance. First, it is uniquely comprehensive and uses the realistic model of endocarditis, which provides conceptual information that is valid for many deep-seated and systemic infections. Second, it discloses that phage-resistant bacterial mutants

are naturally hampered *in* vivo due to resistance-induced cell surface defects, i.e. phage-resistance is a tradeoff that affects *in vivo* infectivity. This provides novel arguments answering the legitimate worry that phage resistance might rapidly emerge in the clinics. Finally, the observation that a single injection of phages combined with antibiotics might be enough to cure infective endocarditis suggests that, if wisely used, phage therapy may turn into an unprecedented breakthrough in antibacterial therapy.

The present paper was accompanied by an Editorial Commentary by Stratton et al. [145] and the article in the microbe magazine (January 2016, Vol 11, No 1) describing the relation between phage resistance and its concomitant virulence loss.

In addition, developments along this work were awarded best poster prizes at the following meetings:

- ISCVID 2015: International Society of Cardiovascular Infectious Diseases, 04-06.06.15, Rio De Janeiro (Brazil). Best poster prize.

- Interscience Conference on Antimicrobial Agents and Chemotherapy (ICAAC), 18-21.09.15, San Diego (USA). Best poster prize.

- SGM-SSM: 74th Annual Meeting of the Swiss Society of Microbiology, 13-15.06.16, Bern (Switzerland). Best poster prize.

The Journal of Infectious Diseases
MAJOR ARTICLE

Synergistic Interaction Between Phage Therapy and Antibiotics Clears *Pseudomonas Aeruginosa* Infection in Endocarditis and Reduces Virulence

Frank Oechslin,[1] Philippe Piccardi,[1] Stefano Mancini,[1] Jérôme Gabard,[3] Philippe Moreillon,[1] José M. Entenza,[1] Gregory Resch,[1] and Yok-Ai Que[2]

[1]Department of Fundamental Microbiology, University of Lausanne, and [2]Department of Intensive Care Medicine, Bern University Hospital, Switzerland; and [3]Pherecydes Pharma, Romainville, France

Background. Increasing antibiotic resistance warrants therapeutic alternatives. Here we investigated the efficacy of bacteriophage-therapy (phage) alone or combined with antibiotics against experimental endocarditis (EE) due to *Pseudomonas aeruginosa*, an archetype of difficult-to-treat infection.

Methods. In vitro fibrin clots and rats with aortic EE were treated with an antipseudomonas phage cocktail alone or combined with ciprofloxacin. Phage pharmacology, therapeutic efficacy, and resistance were determined.

Results. In vitro, single-dose phage therapy killed 7 log colony-forming units (CFUs)/g of fibrin clots in 6 hours. Phage-resistant mutants regrew after 24 hours but were prevented by combination with ciprofloxacin (2.5 × minimum inhibitory concentration). In vivo, single-dose phage therapy killed 2.5 log CFUs/g of vegetations in 6 hours ($P < .001$ vs untreated controls) and was comparable with ciprofloxacin monotherapy. Moreover, phage/ciprofloxacin combinations were highly synergistic, killing >6 log CFUs/g of vegetations in 6 hours and successfully treating 64% (n = 7/11) of rats. Phage-resistant mutants emerged in vitro but not in vivo, most likely because resistant mutations affected bacterial surface determinants important for infectivity (eg, the *pilT* and *galU* genes involved in pilus motility and LPS formation).

Conclusions. Single-dose phage therapy was active against *P. aeruginosa* EE and highly synergistic with ciprofloxacin. Phage-resistant mutants had impaired infectivity. Phage-therapy alone or combined with antibiotics merits further clinical consideration.

Keywords. bacteriophage; phage therapy; endocarditis; *Pseudomonas aeruginosa*; resistance; antibiotic.

The global increase in antibiotic resistance is reviving the need for alternative antimicrobial strategies, including phage therapy. This "forgotten cure" was developed in parallel to antibiotics during the first half of the 20th century and is still commonly used in countries of the former Soviet Union [1]. However, it was not developed on a large scale in Western countries, and information on phage pharmacokinetics/pharmacodynamics (PK/PD), drug interactions, in vivo efficacy, and emergence of resistance remains scarce. Phages have been administered by various routes, including inhalation for pneumonia (reviewed in [2]), surgical rinsing for chronic osteomyelitis [3], and intravenous injection for severe systemic infections, such as typhoid fever (reviewed in [4]). However, only a few studies provide a comprehensive picture linking phage pharmacology to antibacterial efficacy [5, 6]. Moreover, with few exceptions [6], the emergence of phage resistance is seldom addressed, even in recent clinical studies [7–9].

Detailed understanding of bacterial resistance to phages is critical if phages were to be used more broadly in the clinical setting. Phage-resistant bacteria can result from several mechanisms, including modification of cell-surface receptors, restriction-modification of incoming (foreign) phage DNA, or interphage immunity [10]. Resistance mutations may arise spontaneously in vitro and are likely to be selected in vivo as well [6]. Some mutations may affect LPS (a common phage receptor) and impact bacterial fitness or virulence [11–13]. However, other kinds of mutations or further mutations restoring virulence cannot be excluded and must be scrutinized.

The intrinsic bactericidal properties of anti-infective compounds are most reliably studied in models of therapeutic sanctuaries, where natural host defenses are poorly involved. Experimental endocarditis (EE) and experimental meningitis are 2 such models. Experimental meningitis implicates a special anatomical setting where drug distribution depends on the blood–brain barrier. In contrast, EE mirrors the general situation encountered in many deep-seated infections. Moreover, endocarditis pathogens surround themselves with amorphous aggregates of platelet-fibrin clots, which cellular host defenses cannot penetrate (for review see [14]). Thus, the capability of antimicrobials to penetrate into vegetations is a critical issue.

Received 26 September 2016; editorial decision 30 November 2016; accepted 19 December 2016.
[a]Y-A. Q. and G. R. contributed equally to this study.
Correspondence: F. Oechslin, PhD, University of Lausanne, Quartier UNIL-Sorge, Bâtiment Biophore, CH-1015 Lausanne, Switzerland (Frank.Oechslin@gmail.ch).

The Journal of Infectious Diseases® 2017;XX:1–10

DOI: 10.1093/infdis/jiw632

In these experiments, we systematically explored the efficacy of a clinically used antipseudomonas phage cocktail (cocktail PP1131 currently investigated in the multicentric Phagoburn clinical trial for treatment of burn-wound infections; http://www.phagoburn.eu) in a dual in vitro and in vivo model of experimental endocarditis due to *Pseudomonas aeruginosa*.

Phage therapy alone was active both in vitro and in animals with EE. Moreover, it was highly synergistic with antibiotics. Although phage-resistant bacteria emerged in vitro, they were not detectable in vivo due to fitness alteration in the animal milieu. These results suggest that phage therapy alone or combined with antibiotics (in this case ciprofloxacin) deserves further consideration for future clinical application.

METHODS

Strains, Phage Cocktail, and Antibiotics

A total of 33 *P. aeruginosa* reference strains and clinical isolates from our own clinical strain collection were used in in vitro susceptibility determinations (Supplementary Table 1). These isolates were not meant to cover the diversity of contemporary pseudomonas from our hospitals but rather to select strains with extreme phenotypes to be tested in our experiments. Growth conditions and reagents are given in the Supplementary Materials.

In Vitro Studies

The host range of the individual phages composing the PP1131 cocktail was determined using spot or plaque assays [15]. Experiments were done in triplicates. Plasma clots were prepared in 96-well microplates, as previously described [16]. Phage titers were measured by plaque assays [15]. The activity of the phage cocktail was considered bactericidal when it killed ≥3 log colony-forming units (CFUs) of the starting inoculum in the clot. Details are provided in the Supplementary Materials.

Animal Studies

Experiments were approved by and in adherence with the guidelines of the Swiss Animal Protection Law, Veterinary office, State of Vaud. Experiments were performed under license number 879.9 and in accordance with the regulations of the cantonal committee on animal experimentation of the State of Vaud, Switzerland. The production of catheter-induced aortic vegetations and the installation of an intravenous line into the superior vena cava, connected to an infusion pump to deliver the phage cocktail, were performed in female Wistar rats as previously described [17]. Details are provided in the Supplementary Materials.

Histology

Semithin and ultrathin sections were prepared as previously described [18] and cut with a Leica Ultracut microtome. Sections were stained for light microscopy using the modified Brown and Brenn method, as previously described [19]. Ultrathin sections of 50 nm were stained as previously described [18]. For phage observation, phage cocktail was adsorbed on copper 200-mesh grid coated with Formvar-carbon and stained with uranyl acetate. Micrographs were taken with a transmission electron microscope FEI CM100 at an acceleration voltage of 80 kV with a TVIPS TemCam-F416 digital camera (EMF, UNIL).

Cytokine Measurements

The serum inflammatory cytokines interleukin 1β (IL-1β), interleukin 6 (IL-6), and tumor necrosis factor α (TNFα) were quantified prior to infection (24 hours after surgery), prior to therapy (18 hours after bacterial inoculation), and at sacrifice (6 hours after onset of therapy). Plasma was kept at −80°C, and cytokines titers were measured using the Biorad Bio-Plex Rat Cytokine Kit in a Luminex 200 system and following manufacturer's recommendations (MEF platform, UNIL).

Detection and Characterization of Phage Resistance

Phage-resistant bacteria were isolated from broth cultures, in vitro fibrin clots, and rat vegetations by plating on blood agar plates containing 10^{10} PFU (plaque forming unit) preabsorbed phages. Resistance rates were determined as the number of bacteria growing on plates preadsorbed with phages divided by the number of bacteria growing on plain plates. In vivo infectivity of phage resistance was assessed by inoculating rats with catheter-induced aortic vegetations as previously described. Full genomic DNA sequencing was performed by the Center for Integrative Genomics (University of Lausanne, Switzerland) using the Pacific Biosciences RSII platform. Total DNA was extracted using the DNeasy Blood and Tissue kit according to manufacturer's instructions. GenDB [20], BLASTn [21], and BRIG [22] were used for genomic analysis. Subsurface twitching motility tests were performed as described [23]. LPS was extracted using the iNTRON LPS extraction kit, resolved on NuPAGE 4%–12% BisTris gels, and silver stained as previously described [24]. Details are provided in the Supplementary Materials.

RESULTS

Pseudomonas aeruginosa Host Range of Individual Phages of the PP1131 Cocktail

The 12 phages contained in the PP1131 cocktail were evaluated for their ability to lyse a panel of 33 laboratory and clinical isolates of *P. aeruginosa* from our own collection using spot assays (Supplementary Tables 1 and 2). This test showed that 31 of 33 (94%) of the *P. aeruginosa* isolates were lysed by at least 2 phages, whereas only strains PA7 and PA10 were resistant to the 12 phages. The relatedness of the 12 phages regarding strain specificity was further evaluated by hierarchical cluster analysis based on a binary matrix derived from the spot assay.

Supplementary Figure 1 indicates that the phages of the cocktail were different from each other regarding their host specificity profiles, thus ensuring coverage of multiple strains.

Of note, spot assays indicate both lysis from within (due to productive phage infection) and lysis from without (due to phage attachment only). Therefore, although they assess specificity of phage–bacteria interactions, they may underestimate genuine productive infectivity. In the present experiments, the PP1331 phage cocktail achieved productive infection in 28 of 33 (84%) of the tested strains (Supplementary Figure 2).

Activity of the Phage Cocktail in the In Vitro Fibrin-Clot Model

The efficacy of the cocktail was tested in fibrin clots simulating endocarditis vegetations [16]. Two *P. aeruginosa* strains were used: namely, strain P7, which was not infected by any of the cocktail's phages, and strain CHA which was susceptible to all of them. For resistant strain PA7, no phage-induced killing and no in situ phage amplification were observed (Figure 1A). Moreover, physical disintegration of the clots, possibly due to the action of bacterial proteases, was observed after 24 hours (Figure 1C).

In contrast, a significant loss of bacterial viability of approximately 6 log CFUs/g was observed after 6 hours when CHA-infected clots were challenged with the cocktail (Figure 1I (P = .0001 compared with the initial bacterial load). Phage-induced killing was accompanied by a phage amplification of 5 log PFUs/g of clots (P = .0001 compared with noninfected clots). In addition, phage-induced bacterial killing prevented bacterial-induced clot disintegration (Figure 1D), indicating that phages diffused through the fibrin meshwork and killed bacteria located inside the clots. Yet, the sharp initial phage-induced killing was followed by bacterial regrowth after 24 hours (Figure 1B). This regrowth was caused by the development of phage-resistant bacterial mutants and was not accompanied by further phage amplification.

Frequency of Phage Resistance in Broth Cultures and Fibrin Clots

In the absence of phages, spontaneous resistant mutants occurred at an average frequency of ca 10^{-7} and at ca 10^{-8} against the whole cocktail (result not shown), both in batch cultures and in fibrin clots after 6 hours and 24 hours (Supplementary Table 3, column 2). In contrast, the proportion of phage-resistant bacteria increased sharply after exposure to phages due to the replacement of phage-susceptible bacteria by resistant subpopulations, (ie, 10^{-4} at 6 hours and 10^{-2} at 24 hours) (Supplementary Table 3, columns 5 and 6).

Prevention of Phage Resistance Using Phage/Antibiotic Combinations

To prevent the development of phage-resistant subpopulations, we attempted to combine phages with antibiotics. Combining the phage cocktail with 2.5 times the minimum inhibitory concentration (MIC) of ciprofloxacin or meropenem inhibited the

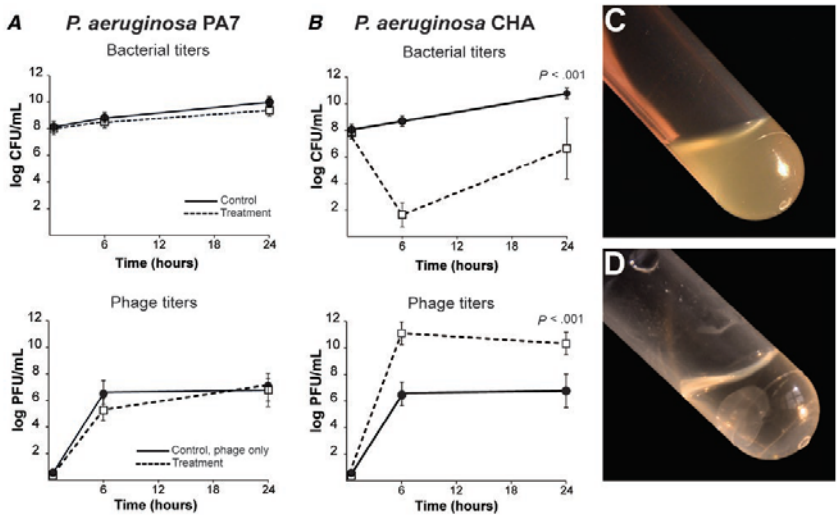

Figure 1. Activity of phage cocktail PP1131 in in vitro fibrin clots. Clots were produced from rat plasma and infected with 10^8 colony-forming units (CFUs)/mL of either phage-resistant *Pseudomonas aeruginosa* strain PA7 (*A*) or phage-susceptible strain CHA (*B*). Clots were left untreated (solid lines) or exposed to 10^8 PFUs/mL of PP1131 for 24 hours at 37°C (dashed lines). Phage titers in noninfected clots (solid lines) and in PA7-infected or CHA-infected clots (dashed lines) were determined 6 hours and 24 hours after exposure to the phage cocktail. Clots infected with strain PA7 lysed in spite of phage treatment (*C*), whereas those infected with phage-susceptible CHA and treated with phages remained intact (*D*). *P* values were determined using the Mann-Whitney test.

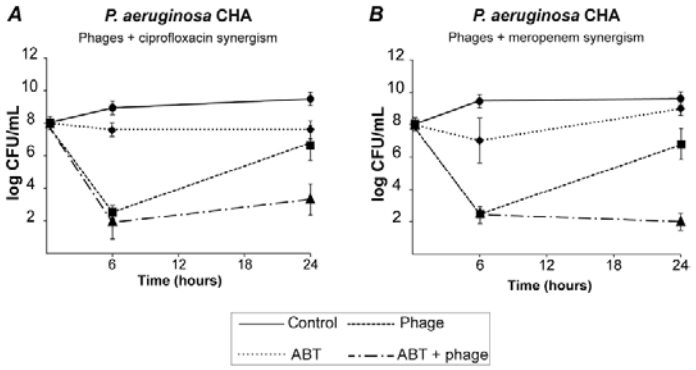

Figure 2. Bactericidal synergism between phages and selected antibiotics. Bacterial killing by phage-antibiotic combinations was tested by using 10^8 PFUs/mL of PP1131 with 2.5-times the minimum inhibitory concentration (MIC) of ciprofloxacin (*A*) or meropenem (*B*) (MIC of 0.19 μg/mL and 0.125 μg/mL, respectively). Each value represents the mean ± SD of 4–16 independent clots. Abbreviation: ABT, antibiotic.

regrowth of phage-resistant mutants after 24 hours (Figure 2A and 2B, dashed dotted lines, respectively). Moreover, the 2 antibiotics were highly synergistic with phages at 24 hours, as defined by a ≥3 log CFUs/mL decrease in bacterial viable counts when compared with single phage or antibiotic therapy alone.

Phage Pharmacokinetics

The pharmacokinetics of the phage cocktail were assessed in the plasma and tissues of noninfected rats with catheter-induced aortic vegetations following a single intravenous bolus injection or during continuous infusion (Figure 3A, solid and dashed line, respectively). A high plasma titer (8.5 ± 1.5 log PFUs/mL) was measured 1 hour after bolus injection, followed by a continuous decrease to 4.9 ± 0.6 log PFUs/mL at 24 hours (elimination half-life = ca 2.3 hours). In parallel, the concentrations of phages in vegetations decreased from 7.5 ± 0.3 to 6.2 ± 0.9 log PFUs/g between 6 hours and 24 hours after administration. A similar tendency was observed in the spleen, kidney, liver, lung, and brain (elimination half-life = ca 9 hours) (Supplementary Figure 3). This demonstrated phage diffusion into the organs and delayed phage clearance compared with plasma. During continuous infusion, phage titers in plasma progressively increased to reach a plateau of 8.5 ± 0.2 log PFUs/mL after 6 hours, which is comparable with to the concentration achieved after 1 hour following bolus injection. Phage concentrations in the vegetations and organs remained high after 24 hours (7.4 ± 0.9 log PFUs/mL) (Supplementary Figure 3).

Treatment of Experimental Endocarditis

Inoculation with 10^8 CFUs of *P. aeruginosa* CHA induced EE with bacterial loads in vegetations of control rats of >8 log CFUs/g 18 hours after bacterial challenge (Figure 3B). Administration of the phage cocktail 18 hours after bacterial challenge by either continuous or bolus injection decreased median vegetation bacterial titers by 3.0 and 2.3 log CFUs/g, respectively, within 6 hours of therapy (Figure 3B) ($P < .0001$ compared with treatment onset). No significant difference between the 2 routes of administration was observed. Notably, a single bolus injection of ciprofloxacin simulating a single oral dose of 750 mg in adults [17] decreased median vegetation bacterial titers by 2.6 log CFUs/g (Figure 3B), which was comparable with phage therapy. Moreover, the combination of phages with ciprofloxacin was highly synergistic, resulting in negative vegetation cultures in 7 of 11 rats receiving combined therapy after 6 hours, as compared with 0 of 28 in phage-alone or ciprofloxacin-alone treated groups (Figure 3B) ($P < .005$). Likewise, the residual median vegetation bacterial titers of ≤2 log CFUs/g in the combined therapy group were significantly lower than the ≥6 log CFUs/g titers detected in the monotherapy groups ($P < .0001$).

In Situ Penetration of Phages in Valve Tissues

Optical microscopy and transmission electron microscopy were performed on vegetation samples to visualize the presence and activity of phages inside the vegetations. Figure 4 presents relevant pictures of these experiments, including intravegetation *P. aeruginosa* in untreated rats (Figure 4A and 4B), negatively stained phages from the cocktail with a capsid size of ca 70 nm (Figure 4C), and intravegetation lysed bacteria in phage-treated rats with bacterial ghosts containing phage particles (Figure 4D).

Correlation Between Phage Multiplication, Antimicrobial Activity, and Cytokine Production

In vivo antibacterial activity correlated with phage amplification (ca 3 log PFUs/g of vegetations) after both continuous and

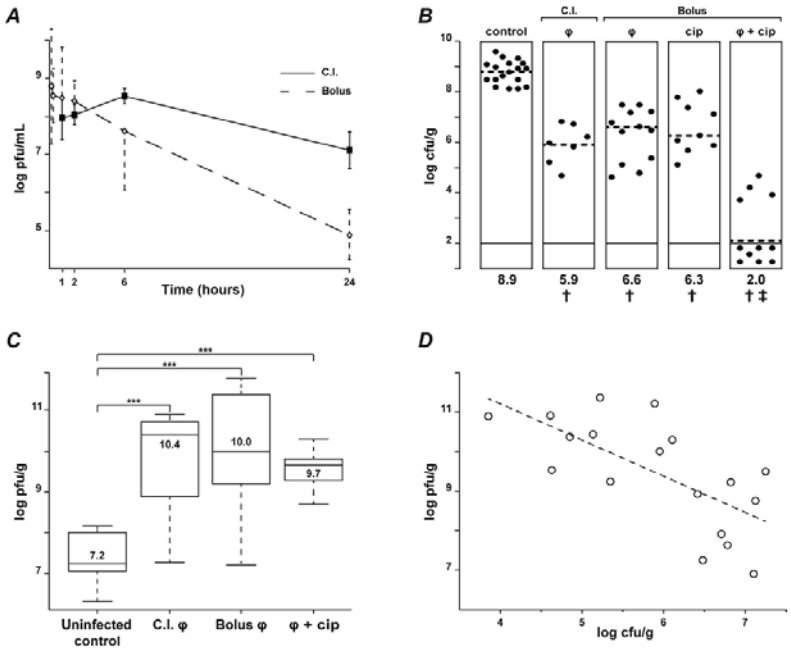

Figure 3. Pharmacokinetics/pharmacodynamics (PK/PD) and therapeutic efficacy of phage cocktail PP1131 and ciprofloxacin in rats with experimental endocarditis (EE) due to *Pseudomonas aeruginosa* CHA. *A*, Pharmacokinetics in the absence of infection of phage cocktail PP1131 in rat plasma after either a single intravenous bolus injection (1 mL of 10^{10} PFUs/mL in 1 minute, dashed line, Bolus) or the same amount of phages administered through continuous infusion (0.1 mL/h of 10^{10} PFUs/mL over 24 hours, solid line: continuous infusion). Each value represents the mean ± SD from 8–10 individual animals. *B*, Bacterial loads of infected vegetations after 6 hours of phage treatment administered through continuous infusion or in single bolus and treatment with ciprofloxacin alone or combined with phages. Each dot represents the vegetation of a single animal. The mode of injection and type of treatment are indicated at the top of columns (C.I.: continuous infusion; φ: phages). Statistical results are indicated at the bottom of columns (†: control vs all types of treatment, $P < .0005$; ‡: combination vs control and all other types of treatments, $P < .0001$; results were compared by the Mann-Whitney test). *C*, Phage titers in vegetations measured in uninfected rats treated with bolus phage injection (control) or infected rats treated with the same regimens as in Figure 2*B* (***, $P < .0001$ using the Mann-Whitney test). *D*, Correlation between the decrease in vegetation bacterial loads and the vegetation phage titers resulting from in situ phage amplification (continuous infusion and bolus injection pooled together; correlation value [*r*] = –0.66; Pearson 2-tailed correlation test: $P = .003$). Abbreviation: cip, ciprofloxacin.

bolus injection (Figure 3C). This relation was further underlined by the scatter plot presented in Figure 3D, which showed a significant inverse correlation between phage and bacterial concentrations in the vegetations (correlation value $r = -0.66$, Pearson 2-tailed correlation test; $P = .003$).

Successful phage therapy also correlated with the production of specific inflammatory cytokines (Figure 5). Concentrations of IL-1β, IL-6, and TNFα in plasma were quantified by Luminex first before inoculation, second before treatment onset, and lastly after 6 hours of phage therapy in uninfected and infected rats (Figure 5A). Several observations were drawn from these measurements. First, although there were trends in cytokine-induction by bacteria and phages alone, these were not statistically significant. Second, TNFα levels remained essentially unaltered in all of the groups throughout the experiment. Finally, only phage treatment, but not ciprofloxacin, significantly increased plasma levels of IL-1β and IL-6 (Figure 5B). Because ciprofloxacin is not bacteriolytic, the increase in IL-1β and IL-6 levels was likely related to phage-induced bacterial lysis.

Phage Resistance in Experimental Endocarditis

Because spontaneous phage-resistant mutants occurred at a rate of 10^{-7} in batch cultures and fibrin clots, they were also expected to emerge in infected vegetations. To test this assumption, phage-resistant mutants were sought in infected valves by plating vegetation extracts directly on agar plates containing preadsorbed phages. Unexpectedly, no phage-resistant mutants could be isolated from the infected vegetations either before or after therapy, therefore suggesting that phage resistance might result in altered virulence or fitness and interfere with successful bacterial survival or growth in vivo. Two resistant isolates recovered from fibrin clots, 19/2 and 24/2, which showed different phage resistance patterns, were further characterized to

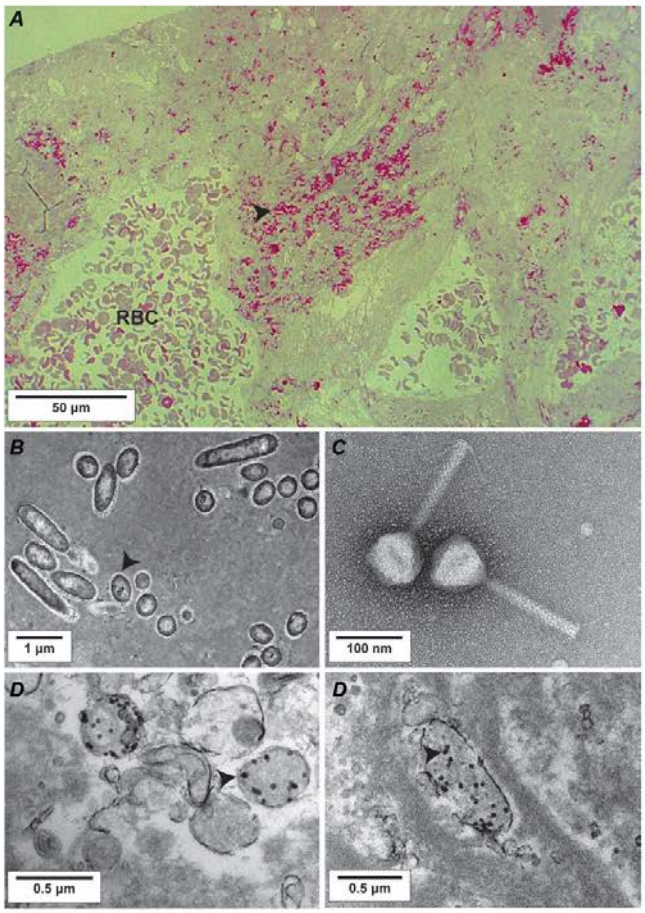

Figure 4. Light microscopy and transmission electron microscopy of rat vegetations after 6 hours of phage therapy. *A*, Semithin section (200 nm) of control vegetation infected with *Pseudomonas aeruginosa* CHA stained using the modified Braun Brenn staining protocol [37]. Arrows indicate bacteria, stained in red. *B*, Transmission electron microscopy of ultrathin sections (50 nm) of control vegetation infected with *P. aeruginosa* CHA positive-stained using uranium acetate and lead citrate. Arrows indicate bacteria. *C*, Example of a negative staining of a myoviridae phage present in the cocktail; other phages morphotypes including podoviridae were also present. *D*, Transmission electron microscopy of vegetation infected by *P. aeruginosa* CHA and treated with the phage cocktail. Arrows indicate phage capsids inside lysed bacteria. Abbreviation: RBC, red blood cell.

verify this hypothesis. Figure 6A shows that these resistant isolates had markedly different phage susceptibility profiles when compared with the parent strain. Mutant 24/2 conferred turbid plaques, whereas mutant 19/2 was resistant to 10 of the 12 phages and displayed a melanized (dark colonies) phenotype.

To determine whether these mutants had altered virulence, they were tested for their capability to infect sterile vegetations. A single bolus of 10^8 CFUs (ie, infective dose 90% of parent strain) led to the infection of <60% ($P < .05$) and <30% ($P < .01$) of vegetations for mutants 19/2 and 24/2, respectively (Figure 6B). Moreover, the median bacterial densities in the infected vegetations were significantly lower than in rats infected with the parent strain (CHA: 8.9 CFUs/g; 24/2: 7.3 CFUs/g; and 19/2: 6.8 CFUs/g; $P < .05$), and blood cultures were negative.

To further investigate the origin of this impaired in vivo infectivity, the genomic DNA of the parent strain CHA and the 2 mutants was sequenced, assembled, and compared (Figure 7A). Mutant 24/2 displayed a 15-basepair deletion at the 3' end of the *pilT* gene (Supplementary Figure 4), which encodes an ATPase involved in motility [25]. As a result, mutant 24/2 exhibited loss

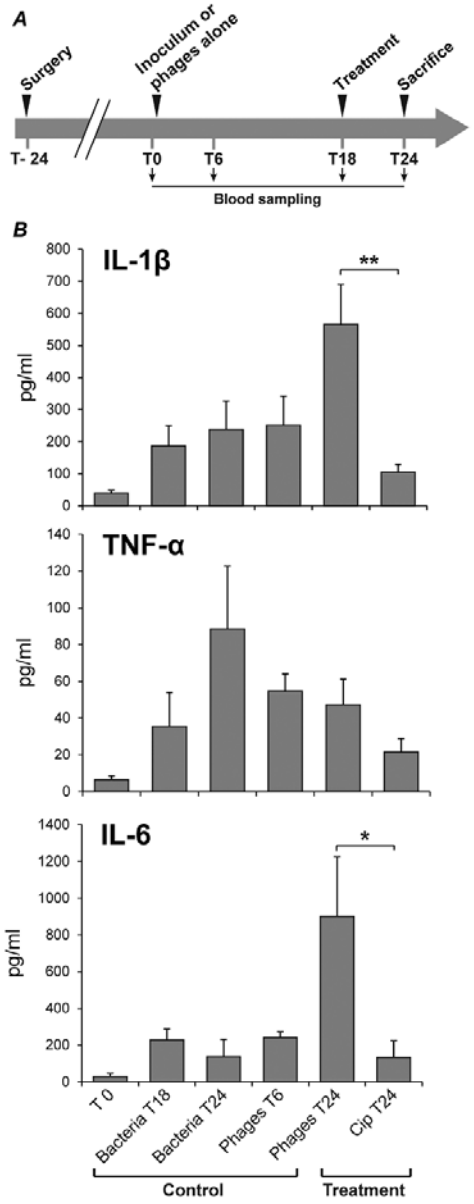

Figure 5. Cytokine quantification in rat plasma during experimental endocarditis. *A*, Protocol of blood sampling for cytokine quantification. *B*, Levels of interleukin 1β (IL-1β), interleukin 6 (IL-6), and tumor necrosis factor α (TNF-α) measured after 6 hours of phage or antibiotherapy (treatment). Controls included rats 24 hours after surgery (inoculum, T0), untreated but infected rats for 18 hours or 24 hours (bacteria T18 and T24), and uninfected rats receiving phage for 6 hours (Phages T6). Each value represents the mean ± SEM from 4–10 individual animals (*, $P = .03$; **, $P = .005$ using the Mann-Whitney test). Abbreviation: cip, ciprofloxacin.

of twitching motility (Figure 7B). Mutant 19/2 had a 362-kb genomic deletion encompassing 342 genes. These included the *galU* gene, which is involved in *P. aeruginosa* LPS core synthesis. *galU* deletion was shown to be responsible for phage resistance [26]. The resulting absence of O antigen and LPS core truncation was confirmed by LPS extraction followed by gel electrophoresis (Figure 7C). Mutant 19/2 also showed a 3-fold decrease in its MIC of ciprofloxacin (0.064 vs 0.192 µg/mL for mutant 19/2 and parent CHA, respectively).

DISCUSSION

Although phage therapy is a promising alternative to antibiotics against specific and difficult-to-treat infections, careful appraisal of its therapeutic potential is an absolute prerequisite before clinical application.

Here we evaluated the in vitro activity of the whole phage cocktail and its individual phage components against a panel of independent *P. aeruginosa* isolates in test tubes and in fibrin clots. This revealed the presence of bacterial strains with opposite susceptibility profiles, either resistant to all of the cocktail's phages (eg, strain PA7) or susceptible to all of them (eg, strain CHA). The frequency of spontaneous phage resistance mutations of the susceptible strain CHA was found to be ca 10^{-7}. This predicted that phage resistance would emerge in infected fibrin clots, which contained $\geq 10^8$ CFUs/g. This was indeed the case. However, these approach experiments highlighted 2 additional important facts. First, phages could readily diffuse into clots, kill the overwhelming majority of phage-susceptible bacteria in situ, and protect the fibrin matrix from bacterial-induced disintegration. Second, combining phages with low concentrations of ciprofloxacin or meropenem (2.5 × the MIC) inhibited the regrowth of phage-resistant mutants, suggesting potential success of in vivo therapy.

The in vivo experiments provided further critical information. Regarding PK/PD parameters, phages were relatively stable in plasma (elimination half-life of ca 2.3 hours following bolus administration) and persisted longer in organs (half-life up to 9 hours). These values were consistent with those observed in previous work [27] and confirmed that phages, whose sizes vary from ca 50 nm to 200 nm, can diffuse into various body compartments [5, 6, 28]. As a result, phages were able to kill bacteria inside valve vegetations and multiply locally by up to 3 log PFUs/g within 6 hours. Phage-induced killing correlated with a burst of IL-1β and IL-6. Because cytokine levels were measured only at a single time point, the data did not permit extrapolating the dynamics of cytokine responses over time. However, the significant increase in IL-1β and IL-6 levels in rats treated with phages—as compared with rats treated with ciprofloxacin—most likely reflected the release of cell debris by phage-mediated lysis. Accordingly, it is known that both cytokines are inducible by LPS [29] and that similar results were obtained in EE using a bactericidal phage lysin [30].

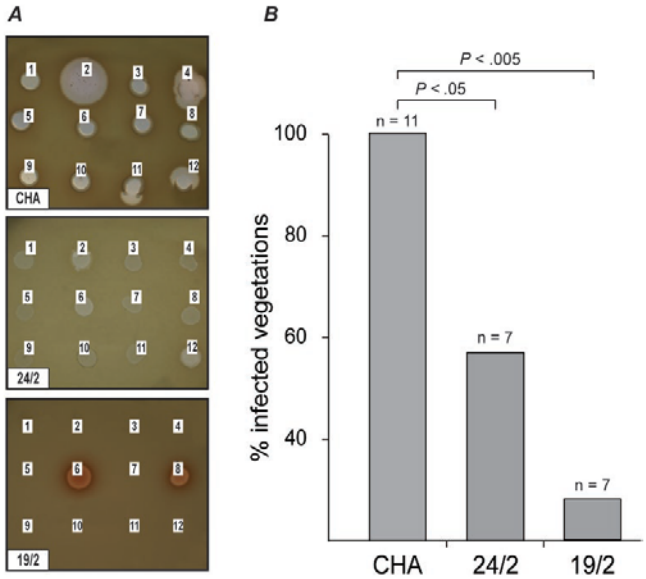

Figure 6. Infectivity of phage-resistant *Pseudomonas aeruginosa* mutants in rats with catheter-induced vegetations. *A*, Two phage resistant *P. aeruginosa* mutants, 24/2 and 19/2, were isolated in vitro from fibrin clots and showed different phage resistance patterns. Lysis zones at the site of the phage deposits indicated phage-sensitivity. The absence of lysis indicated phage resistance. *B*, The isolates' infectivity was tested in rats with catheter-induced vegetations. Both variants showed a loss of infectivity (>40% for 24/2 and >70% for 19/2) as compared with the parent strain CHA. *P* values were determined using Fisher's exact test.

From a therapeutic point of view, the combination of phages with ciprofloxacin exhibited a highly synergistic effect and resulted in 7 of 11 (64%) negative valve cultures within 6 hours. This remarkable result has no precedent in antimicrobial therapy of EE with virtually any drug or pathogen, especially not with *P. aeruginosa* [31–33].

Phage-antibiotic (or PAS) synergism has been formerly reported [34–37]. The mechanism of PAS is proposed to result from antibiotic-induced bacterial elongation, which may facilitate the access of phages to their bacterial target [37]. However, none of the previous PAS studies were done in vivo, and none of them demonstrated the extensive killing of >7 orders of magnitude in 6 hours reported herein [34–37]. Interestingly, phage-resistant subpopulations were readily detected in broth cultures and infected clots, but not in vegetations. This suggests that preexisting phage-resistant mutants might be hampered in vivo, as proposed by others [6, 11, 12, 38, 39].

In fact, the mutations that conferred resistance to the phage cocktail came at a great physiological cost. The present experiments provide 2 examples supporting this notion. Mutant 24/2 exhibited defective cell motility due to disruption of the *pilT* gene, whose product is an ATPase providing energy for type IV pilus contraction and bacterial twitching [25]. Type IV pilus is also a phage receptor, and pilus contraction is believed to bring the phages closer to the bacterial envelope [40]. Mutant 19/2 had a truncated LPS resulting from a large deletion encompassing the *galU* gene involved in the synthesis of the LPS core [26, 41]. LPS can also act as a phage receptor, and its alteration can confer phage resistance [13]. Both type IV pili and LPS are major virulence factors in *P. aeruginosa*, and their mutation can result in attenuated virulence [13, 42]. Thus, while these mutations confer resistance to phages, they may also decrease fitness in animals while preserving normal growth in less stringent in vitro conditions.

Although these observations are promising regarding phage antibacterial activity, caution should be raised as to the use of phage cocktails versus single-phage preparations. Although phage cocktails provide broader strain coverage than single phages, they also carry greater risks of unwanted gene transfer and interphage interference. Ideally phages should be tailored against their target pathogen, and specificity should be preferred to exhaustiveness, just like for antibiotic therapy.

Altogether our results provide a strong proof of concept for phage therapy of deep-seated and systemic infections. Moreover they raise the provocative possibility that certain infections might be cured by a single phage injection most efficiently

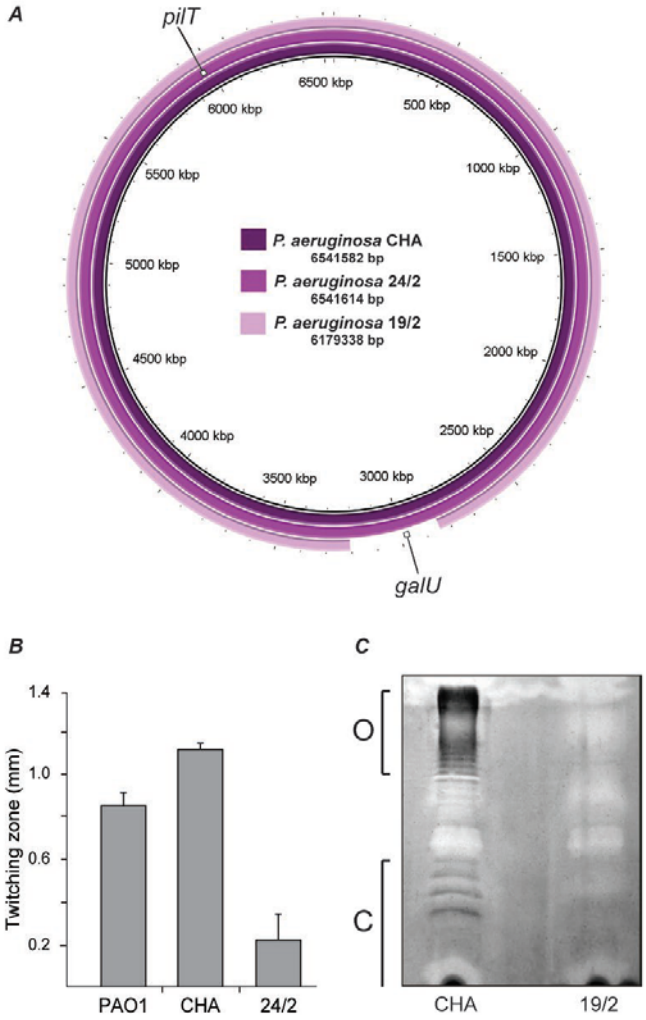

Figure 7. Characterization of phage-resistant *Pseudomonas aeruginosa* mutants. The 2 phage-resistant *P. aeruginosa* mutants, 24/2 and 19/2, isolated in vitro were further characterized regarding to genomic content and phenotypes. *A*, Variant 24/2 displayed a 15-basepair deletion in the *pilT* gene, and variant 19/2 displayed a 362-kb chromosomal deletion that encompassed the *galU* gene. *B*, Impaired twitching motility resulting from the *pilT* alteration in variant 24/2, as compared with wild-type PAO1 and parent CHA. *C*, Impaired LPS synthesis resulting from the *galU* deletion in variant 19/2 with absence of O-antigen (O) and LPS core (C), as compared with parent CHA.

combined with synergistic antibiotics. Indeed, once locally established, phages can multiply in situ and do not necessitate further administration.

Supplementary Data

Supplementary materials are available at *The Journal of Infectious Diseases* online. Consisting of data provided by the authors to benefit the reader, the posted materials are not copyedited and are the sole responsibility of the authors, so questions or comments should be addressed to the corresponding author.

Notes

Acknowledgments. We are indebted to Marlyse Giddey, Matthew Parkan, Sara Mitri, Glib Mazepa, Shawna McCallin, Jean Daraspe, and Gilles Willemen for their invaluable technical support and fruitful discussions.

Financial support. This work was supported in part by the Swiss National Research Foundation (CR31I3_166124 to Y. A. Q.,

310030-143799 to J. M. E.) and the European Commission research grant (FP7-PHAGOBURN to Y. A. Q.). This work was also supported by a non-restricted grant from the Loterie Suisse Romande (to Y. A. Q.). The funders had no role in study design, data collection and interpretation, or the decision to submit the work for publication.

Potential conflict of interest. J. G. is employed by the commercial company Pherecydes Pharma as COO. The bacteriophage cocktail PP1131 used in this study is produced under license by the company Pherecydes Pharma and used in a human clinical trial (Phagoburn, NCT02116010, http://www.phagoburn.eu/). Y. A. Q. is coinvestigator in the clinical trial Phagoburn, which uses the PP1131 bacteriophage cocktail. All authors have submitted the ICMJE Form for Potential Conflicts of Interest. Conflicts that the editors consider relevant to the content of the manuscript have been disclosed.

References

1. Chanishvili N. Phage therapy—history from Twort and d'Herelle through Soviet experience to current approaches. Adv Virus Res 2012; 83:3–40.
2. Abedon ST. Phage therapy of pulmonary infections. Bacteriophage 2015; 5:e1020260.
3. Lang G, Kehr P, Mathevon H, Clavert JM, Séjourne P, Pointu J. Bacteriophage therapy of septic complications of orthopaedic surgery. Rev Chir Orthop Reparatrice Appar Mot 1979; 65:33–7.
4. Speck P, Smithyman A. Safety and efficacy of phage therapy via the intravenous route. FEMS Microbiol Lett 2016; 363.
5. Chhibber S, Kaur S, Kumari S. Therapeutic potential of bacteriophage in treating *Klebsiella pneumoniae* B5055-mediated lobar pneumonia in mice. J Med Microbiol 2008; 57:1508–13.
6. Pouillot F, Chomton M, Blois H, et al. Efficacy of bacteriophage therapy in experimental sepsis and meningitis caused by a clone O25b:H4-ST131 *Escherichia coli* strain producing CTX-M-15. Antimicrob Agents Chemother 2012; 56:3568–75.
7. Marza JA, Soothill JS, Boydell P, Collyns TA. Multiplication of therapeutically administered bacteriophages in *Pseudomonas aeruginosa* infected patients. Burns 2006; 32:644–6.
8. Wright A, Hawkins CH, Anggård EE, Harper DR. A controlled clinical trial of a therapeutic bacteriophage preparation in chronic otitis due to antibiotic-resistant *Pseudomonas aeruginosa*; a preliminary report of efficacy. Clin Otolaryngol 2009; 34:349–57.
9. Rhoads DD, Wolcott RD, Kuskowski MA, Wolcott BM, Ward LS, Sulakvelidze A. Bacteriophage therapy of venous leg ulcers in humans: results of a phase I safety trial. J Wound Care 2009; 18:237–8, 40–3.
10. Labrie SJ, Samson JE, Moineau S. Bacteriophage resistance mechanisms. Nat Rev Microbiol 2010; 8:317–27.
11. Lenski RE. Experimental studies of pleiotropy and epistasis in *Escherichia coli* variation in competitive fitness among mutants resistant to virus T4. Evolution 1988; 42:425–32.
12. Scanlan PD, Buckling A, Hall AR. Experimental evolution and bacterial resistance: (co)evolutionary costs and trade-offs as opportunities in phage therapy research. Bacteriophage 2015; 5:e1050153.
13. Le S, Yao X, Lu S, et al. Chromosomal DNA deletion confers phage resistance to *Pseudomonas aeruginosa*. Sci Rep 2014; 4:4738.
14. Que YA, Moreillon P. Infective endocarditis. Nat Rev Cardiol 2011; 8:322–36.
15. Clokie MRJ, Kropinski AM. Bacteriophages. Methods and protocols. Volume 1: Isolation, characterization, and interactions. New York: Humana Press, 2009.
16. Entenza JM, Haldimann A, Giddey M, Lociuro S, Hawser S, Moreillon P. Efficacy of iclaprim against wild-type and thymidine kinase-deficient methicillin-resistant *Staphylococcus aureus* isolates in an in vitro fibrin clot model. Antimicrob Agents Chemother 2009; 53:3635–41.
17. Entenza JM, Vouillamoz J, Glauser MP, Moreillon P. Levofloxacin versus ciprofloxacin, flucloxacillin, or vancomycin for treatment of experimental endocarditis due to methicillin-susceptible or -resistant *Staphylococcus aureus*. Antimicrob Agents Chemother 1997; 41:1662–7.
18. Broskey NT, Daraspe J, Humbel BM, Amati F. Skeletal muscle mitochondrial and lipid droplet content assessed with standardized grid sizes for stereology. J App Physio 2013; 115:765–70.
19. Taylor RD. Modification of the Brown and Brenn gram stain for the differential staining of gram-positive and gram-negative bacteria in tissue sections. Am J Clin Pathol 1966; 46:472–4.
20. Meyer F, Goesmann A, McHardy AC, et al. GenDB—an open source genome annotation system for prokaryote genomes. Nucleic Acids Res 2003; 31:2187–95.
21. Altschul SF, Gish W, Miller W, Myers EW, Lipman DJ. Basic local alignment search tool. J Mol Biol 1990; 215:403–10.
22. Alikhan NF, Petty NK, Ben Zakour NL, Beatson SA. BLAST ring image generator (BRIG): simple prokaryote genome comparisons. BMC Genomics 2011; 12:402.
23. Semmler AB, Whitchurch CB, Mattick JS. A re-examination of twitching motility in *Pseudomonas aeruginosa*. Microbiology 1999; 145:2863–73.
24. Zhu ZX, Cong WT, Ni MW, et al. An improved silver stain for the visualization of lipopolysaccharides on polyacrylamide gels. Electrophoresis 2012; 33:1220–3.
25. Mattick JS. Type IV pili and twitching motility. Annu Rev Microbiol 2002; 56:289–314.
26. Dean CR, Goldberg JB. *Pseudomonas aeruginosa* galU is required for a complete lipopolysaccharide core and repairs a secondary mutation in a PA103 (serogroup O11) wbpM mutant. FEMS Microbiol Lett 2002; 210:277–83.
27. Merril CR, Biswas B, Carlton R, et al. Long-circulating bacteriophage as antibacterial agents. Proc Natl Acad Sci U S A 1996; 93:3188–92.
28. Górski A, Wazna E, Dabrowska BW, Dabrowska K, Switała-Jeleń K, Miedzybrodzki R. Bacteriophage translocation. FEMS Immunol Med Microbiol 2006; 46:313–9.
29. de Bont N, Netea MG, Rovers C, et al. LPS-induced release of IL-1 beta, IL-1Ra, IL-6, and TNF-alpha in whole blood from patients with familial hypercholesterolemia: no effect of cholesterol-lowering treatment. J Interferon Cytokine Res 2006; 26:101–7.
30. Entenza JM, Loeffler JM, Grandgirard D, Fischetti VA, Moreillon P. Therapeutic effects of bacteriophage Cpl-1 lysin against *Streptococcus pneumoniae* endocarditis in rats. Antimicrob Agents Chemother 2005; 49:4789–92.
31. Papadakis JA, Samonis G, Maraki S, Boutsikakis J, Petrocheilou V, Saroglou G. Efficacy of amikacin, ofloxacin, pefloxacin, ciprofloxacin, enoxacin and fleroxacin in experimental left-sided *Pseudomonas aeruginosa* endocarditis. Chemotherapy 2000; 46:116–21.
32. Bayer AS, Norman D, Kim KS. Efficacy of amikacin and ceftazidime in experimental aortic valve endocarditis due to *Pseudomonas aeruginosa*. Antimicrob Agents Chemother 1985; 28:781–5.
33. Robaux MA, Dube L, Caillon J, et al. In vivo efficacy of continuous infusion versus intermittent dosing of ceftazidime alone or in combination with amikacin relative to human kinetic profiles in a *Pseudomonas aeruginosa* rabbit endocarditis model. J Antimicrob Chemother 2001; 47:617–22.
34. Ryan EM, Alkawareek MY, Donnelly RF, Gilmore BF. Synergistic phage-antibiotic combinations for the control of *Escherichia coli* biofilms in vitro. FEMS Immunol Med Microbiol 2012; 65:395–8.
35. Knezevic P, Curcin S, Aleksic V, Petrusic M, Vlaski L. Phage-antibiotic synergism: a possible approach to combatting *Pseudomonas aeruginosa*. Res Microbiol 2013; 164:55–60.
36. Kamal F, Dennis JJ. Burkholderia cepacia complex phage-antibiotic synergy (PAS): antibiotics stimulate lytic phage activity. Appl Environ Microbiol 2015; 81:1132–8.
37. Comeau AM, Tétart F, Trojet SN, Prère MF, Krisch HM. Phage-antibiotic synergy (PAS): beta-lactam and quinolone antibiotics stimulate virulent phage growth. PLoS One 2007; 2:e799.
38. Scanlan PD, Hall AR, Blackshields G, et al. Coevolution with bacteriophages drives genome-wide host evolution and constrains the acquisition of abiotic-beneficial mutations. Mol Biol Evol 2015; 32:1425–35.
39. Smith HW, Huggins MB, Shaw KM. The control of experimental *Escherichia coli* diarrhoea in calves by means of bacteriophages. J Gen Microbiol 1987; 133:1111–26.
40. Bradley DE. Shortening of *Pseudomonas aeruginosa* pili after RNA-phage adsorption. J Gen Microbiol 1972; 72:303–19.
41. Rodríguez-Rojas A, Mena A, Martín S, Borrell N, Oliver A, Blázquez J. Inactivation of the hmgA gene of *Pseudomonas aeruginosa* leads to pyomelanin hyperproduction, stress resistance and increased persistence in chronic lung infection. Microbiology 2009; 155:1050–7.
42. Comolli JC, Hauser AR, Waite L, Whitchurch CB, Mattick JS, Engel JN. *Pseudomonas aeruginosa* gene products PilT and PilU are required for cytotoxicity in vitro and virulence in a mouse model of acute pneumonia. Infect Immun 1999; 67:3625–30.

SUPPLEMENTARY FIGURES

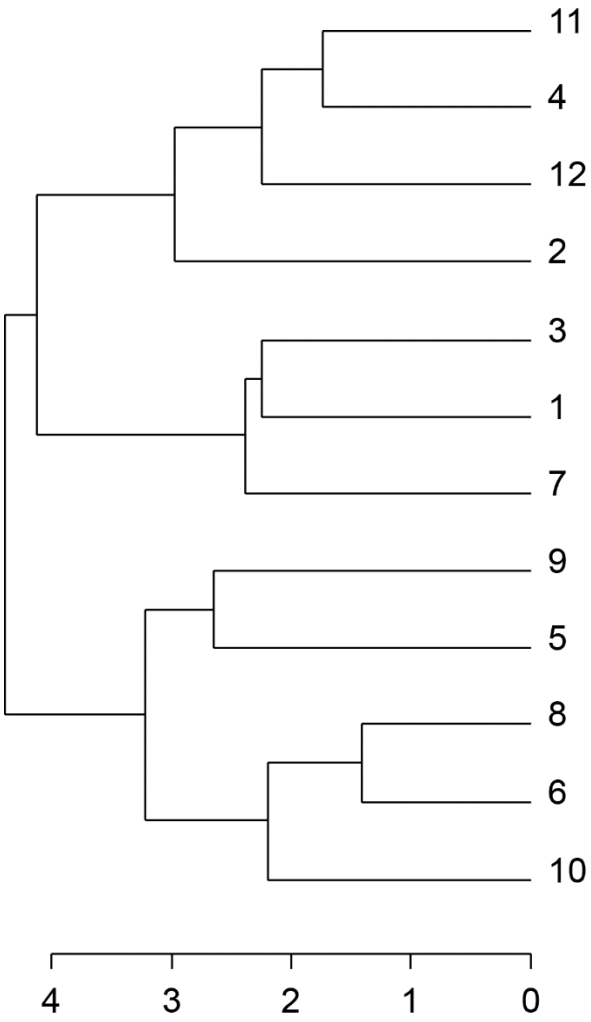

Supplementary Figure 1. Infectivity relatedness of the different phages of the PP1131 cocktail. The 12 phages present in the cocktail were evaluated by statistical analysis regarding the similarity of their host range. A distance matrix was produced according to the results presented in Supplementary Table 2 and hierarchical clustering was used to produce a dendrogram that schematizes the similarity between the different phages according to their infectivity. The horizontal axis indicates relative distance (or dissimilarity) between phage clusters. Thus, when looking at branching

points (i.e. clusters), high values indicate high dissimilarity and low values indicate low dissimilarity.

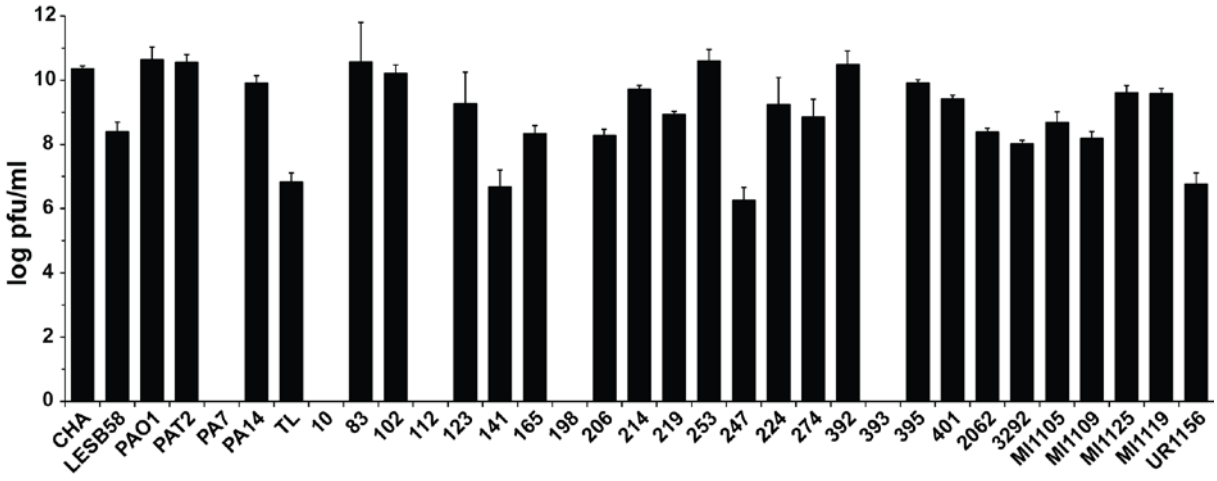

Supplementary Figure 2. Host range of the PP1131 cocktail regarding different *P. aeruginosa* isolates. The host range of the cocktail was evaluated against a panel of 33 laboratory and clinical *P. aeruginosa* isolates using a plaque assay method. By using this technique, the phage cocktail achieved a productive infection in 28/33 (84%) of the strains with a phage titer ranging from c.a. 6 to 10 log pfu/ml. Experiments were done in triplicate.

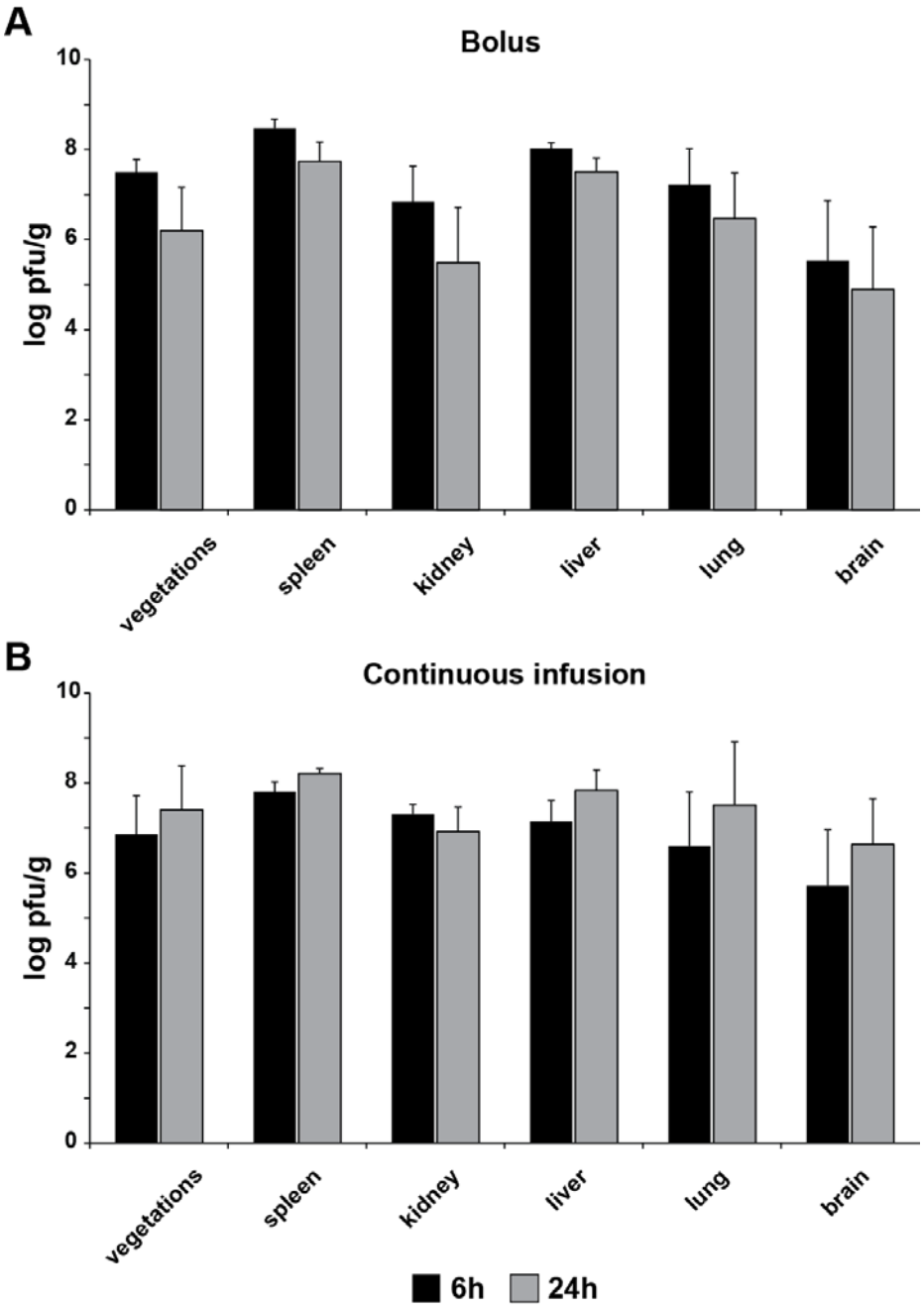

Supplementary Figure 3. Pharmacokinetics of phage cocktail PP1141 in uninfected rat organs. Phage titers were measured 6 h or 24 h after treatment onset (black and grey, respectively) in rat vegetations, spleens, kidneys, livers, lungs, and brains after either (A) a single i.v. bolus injection of 10^{10} PFU of the cocktail or (B) the same amount of phages administered through continuous infusion. Each value represents the mean +/- SD from 8 to 10 individual animals.

```
CHA     MDITELLAFSAKQGASDLHLSAGLPPMIRVDGDVRRINLPPLEHKQVHALIYDIMNDKQR 60
24/2    MDITELLAFSAKQGASDLHLSAGLPPMIRVDGDVRRINLPPLEHKQVHALIYDIMNDKQR 60
        ************************************************************

CHA     KDFEEFLETDFSFEVPGVARFRVNAFNQNRGAGAVFRTIPSKVLTMEELGMGEVFKRVSD 120
24/2    KDFEEFLETDFSFEVPGVARFRVNAFNQNRGAGAVFRTIPSKVLTMEELGMGEVFKRVSD 120
        ************************************************************

CHA     VPRGLVLVTGPTGSGKSTTLAAMLDYLNNTKYHHILTIEDPIEFVHESKKCLVNQREVHR 180
24/2    VPRGLVLVTGPTGSGKSTTLAAMLDYLNNTKYHHILTIEDPIEFVHESKKCLVNQREVHR 180
        ************************************************************

CHA     DTLGFSEALRSALREDPDIILVGEMRDLETIRLALTAAETGHLVFGTLHTTSAAKTIDRV 240
24/2    DTLGFSEALRSALREDPDIILVGEMRDLETIRLALTAAETGHLVFGTLHTTSAAKTIDRV 240
        ************************************************************

CHA     VDVFPAEEKAMVRSMLSESLQSVISQTLIKKIGGGRVAAHEIMIGTPAIRNLIREDKVAQ 300
24/2    VDVFPAEEKAMVRSMLSESLQSVISQTLIKKIGGGRVAAHEIMIGTPAIRNLIREDKVAQ 300
        ************************************************************

CHA     MYSAIQTGGSLGMQTLDMCLKGLVAKGLISRENAREKAKIPENF- 344
24/2    MYSAIQTGGSLGMQTLDMCLK-----GLISRENAREKAKIPENF- 339
        **********************     ******************
```

Supplementary Figure 4. Alignment of *pilT* present in the parent strain CHA and the variant 24/2.

Pairwise alignment using Clustal Omega.

SUPPLEMENTARY TABLES

Supplementary Table 1. Bacterial strains used in this study.

Pseudomonas strains	Characteristics and/or source
PAO1	Burn wound isolate[a]
CHA	Cystic fibrosis isolate[a]
LESB 58	Cystic fibrosis , -lactam resistant, Gmr Azr Imr[a]
PAT2	Burn wound isolate[a]
PA7	Non-respiratory human isolate[a]
PA14	Wild type, UCBPP-PA14, human isolate[a]
TL	Clinical isolate[b]
10	Bacteremia[b]
83	Bacteremia[b]
102	Bronchosaspiration[b]
112	Peritoneal liquid[b]
123	Hemoculture[b]
141	Skin biopsy[b]
165	Bronchoalveolar lavage [b]
198	Urine[b]
206	Ureteral swab[b]
214	Peritoneal liquid[b]
219	Hemoculture[b]
253	Urine[b]
247	Peritoneal liquid[b]
224	Skin[b]
274	Hemoculture[b]

392	Hemoculture[b]
393	Hemoculture[b]
395	Hemoculture[b]
401	Hemoculture[b]
2062	Hemoculture[b]
3292	Hemoculture[b]
MI1105	Skin biopsy[b]
MI1109	Skin swab[b]
MI1125	Skin swab[b]
MI1119	Hemoculture[b]
UR1156	Urine[b]

[a] Kindly provided by C. Reimmann. [b] Isolated from different geographical areas.

Supplementary Table 2. *P. aeruginosa* host range of individual bacteriophages composing the PP1131 cocktail.

Phages													
Isolates	1	2	3	4	5	6	7	8	9	10	11	12	C
CHA	S	S	S	S	S	S	S	S	S	S	S	S	S
LESB58	S	S	S	R	R	S	S	S	S	S	S	S	S
PAO1	S	S	S	S	S	S	S	S	S	S	S	S	S
PAT2	S	S	S	S	S	S	S	S	S	S	S	S	S
PA7	R	R	R	R	R	R	R	R	R	R	R	R	R
PA14	R	R	S	R	R	S	S	S	S	S	S	R	S
TL	S	R	S	R	S	S	S	S	S	S	R	S	S
10	R	R	R	R	R	R	R	R	R	R	R	R	R
83	S	S	S	S	S	S	S	S	S	S	S	S	S
102	S	R	S	S	S	S	S	S	S	S	S	S	S
112	S	R	S	R	S	R	R	R	R	R	R	R	S
123	S	S	S	S	S	S	R	S	S	S	S	S	S
141	R	R	S	S	S	S	S	S	R	S	S	S	S
165	S	S	S	S	S	R	R	S	S	R	S	S	S
198	R	S	R	R	R	S	R	S	R	R	R	R	S
206	S	R	S	S	R	S	S	S	S	S	S	R	S
214	S	S	S	S	S	S	S	S	S	S	S	S	S
219	R	S	R	S	R	R	R	R	R	R	R	R	S
253	S	S	S	S	S	S	S	S	S	S	S	S	S
247	S	S	S	S	S	S	S	S	S	S	S	S	S
224	R	R	S	S	S	S	R	S	S	S	S	R	S
274	R	S	R	S	S	S	R	S	S	S	S	S	S
392	S	S	S	S	R	R	S	S	R	S	S	S	S

393	S	R	S	R	R	R	S	R	S	R	R	R	S
395	R	R	S	R	S	S	R	S	S	S	R	R	S
401	S	R	S	S	S	S	S	S	S	S	S	S	S
2062	S	S	S	S	S	S	S	S	S	S	S	S	S
3292	R	S	S	S	S	S	S	S	S	S	S	S	S
MI1105	S	S	S	S	S	S	S	S	S	S	S	S	S
MI1109	S	S	S	S	S	S	S	S	S	S	S	S	S
MI1125	S	S	S	S	R	S	S	S	R	R	S	S	S
MI1119	S	S	S	S	S	S	S	S	S	S	S	S	S
UR1156	R	R	R	R	R	S	R	S	R	R	R	R	S

The host range of the 12 individual phages composing the PP1131 cocktail was evaluated against a panel of 33 laboratory and clinical *P. aeruginosa* isolates using the spot assay method. Lysis zones around phage deposits indicated phage-sensitivity and were recorded as “S” for Sensitive. Absence of lysis indicated phage-resistance and was recorded as “R” for Resistant. *P. aeruginosa* strain PA7 and strain 10 were resistant to the 12 phages of the cocktail, whereas each of the 31 remaining isolates could be lysed by at least two different phages. Same results were observed for the whole bacteriophage cocktail PP1131 (referred as C).

Supplementary Table 3. Frequencies of phage resistance in *in vitro* fibrin clots.

Phages	Broth culture	Clots 6 h Control	Clots 24 h Control	Clots 6 h Phages	Clots 24 h Phages
1	$5.3 \cdot 10^{-7}$	$6.1 \cdot 10^{-7}$	$5.3 \cdot 10^{-7}$	$1.7 \cdot 10^{-4}$	$3.2 \cdot 10^{-3}$
2	$5.9 \cdot 10^{-7}$	$8.7 \cdot 10^{-8}$	$1.7 \cdot 10^{-7}$	$2.5 \cdot 10^{-4}$	$2.1 \cdot 10^{-1}$
3	$5.8 \cdot 10^{-7}$	$1.4 \cdot 10^{-7}$	$1.9 \cdot 10^{-7}$	$1.4 \cdot 10^{-4}$	$5.7 \cdot 10^{-3}$
4	$5.0 \cdot 10^{-7}$	$3.6 \cdot 10^{-7}$	$2.0 \cdot 10^{-7}$	$2.0 \cdot 10^{-4}$	$1.7 \cdot 10^{-1}$
5	$6.6 \cdot 10^{-7}$	$2.6 \cdot 10^{-7}$	$8.0 \cdot 10^{-7}$	$3.0 \cdot 10^{-4}$	$1.4 \cdot 10^{-3}$
6	$5.1 \cdot 10^{-7}$	$5.6 \cdot 10^{-7}$	$1.7 \cdot 10^{-7}$	$2.7 \cdot 10^{-4}$	$6.8 \cdot 10^{-3}$
7	$7.4 \cdot 10^{-7}$	$6.8 \cdot 10^{-7}$	$2.0 \cdot 10^{-7}$	$1.7 \cdot 10^{-4}$	$1.3 \cdot 10^{-1}$
8	$5.9 \cdot 10^{-7}$	$2.3 \cdot 10^{-7}$	$8.3 \cdot 10^{-7}$	$2.5 \cdot 10^{-4}$	$1.6 \cdot 10^{-2}$
9	$4.1 \cdot 10^{-7}$	$8.0 \cdot 10^{-8}$	$3.0 \cdot 10^{-7}$	$1.2 \cdot 10^{-4}$	$1.5 \cdot 10^{-3}$
10	$4.1 \cdot 10^{-7}$	$1.2 \cdot 10^{-6}$	$1.7 \cdot 10^{-7}$	$1.4 \cdot 10^{-4}$	$5.9 \cdot 10^{-2}$
11	$4.2 \cdot 10^{-7}$	$5.0 \cdot 10^{-7}$	$1.4 \cdot 10^{-7}$	$1.9 \cdot 10^{-4}$	$8.5 \cdot 10^{-3}$
12	$7.1 \cdot 10^{-7}$	$6.0 \cdot 10^{-7}$	$3.4 \cdot 10^{-7}$	$1.8 \cdot 10^{-4}$	$8.5 \cdot 10^{-2}$
Mean	$5.6 \cdot 10^{-7}$	$4.4 \cdot 10^{-7}$	$3.4 \cdot 10^{-7}$	$1.6 \cdot 10^{-4}$	$5.9 \cdot 10^{-2}$

The frequencies of phage resistance were measured in the bacterial populations isolated during *in vitro* phage therapy for each of the 12 individual phages of the PP1131 cocktail. Serial dilutions of bacteria were plated on Petri dishes with a saturating amount of absorbed phages (10^{10} PFU).

SUPPLEMENTARY METHODS

Strains, phage cocktail and antibiotics. Strain CHA was selected for further *in vivo* studies. All strains were grown at 37°C with aeration (200 rpm) either in tryptic soy broth (TSB; Difco™, Becton Dickinson, Sparks, MD, USA) or on tryptic soy blood agar (TSA) plates (bioMérieux SA, Marcy l'Etoile, France). The cocktail PP1131, composed of 12 different phages, was manufactured and provided by Pherecydes Pharma (PHERECYDES PHARMA, Biocitech, Romainville, France). Ciprofloxacin (Bayer AG, Zurich, Switzerland) and meropenem (Labatec Pharma, Meyrin, Switzerland) were purchased commercially.

***In vitro* studies**. The host range of the individual phages composing the PP1131 cocktail was determined using spot assays [34]. Experiments were done in triplicates. Plasma clots were prepared in 96-well microplates, as previously described [15]. The resulting clots (mean weight of 0.1 ± 0.01 g) were transferred into 5 ml polypropylene round-bottom tubes containing 500 µl of either saline (sterile solution of 0.9% NaCl in water), or saline plus the phage cocktail (10^8 PFU/ml), antibiotics (0.47 µg/ml of ciprofloxacin or 0.31 µg/ml of meropenem), or combinations of phages and antibiotics and incubated with shaking at 37°C. Clots were removed after 0, 6 and 24 h of incubation, washed with saline, and lysed with 25 µl of trypsin (20 mg/ml; Sigma-Aldrich, Saint Louis, MO, USA). After 5 min of centrifugation at 14'000 rpm, the supernatant was removed for phage titration, and the cell pellet was resuspended in the initial volume of saline and plated for colony counting. The removal of supernatant plus the dilution procedure minimized the potential of phage carryover. Phage titers

were measured by plaque assays [34]. The activity of the phage cocktail was considered bactericidal when it killed ≥ 3 log CFU of the starting inoculum in the clot.

Animal studies. Experiments were approved by and in adherence with the guidelines of the Swiss Animal Protection Law, Veterinary office, State of Vaud. Experiments were performed under license number 879.9 and in accordance with the regulations of the cantonal committee on animal experimentation of the State of Vaud, Switzerland.

A mixture of ketamine (75 mg/kg) and midazolam (5 mg/kg) anaesthetics was administered to the animals before any surgical procedure. The production of catheter-induced aortic vegetations and the installation of an i.v. line into the superior vena cava, connected to an infusion pump to deliver the phage cocktail, were performed in female Wistar rats as previously described [16].

Twenty-four hours after catheterization, rats were inoculated i.v. with 10^8 CFU *P. aeruginosa* CHA. Eighteen hours later, animals were treated with: (i) a single i.v. bolus (1 ml in 1 min) of phages cocktail at 10^{10} PFU/ml; (ii) the same concentration of phages progressively infused at a pace of 100 µl/h; (iii) a single i.v. bolus (1 ml in 1 min) of ciprofloxacin to a total of 20 mg/kg (mimicking human-like kinetics of a single oral dose of 750 mg [16]) ; and (iv) a combination of single boluses of phage cocktail and ciprofloxacin. Ciprofloxacin was chosen for the *in vivo* studies because, like phages, it exhibits a rapid bactericidal activity. Control rats were euthanized at the onset of therapy and treated rats 6 h after treatment onset.

Plasma pharmacokinetics were determined in catheterized, but uninfected rats using the different modes of treatment described above. For phages, blood samples were collected 1, 2, 6 and 24 h after phage administration. For ciprofloxacin, blood samples

were collected 30 min and 6 h after treatment onset. Vegetations and organs (spleen, liver, kidney, lung, and brain) were collected after 6 and 24 h and homogenized in PBS. Phage titers in plasma and organs were assessed using the plaque assay method as described above. Ciprofloxacin concentrations were determined by the agar diffusion assay with antibiotic medium 1 (Difco; Becton Dickinson), using *Bacillus subtilis* ATCC 6633 as an indicator, as previously described [16]. Standard solutions were prepared in rat plasma.

Detection and characterization of phage resistance. Bacteria grown in broth cultures and bacteria isolated from *in vitro* fibrin clots or rat vegetations were serially diluted and plated on blood agar plates containing 10^{10} PFU pre-absorbed phages. The procedure was done separately for each phage composing the cocktail. After overnight incubation at 37°C, phage-resistant colonies were enumerated. To detect possible slow growing colonies, plates were observed for an additional 48 h at room temperature. Resistance rates were determined as the number of bacteria growing on plates pre-adsorbed with phages divided by the number of bacteria growing on plain plates. Two phage-resistant variants obtained *in vitro* from the fibrin clots were further assessed for their *in vivo* infectivity by inoculating rats with catheter-induced aortic vegetations i.v. with 10^8 CFU of either the *P. aeruginosa* CHA parent strain or the phage-resistant variants. Eighteen hours later, rats were euthanized and bacterial burden in vegetations were quantified, as previously described.

Full genomic DNA sequencing of the two phage-resistant variants and the parent strain CHA was performed by the core sequencing facility of the Center for Integrative Genomics (CIG; University of Lausanne, Switzerland) using the Pacific Biosciences

RSII platform (Pacific Bioscience, Menlo Park, CA). Total DNA was extracted using the DNeasy Blood and Tissue kit (Qiagen, Valencia, CA, USA) according to manufacturer's instructions. After assembly, open reading frames (ORFs) were extracted from contigs using the GenDB open source genome annotation system [37] and the ORFeome of the parent strain CHA was used as a reference for BLASTn [38] comparison. ORFs in the two mutants showing < 100% identity to ORFs present in the parent strain were identified and analyzed. Circular visualization for the comparison of ORFeomes of the parent strain and the two mutants was done using BLAST Ring Image Generator (BRIG) [39]. Subsurface twitching motility tests were performed as described [40]. LPS was extracted using the iNTRON LPS extraction kit (iNtRON biotechnology, Daejeon, South Korea), resolved on NuPAGE 4-12% BisTris gels (Invitrogen, Carlsbad, CA, USA), and silver stained according to [41].

Statistical analyses. A hierarchical clustering based on the Euclidean distance of binary host infection arrays was used to evaluate the similarity of the phages composing the cocktail. The Mann Whitney test was used to examine differences in bacterial or phage counts between the control and the treated groups. The Pearson two-tailed correlation test was used to examine the relation between phage and bacterial concentrations *in vivo*. The difference in infectivity between the wild type CHA strain and the resistant variants was assessed with the Fisher's exact test. A *p*-value < 0.05 was considered as statistically significant.

References

1. Taylor LH, Latham SM, Woolhouse ME. Risk factors for human disease emergence. Philosophical transactions of the Royal Society of London Series B, Biological sciences. 2001;356(1411):983-9. Epub 2001/08/23. doi: 10.1098/rstb.2001.0888. PubMed PMID: 11516376; PubMed Central PMCID: PMCPMC1088493.

2. Wertheim HF, Walsh E, Choudhurry R, Melles DC, Boelens HA, Miajlovic H, et al. Key role for clumping factor B in Staphylococcus aureus nasal colonization of humans. PLoS medicine. 2008;5(1):e17. Epub 2008/01/18. doi: 10.1371/journal.pmed.0050017. PubMed PMID: 18198942; PubMed Central PMCID: PMCPMC2194749.

3. Tong SY, Davis JS, Eichenberger E, Holland TL, Fowler VG, Jr. Staphylococcus aureus infections: epidemiology, pathophysiology, clinical manifestations, and management. Clinical microbiology reviews. 2015;28(3):603-61. Epub 2015/05/29. doi: 10.1128/cmr.00134-14. PubMed PMID: 26016486; PubMed Central PMCID: PMCPMC4451395.

4. Gordon RJ, Lowy FD. Pathogenesis of Methicillin-Resistant Staphylococcus aureus Infection. Clinical infectious diseases : an official publication of the Infectious Diseases Society of America. 2008;46(Suppl 5):S350-9. doi: 10.1086/533591. PubMed PMID: 18462090; PubMed Central PMCID: PMCPMC2474459.

5. Weese JS. Methicillin-resistant Staphylococcus aureus in animals. ILAR journal. 2010;51(3):233-44. Epub 2010/12/07. PubMed PMID: 21131724.

6. Deb R, Kumar A, Chakraborty S, Verma AK, Tiwari R, Dhama K, et al. Trends in diagnosis and control of bovine mastitis: a review. Pakistan journal of biological sciences : PJBS. 2013;16(23):1653-61. Epub 2014/02/11. PubMed PMID: 24506032.

7. JA L. Staphylococcus Molecular Genetics: Caister Academic Press; 2008.

8. Alibayov B, Baba-Moussa L, Sina H, Zdenkova K, Demnerova K. Staphylococcus aureus mobile genetic elements. Molecular biology reports. 2014;41(8):5005-18. Epub 2014/04/15. doi: 10.1007/s11033-014-3367-3. PubMed PMID: 24728610.

9. Novick RP, Subedi A. The SaPIs: mobile pathogenicity islands of Staphylococcus. Chemical immunology and allergy. 2007;93:42-57. Epub 2007/03/21. doi: 10.1159/0000100857. PubMed PMID: 17369699.

10. Peacock SJ, Paterson GK. Mechanisms of Methicillin Resistance in Staphylococcus aureus. Annual review of biochemistry. 2015;84:577-601. Epub 2015/06/04. doi: 10.1146/annurev-biochem-060614-034516. PubMed PMID: 26034890.

11. Paterson GK, Larsen AR, Robb A, Edwards GE, Pennycott TW, Foster G, et al. The newly described mecA homologue, mecALGA251, is present in methicillin-resistant Staphylococcus aureus isolates from a diverse range of host species. The Journal of antimicrobial chemotherapy. 2012;67(12):2809-13. Epub 2012/09/04. doi:

10.1093/jac/dks329. PubMed PMID: 22941897; PubMed Central PMCID: PMCPMC3494845.

12. Fitzgerald JR, Meaney WJ, Hartigan PJ, Smyth CJ, Kapur V. Fine-structure molecular epidemiological analysis of Staphylococcus aureus recovered from cows. Epidemiology and infection. 1997;119(2):261-9. Epub 1997/11/18. PubMed PMID: 9363026; PubMed Central PMCID: PMCPMC2808849.

13. Kapur V, Sischo WM, Greer RS, Whittam TS, Musser JM. Molecular population genetic analysis of Staphylococcus aureus recovered from cows. Journal of clinical microbiology. 1995;33(2):376-80. Epub 1995/02/01. PubMed PMID: 7714195; PubMed Central PMCID: PMCPMC227951.

14. Schlegelova J, Dendis M, Benedik J, Babak V, Rysanek D. Staphylococcus aureus isolates from dairy cows and humans on a farm differ in coagulase genotype. Veterinary microbiology. 2003;92(4):327-34. Epub 2003/01/30. PubMed PMID: 12554102.

15. Smith EM, Green LE, Medley GF, Bird HE, Fox LK, Schukken YH, et al. Multilocus sequence typing of intercontinental bovine Staphylococcus aureus isolates. Journal of clinical microbiology. 2005;43(9):4737-43. Epub 2005/09/08. doi: 10.1128/jcm.43.9.4737-4743.2005. PubMed PMID: 16145135; PubMed Central PMCID: PMCPMC1234155.

16. Zadoks RN, van Leeuwen WB, Kreft D, Fox LK, Barkema HW, Schukken YH, et al. Comparison of Staphylococcus aureus isolates from bovine and human skin, milking equipment, and bovine milk by phage typing, pulsed-field gel electrophoresis, and binary typing. Journal of clinical microbiology. 2002;40(11):3894-902. Epub 2002/11/01. PubMed PMID: 12409348; PubMed Central PMCID: PMCPMC139627.

17. Sung JM, Lloyd DH, Lindsay JA. Staphylococcus aureus host specificity: comparative genomics of human versus animal isolates by multi-strain microarray. Microbiology (Reading, England). 2008;154(Pt 7):1949-59. Epub 2008/07/05. doi: 10.1099/mic.0.2007/015289-0. PubMed PMID: 18599823.

18. Lowder BV, Guinane CM, Ben Zakour NL, Weinert LA, Conway-Morris A, Cartwright RA, et al. Recent human-to-poultry host jump, adaptation, and pandemic spread of Staphylococcus aureus. Proceedings of the National Academy of Sciences of the United States of America. 2009;106(46):19545-50. Epub 2009/11/04. doi: 10.1073/pnas.0909285106. PubMed PMID: 19884497; PubMed Central PMCID: PMCPMC2780746.

19. Harrison EM, Paterson GK, Holden MT, Larsen J, Stegger M, Larsen AR, et al. Whole genome sequencing identifies zoonotic transmission of MRSA isolates with the novel mecA homologue mecC. EMBO molecular medicine. 2013;5(4):509-15. Epub

2013/03/26. doi: 10.1002/emmm.201202413. PubMed PMID: 23526809; PubMed Central PMCID: PMCPMC3628104.

20. Fitzgerald JR. Human origin for livestock-associated methicillin-resistant Staphylococcus aureus. mBio. 2012;3(2):e00082-12. Epub 2012/04/19. doi: 10.1128/mBio.00082-12. PubMed PMID: 22511352; PubMed Central PMCID: PMCPMC3345579.

21. Price LB, Stegger M, Hasman H, Aziz M, Larsen J, Andersen PS, et al. Staphylococcus aureus CC398: Host Adaptation and Emergence of Methicillin Resistance in Livestock: mBio. 2013 Jan-Feb;4(1):e00520-12. doi:10.1128/mBio.00520-12.

22. Sakwinska O, Giddey M, Moreillon M, Morisset D, Waldvogel A, Moreillon P. Staphylococcus aureus host range and human-bovine host shift. Applied and environmental microbiology. 2011;77(17):5908-15. Epub 2011/07/12. doi: 10.1128/aem.00238-11. PubMed PMID: 21742927; PubMed Central PMCID: PMCPMC3165375.

23. Tenover FC, Goering RV. Methicillin-resistant Staphylococcus aureus strain USA300: origin and epidemiology. The Journal of antimicrobial chemotherapy. 2009;64(3):441-6. Epub 2009/07/18. doi: 10.1093/jac/dkp241. PubMed PMID: 19608582.

24. Resch G, Francois P, Morisset D, Stojanov M, Bonetti EJ, Schrenzel J, et al. Human-to-bovine jump of Staphylococcus aureus CC8 is associated with the loss of a beta-hemolysin converting prophage and the acquisition of a new staphylococcal cassette chromosome. PloS one. 2013;8(3):e58187. Epub 2013/03/19. doi: 10.1371/journal.pone.0058187. PubMed PMID: 23505465; PubMed Central PMCID: PMCPMC3594393.

25. Graber HU, Naskova J, Studer E, Kaufmann T, Kirchhofer M, Brechbuhl M, et al. Mastitis-related subtypes of bovine Staphylococcus aureus are characterized by different clinical properties. Journal of dairy science. 2009;92(4):1442-51. Epub 2009/03/25. doi: 10.3168/jds.2008-1430. PubMed PMID: 19307625.

26. Boss R, Cosandey A, Luini M, Artursson K, Bardiau M, Breitenwieser F, et al. Bovine Staphylococcus aureus: Subtyping, evolution, and zoonotic transfer. Journal of dairy science. 2016;99(1):515-28. Epub 2015/11/26. doi: 10.3168/jds.2015-9589. PubMed PMID: 26601578.

27. Sartori C, Boss R, Ivanovic I, Graber HU. Development of a new real-time quantitative PCR assay for the detection of Staphylococcus aureus genotype B in cow milk, targeting the new gene adlb. Journal of dairy science. 2017;100(10):7834-45. Epub 2017/08/02. doi: 10.3168/jds.2017-12820. PubMed PMID: 28755929.

28. Stojanov M, Sakwinska O, Moreillon P. Expression of SCCmec cassette chromosome recombinases in methicillin-resistant Staphylococcus aureus and Staphylococcus epidermidis. The Journal of antimicrobial chemotherapy.

2013;68(4):749-57. Epub 2012/12/20. doi: 10.1093/jac/dks494. PubMed PMID: 23249841.

29. Hernandez D, Francois P, Farinelli L, Osteras M, Schrenzel J. De novo bacterial genome sequencing: millions of very short reads assembled on a desktop computer. Genome research. 2008;18(5):802-9. Epub 2008/03/12. doi: 10.1101/gr.072033.107. PubMed PMID: 18332092; PubMed Central PMCID: PMCPMC2336802.

30. Aziz RK, Bartels D, Best AA, DeJongh M, Disz T, Edwards RA, et al. The RAST Server: rapid annotations using subsystems technology. BMC genomics. 2008;9:75. Epub 2008/02/12. doi: 10.1186/1471-2164-9-75. PubMed PMID: 18261238; PubMed Central PMCID: PMCPMC2265698.

31. Katoh K, Standley DM. MAFFT multiple sequence alignment software version 7: improvements in performance and usability. Molecular biology and evolution. 2013;30(4):772-80. Epub 2013/01/19. doi: 10.1093/molbev/mst010. PubMed PMID: 23329690; PubMed Central PMCID: PMCPMC3603318.

32. Price MN, Dehal PS, Arkin AP. FastTree 2--approximately maximum-likelihood trees for large alignments. PloS one. 2010;5(3):e9490. Epub 2010/03/13. doi: 10.1371/journal.pone.0009490. PubMed PMID: 20224823; PubMed Central PMCID: PMCPMC2835736.

33. Perriere G, Gouy M. WWW-query: an on-line retrieval system for biological sequence banks. Biochimie. 1996;78(5):364-9. Epub 1996/01/01. PubMed PMID: 8905155.

34. Que YA, Haefliger JA, Francioli P, Moreillon P. Expression of Staphylococcus aureus Clumping Factor A in Lactococcus lactis subsp. cremoris Using a New Shuttle Vector. Infection and immunity. 2000;68(6):3516-22. PubMed PMID: 10816506; PubMed Central PMCID: PMCPMC97637.

35. Towbin H, Staehelin T, Gordon J. Electrophoretic transfer of proteins from polyacrylamide gels to nitrocellulose sheets: procedure and some applications. Proceedings of the National Academy of Sciences of the United States of America. 1979;76(9):4350-4. Epub 1979/09/01. PubMed PMID: 388439; PubMed Central PMCID: PMCPMC411572.

36. Yao J, Zhong J, Fang Y, Geisinger E, Novick RP, Lambowitz AM. Use of targetrons to disrupt essential and nonessential genes in Staphylococcus aureus reveals temperature sensitivity of Ll.LtrB group II intron splicing. RNA (New York, NY). 2006;12(7):1271-81. Epub 2006/06/03. doi: 10.1261/rna.68706. PubMed PMID: 16741231; PubMed Central PMCID: PMCPMC1484445.

37. Wolz C, McDevitt D, Foster TJ, Cheung AL. Influence of agr on fibrinogen binding in Staphylococcus aureus Newman. Infection and immunity. 1996;64(8):3142-7. PubMed PMID: 8757845; PubMed Central PMCID: PMCPMC174199.

38. Geoghegan JA, Corrigan RM, Gruszka DT, Speziale P, O'Gara JP, Potts JR, et al. Role of surface protein SasG in biofilm formation by Staphylococcus aureus. Journal

of bacteriology. 2010;192(21):5663-73. Epub 2010/09/08. doi: 10.1128/jb.00628-10. PubMed PMID: 20817770; PubMed Central PMCID: PMCPMC2953683.

39. Katayama Y, Ito T, Hiramatsu K. A new class of genetic element, staphylococcus cassette chromosome mec, encodes methicillin resistance in Staphylococcus aureus. Antimicrobial agents and chemotherapy. 2000;44(6):1549-55. Epub 2000/05/19. PubMed PMID: 10817707; PubMed Central PMCID: PMCPMC89911.

40. Bateman A, Holden MT, Yeats C. The G5 domain: a potential N-acetylglucosamine recognition domain involved in biofilm formation. Bioinformatics (Oxford, England). 2005;21(8):1301-3. Epub 2004/12/16. doi: 10.1093/bioinformatics/bti206. PubMed PMID: 15598841.

41. van Wamel WJ, Rooijakkers SH, Ruyken M, van Kessel KP, van Strijp JA. The innate immune modulators staphylococcal complement inhibitor and chemotaxis inhibitory protein of Staphylococcus aureus are located on beta-hemolysin-converting bacteriophages. Journal of bacteriology. 2006;188(4):1310-5. doi: 10.1128/JB.188.4.1310-1315.2006. PubMed PMID: 16452413; PubMed Central PMCID: PMCPMC1367213.

42. Mazmanian SK, Liu G, Ton-That H, Schneewind O. Staphylococcus aureus sortase, an enzyme that anchors surface proteins to the cell wall. Science. 1999;285(5428):760-3. PubMed PMID: 10427003.

43. Frenay HM, Bunschoten AE, Schouls LM, van Leeuwen WJ, Vandenbroucke-Grauls CM, Verhoef J, et al. Molecular typing of methicillin-resistant Staphylococcus aureus on the basis of protein A gene polymorphism. Eur J Clin Microbiol Infect Dis. 1996;15(1):60-4. PubMed PMID: 8641305.

44. Edwards AM, Potts JR, Josefsson E, Massey RC. Staphylococcus aureus host cell invasion and virulence in sepsis is facilitated by the multiple repeats within FnBPA. PLoS Pathog. 2010;6(6):e1000964. doi: 10.1371/journal.ppat.1000964. PubMed PMID: 20585570; PubMed Central PMCID: PMCPMC2891841.

45. Xia G, Wolz C. Phages of Staphylococcus aureus and their impact on host evolution. Infect Genet Evol. 2014;21:593-601. doi: 10.1016/j.meegid.2013.04.022. PubMed PMID: 23660485.

46. Kaneko J, Kimura T, Narita S, Tomita T, Kamio Y. Complete nucleotide sequence and molecular characterization of the temperate staphylococcal bacteriophage phiPVL carrying Panton-Valentine leukocidin genes. Gene. 1998;215(1):57-67. PubMed PMID: 9666077.

47. Baba T, Takeuchi F, Kuroda M, Yuzawa H, Aoki K, Oguchi A, et al. Genome and virulence determinants of high virulence community-acquired MRSA. Lancet (London, England). 2002;359(9320):1819-27. PubMed PMID: 12044378.

48. Price LB, Stegger M, Hasman H, Aziz M, Larsen J, Andersen PS, et al. Staphylococcus aureus CC398: Host Adaptation and Emergence of Methicillin

Resistance in Livestock. mBio. 2012;3(1). Epub 2012/02/23. doi: 10.1128/mBio.00305-11. PubMed PMID: 22354957; PubMed Central PMCID: PMC3280451.

49. Katayama Y, Baba T, Sekine M, Fukuda M, Hiramatsu K. Beta-hemolysin promotes skin colonization by Staphylococcus aureus. Journal of bacteriology. 2013;195(6):1194-203. doi: 10.1128/JB.01786-12. PubMed PMID: 23292775; PubMed Central PMCID: PMCPMC3592002.

50. Gasson MJ, Davies FL. Prophage-Cured Derivatives of Streptococcus lactis and Streptococcus cremoris. Applied and environmental microbiology. 1980;40(5):964-6. Epub 1980/11/01. PubMed PMID: 16345661; PubMed Central PMCID: PMCPMC291696.

51. Kreiswirth BN, Lofdahl S, Betley MJ, O'Reilly M, Schlievert PM, Bergdoll MS, et al. The toxic shock syndrome exotoxin structural gene is not detectably transmitted by a prophage. Nature. 1983;305(5936):709-12. Epub 1983/10/20. PubMed PMID: 6226876.

52. Kuroda M, Ohta T, Uchiyama I, Baba T, Yuzawa H, Kobayashi I, et al. Whole genome sequencing of meticillin-resistant Staphylococcus aureus. Lancet (London, England). 2001;357(9264):1225-40. Epub 2001/06/22. PubMed PMID: 11418146.

53. Conrady DG, Brescia CC, Horii K, Weiss AA, Hassett DJ, Herr AB. A zinc-dependent adhesion module is responsible for intercellular adhesion in staphylococcal biofilms. Proceedings of the National Academy of Sciences of the United States of America. 2008;105(49):19456-61. Epub 2008/12/03. doi: 10.1073/pnas.0807717105. PubMed PMID: 19047636; PubMed Central PMCID: PMCPMC2592360.

54. Hambly E, Suttle CA. The viriosphere, diversity, and genetic exchange within phage communities. Current opinion in microbiology. 2005;8(4):444-50. Epub 2005/06/28. doi: 10.1016/j.mib.2005.06.005. PubMed PMID: 15979387.

55. Chibani-Chennoufi S, Bruttin A, Dillmann ML, Brussow H. Phage-host interaction: an ecological perspective. Journal of bacteriology. 2004;186(12):3677-86. Epub 2004/06/04. doi: 10.1128/jb.186.12.3677-3686.2004. PubMed PMID: 15175280; PubMed Central PMCID: PMCPMC419959.

56. Ackermann HW. Frequency of morphological phage descriptions in the year 2000. Brief review. Archives of virology. 2001;146(5):843-57. Epub 2001/07/13. PubMed PMID: 11448025.

57. Matsuzaki S, Rashel M, Uchiyama J, Sakurai S, Ujihara T, Kuroda M, et al. Bacteriophage therapy: a revitalized therapy against bacterial infectious diseases. Journal of infection and chemotherapy : official journal of the Japan Society of Chemotherapy. 2005;11(5):211-9. Epub 2005/11/01. doi: 10.1007/s10156-005-0408-9. PubMed PMID: 16258815.

58. Wang IN, Smith DL, Young R. Holins: the protein clocks of bacteriophage infections. Annual review of microbiology. 2000;54:799-825. Epub 2000/10/06. doi: 10.1146/annurev.micro.54.1.799. PubMed PMID: 11018145.

59. Fischetti VA. Using phage Lytic Enzymes to Control Pathogenic Bacteria. BMC Oral Health. 2006;6(Suppl 1):S16. doi: 10.1186/1472-6831-6-s1-s16. PubMed PMID: 16934117; PubMed Central PMCID: PMCPMC2147602.

60. Loeffler JM, Nelson D, Fischetti VA. Rapid killing of Streptococcus pneumoniae with a bacteriophage cell wall hydrolase. Science (New York, NY). 2001;294(5549):2170-2. Epub 2001/12/12. doi: 10.1126/science.1066869. PubMed PMID: 11739958.

61. Loessner MJ. Bacteriophage endolysins--current state of research and applications. Current opinion in microbiology. 2005;8(4):480-7. Epub 2005/06/28. doi: 10.1016/j.mib.2005.06.002. PubMed PMID: 15979390.

62. Hermoso JA, Monterroso B, Albert A, Galan B, Ahrazem O, Garcia P, et al. Structural basis for selective recognition of pneumococcal cell wall by modular endolysin from phage Cp-1. Structure (London, England : 1993). 2003;11(10):1239-49. Epub 2003/10/07. PubMed PMID: 14527392.

63. Veiga-Crespo P, Villa T. Enzybiotics: Antibiotic Enzymes as Drugs and Therapeutics2010.

64. Loessner MJ, Kramer K, Ebel F, Scherer S. C-terminal domains of Listeria monocytogenes bacteriophage murein hydrolases determine specific recognition and high-affinity binding to bacterial cell wall carbohydrates. Molecular microbiology. 2002;44(2):335-49. Epub 2002/04/26. PubMed PMID: 11972774.

65. McGowan S, Buckle AM, Mitchell MS, Hoopes JT, Gallagher DT, Heselpoth RD, et al. X-ray crystal structure of the streptococcal specific phage lysin PlyC. Proceedings of the National Academy of Sciences of the United States of America. 2012;109(31):12752-7. Epub 2012/07/19. doi: 10.1073/pnas.1208424109. PubMed PMID: 22807482; PubMed Central PMCID: PMCPMC3412044.

66. García JL, García E, Arrarás A, García P, Ronda C, López R. Cloning, purification, and biochemical characterization of the pneumococcal bacteriophage Cp-1 lysin. Journal of Virology. 1987;61(8):2573-80. PubMed PMID: 3298686; PubMed Central PMCID: PMCPMC255702.

67. Fenton M, Ross P, McAuliffe O, O'Mahony J, Coffey A. Recombinant bacteriophage lysins as antibacterials. Bioengineered Bugs. 2010;1(1):9-16. Epub 2011/02/18. doi: 10.4161/bbug.1.1.9818. PubMed PMID: 21327123; PubMed Central PMCID: PMCPMC3035150.

68. Pritchard DG, Dong S, Baker JR, Engler JA. The bifunctional peptidoglycan lysin of Streptococcus agalactiae bacteriophage B30. Microbiology (Reading, England). 2004;150(Pt 7):2079-87. Epub 2004/07/17. doi: 10.1099/mic.0.27063-0. PubMed PMID: 15256551.

69. Jado I, Lopez R, Garcia E, Fenoll A, Casal J, Garcia P. Phage lytic enzymes as therapy for antibiotic-resistant Streptococcus pneumoniae infection in a murine sepsis

model. The Journal of antimicrobial chemotherapy. 2003;52(6):967-73. Epub 2003/11/14. doi: 10.1093/jac/dkg485. PubMed PMID: 14613958.

70. Entenza JM, Loeffler JM, Grandgirard D, Fischetti VA, Moreillon P. Therapeutic effects of bacteriophage Cpl-1 lysin against Streptococcus pneumoniae endocarditis in rats. Antimicrobial agents and chemotherapy. 2005;49(11):4789-92. Epub 2005/10/28. doi: 10.1128/aac.49.11.4789-4792.2005. PubMed PMID: 16251333; PubMed Central PMCID: PMCPMC1280127.

71. Grandgirard D, Loeffler JM, Fischetti VA, Leib SL. Phage lytic enzyme Cpl-1 for antibacterial therapy in experimental pneumococcal meningitis. The Journal of infectious diseases. 2008;197(11):1519-22. Epub 2008/05/13. doi: 10.1086/587942. PubMed PMID: 18471063.

72. Witzenrath M, Schmeck B, Doehn JM, Tschernig T, Zahlten J, Loeffler JM, et al. Systemic use of the endolysin Cpl-1 rescues mice with fatal pneumococcal pneumonia. Critical care medicine. 2009;37(2):642-9. Epub 2008/12/31. doi: 10.1097/CCM.0b013e31819586a6. PubMed PMID: 19114881.

73. Djurkovic S, Loeffler JM, Fischetti VA. Synergistic Killing of Streptococcus pneumoniae with the Bacteriophage Lytic Enzyme Cpl-1 and Penicillin or Gentamicin Depends on the Level of Penicillin Resistance. Antimicrobial agents and chemotherapy. 2005;49(3):1225-8. doi: 10.1128/aac.49.3.1225-1228.2005. PubMed PMID: 15728935; PubMed Central PMCID: PMCPMC549239.

74. Loeffler JM, Fischetti VA. Synergistic lethal effect of a combination of phage lytic enzymes with different activities on penicillin-sensitive and -resistant Streptococcus pneumoniae strains. Antimicrobial agents and chemotherapy. 2003;47(1):375-7. Epub 2002/12/25. PubMed PMID: 12499217; PubMed Central PMCID: PMCPMC149014.

75. Nelson D, Schuch R, Chahales P, Zhu S, Fischetti VA. PlyC: a multimeric bacteriophage lysin. Proceedings of the National Academy of Sciences of the United States of America. 2006;103(28):10765-70. Epub 2006/07/05. doi: 10.1073/pnas.0604521103. PubMed PMID: 16818874; PubMed Central PMCID: PMCPMC1487170.

76. Cheng Q, Nelson D, Zhu S, Fischetti VA. Removal of group B streptococci colonizing the vagina and oropharynx of mice with a bacteriophage lytic enzyme. Antimicrobial agents and chemotherapy. 2005;49(1):111-7. Epub 2004/12/24. doi: 10.1128/aac.49.1.111-117.2005. PubMed PMID: 15616283; PubMed Central PMCID: PMCPMC538902.

77. Pritchard DG, Dong S, Kirk MC, Cartee RT, Baker JR. LambdaSa1 and LambdaSa2 prophage lysins of Streptococcus agalactiae. Applied and environmental microbiology. 2007;73(22):7150-4. Epub 2007/10/02. doi: 10.1128/aem.01783-07. PubMed PMID: 17905888; PubMed Central PMCID: PMCPMC2168211.

78. Tang F, Li D, Wang H, Ma Z, Lu C, Dai J. Prophage lysin Ply30 protects mice from Streptococcus suis and Streptococcus equi subsp. zooepidemicus infections. Applied and environmental microbiology. 2015;81(21):7377-84. Epub 2015/08/09. doi:

10.1128/aem.02300-15. PubMed PMID: 26253669; PubMed Central PMCID: PMCPMC4592866.

79. Gilmer DB, Schmitz JE, Thandar M, Euler CW, Fischetti VA. The Phage Lysin PlySs2 Decolonizes Streptococcus suis from Murine Intranasal Mucosa. PLoS ONE. 2017;12(1). doi: 10.1371/journal.pone.0169180. PubMed PMID: 28046082; PubMed Central PMCID: PMCPMC5207509.

80. Oechslin F, Daraspe J, Giddey M, Moreillon P, Resch G. In vitro characterization of PlySK1249, a novel phage lysin, and assessment of its antibacterial activity in a mouse model of Streptococcus agalactiae bacteremia. Antimicrobial agents and chemotherapy. 2013;57(12):6276-83. Epub 2013/10/09. doi: 10.1128/aac.01701-13. PubMed PMID: 24100496; PubMed Central PMCID: PMCPMC3837886.

81. Donovan DM, Foster-Frey J, Dong S, Rousseau GM, Moineau S, Pritchard DG. The cell lysis activity of the Streptococcus agalactiae bacteriophage B30 endolysin relies on the cysteine, histidine-dependent amidohydrolase/peptidase domain. Applied and environmental microbiology. 2006;72(7):5108-12. Epub 2006/07/06. doi: 10.1128/aem.03065-05. PubMed PMID: 16820517; PubMed Central PMCID: PMCPMC1489305.

82. Cheng Q, Fischetti VA. Mutagenesis of a bacteriophage lytic enzyme PlyGBS significantly increases its antibacterial activity against group B streptococci. Applied microbiology and biotechnology. 2007;74(6):1284-91. Epub 2006/12/23. doi: 10.1007/s00253-006-0771-1. PubMed PMID: 17186236.

83. Gilmer DB, Schmitz JE, Euler CW, Fischetti VA. Novel bacteriophage lysin with broad lytic activity protects against mixed infection by Streptococcus pyogenes and methicillin-resistant Staphylococcus aureus. Antimicrobial agents and chemotherapy. 2013;57(6):2743-50. Epub 2013/04/11. doi: 10.1128/aac.02526-12. PubMed PMID: 23571534; PubMed Central PMCID: PMCPMC3716137.

84. Fischetti VA. Exploiting what phage have evolved to control gram-positive pathogens. Bacteriophage. 2011;1(4):188-94. doi: 10.4161/bact.1.4.17747. PubMed PMID: 23050211; PubMed Central PMCID: PMCPMC3448103.

85. Hyman P, Abedon ST. Bacteriophages in Health and Disease: CAB International.

86. Donovan DM, Foster-Frey J. LambdaSa2 prophage endolysin requires Cpl-7-binding domains and amidase-5 domain for antimicrobial lysis of streptococci. FEMS microbiology letters. 2008;287(1):22-33. Epub 2008/08/05. doi: 10.1111/j.1574-6968.2008.01287.x. PubMed PMID: 18673393.

87. Horgan M, O'Flynn G, Garry J, Cooney J, Coffey A, Fitzgerald GF, et al. Phage lysin LysK can be truncated to its CHAP domain and retain lytic activity against live antibiotic-resistant staphylococci. Applied and environmental microbiology. 2009;75(3):872-4. Epub 2008/12/03. doi: 10.1128/aem.01831-08. PubMed PMID: 19047377; PubMed Central PMCID: PMCPmc2632115.

88. Loessner MJ, Gaeng S, Wendlinger G, Maier SK, Scherer S. The two-component lysis system of Staphylococcus aureus bacteriophage Twort: a large TTG-start holin and an associated amidase endolysin. FEMS microbiology letters. 1998;162(2):265-74. Epub 1998/06/17. PubMed PMID: 9627962.

89. Yokoi KJ, Kawahigashi N, Uchida M, Sugahara K, Shinohara M, Kawasaki K, et al. The two-component cell lysis genes holWMY and lysWMY of the Staphylococcus warneri M phage varphiWMY: cloning, sequencing, expression, and mutational analysis in Escherichia coli. Gene. 2005;351:97-108. Epub 2005/04/26. doi: 10.1016/j.gene.2005.03.006. PubMed PMID: 15848115.

90. Low LY, Yang C, Perego M, Osterman A, Liddington RC. Structure and lytic activity of a Bacillus anthracis prophage endolysin. The Journal of biological chemistry. 2005;280(42):35433-9. Epub 2005/08/17. doi: 10.1074/jbc.M502723200. PubMed PMID: 16103125.

91. Becker SC, Dong S, Baker JR, Foster-Frey J, Pritchard DG, Donovan DM. LysK CHAP endopeptidase domain is required for lysis of live staphylococcal cells. FEMS microbiology letters. 2009;294(1):52-60. Epub 2009/06/06. doi: 10.1111/j.1574-6968.2009.01541.x. PubMed PMID: 19493008.

92. Fischetti VA. Bacteriophage lysins as effective antibacterials. Current opinion in microbiology. 2008;11(5):393-400. Epub 2008/10/01. doi: 10.1016/j.mib.2008.09.012. PubMed PMID: 18824123; PubMed Central PMCID: PMCPMC2597892.

93. Schmelcher M, Donovan DM, Loessner MJ. Bacteriophage endolysins as novel antimicrobials. Future microbiology. 2012;7(10):1147-71. Epub 2012/10/04. doi: 10.2217/fmb.12.97. PubMed PMID: 23030422; PubMed Central PMCID: PMCPMC3563964.

94. Watnick P, Kolter R. Biofilm, city of microbes. Journal of bacteriology. 2000;182(10):2675-9. Epub 2000/04/27. PubMed PMID: 10781532; PubMed Central PMCID: PMCPMC101960.

95. Whiteley M, Bangera MG, Bumgarner RE, Parsek MR, Teitzel GM, Lory S, et al. Gene expression in Pseudomonas aeruginosa biofilms. Nature. 2001;413(6858):860-4. Epub 2001/10/26. doi: 10.1038/35101627. PubMed PMID: 11677611.

96. Wang X, Kim Y, Wood TK. Control and benefits of CP4-57 prophage excision in Escherichia coli biofilms. The ISME journal. 2009;3(10):1164-79. Epub 2009/05/22. doi: 10.1038/ismej.2009.59. PubMed PMID: 19458652; PubMed Central PMCID: PMCPMC2754048.

97. Luke K, Radek A, Liu X, Campbell J, Uzan M, Haselkorn R, et al. Microarray analysis of gene expression during bacteriophage T4 infection. Virology. 2002;299(2):182-91. Epub 2002/08/31. PubMed PMID: 12202221.

98. McPheeters DS, Christensen A, Young ET, Stormo G, Gold L. Translational regulation of expression of the bacteriophage T4 lysozyme gene. Nucleic acids

research. 1986;14(14):5813-26. PubMed PMID: 3526285; PubMed Central PMCID: PMCPMC311593.

99. Sao-Jose C, Parreira R, Vieira G, Santos MA. The N-terminal region of the Oenococcus oeni bacteriophage fOg44 lysin behaves as a bona fide signal peptide in Escherichia coli and as a cis-inhibitory element, preventing lytic activity on oenococcal cells. Journal of bacteriology. 2000;182(20):5823-31. Epub 2000/09/27. PubMed PMID: 11004183; PubMed Central PMCID: PMCPMC94706.

100. Young R. Bacteriophage holins: deadly diversity. Journal of molecular microbiology and biotechnology. 2002;4(1):21-36. Epub 2002/01/05. PubMed PMID: 11763969.

101. Young R. Phage lysis: three steps, three choices, one outcome. Journal of microbiology (Seoul, Korea). 2014;52(3):243-58. Epub 2014/03/04. doi: 10.1007/s12275-014-4087-z. PubMed PMID: 24585055; PubMed Central PMCID: PMCPMC4012431.

102. Nelson DC, Schmelcher M, Rodriguez-Rubio L, Klumpp J, Pritchard DG, Dong S, et al. Endolysins as antimicrobials. Advances in virus research. 2012;83:299-365. Epub 2012/07/04. doi: 10.1016/b978-0-12-394438-2.00007-4. PubMed PMID: 22748813.

103. Fischetti VA. Bacteriophage endolysins: a novel anti-infective to control Gram-positive pathogens. International journal of medical microbiology : IJMM. 2010;300(6):357-62. Epub 2010/05/11. doi: 10.1016/j.ijmm.2010.04.002. PubMed PMID: 20452280; PubMed Central PMCID: PMCPMC3666336.

104. Schleifer KH, Kandler O. Peptidoglycan types of bacterial cell walls and their taxonomic implications. Bacteriological reviews. 1972;36(4):407-77. Epub 1972/12/01. PubMed PMID: 4568761; PubMed Central PMCID: PMCPMC408328.

105. Vollmer W, Blanot D, de Pedro MA. Peptidoglycan structure and architecture. FEMS microbiology reviews. 2008;32(2):149-67. Epub 2008/01/16. doi: 10.1111/j.1574-6976.2007.00094.x. PubMed PMID: 18194336.

106. Briers Y, Schmelcher M, Loessner MJ, Hendrix J, Engelborghs Y, Volckaert G, et al. The high-affinity peptidoglycan binding domain of Pseudomonas phage endolysin KZ144. Biochemical and biophysical research communications. 2009;383(2):187-91. Epub 2009/04/08. doi: 10.1016/j.bbrc.2009.03.161. PubMed PMID: 19348786.

107. O'Flaherty S, Coffey A, Meaney W, Fitzgerald GF, Ross RP. The recombinant phage lysin LysK has a broad spectrum of lytic activity against clinically relevant staphylococci, including methicillin-resistant Staphylococcus aureus. Journal of bacteriology. 2005;187(20):7161-4. Epub 2005/10/04. doi: 10.1128/jb.187.20.7161-7164.2005. PubMed PMID: 16199588; PubMed Central PMCID: PMCPMC1251611.

108. Navarre WW, Ton-That H, Faull KF, Schneewind O. Multiple enzymatic activities of the murein hydrolase from staphylococcal phage phi11. Identification of a

D-alanyl-glycine endopeptidase activity. The Journal of biological chemistry. 1999;274(22):15847-56. Epub 1999/05/21. PubMed PMID: 10336488.

109. Rashel M, Uchiyama J, Ujihara T, Uehara Y, Kuramoto S, Sugihara S, et al. Efficient elimination of multidrug-resistant Staphylococcus aureus by cloned lysin derived from bacteriophage phi MR11. The Journal of infectious diseases. 2007;196(8):1237-47. Epub 2007/10/24. doi: 10.1086/521305. PubMed PMID: 17955443.

110. Sass P, Bierbaum G. Lytic activity of recombinant bacteriophage phi11 and phi12 endolysins on whole cells and biofilms of Staphylococcus aureus. Applied and environmental microbiology. 2007;73(1):347-52. Epub 2006/11/07. doi: 10.1128/aem.01616-06. PubMed PMID: 17085695; PubMed Central PMCID: PMCPMC1797112.

111. Low LY, Yang C, Perego M, Osterman A, Liddington R. Role of net charge on catalytic domain and influence of cell wall binding domain on bactericidal activity, specificity, and host range of phage lysins. The Journal of biological chemistry. 2011;286(39):34391-403. Epub 2011/08/06. doi: 10.1074/jbc.M111.244160. PubMed PMID: 21816821; PubMed Central PMCID: PMCPMC3190764.

112. Wong JE, Midtgaard SR, Gysel K, Thygesen MB, Sorensen KK, Jensen KJ, et al. An intermolecular binding mechanism involving multiple LysM domains mediates carbohydrate recognition by an endopeptidase. Acta crystallographica Section D, Biological crystallography. 2015;71(Pt 3):592-605. Epub 2015/03/12. doi: 10.1107/s139900471402793x. PubMed PMID: 25760608; PubMed Central PMCID: PMCPMC4356369.

113. Visweswaran GR, Leenhouts K, van Roosmalen M, Kok J, Buist G. Exploiting the peptidoglycan-binding motif, LysM, for medical and industrial applications. Applied microbiology and biotechnology. 2014;98(10):4331-45. Epub 2014/03/22. doi: 10.1007/s00253-014-5633-7. PubMed PMID: 24652063; PubMed Central PMCID: PMCPMC4004799.

114. Buist G, Steen A, Kok J, Kuipers OP. LysM, a widely distributed protein motif for binding to (peptido)glycans. Molecular microbiology. 2008;68(4):838-47. Epub 2008/04/24. doi: 10.1111/j.1365-2958.2008.06211.x. PubMed PMID: 18430080.

115. Herbold DR, Glaser L. Interaction of N-acetylmuramic acid L-alanine amidase with cell wall polymers. The Journal of biological chemistry. 1975;250(18):7231-8. Epub 1975/09/25. PubMed PMID: 809432.

116. Rigden DJ, Jedrzejas MJ, Galperin MY. Amidase domains from bacterial and phage autolysins define a family of gamma-D,L-glutamate-specific amidohydrolases. Trends in biochemical sciences. 2003;28(5):230-4. Epub 2003/05/27. PubMed PMID: 12765833.

117. Wang X, Wilkinson BJ, Jayaswal RK. Sequence analysis of a Staphylococcus aureus gene encoding a peptidoglycan hydrolase activity. Gene. 1991;102(1):105-9. Epub 1991/06/15. PubMed PMID: 1677905.

118. Gu J, Xu W, Lei L, Huang J, Feng X, Sun C, et al. LysGH15, a novel bacteriophage lysin, protects a murine bacteremia model efficiently against lethal methicillin-resistant Staphylococcus aureus infection. Journal of clinical microbiology. 2011;49(1):111-7. Epub 2010/11/05. doi: 10.1128/jcm.01144-10. PubMed PMID: 21048011; PubMed Central PMCID: PMCPMC3020447.

119. Broskey NT, Daraspe J, Humbel BM, Amati F. Skeletal muscle mitochondrial and lipid droplet content assessed with standardized grid sizes for stereology. Journal of applied physiology (Bethesda, Md : 1985). 2013;115(5):765-70. Epub 2013/06/22. doi: 10.1152/japplphysiol.00063.2013. PubMed PMID: 23788579.

120. Majcherczyk PA, Langen H, Heumann D, Fountoulakis M, Glauser MP, Moreillon P. Digestion of Streptococcus pneumoniae cell walls with its major peptidoglycan hydrolase releases branched stem peptides carrying proinflammatory activity. The Journal of biological chemistry. 1999;274(18):12537-43. Epub 1999/04/23. PubMed PMID: 10212231.

121. Schmelcher M, Shen Y, Nelson DC, Eugster MR, Eichenseher F, Hanke DC, et al. Evolutionarily distinct bacteriophage endolysins featuring conserved peptidoglycan cleavage sites protect mice from MRSA infection. The Journal of antimicrobial chemotherapy. 2015;70(5):1453-65. Epub 2015/01/30. doi: 10.1093/jac/dku552. PubMed PMID: 25630640; PubMed Central PMCID: PMCPMC4398471.

122. Glauner B. Separation and quantification of muropeptides with high-performance liquid chromatography. Analytical biochemistry. 1988;172(2):451-64. Epub 1988/08/01. PubMed PMID: 3056100.

123. Catalao MJ, Gil F, Moniz-Pereira J, Sao-Jose C, Pimentel M. Diversity in bacterial lysis systems: bacteriophages show the way. FEMS microbiology reviews. 2013;37(4):554-71. Epub 2012/10/10. doi: 10.1111/1574-6976.12006. PubMed PMID: 23043507.

124. Pohane AA, Jain V. Insights into the regulation of bacteriophage endolysin: multiple means to the same end. Microbiology (Reading, England). 2015;161(12):2269-76. Epub 2015/10/01. doi: 10.1099/mic.0.000190. PubMed PMID: 26419630.

125. Regulski K, Courtin P, Meyrand M, Claes IJ, Lebeer S, Vanderleyden J, et al. Analysis of the peptidoglycan hydrolase complement of Lactobacillus casei and characterization of the major gamma-D-glutamyl-L-lysyl-endopeptidase. PLoS ONE. 2012;7(2):e32301. Epub 2012/03/03. doi: 10.1371/journal.pone.0032301. PubMed PMID: 22384208; PubMed Central PMCID: PMCPMC3288076.

126. Claes IJ, Schoofs G, Regulski K, Courtin P, Chapot-Chartier MP, Rolain T, et al. Genetic and biochemical characterization of the cell wall hydrolase activity of the major secreted protein of Lactobacillus rhamnosus GG. PLoS ONE. 2012;7(2):e31588. Epub 2012/02/24. doi: 10.1371/journal.pone.0031588. PubMed PMID: 22359601; PubMed Central PMCID: PMCPMC3281093.

127. Steen A, Palumbo E, Deghorain M, Cocconcelli PS, Delcour J, Kuipers OP, et al. Autolysis of Lactococcus lactis Is Increased upon d-Alanine Depletion of Peptidoglycan and Lipoteichoic Acids. Journal of bacteriology. 2005;187(1):114-24. doi: 10.1128/jb.187.1.114-124.2005. PubMed PMID: 15601695; PubMed Central PMCID: PMCPMC538808.

128. Buist G, Venema G, Kok J. Autolysis of Lactococcus lactis is influenced by proteolysis. Journal of bacteriology. 1998;180(22):5947-53. Epub 1998/11/13. PubMed PMID: 9811653; PubMed Central PMCID: PMCPMC107669.

129. Eckert C, Lecerf M, Dubost L, Arthur M, Mesnage S. Functional analysis of AtlA, the major N-acetylglucosaminidase of Enterococcus faecalis. Journal of bacteriology. 2006;188(24):8513-9. Epub 2006/10/17. doi: 10.1128/jb.01145-06. PubMed PMID: 17041059; PubMed Central PMCID: PMCPMC1698247.

130. Fan DP. Autolysin(s) of Bacillus subtilis as dechaining enzyme. Journal of bacteriology. 1970;103(2):494-9. Epub 1970/08/01. PubMed PMID: 4988246; PubMed Central PMCID: PMCPMC248109.

131. Layec S, Gerard J, Legue V, Chapot-Chartier MP, Courtin P, Borges F, et al. The CHAP domain of Cse functions as an endopeptidase that acts at mature septa to promote Streptococcus thermophilus cell separation. Molecular microbiology. 2009;71(5):1205-17. Epub 2009/01/28. doi: 10.1111/j.1365-2958.2009.06595.x. PubMed PMID: 19170887.

132. Kerr KG, Snelling AM. Pseudomonas aeruginosa: a formidable and ever-present adversary. The Journal of hospital infection. 2009;73(4):338-44. Epub 2009/08/25. doi: 10.1016/j.jhin.2009.04.020. PubMed PMID: 19699552.

133. Mayhall CG. The epidemiology of burn wound infections: then and now. Clinical infectious diseases : an official publication of the Infectious Diseases Society of America. 2003;37(4):543-50. Epub 2003/08/09. doi: 10.1086/376993. PubMed PMID: 12905139.

134. Norbury W, Herndon DN, Tanksley J, Jeschke MG, Finnerty CC. Infection in Burns. Surgical infections. 2016;17(2):250-5. Epub 2016/03/16. doi: 10.1089/sur.2013.134. PubMed PMID: 26978531; PubMed Central PMCID: PMCPMC4790211.

135. Mesaros N, Nordmann P, Plesiat P, Roussel-Delvallez M, Van Eldere J, Glupczynski Y, et al. Pseudomonas aeruginosa: resistance and therapeutic options at the turn of the new millennium. Clinical microbiology and infection : the official publication of the European Society of Clinical Microbiology and Infectious Diseases. 2007;13(6):560-78. Epub 2007/02/03. doi: 10.1111/j.1469-0691.2007.01681.x. PubMed PMID: 17266725.

136. Dublanchet A, Bourne S. The epic of phage therapy. The Canadian journal of infectious diseases & medical microbiology = Journal canadien des maladies infectieuses et de la microbiologie medicale. 2007;18(1):15-8. Epub 2008/10/17. PubMed PMID: 18923688; PubMed Central PMCID: PMCPMC2542892.

137. Kutter E, De Vos D, Gvasalia G, Alavidze Z, Gogokhia L, Kuhl S, et al. Phage therapy in clinical practice: treatment of human infections. Current pharmaceutical biotechnology. 2010;11(1):69-86. Epub 2009/01/01. PubMed PMID: 20214609.

138. Sansom C. Phage therapy for severe infections tested in the first multicentre trial. The Lancet Infectious diseases. 2015;15(12):1384-5. Epub 2015/11/27. doi: 10.1016/s1473-3099(15)00420-x. PubMed PMID: 26607127.

139. Moreillon P, Que YA. Infective endocarditis. Lancet (London, England). 2004;363(9403):139-49. Epub 2004/01/17. doi: 10.1016/s0140-6736(03)15266-x. PubMed PMID: 14726169.

140. Habib G, Hoen B, Tornos P, Thuny F, Prendergast B, Vilacosta I, et al. Guidelines on the prevention, diagnosis, and treatment of infective endocarditis (new version 2009): the Task Force on the Prevention, Diagnosis, and Treatment of Infective Endocarditis of the European Society of Cardiology (ESC). Endorsed by the European Society of Clinical Microbiology and Infectious Diseases (ESCMID) and the International Society of Chemotherapy (ISC) for Infection and Cancer. European heart journal. 2009;30(19):2369-413. Epub 2009/08/29. doi: 10.1093/eurheartj/ehp285. PubMed PMID: 19713420.

141. Sousa C, Botelho C, Rodrigues D, Azeredo J, Oliveira R. Infective endocarditis in intravenous drug abusers: an update. European journal of clinical microbiology & infectious diseases : official publication of the European Society of Clinical Microbiology. 2012;31(11):2905-10. Epub 2012/06/21. doi: 10.1007/s10096-012-1675-x. PubMed PMID: 22714640.

142. Watanabe R, Matsumoto T, Sano G, Ishii Y, Tateda K, Sumiyama Y, et al. Efficacy of bacteriophage therapy against gut-derived sepsis caused by Pseudomonas aeruginosa in mice. Antimicrobial agents and chemotherapy. 2007;51(2):446-52. Epub 2006/11/23. doi: 10.1128/aac.00635-06. PubMed PMID: 17116686; PubMed Central PMCID: PMCPMC1797723.

143. Pouillot F, Chomton M, Blois H, Courroux C, Noelig J, Bidet P, et al. Efficacy of Bacteriophage Therapy in Experimental Sepsis and Meningitis Caused by a Clone O25b:H4-ST131 Escherichia coli Strain Producing CTX-M-15. Antimicrobial agents and chemotherapy. 2012;56(7):3568-75. doi: 10.1128/aac.06330-11. PubMed PMID: 22491690; PubMed Central PMCID: PMCPMC3393425.

144. Biswas B, Adhya S, Washart P, Paul B, Trostel AN, Powell B, et al. Bacteriophage therapy rescues mice bacteremic from a clinical isolate of vancomycin-resistant Enterococcus faecium. Infection and immunity. 2002;70(1):204-10. Epub 2001/12/19. PubMed PMID: 11748184; PubMed Central PMCID: PMCPMC127648.

145. Stratton CW. Phages, Fitness, Virulence, and Synergy: A Novel Approach for the Therapy of Infections Caused by Pseudomonas aeruginosa. The Journal of infectious diseases. 2017;215(5):668-70. Epub 2016/12/23. doi: 10.1093/infdis/jiw634. PubMed PMID: 28007923.

ANNEXES

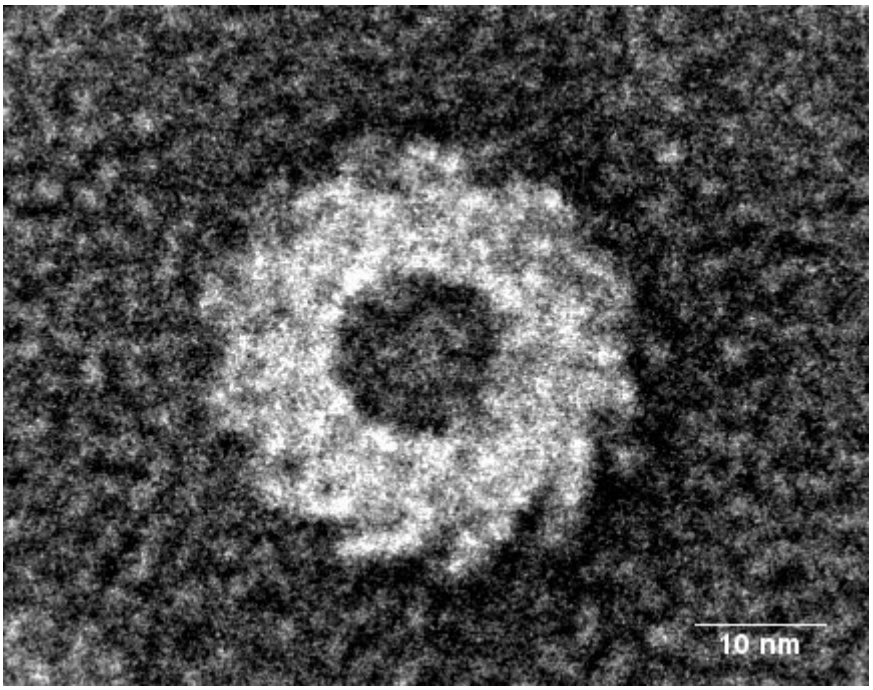

Phage tail, view from the top. Negative staining. 2016. F. Oechslin

Annexes

This annex section is composed of three published manuscripts, which I finished or contributed during the course of my thesis.

- **Oechslin F**, Daraspe J, Giddey M, Moreillon P, Resch G. In vitro characterization of PlySK1249, a novel phage lysin, and assessment of its antibacterial activity in a mouse model of Streptococcus agalactiae bacteremia. Antimicrobial agents and chemotherapy. 2013.
- Mancini S, Menzi C, **Oechslin F**, Moreillon P, Entenza JM. Antibodies Targeting Hsa and PadA Prevent Platelet Aggregation and Protect Rats against Experimental Endocarditis Induced by Streptococcus gordonii. Infection and immunity. 2016.
- Veloso TR, **Oechslin F**, Que YA, Moreillon P, Entenza JM, Mancini S. Aspirin plus ticlopidine prevented experimental endocarditis due to Enterococcus faecalis and Streptococcus gallolyticus. Pathogens and disease. 2015.

In addition, I was also involved in the two following manuscript which are already submitted:

- In vitro Characterization of PlyE146, A Novel Phage Lysin That Targets Gram-negative Bacteria. Yu Larpin, **Frank Oechslin**, Philippe Moreillon, Gregory resch, Jose Entenza, and Stefano Mancini. Antimicrobial Agent and Chemotherapy.

- Marginal Role of von Willebrand Factor-Binding Protein and Coagulase in the Initiation of Endocarditis in Rats with Catheter-Induced Aortic Vegetations. Stefano Mancini, **Frank Oechslin**, Carmen Menzi, Yok-Ai Que, Jorien Claes, Ruth Heying, Tiago Rafael Veloso, Philippe Moreillon, José Manuel Entenza. The Journal of Infectious Diseases.

Finally, I was also involved in the patent number WO2015008214. Resch G, **Oechslin F**, Moreillon P. Bacterial lysins and uses thereof. University of Lausanne.

AAC
Journals.ASM.org

In Vitro Characterization of PlySK1249, a Novel Phage Lysin, and Assessment of Its Antibacterial Activity in a Mouse Model of *Streptococcus agalactiae* Bacteremia

Frank Oechslin,[a] Jean Daraspe,[b] Marlyse Giddey,[a] Philippe Moreillon,[a] Grégory Resch[a]

Department of Fundamental Microbiology, University of Lausanne, Lausanne, Switzerland[a]; Electron Microscopy Facility, University of Lausanne, Lausanne, Switzerland[b]

Beta-hemolytic *Streptococcus agalactiae* is the leading cause of bacteremia and invasive infections. These diseases are treated with β-lactams or macrolides, but the emergence of less susceptible and even fully resistant strains is a cause for concern. New bacteriophage lysins could be promising alternatives against such organisms. They hydrolyze the bacterial peptidoglycan at the end of the phage cycle, in order to release the phage progeny. By using a bioinformatic approach to screen several beta-hemolytic streptococci, a gene coding for a lysin was identified on a prophage carried by *Streptococcus dysgalactiae* subsp. *equisimilis* SK1249. The gene product, named PlySK1249, harbored an original three-domain structure with a central cell wall-binding domain surrounded by an N-terminal amidase and a C-terminal CHAP domain. Purified PlySK1249 was highly lytic and bactericidal for *S. dysgalactiae* (2-$\log_{10}$ CFU/ml decrease within 15 min). Moreover, it also efficiently killed *S. agalactiae* (1.5-$\log_{10}$ CFU/ml decrease within 15 min) but not several streptococcal commensal species. We further investigated the activity of PlySK1249 in a mouse model of *S. agalactiae* bacteremia. Eighty percent of the animals ($n = 10$) challenged intraperitoneally with 10^6 CFU of *S. agalactiae* died within 72 h, whereas repeated injections of PlySK1249 (45 mg/kg 3 times within 24 h) significantly protected the mice ($P < 0.01$). Thus, PlySK1249, which was isolated from *S. dysgalactiae*, demonstrated high cross-lytic activity against *S. agalactiae* both *in vitro* and *in vivo*. These encouraging results indicated that PlySK1249 might represent a good candidate to be developed as a new enzybiotic for the treatment of systemic *S. agalactiae* infections.

Streptococcus agalactiae, or group B *Streptococcus* (GBS) (1), is a common inhabitant of the gastrointestinal and genital tracts, with an asymptomatic-carriage rate of 9% to 30% in adults. It is the leading cause of invasive neonatal infections in children (2), in whom it may cause bacteremia, pneumonia, and meningitis, with mortality rates ranging from 5% to 20% (3). In addition, GBS infection is now also increasingly reported in older children and adults, in whom it provokes severe sepsis often complicated by multiple deep-seated abscesses and sometimes endocarditis (4–6).

A major source of neonate GBS infection is asymptomatic vaginal carriage by the mother. Therefore, prevention guidelines aim at interfering with mother-to-child transmission at the time of birth and advocate parenteral administration of penicillin G or amoxicillin to GBS-colonized women 4 h before delivery (7). Recently, concerns regarding GBS isolates with decreased susceptibility to penicillin (8, 9) and even resistance to penicillin G and ceftriaxone have emerged (10). Moreover, in some U.S. states, the prevalence of GBS resistant to erythromycin and clindamycin has increased from 15.8% to 32.8% and 10.5% to 15%, respectively, between 1996 and 2003 (11). In parallel, Bergseng et al. (12) also reported erythromycin and clindamycin resistance in Norway, as well as an increase in the rate of mortality from neonatal GBS infections (from 6.5% in 1996 to 16.5% in 2005), which seemed to correlate with the drug resistance phenotype. This supports the necessity of searching for alternative compounds against drug-resistant bacteria in general and *S. agalactiae* in particular.

Bacteriophage lysins having peptidoglycan hydrolase activities represent one such compound (13). These enzymes are produced by both temperate and lytic phages in order to lyse their host cells and release their progeny at the end of their life cycle. Because purified lysins are able to reach and destroy the peptidoglycan of Gram-positive bacterial cells when added from the outside, they were successfully used either topically, to decontaminate colonized tissues, or parenterally, in cases of severe infections (13). Since a temperate bacteriophage integrates its genome into the host chromosome, we used a bioinformatic approach to screen sequenced bacterial genomes of beta-hemolytic streptococci in order to identify new bacteriophage lysin genes. Here we describe a new lysin encoded on a prophage-like region inserted into the genome of *Streptococcus dysgalactiae* subsp. *equisimilis* strain SK1249. The purified lysin, named PlySK1249, showed an uncommon architecture with a central cell wall-binding domain. It not only efficiently lysed and killed *S. dysgalactiae* but also had cross-lytic activity against GBS and several representatives of beta-hemolytic streptococci *in vitro*. Accordingly, PlySK1249 was very potent in curing mice suffering from GBS-induced bacteremia. Our results underline the cross-lytic activity of PlySK1249 between beta-hemolytic streptococci and suggest that it could constitute a new alternative for the prevention and the treatment of bacterial infections due to GBS.

Received 6 August 2013 **Returned for modification** 21 September 2013
Accepted 29 September 2013
Published ahead of print 7 October 2013
Address correspondence to Grégory Resch, gregory.resch@unil.ch.
Supplemental material for this article may be found at http://dx.doi.org/10.1128/AAC.01701-13.

doi:10.1128/AAC.01701-13

TABLE 1 Bacterial strains, plasmids, and oligonucleotides used in this study

Strain, plasmid, or oligonucleotide	Characteristics or origin[a]	Source or reference
Bacterial strains		
E. coli BL21(DE3)pLysS	F^- *ompT hsdSB* (r_B^- m_B^-) *dcm*$^+$ *gal* (DE3) pLysS (Cam^r)	Stratagene
E. coli BL21/pPlySK1249^{15b}	*E. coli* BL21(DE3)(pLysS) transformed with pPlySK1249^{15b}	This study
E. coli BL21/pPlySK1249^{28a}	*E. coli* BL21(DE3)(pLysS) transformed with pPlySK1249^{28a}	This study
S. dysgalactiae SK1249	Human, hemoculture	
GBS FSL-S3-026	Bovine	
GBS 17–2167	Human, endocarditis	
GBS 532	Human	
GBS GF	Human, hemoculture	
S. pyogenes ATCC 19615	Human, sore throat	
S. gordonii DL1	Human	
S. mutans ATCC 25175	Human, carious dentine	
S. suis 19	Porcine	
S. uberis ATCC 700407	Bovine	
S. mutans ATCC 25175	Human, carious dentine	
E. faecalis ATCC 29212	Human, urine	
E. faecium D344	Human	
S. pneumoniae D39	Human	
S. aureus M32	Bovine, subclinical mastitis	
S. aureus Laus102	Human, healthy patient	
E. faecalis ATCC 29212	Human, urine	
Plasmids		
pET-15b	Expression vector; Amp^r	Novagen
pET-28a	Expression vector; Kan^r	Novagen
pPlySK1249^{15b}	pET-15b carrying *PlySK1249*	This study
pPlySK1249^{28a}	pET-28a carrying *PlySK1249*	This study
Oligonucleotides		
plySK15bNdeIFw	5′-GGAATTCCATATGGGAAAACATCTAGTCATTTGTGGTCATGGGCAAGGGCG-3′	This study
plySK15bBamHIRv	5′-CGCGGATCCTTAATGAAATTCTAAACCAACCAACAACTTTTCCAAGTTTAACTGTTCCAG-3′	This study
plySK28aNcoIFw	5′-GCATGCCATGGGAAAACATCTAGTGATTTGTGGACATGGGCAAGGACG-3′	This study
plySK28aXhoIRv	5′-GCCGCTCGAGTGAAATTCTAAACCAACCTACAACTTTTCCAAGTTTAACTGTTCCAG-3′	This study
Universal T7 primer Fw	5′-TAATACGACTCACTATAGGG-3′	Microsynth
Universal T7 primer Rv	5′-GCTAGTTATTGCTCAGCGG-3′	Microsynth

[a] Amp^r, ampicillin resistance; Cam^r, chloramphenicol resistance; Kan^r kanamycin resistance. Restriction sites in oligonucleotides are underlined.

MATERIALS AND METHODS

Bacterial strains and reagents. Unless otherwise specified, chemicals used in this study were purchased from Sigma-Aldrich (St. Louis, MO). Restriction enzymes were obtained from Promega (Madison, WI), and primers were synthesized by Microsynth AG (Balgach, Switzerland). All strains used in this study (Table 1) were grown at 37°C with aeration (250-rpm shaking), except for *Streptococcus pneumoniae*, which was grown without aeration. Streptococci and enterococci were cultured in brain heart infusion (BHI) and plated on Mueller-Hinton agar containing 5% sheep blood (bioMérieux SA, Marcy l'Etoile, France) and BHI agar, respectively. *Staphylococcus aureus* was grown in tryptic soy broth (TSB) and plated as streptococci. *Escherichia coli* strains were grown in Luria-Bertani (LB) broth and plated on LB agar. Frozen stocks were made from cultures in the exponential phase of growth supplemented with 20% glycerol (vol/vol).

Cloning of *PlySK1249*. The gene *HMPREF9964_0831*, potentially encoding a functional lysin, was identified using a bioinformatic approach and is referred to as *PlySK1249* for convenience throughout this paper, as described in Results. To further clone *PlySK1249*, genomic DNA was prepared from *S. dysgalactiae* strain SK1249 using the DNeasy blood and tissue kit (Qiagen, Valencia, CA) according to the manufacturer's instructions. *PlySK1249* was PCR amplified with specific primer pairs, i.e., plySK15bNdeIFw/plySK15bBamHIRv and plySK28aNcoIFw/plySK28aXhoIRv (Table 1). PCR products were digested with compatible restrictions endonucleases and ligated into expression vectors pET-15b and pET-28a (Merck KGaA, Darmstadt, Germany). Two plasmids, namely, pPlySK1249^{15b} and pPlySK1249^{28a} (Table 1), were obtained in which the His tag was located at either the 5′ or 3′ end of *PlySK1249*, respectively. Constructs were transformed in One Shot BL21(DE3)pLysS chemically competent *E. coli* cells (Life Technologies Europe B.V., Zug, Switzerland) and propagated on LB plates or broth supplemented with ampicillin (100 μg/ml) and chloramphenicol (25 μg/ml) for *E. coli* BL21/pPlySK1249^{15b} or kanamycin (30 μg/ml) and chloramphenicol (25 μg/ml) for *E. coli* BL21/pPlySK1249^{28a}. All constructs were validated by DNA sequencing using universal T7 primers (Table 1).

***PlySK1249* expression and activity screening of the gene product.** In order to identify a clone expressing active PlySK1249 lysin, a protocol was adapted from the work of Schmitz et al. (14). Briefly, BL21/pPlySK1249^{15b} and BL21/pPlySK1249^{28a} transformants (Table 1) were replica plated on LB agar supplemented with the appropriate antibiotics and 0.4 mM isopropyl-1-thio-β-D-galactopyranoside (IPTG). Following overnight incubation at 37°C, colonies were exposed to chloroform vapors for 20 min. Permeabilized cells were further overlaid with 15 ml of molten soft agar containing autoclaved *S. dysgalactiae* SK1249 cells. Plates were incubated at 37°C and observed for clearing zones surrounding colonies for up to 24 h. To prepare molten soft agar, an overnight culture of *S. dysgalactiae*

SK1249 was centrifuged, washed with 1 vol of 0.9% NaCl, and resuspended in 0.25 vol of PBS, pH 7.4. The cell suspension was further supplemented with granulated agar (7.5 g/liter), autoclaved for 15 min at 120°C, and stored at 4°C.

Purification of PlySK1249. A starter culture from an *E. coli* colony carrying the BL21/pPlySK1249[28a] construct and surrounded by a large lysis zone in the above-mentioned screening test was grown overnight in LB supplemented with kanamycin (30 μg/ml) and chloramphenicol (50 μg/ml). The following morning, 25 ml of the culture was diluted with 20 vol of preheated fresh LB and further grown at 37°C. At an optical density at 600 nm (OD_{600}) of 0.7, the culture was induced for 20 h at 18°C by the addition of 0.4 mM IPTG. Cells were centrifuged, washed with 30 ml of 0.9% NaCl, and resuspended in 30 ml of binding buffer (20 mM imidazole, 20 mM phosphate buffer, 0.5 M NaCl [pH 7.4]). Aliquots of 15 ml were frozen at −80°C, thawed, and sonicated on ice (Sonopuls; Bandelin Electronics, Berlin, Germany). Cell debris was removed from pooled supernatants by centrifugation (15,000 rpm, 30 min, 4°C). Supernatant were further treated with 1 μg/ml RNase A and DNase I (Roche AG, Basel, Switzerland) for 45 min at 4°C and filtered through 0.45-μm Acrodisc filters (Pall, Ann Arbor, MI). The filtrate was applied to a 5-ml HisTrap HP column (GE Healthcare, Glattbrugg, Switzerland) previously equilibrated with binding buffer and coupled to an ÄKTA Prime apparatus (GE Healthcare). After a washing with 50 ml of buffer A (50 mM imidazole, 20 mM phosphate buffer, 0.5 M NaCl [pH 7.4]), His-tagged PlySK1249 was eluted in buffer B (500 mM imidazole, 20 mM phosphate buffer, 0.5 M NaCl [pH 7.4]). Imidazole was removed by extensive dialysis against lysin buffer (500 mM L-arginine, 50 mM phosphate buffer [pH 7.4]) using a membrane tubing (molecular weight cutoff [MWCO], 12,000 to 14,000; Spectra/Por, Rancho Dominguez, CA). PlySK1249 was analyzed on NuPage 4 to 12% bis-Tris gels (Invitrogen, Carlsbad, CA).

In vitro quantification of PlySK1249 activity against *S. dysgalactiae*: effect of bacterial growth phase and pH. PlySK1249 activity was measured by following the decrease in turbidity of a solution of *S. dysgalactiae* SK1249 cells resuspended in lysis buffer (40 mM phosphate buffer, 200 mM NaCl [pH 7.4]). Briefly, bacterial cells were liquid cultured overnight, subcultured (1:100) to an OD_{600} of ~0.4 the next morning, and harvested by centrifugation before being washed with 0.9% NaCl and finally resuspended in lysis buffer to an OD_{600} of 1. Activity was measured by mixing 150 μl of the bacterial cell suspension with 150 μl of serial 2-fold dilutions of PlySK1249 in 96-well microtiter plates. Serial dilutions of the enzyme were done in lysin buffer. The decrease in OD_{600} was monitored each min for 1 h with an EL808 absorbance microplate reader run with Gen5 software (BioTek, Winooski, VT) and set to 37°C. The well in which a decrease in the optical density of half in 15 min was observed was defined as containing one unit (1 U) of purified enzyme (15). In order to test the effect of the growth phase on the susceptibility of *S. dysgalactiae* to PlySK1249, subcultured cells were harvested at OD_{600} of 0.13, 0.48, 0.85, and 1.02 before being exposed to purified lysin (final concentration, 3.3 U/ml). To test the effect of pH on the PlySK1249 activity, *S. dysgalactiae* cell suspensions and PlySK1249 solutions were both prepared in buffers with pH values ranging from 4.0 to 9.0. Cells were then exposed to PlySK1249 (final concentration, 3.3 U/ml), and the decrease in OD_{600} was monitored after 15 min incubation at 37°C. All reactions were performed in triplicate.

PlySK1249 host range. In order to determine the PlySK1249 host range, subcultures of different bacterial species (Table 1) were harvested at an OD_{600} of ~0.4 and processed as described above before being exposed to purified PlySK1249 (final concentration, 3.3 U/ml). The decrease in OD_{600} was monitored after 15 min incubation at 37°C. All reactions were performed in triplicate.

***In vitro* time-kill assays.** To determine bacterial viability, time-kill assays were performed in triplicate by exposing either a solution of *S. dysgalactiae* SK1249 at 10^9 CFU/ml or a solution of GBS clinical strain 17-2167 at 5×10^8 CFU/ml resuspended in lysin buffer to purified PlySK1249 (final concentration, 3.3 U/ml) at 37°C. At different times over 1 h of incubation, 100-μl aliquots were collected, serially diluted in 10 ml 0.9% ice-cold NaCl, and plated for colony counts. Viable colonies were enumerated after 24 h of incubation at 37°C.

Transmission electron microscopy (TEM). *S. dysgalactiae* SK1249 was grown to an OD_{600} of 0.4, centrifuged, and resuspended in lysis buffer to an OD_{600} of 1.0. Then 150 μl of this bacterial suspension was mixed with 150 μl of PlySK1249 (final concentration, 3.3 U/ml). After 15 min of incubation at 37°C, 1 μl of this solution was adsorbed on a glow-discharged copper 200-mesh grid coated with Formvar-carbon (EMS, Hatfield, PA) during 1 min at room temperature (RT). The grid was then washed with two drops of distilled water followed by staining with 1% of uranyl acetate in H_2O (Sigma, St. Louis, MO) for 1 min. Excess uranyl acetate was removed with blotting paper, and the grid was dried for 10 min before image acquisition. Micrographs were taken with an FEI CM100 transmission electron microscope (FEI, Eindhoven, The Netherlands) at an acceleration voltage of 80 kV and 11,000× magnification (pixel size of 0.93 nm) with a TVIPS TemCam-F416 digital camera (TVIPS GmbH, Gauting, Germany).

PlySK1249 therapeutic trials in mice. Animal experimentation was carried out in strict accordance with the recommendations of the Swiss Federal Act on Animal Protection, and the protocol was approved by the Committee on the Ethics of Animal Experiments of the Consumer and Veterinary Affairs Department of the State of Vaud (permit number 2395). A total of 35 six-week-old CD1 Swiss female mice (Charles River Laboratories, L'Arbresle, France) with an average weight of 22 ± 1 g were used. In order to validate the bacteremic state of mice at the time of the initial treatment injection, i.e., 1 h after the bacterial challenge, the left kidney and spleen were removed aseptically from three mice 45 min after i.p injection of 10^6 CFU of GBS clinical strain 17-2167. Organs were homogenized in 1 ml of saline and briefly centrifuged, and supernatants were plated on blood agar plates to determine the number of viable organisms in tissues. For therapeutic experiments, animal sample sizes were estimated with the formula for dichotomous variables (16). In a first series of experiments conducted to evaluate the effect of a single bolus injection of PlySK1249, two groups of mice were injected intraperitoneally (i.p.) with 10^6 CFU of the GBS 17-2167. Group 1 (treatment group) received 22.5 mg/kg of PlySK1249 in 200 μl i.p. 1 h after the bacterial challenge, while group 2 (control group) received 200 μl of lysin buffer i.p. in parallel.

A second series of experiments was run to test the effect of dose escalation. Two groups of mice were injected i.p. with 10^6 CFU of the GBS 17-2167, with the treatment group receiving 45 mg/kg of PlySK1249 in 200 μl i.p. 2, 20, and 24 h after the bacterial challenge, while the control or untreated group received 200 μl of lysin buffer i.p at the same times. Survival curves were drawn, analyzed, and compared with log rank (Mantel-Cox) and Gehan-Breslow-Wilcoxon tests using GraphPad Prism version 5.00 for Windows (GraphPad Software, San Diego, CA).

Nucleotide sequence accession numbers. The full genomic sequence of *S. dysgalactiae* SK1249 has been deposited in GenBank as a whole-genome shotgun sequencing project under accession number AFIN00000000. The sequence of PlySK1249 has been submitted to GenBank under accession number EGL49245.1.

RESULTS

Identification of prophage-like regions in the genome of *S. dysgalactiae* strain SK1249 and identification of *PlySK1249*. Phage search tool (PHAST) (17), a web tool finder and annotator of prophage regions within bacterial genomes, found nine prophage-related regions in the sequenced genome of *S. dysgalactiae* SK1249 (http://phast.wishartlab.com/cgi-bin/change_to_html.cgi?num=AFIN00000000).

HMPREF9964_0831, encoding a potential lysin, was identified at chromosomal positions 550,441 to 551,910 within prophage-related region 2, annotated as a questionable prophage by PHAST (data not shown), and renamed *PlySK1249* for convenience in this

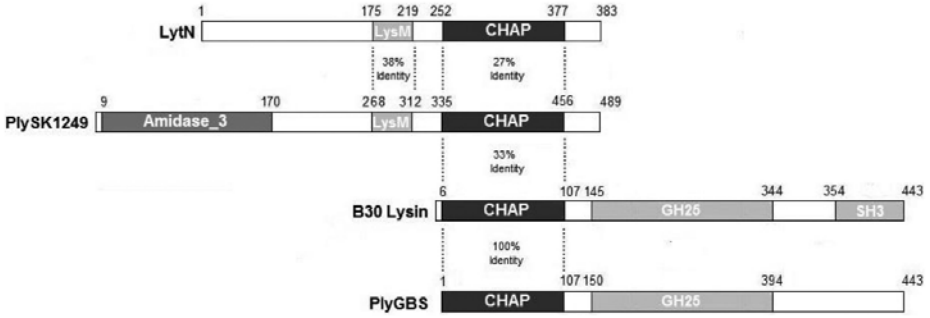

FIG 1 Schematic representation of relevant lysins. MurNac-LAA, amidase catalytic domain; CHAP, cysteine histidine-dependent aminohydrolase/peptidase catalytic domain; GH25, glycoside hydrolase family 25 catalytic domain; LysM and SH3, substrate binding domains. Amino acid identities are presented between the considered domains.

study. The analysis of the deduced gene product, named PlySK1249, revealed a putative 489-amino-acid LysM domain protein with a calculated molecular mass of ca. 53 kDa. PlySK1249 shares 98% and 80% identity with phage-associated cell wall hydrolases found in *Streptococcus suis* R61 (EHC01546.1) and *S. agalactiae* FSL S3-026 (ZP_11943978.1), respectively.

The predicted primary structure of PlySK1249 is depicted in Fig. 1. Conserved domain analysis using the Conserved Domains Database (CDD) (http://www.ncbi.nlm.nih.gov/Structure/cdd/cdd.shtml) indicated that PlySK1249 harbors three putative functional domains: (i) an N-terminal catalytic domain with predicted amidase activity; (ii) a central LysM cell wall-binding domain that shares 38% identity (100% coverage) with a similar domain found in the *S. aureus* LytN autolysin (18), and (iii) a C-terminal catalytic domain that shares 27% (71% coverage) and 33% (40% coverage) identity with the cysteine histidine-dependent aminohydrolase/peptidase (CHAP) domains of the LytN autolysin (18) and the B30 lysin (19, 20), respectively. The conserved cysteine and histidine residues of the CHAP domain were found at positions 353 and 414 of the PlySK1249 sequence (see Fig. S1 in the supplemental material).

Cloning of *PlySK1249* and screening of PlySK1249 lytic activity. *PlySK1249* was successfully amplified by PCR from purified genomic DNA of *S. dysgalactiae* SK1249 and cloned into pET-15b and pET-28a expression vectors (leading to the constructs pPlySK1249^{15b} and pPlySK1249^{28a}, respectively). Constructs were transformed into *E. coli* BL21 cells (Table 1), and transformants were recovered on LA plates supplemented with antibiotics as described in Materials and Methods. Following IPTG induction, chloroform permeabilization, and overlay with soft agar containing autoclaved *S. dysgalactiae* SK1249 cells, lysis zones developed around BL21/pPlySK1249^{28a} colonies within 12 h of incubation (see Fig. S2 in the supplemental material). In contrast, no lysis zones were observed around BL21/pet28a and BL21/pPlySK1249^{15b} colonies (Fig. S2 and data not shown, respectively). One BL21/pPlySK1249^{28a} colony, surrounded by a large halo, was selected and further grown in order to purify PlySK1249.

Purification of PlySK1249. We obtained 8 mg of PlySK1249 from 1 liter of culture by a single-step passage of the crude extract, obtained after sonication, on a 5-ml HisTrap HP column. PlySK1249 was expressed, was soluble, and migrated at the expected molecular mass of 53 kDa on a 4 to 12% Novex bis-Tris gel (Fig. 2, lanes 2.1, 2.2, and 3.1). A purity of ca. 90% was achieved (Fig. 2, lane 3.1; also, see Fig. S3 in the supplemental material). Purified PlySK1249 was stored at 4°C in lysin buffer (500 mM L-arginine, 50 mM phosphate buffer [pH 7.4]) until further use.

***In vitro* quantification of PlySK1249 activity; effect of bacterial growth phase and pH.** The antibacterial activity of purified lysins is commonly quantified by determining their capacity to decrease the turbidity of a suspension of bacterial cells over time. In such turbidity assays, 1 U of enzyme is defined as the amount of enzyme that results in a 50% drop in turbidity (OD_{600}) in 15 min and at 37°C in a suspension of bacterial cells harvested in mid-

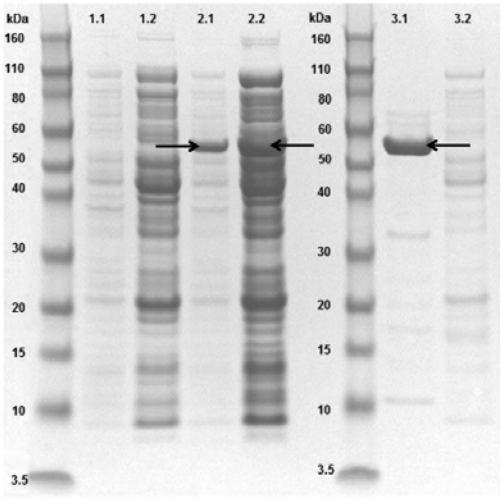

FIG 2 Electrophoretic profile of overexpressed PlySK1249. Lanes: 1.1 and 1.2, noninduced total and cytoplasmic fractions, respectively; 2.1 and 2.2, induced total and cytoplasmic fractions, respectively; 3.1 and 3.2, purified PlySK1249 and column flowthrough, respectively. Arrows indicate overexpressed PlySK1249. Molecular masses of the Novex Sharp standard are given.

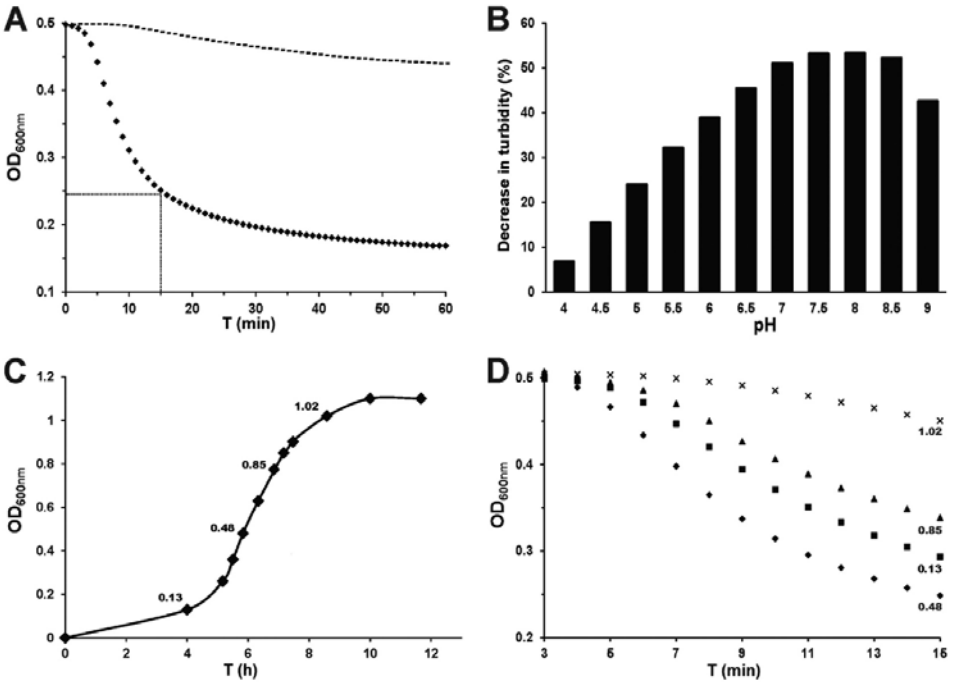

FIG 3 PlySK1249 *in vitro* activity. All experiments were done in OD_{600} turbidity assays using *S. dysgalactiae* SK1249 as the target. (A) The specific activity of PlySK1249 was 1 U/μg. One unit of activity was defined as the amount of lysin resulting in a 50% decrease in OD_{600} in 15 min (closed diamonds, PlySK1249; dotted line, controls). (B) The optimum pH was between 7 and 8.5, determined after a 15-min exposure of the cells to PlySK1249 (final concentration, 3.3 U/ml). (C and D) PlySK1249 was more active against bacteria in the early than the late stage of growth. The OD_{600} at which the cells were harvested before challenge with PlySK1249 (final concentration, 3.3 U/ml) are indicated.

logarithmic growth phase. Using this definition, which is commonly accepted, the calculated specific activity was 1 U/μg, which was equivalent to 50 U/nmol of PlySK1249 (Fig. 3A).

Figure 3B depicts the pH activity profile in the presence of 3.3 U/ml of PlySK1249. The optimal pH was found to be between pH 7 and 8.5, with a ca. 50% decrease in OD_{600} achieved at these pH values in 15 min. The activity was lower at acidic and basic pHs, with, for instance, only a 7% OD_{600} decrease at pH 4.

It is well known that the activity of phage lysins is dependent on the growth phase the bacterial targets are in when they are challenged by the enzyme. In order to test this growth phase-dependent sensitivity to PlySK1249, aliquots of *S. dysgalactiae* SK1249 were harvested at different stages of growth (Fig. 3C) and further challenged by purified PlySK1249 in turbidity assays (Fig. 3D). We observed that bacterial cells harvested at early exponential and mid-exponential phases were much more susceptible to PlySK1249-induced lysis than cells harvested in the late exponential or stationary phase. For instance, while the turbidity of a solution of cells harvested in the exponential growth phase (i.e., at an OD_{600} of 0.48) decreased by 50% in 15 min, that of cells harvested in the early stationary growth phase decreased by only ca. 5% (i.e., at an OD_{600} of 1.02) (Fig. 3D).

Host range. We used the turbidity assay to further determine the activity of PlySK1249 against several different bacterial species. All beta-hemolytic species tested (*S. dysgalactiae*, GBS, and *Streptococcus pyogenes*) were susceptible to PlySK1249, with some strain-to-strain variation for GBS (Fig. 4). Indeed, while a ca. 65% turbidity decrease was observed for the GBS strain FSL-03, only a ca. 15% decrease was achieved under the same conditions with strain 532. Interestingly, *Streptococcus uberis* and *Streptococcus suis* were also susceptible, with ca. 20% and ca. 30% decreases in turbidity, respectively. PlySK1249 was active against *Streptococcus gordonii* strain DL1 (ca. 45% turbidity decrease) but not against *Streptococcus mutans*, *S. pneumoniae*, *S. aureus*, *Enterococcus faecalis*, or *Enterococcus faecium* (<10% turbidity decreases in all cases) (Fig. 4).

***In vitro* time-kill assays.** In order to determine if the observed loss of turbidity resulted from cell bursting and subsequent death, we further tested the viability of bacterial cells exposed to PlySK1249 in time-kill experiments (Fig. 5) and observed the effect of lysin on the cells by TEM (Fig. 6). To this end, a suspension of *S. dysgalactiae* SK1249 harvested in mid-log phase was challenged with 3.3 U/ml of lysin and plated for numeration at different incubation times (Fig. 5). Our data showed a ca. 2-log CFU/ml decrease in 15 min, which was in agreement with the observed decrease in turbidity. Similarly, a ca. 2-$\log_{10}$ CFU/ml decrease in

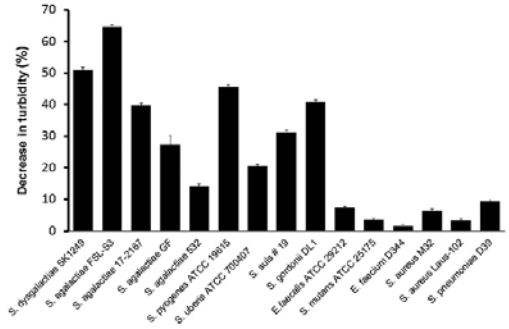

FIG 4 Host range. All experiments were done in turbidity assays in the presence of purified PlySK1249 (final concentration, 3.3 U/ml) and bacterial cells harvested in mid-exponential growth phase (i.e., at an OD_{600} of ~0.5), which had been previously washed and adjusted to an OD_{600} of ~0.5 in lysis buffer. Values are means and standard deviations from triplicates.

15 min was achieved with the same amount of PlySK1249 for the GBS clinical strain 17-2167, which was used in the mouse model of GBS-induced bacteremia. In parallel, TEM imaging of aliquots of unchallenged (Fig. 6A) and challenged (Fig. 6B) *S. dysgalactiae* cells revealed that exposure to PlySK1249 led to cytoplasm extrusion, resulting in ghost cells.

PlySK1249 efficacy in a mouse model of GBS-induced bacteremia. The therapeutic potential of PlySK1249 was tested in a mouse model of GBS-induced bacteremia. To determine the natural history of early infection, three mice were challenged i.p. with 10^6 CFU of GBS 17-2167 in 100 μl of 0.9% NaCl. Animals were euthanized 1 h postinfection, and various organs were tested for viable GBS. We found $>10^5$ CFU/g in the spleen and kidneys (data not shown), demonstrating that extensive bacterial seeding had already occurred in the organs at this time point. On this basis, PlySK1249 treatment was started 1 h after bacterial challenge in all subsequent experiments.

In a first series of therapeutic experiments, mice were infected by i.p. injection of 10^6 CFU of GBS 17-2167 in 100 μl of 0.9% NaCl

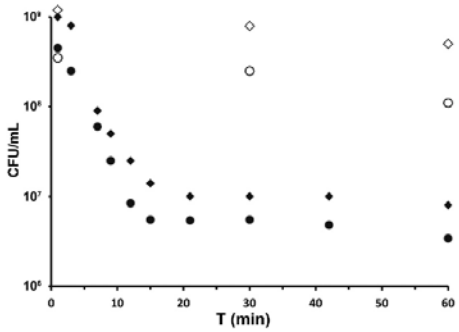

FIG 5 *In vitro* time-kill assays. *S. dysgalactiae* SK1249 (closed diamonds) and *S. agalactiae* clinical strain 17-2167 (closed circles) were exposed to PlySK1249 (final concentration, 3.3 U/ml). Controls (open diamonds and circles) were exposed to lysin buffer only. Each dot represents the mean of triplicates.

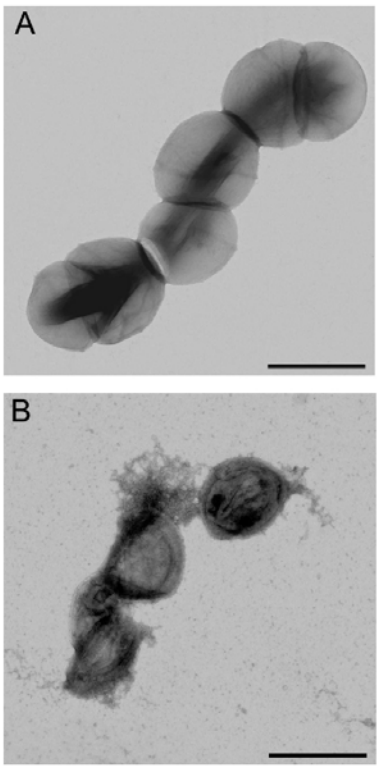

FIG 6 Visualization of PlySK1249 lytic activity by TEM (magnification, ×11,000). (A) *S. dysgalactiae* SK1249 treated with lysis buffer was not disturbed. (B) *S. dysgalactiae* SK1249 treated for 15 min with PlySK1249 (final concentration, 3.3 U/ml) showed cytoplasmic extrusion and ghost cells. Scale bar, 1 μm.

and treated i.p. 1 h later with either a single dose of 22.5 mg/kg PlySK1249 in 100 μl lysin buffer (8 animals) or 100 μl of lysin buffer alone (7 animals). Figure 7A shows that PlySK1249 improved survival at 48 h and 72 h in this single-dose experiment. However, the difference from untreated controls was not statistically significant ($P > 0.05$). Therefore, a second series of experiments was attempted in which the total dosage and the frequency of PlySK1249 injections were increased. Animals received three injections of 45 mg/kg of PlySK1249 at 2, 20, and 24 h after bacterial challenge (Fig. 7B, arrows). This multidose treatment significantly improved survival at any time. Indeed, while only 2/10 (20%) of mice were still alive 5 days after bacterial challenge in the control group, 8/10 (80%) of mice survived during the same period in the PlySK1249 treatment group ($P < 0.01$) (Fig. 7B).

DISCUSSION

Searching for potential new phage lysins against beta-hemolytic streptococci, we focused on PlySK1249 of *S. dysgalactiae* SK1249 because of its unusual predicted three-domain structure, in which the binding domain lay between the two catalytic domains. More-

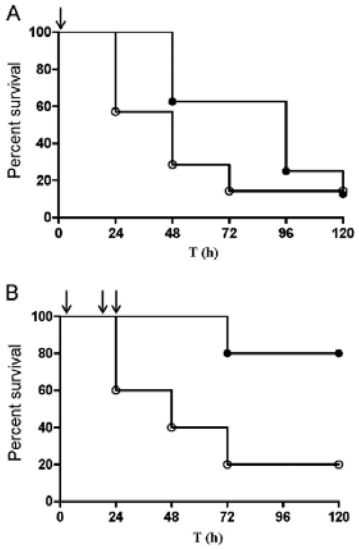

FIG 7 Therapeutic effect of PlySK1249 in a mouse model of GBS-induced bacteremia. (A) CD1 Swiss mice were i.p. injected with 10^6 CFU of the GBS clinical strain 17-2167. At 1 h postinfection (black arrow), animals received an i.p. injection of 22.5 mg/kg PlySK1249 (closed circles). A control group received lysin buffer only (open circles). (B) Mice were i.p. injected with 10^6 CFU of the GBS clinical strain 17-2167. At 2, 20, and 24 h postinfection (arrows), animals received an i.p. injection of 45 mg/kg, i.e., a total of 135 mg/kg over the first 24 h, of PlySK1249 (closed circles). A control group received lysin buffer only (open circles). Mice were monitored for survival over a period of 5 days, and results were plotted in Kaplan-Meier survival curves. Survival curves were compared with the log rank (Mantel-Cox) and Gehan-Breslow-Wilcoxon tests.

over, PlySK1249 was also interesting from the functional point of view, as it demonstrated cross-lytic activity against several beta-hemolytic streptococci (plus a selection of other streptococci) and could successfully prevent mortality in a mouse model of GBS bacteremia.

First, from the structure point of view, the PlySK1249 lysin was different from the four anti-GBS lysins that have been described so far. These include lysin B30 (isolated from GBS bacteriophage B30) (19), PlyGBS (21), and LambdaSa1 and LambdaSa2, which were isolated from GBS as well (22). Like PlySK1249, lysin B30 and PlyGBS carried two different catalytic domains. However, the primary structure and the organization of these domains were quite different, as shown in Fig. 1. For instance, although the three enzymes contained a CHAP (for "cysteine histidine-dependent amidohydrolase/peptidase") endopeptidase domain, the second functional domain of PlySK1249 was predicted to be an amidase, whereas that of lysin B30 and PlyGBS was a glycoside hydrolase of the GH25 family (19, 21). Likewise, PlySK1249 was also different from LambdaSa1 and LambdaSa2 lysins, which harbored different catalytic and binding domains (22). Finally, although some hydrolytic functions were shared among these lysin species, their overall amino acid homology was low, i.e., <40%.

Second, from the structure-function point of view, it was interesting that double-layer screening assays detected lytic activities only around *E. coli* transformed with C-terminally His-tagged pPlySK1249[28a] constructs, not those transformed with N-terminally His-tagged pPlySK1249[15b] constructs. This suggests that either the product of N-terminally His-tagged constructs was not expressed or the His tag positioned at the N-terminal end (but not the C-terminal end) of PlySK1249 abrogated the enzyme lytic activity. Although we did not work out the definitive answer to this question, it was previously shown that His tagging can affect enzymatic functions (23). Thus, it is quite possible that the N-terminal amidase domain of PlySK1249 carried the major part of the enzyme's lytic activity and that this function was affected by the His tag. As a consequence, any further development of this enzyme as a potential antimicrobial agent should take this point into consideration.

Third, from the functional point of view, some salient aspects of the PlySK1249 activity are relevant here, including pH and growth phase dependency. The optimal pH-activity relationship is well known for enzymatic activities in general and lysins in particular. For instance, lysin B30 and PlyGBS are mostly active at pH 4.5 to 6 and 4 to 6, respectively (19, 21), the optimal pH of the major autolysin LytA is around 7 (24), and the optimal pH for PlySK1249 is between 7.0 and 8.5. Beyond academic interest, these differences may have pharmacokinetic/pharmacodynamic (PK/PD) implications the development of these proteins for medical purposes. Indeed, an optimal pH of 4.5 might be more adapted to GBS decolonization of the vagina, where the surrounding pH is acidic, as shown for the PlyGBS lysin (21). Therefore, lysins with neutral optimal pH, such as PlySK1249, might have to be delivered in an appropriate buffering carrier to circumvent this issue. In contrast, PlySK1249 would be more suitable in any other infected area, especially for parenteral therapy of severe GBS infection (although the case of abscess environments, which are slightly acidic, should be tested as well). Regarding growth dependency, lysis induced by PlySK1249 (as determined *in vitro*) was faster in cells in the exponential growth phase than cells in stationary phase. Similar observations were reported for other lysins, including the B30 lysin (19). A greater susceptibility of the nascent peptidoglycan was also shown for PlyGBS, since lysin-induced extrusion and rupture of the cytoplasmic membrane occurred during cell division in the region of the septum (21). The pertinence of these observations for potential *in vivo* treatment success is not known. Bacteria at infected sites are likely to span the whole array between vegetative and dormant cells. However, the observation is conceptually similar to that made with the very large majority of antibiotics, which are active on growing but not dormant cells. Yet they do confer treatment success. Thus, the definite proof of efficacy must come from *in vivo* experimentation.

Toward this end, we tested the therapeutic potential of PlySK249 in a mouse model of GBS-induced bacteremia. While <20% of untreated control animals survived, 80% survival was observed in the animals treated with PlySK1249. Therapeutic efficacy was dose dependent, which is compatible with *in vivo* observations made with other lysins, such as the anti-pneumococcal lysin Cpl-1 (25). Moreover, although we did not perform sophisticated PK/PD measurements in these experiments, it is worth noting that the specific activity of PlySK1249 (1 U/μg) was in the same range as that of Cpl-1 (15).

Taken together, the present results demonstrate the *in vitro* efficacy and the proof of concept for successful *in vivo* therapy

against GBS with the new PlySK249 lysin. Moreover, PlySK1249 represent a new lysin with cross-species lytic activity (26) against several beta-hemolytic streptococci, including GBS, and some other streptococcal species. This makes PlySK1249 a good candidate for more thorough preclinical testing. Larger-scale antimicrobial screening should be performed to broaden the information on its spectrum. In addition, more *in vivo* studies could be carried out in relevant situations before human trials are initiated, for instance, in the veterinarian field against bovine- and swine-associated pathogenic streptococci.

ACKNOWLEDGMENTS

We thank Mogens Killian, Marisa Haenni, and John McCullers for having kindly provided us with *S. dysgalactiae* SK1249, *S. suis* 19, and *S. pneumoniae* D39, respectively. We are grateful to José M. Entenza and Shawna E. McCallin for very fruitful discussions and comments on the manuscript.

REFERENCES

1. Lancefield RC. 1933. A serological differentiation of human and other groups of hemolytic streptococci. J. Exp. Med. 57:571–595.
2. Phares CR, Lynfield R, Farley MM, Mohle-Boetani J, Harrison LH, Petit S, Craig AS, Schaffner W, Zansky SM, Gershman K, Stefonek KR, Albanese BA, Zell ER, Schuchat A, Schrag SJ. 2008. Epidemiology of invasive group B streptococcal disease in the United States, 1999–2005. JAMA 299:2056–2065.
3. Money DM, Dobson S. 2004. The prevention of early-onset neonatal group B streptococcal disease. J. Obstet. Gynaecol. Can. 26:826–840.
4. Muller AE, Oostvogel PM, Steegers EA, Dorr PJ. 2006. Morbidity related to maternal group B streptococcal infections. Acta Obstet. Gynecol. Scand. 85:1027–1037.
5. Jackson LA, Hilsdon R, Farley MM, Harrison LH, Reingold AL, Plikaytis BD, Wenger JD, Schuchat A. 1995. Risk factors for group B streptococcal disease in adults. Ann. Intern. Med. 123:415–420.
6. Yanai H, Hamasaki H, Tsuda N, Adachi H, Yoshikawa N, Moriyama S, Masui Y, Mishima S. 2012. Group B streptococcus infection and diabetes: a review. J. Microbiol. Antimicrob. 4:1–5.
7. Centers for Disease Control and Prevention. 2010. Prevention of perinatal group B streptococcal disease. Morb. Mortal. Wkly. Rep. 59:1–4.
8. Kimura K, Suzuki S, Wachino J, Kurokawa H, Yamane K, Shibata N, Nagano N, Kato H, Shibayama K, Arakawa Y. 2008. First molecular characterization of group B streptococci with reduced penicillin susceptibility. Antimicrob. Agents Chemother. 52:2890–2897.
9. Dahesh S, Hensler ME, Van Sorge NM, Gertz RE, Jr, Schrag S, Nizet V, Beall BW. 2008. Point mutation in the group B streptococcal pbp2x gene conferring decreased susceptibility to beta-lactam antibiotics. Antimicrob. Agents Chemother. 52:2915–2918.
10. Sendi P, Zimmerli W. 2012. Comment on: Prosthetic hip joint infection with a *Streptococcus agalactiae* isolate not susceptible to penicillin G and ceftriaxone. J. Antimicrob. Chemother. 67:1050–1051.
11. Castor ML, Whitney CG, Como-Sabetti K, Facklam RR, Ferrieri P, Bartkus JM, Juni BA, Cieslak PR, Farley MM, Dumas NB, Schrag SJ, Lynfield R. 2008. Antibiotic resistance patterns in invasive group B streptococcal isolates. Infect. Dis. Obstet. Gynecol. 2008:727505. doi:10.1155/2008/727505.
12. Bergseng H, Afset JE, Radtke A, Loeseth K, Lyng RV, Rygg M, Bergh K. 2009. Molecular and phenotypic characterization of invasive group B streptococcus strains from infants in Norway 2006–2007. Clin. Microbiol. Infect. 15:1182–1185.
13. Fischetti VA. 2008. Bacteriophage lysins as effective antibacterials. Curr. Opin. Microbiol. 11:393–400.
14. Schmitz JE, Schuch R, Fischetti VA. 2010. Identifying active phage lysins through functional viral metagenomics. Appl. Environ. Microbiol. 76:7181–7187.
15. Loeffler JM, Djurkovic S, Fischetti VA. 2003. Phage lytic enzyme Cpl-1 as a novel antimicrobial for pneumococcal bacteremia. Infect. Immun. 71:6199–6204.
16. Dell RB, Holleran S, Ramakrishnan R. 2002. Sample size determination. ILAR J. 43:207–213.
17. Zhou Y, Liang Y, Lynch KH, Dennis JJ, Wishart DS. 2011. PHAST: a fast phage search tool. Nucleic Acids Res. 39:W347–W352.
18. Frankel MB, Hendrickx AP, Missiakas DM, Schneewind O. 2011. LytN, a murein hydrolase in the cross-wall compartment of *Staphylococcus aureus*, is involved in proper bacterial growth and envelope assembly. J. Biol. Chem. 286:32593–32605.
19. Pritchard DG, Dong S, Baker JR, Engler JA. 2004. The bifunctional peptidoglycan lysin of *Streptococcus agalactiae* bacteriophage B30. Microbiology 150:2079–2087.
20. Baker JR, Liu C, Dong S, Pritchard DG. 2006. Endopeptidase and glycosidase activities of the bacteriophage B30 lysin. Appl. Environ. Microbiol. 72:6825–6828.
21. Cheng Q, Nelson D, Zhu S, Fischetti VA. 2005. Removal of group B streptococci colonizing the vagina and oropharynx of mice with a bacteriophage lytic enzyme. Antimicrob. Agents Chemother. 49:111–117.
22. Pritchard DG, Dong S, Kirk MC, Cartee RT, Baker JR. 2007. LambdaSa1 and LambdaSa2 prophage lysins of *Streptococcus agalactiae*. Appl. Environ. Microbiol. 73:7150–7154.
23. Arnau J, Lauritzen C, Petersen GE, Pedersen J. 2006. Current strategies for the use of affinity tags and tag removal for the purification of recombinant proteins. Protein Expr. Purif 48:1–13.
24. Holtje JV, Tomasz A. 1976. Purification of the pneumococcal N-acetylmuramyl-L-alanine amidase to biochemical homogeneity. J. Biol. Chem. 251:4199–4207.
25. Entenza JM, Loeffler JM, Grandgirard D, Fischetti VA, Moreillon P. 2005. Therapeutic effects of bacteriophage Cpl-1 lysin against *Streptococcus pneumoniae* endocarditis in rats. Antimicrob. Agents Chemother. 49:4789–4792.
26. Gilmer DB, Schmitz JE, Euler CW, Fischetti VA. 2013. Novel bacteriophage lysin with broad lytic activity protects against mixed infection by *Streptococcus pyogenes* and methicillin-resistant *Staphylococcus aureus*. Antimicrob. Agents Chemother. 57:2743–2750.

FEMS Pathogens and Disease, 73, 2015, ftv060

doi: 10.1093/femspd/ftv060
Advance Access Publication Date: 26 August 2015
Short Communication

SHORT COMMUNICATION

Aspirin plus ticlopidine prevented experimental endocarditis due to *Enterococcus faecalis* and *Streptococcus gallolyticus*

Tiago Rafael Veloso[1,†], Frank Oechslin[1], Yok-Ai Que[2], Philippe Moreillon[1], José Manuel Entenza[1,*] and Stefano Mancini[1]

[1]Department of Fundamental Microbiology, University of Lausanne, CH-1015 Lausanne, Switzerland and [2]Department of Intensive Care Medicine, Lausanne University Hospital Center (CHUV), CH-1011 Lausanne, Switzerland

***Corresponding author:** Department of Fundamental Microbiology, University of Lausanne, CH-1015 Lausanne, Switzerland. Tel: +41-21-6925612; Fax: +41-21-6925605; E-mail: jose.entenza@unil.ch
†Present address: Department of Cardiovascular Sciences, Centre for Molecular and Vascular Biology, Katholieke Universiteit Leuven, Leuven, Belgium
One sentence summary: Antiplatelets may be useful for the prevention of infective endocarditis.
Editor: Eric Oswald

ABSTRACT

Enterococcus faecalis and *Streptococcus gallolyticus* cause infective endocarditis (IE), which can originate from the continuous release or translocation of low bacterial numbers into the bloodstream. In this context, IE cannot be prevented with antibiotics. We previously demonstrated that aspirin plus ticlopidine protected rats from IE due to *S. gordonii* and *Staphylococcus aureus*. Here we showed that aspirin plus ticlopidine significantly reduced vegetation weight and protected 73 and 64% rats ($P < 0.005$) from IE due to *E. faecalis* and *S. gallolyticus*, respectively. These results further support the potential use of aspirin plus ticlopidine for a global prevention of IE in high-risk patients.

Keywords: antiplatelets; prophylaxis; experimental endocarditis; *Enterococcus faecalis*; *Streptococcus gallolyticus*

Enterococcus faecalis and *Streptococcus gallolyticus* are important etiologic agents of infective endocarditis (IE) in humans, with high incidence in elderly people (Slipczuk *et al.* 2013). IE induced by these bacteria is often caused by low-level bacteremia resulting from an infected medical device (Yagupsky and Nolte 1990; Sandoe *et al.* 2002) or from continuous translocation in small numbers from the gastrointestinal tract (Berg 1995).

New guidelines for IE prophylaxis restrict the use of antibiotics to high-risk patients, i.e. those with prosthetic valves or with a history of IE and impending medical procedure with high risk to contract bacteremia (Wilson *et al.* 2007). Nevertheless, the new guidelines do not propose any valuable alternative for the prevention of IE resulting from recurrent low-level bacteremia. In this context, general protective strategies that do not involve the use of antibiotics would greatly benefit at-risk patients (Chirouze, Hoen and Duval 2012). Since platelets are key elements in vegetation formation and growth, the use of antiaggregating agents appears a sensible strategy for IE prevention. We recently demonstrated that the combination of the antiplatelet oral drugs aspirin and ticlopidine was effective in the prophylaxis of experimental IE induced by *S. gordonii* and *Staphylococcus aureus* (Veloso *et al.* 2015). Here we investigated the efficacy of aspirin plus ticlopidine in the prophylaxis of IE induced in rats by *E. faecalis* and *S. gallolyticus*.

Enterococcus faecalis JH2–2 (Yagi and Clewell 1980) and *S. gallolyticus* UCN34 (Rusniok *et al.* 2010) were used. Isolates were

Received: 24 May 2015; **Accepted:** 6 August 2015

grown at 37°C with 5% CO_2 in brain heart infusion broth or agar (Difco; Becton Dickinson, Sparks, MD). Aspirin and ticlopidine did not possess antimicrobial activity against the tested strains, as they displayed minimal inhibitory concentrations of >500 $\mu g\ mL^{-1}$, values which abundantly exceed the pharmacologically relevant concentrations.

Platelet-rich plasma (PRP) and platelet-poor plasma used for the platelet-aggregation tests were obtained from anticoagulated human blood as described previously (Veloso *et al.* 2013). The ability of aspirin (50 $\mu g\ mL^{-1}$), ticlopidine (2 $\mu g\ mL^{-1}$) and the combination thereof to inhibit the aggregation of *E. faecalis* JH2–2 and *S. gallolyticus* UCN34 to human platelets was assessed by light transmission (A_{600nm}) using a fluorimeter Infinite 200® Pro (Tecan, Salzburg, Austria), as previously described (Veloso *et al.* 2015). Platelet response was monitored for a maximum of 20 min. Various inhibitors were compared with regard to the interval between the addition of bacteria to the PRP suspension and the onset of the aggregation response (lag time). Adenosine diphosphate (ADP; 10 μM), a known inducer of platelet aggregation, was used as a positive control. Two independent experiments were performed in quadruplicate.

All animal studies were carried out in strict accordance with the recommendations of the Swiss Federal Act on Animal Protection. All protocols for animal studies were reviewed and approved by the Cantonal Committee on Animal Experiments of the State of Vaud, Switzerland (Permit Number: 879.9). A mixture of ketamine (75 $mg\ kg^{-1}$) and midazolam (5 $mg\ kg^{-1}$) anaesthetics was administered to the animals before any surgical procedure. The production of catheter-induced aortic vegetations was performed in female Wistar rats, as described previously (Veloso *et al.* 2015). Prophylaxis started immediately after the insertion of the intracardiac catheter and lasted for 48 h. Aspirin (8 $mg\ kg^{-1}$) and ticlopidine (10 $mg\ kg^{-1}$), alone or in combination, were administered by an intravenous bolus injection every 12 h (Veloso *et al.* 2015). Control rats received saline. Forty eight hours after starting prophylaxis, animals were inoculated intravenously with 10^6 CFU of *E. faecalis* JH2–2 or *S. gallolyticus* UCN34, progressively delivered at a pace of 0.0017 $mL\ min^{-1}$ over 10 h (Veloso *et al.* 2015). Bacteria were inoculated continuously at low concentrations in order to simulate a protracted, low-level release of bacteria in the bloodstream from an intravenous infected device (Yagupsky and Nolte 1990) or to a constant translocation of low bacterial numbers from the gastrointestinal tract (Berg 1995). Rats were sacrificed 24 h after inoculation. The cardiac vegetations and spleens were sterilely removed, weighed and processed as described elsewhere to determine the number of viable organisms (Veloso *et al.* 2015). The lower limits of detection of bacterial growth were 2 and 1 $\log_{10}$ CFU g^{-1} of vegetation and spleen, respectively. Results of spleen cultures were indicated as positive or negative growth.

The quantification of the lag time prior to platelet aggregation, the weights of the vegetations (expressed as mean ± standard deviation) and the mean bacterial counts of cardiac vegetations were compared by the one way analysis of variance (ANOVA) with Tukey's multiple comparisons test. The percentage of infected tissues was analysed by the Fisher's exact test or the Chi-square test. All statistical analyses were performed with GraphPad Prism software (version 6.05 for Windows; GraphPad Software, La Jolla, CA, USA, www.graphpad.com). Differences were considered significant when $P < 0.05$ by use of two-sided significance levels.

In the absence of either bacteria or drug, the lag time to platelet aggregation was >20 min, whereas in the presence of ADP shrank to nearly 1 min. *Enterococcus faecalis* JH2–2 did not induce platelet aggregation (time to aggregate >20 min), in line with previous studies that showed that platelet aggregation caused by *E. faecalis* is strain and donor dependent (Johansson and Rasmussen 2013).

In contrast to *E. faecalis* JH2–2, *S. gallolyticus* UCN34 rapidly induced platelet aggregation (lag time of 7.5 ± 1.7 min) with a maximum value of 77%. Aspirin or ticlopidine alone did not affect neither the lag time (8.3 ± 1.7 and 6.8 ± 0.9 min, respectively) nor the maximum aggregation value (80 and 75%, respectively) of *S. gallolyticus* UCN34. In contrast, the combination of aspirin and ticlopidine significantly increased the lag time to 19.8 ± 0.4 min and inhibited maximum platelet aggregation to 11% ($P < 0.0001$).

The efficacy of aspirin, ticlopidine and the combination thereof to prevent experimental IE by *E. faecalis* and *S. gallolyticus* is illustrated in Fig. 1. In animals challenged with *E. faecalis* JH2–2, aspirin alone effectively decreased the vegetation weight ($P < 0.05$) and prevented IE in 31% (4/13) of animals. Ticlopidine alone failed to reduce both the vegetation weight and slightly reduced the incidence of infection (11% [1/9] sterile vegetations). By contrast, the combination of aspirin and ticlopidine significantly reduced the vegetation weight ($P < 0.0001$) and effectively prevented IE in 73% (8/11) of animals ($P = 0.001$). Bleeding events occurred only in one animal receiving aspirin. In animals challenged with *S. gallolyticus*, aspirin reduced, albeit not significantly, the vegetation weight and prevented IE in 20% (2/10) of rats while ticlopidine neither reduced the vegetation weight nor prevented IE (10% [1/10] sterile vegetations). By contrast, the combination of aspirin and ticlopidine significantly reduced the vegetation weight ($P < 0.001$) and effectively prevented IE (63% [7/11] of sterile vegetations; $P < 0.001$). No bleeding events were observed. Mean ($\log_{10}$ CFU g^{-1}) bacterial counts in vegetations of control, aspirin, ticlopidine and aspirin plus ticlopidine groups were 7.03, 4.84 ($P < 0.05$ vs controls), 5.00 and 2.89 ($P < 0.05$ vs all the other groups) in rats challenged with *E. faecalis* JH2–2, and 7.25, 5.13 ($P < 0.05$ vs controls), 5.80 and 3.55 ($P < 0.05$ vs all the other groups) in rats challenged with *S. gallolyticus* UCN34, respectively. All (100%) the control animals presented positive spleen cultures. Spleen cultures were also positive in 80–100% of animals receiving aspirin or ticlopidine alone. Spleens from animals receiving aspirin plus ticlopidine were all (100%) infected upon challenge with *E. faecalis* JH2–2 while only 26% (3/11) were positive upon challenge with *S. gallolyticus* UCN34 ($P < 0.05$ vs all the other groups).

Bacterial-induced platelet aggregation plays an important role in the development of IE. However, the mechanisms of interaction between *E. faecalis* or *S. gallolyticus* and platelets are not well defined (Fitzgerald, Foster and Cox 2006; Cox, Kerrigan and Watson 2011). In this work, we report for the first time the ability of *S. gallolyticus* to induce platelet aggregation. Previous studies reported that *E. faecalis* and *S. gallolyticus* bind preferentially to collagen and to a lower extent to fibrinogen and to fibronectin (Sillanpaa *et al.* 2008; Johansson and Rasmussen 2013). Thus, it is plausible that *E. faecalis* and *S. gallolyticus* interact with platelets through the GPVI collagen receptor and to a lesser extent through the GPIIb/IIIa fibrinogen receptor (Michelson 2010).

Aspirin and ticlopidine inhibit platelet aggregation by blocking different effectors of the signal transduction pathway, namely the cyclooxygenase 1 COX1 (an enzyme involved in the thromboxane A_2 [TXA_2] biosynthesis) and the platelet receptor for ADP P_2Y_{12}, respectively (Michelson 2010). Therefore, the inhibitory action of aspirin and ticlopidine occurs downstream of the activating signals transmitted by the interactions between bacteria and platelets, presumably through the

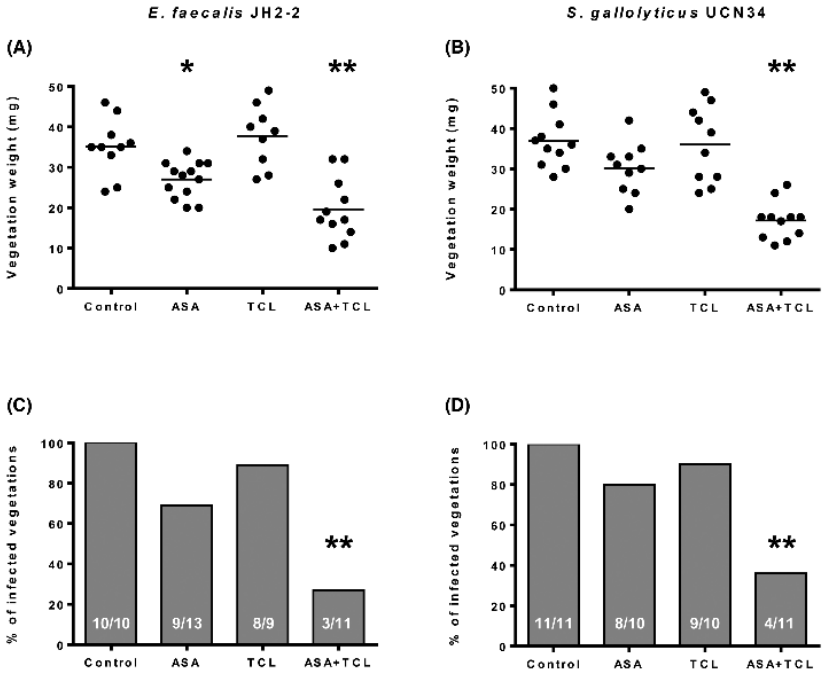

Figure 1. Effect of prophylaxis with aspirin (ASA) and ticlopidine (TCL), alone or in combination, on both the weight of vegetations (A and B) and the prevention of experimental endocarditis (C and D) induced by *E. faecalis* JH2 2 and *S. gallolyticus* UCN41. In panels A and B, each dot represents the vegetation weight for each animal and the mean is represented by the solid line. The total number of animals is indicated at the bottom of each column in panels C and D. *$P < 0.05$ compared to the control group by the ANOVA with Tukey's correction test (vegetation weight). **$P < 0.05$ compared to all the other groups using the ANOVA with Tukey's correction test (vegetation weight), or using either the Fisher's exact or the Chi square tests (infected vegetations).

blockage of platelet-to-platelet interactions. In this study, aspirin and ticlopidine were given prophylactically, i.e. prior to bacterial inoculation. This strategy likely resulted in decreased formation of the nascent platelet/fibrin vegetations, which deprived circulating bacteria of a binding scaffold, necessary first to adhere to the vegetations and then to promote their development. However, additional effects of the drugs other than targeting platelet receptors, i.e. the ability of aspirin to protect the endothelium from oxidative stress and the antiinflammatory effect of ticlopidine, might also contribute to protection of the animals from IE (Veloso *et al.* 2015).

The present results might have major clinical implications in regard of prevention against *E. faecalis* and *S. gallolyticus* IE. As an example, antiplatelet therapy is commonly used for the prevention of cardiovascular and cerebrovascular diseases in elderly patients, a population with high incidence of IE due to *E. faecalis* and *S. gallolyticus* (Slipczuk *et al.* 2013). The implementation of aspirin and ticlopidine (or equivalent newer molecules), which can be administered orally for prolonged periods, might contribute to reduce the incidence of both *E. faecalis* and *S. gallolyticus* IE in this population.

Importantly, the use of antiplatelets, given before the emergence of IE (rather than after IE establishment), is not associated with an increased risk of embolism in case of late IE, which might compromise the validity of this treatment (Anavekar *et al.* 2007, 2011; Eisen *et al.* 2009). Likely, early antiaggregant therapy may decrease the size of nascent vegetations and impede their further enlargement, whereas late antiaggregant therapy might favour vegetation dislodgment and bleeding in embolized areas (Chan *et al.* 2003). The present findings further support the potential beneficial use of antiplatelet agents for the prevention of IE in humans.

ACKNOWLEDGEMENTS

We thank Marlyse Giddey and Jacques Vouillamoz for their continuous help during the course of this work. We thank Christiane Gerscheimer, of the Service and Central Laboratory of Hematology, Lausanne University Hospital (CHUV), for help with aggregometry.

FUNDING

This work was supported by the Swiss National Science Foundation [grant numbers 310030-125325, 310030-143799/1].

Conflict of interest. None declared.

REFERENCES

Anavekar NS, Schultz JC, De Sa DD, *et al.* Modifiers of symptomatic embolic risk in infective endocarditis. *Mayo Clin Proc* 2011;**86**:1068–74.

Anavekar NS, Tleyjeh IM, Anavekar NS, *et al.* Impact of prior antiplatelet therapy on risk of embolism in infective endocarditis. *Clin Infect Dis* 2007;**44**:1180–6.

Berg RD. Bacterial translocation from the gastrointestinal tract. *Trends Microbiol* 1995;**3**:149–54.

Chan KL, Dumesnil JG, Cujec B, *et al.* A randomized trial of aspirin on the risk of embolic events in patients with infective endocarditis. *J Am Coll Cardiol* 2003;**42**:775–80.

Chirouze C, Hoen B, Duval X. Infective endocarditis prophylaxis: moving from dental prophylaxis to global prevention? *Eur J Clin Microbiol Infect Dis* 2012;**31**:2089–95.

Cox D, Kerrigan SW, Watson SP. Platelets and the innate immune system: mechanisms of bacterial-induced platelet activation. *J Thromb Haemost* 2011;**9**:1097–107.

Eisen DP, Corey GR, McBryde ES, *et al.* Reduced valve replacement surgery and complication rate in *Staphylococcus aureus* endocarditis patients receiving acetyl-salicylic acid. *J Infect* 2009;**58**:332–8.

Fitzgerald JR, Foster TJ, Cox D. The interaction of bacterial pathogens with platelets. *Nat Rev Microbiol* 2006;**4**:445–57.

Johansson D, Rasmussen M. Virulence factors in isolates of *Enterococcus faecalis* from infective endocarditis and from the normal flora. *Microb Pathog* 2013;**55**:28–31.

Michelson AD. Antiplatelet therapies for the treatment of cardiovascular disease. *Nat Rev Drug Discov* 2010;**9**:154–69.

Rusniok C, Couve E, Da Cunha V, *et al.* Genome sequence of *Streptococcus gallolyticus*: insights into its adaptation to the bovine rumen and its ability to cause endocarditis. *J Bacteriol* 2010;**192**:2266–76.

Sandoe JA, Witherden IR, Au-Yeung HK, *et al.* Enterococcal intravascular catheter-related bloodstream infection: management and outcome of 61 consecutive cases. *J Antimicrob Chemoth* 2002;**50**:577–82.

Sillanpaa J, Nallapareddy SR, Singh KV, *et al.* Adherence characteristics of endocarditis-derived *Streptococcus gallolyticus* ssp. *gallolyticus* (*Streptococcus bovis* biotype I) isolates to host extracellular matrix proteins. *FEMS Microbiol Lett* 2008;**289**:104–9.

Slipczuk L, Codolosa JN, Davila CD, *et al.* Infective endocarditis epidemiology over five decades: a systematic review. *PLoS One* 2013;**8**:e82665.

Veloso TR, Chaouch A, Roger T, *et al.* Use of a human-like low-grade bacteremia model of experimental endocarditis to study the role of *Staphylococcus aureus* adhesins and platelet aggregation in early endocarditis. *Infect Immun* 2013;**81**:697–703.

Veloso TR, Que YA, Chaouch A, *et al.* Prophylaxis of experimental endocarditis with antiplatelet and antithrombin agents: a role for long-term prevention of infective endocarditis in humans? *J Infect Dis* 2015;**211**:72–9.

Wilson W, Taubert KA, Gewitz M, *et al.* Prevention of infective endocarditis: guidelines from the American Heart Association: a guideline from the American Heart Association Rheumatic Fever, Endocarditis, and Kawasaki Disease Committee, Council on Cardiovascular Disease in the Young, and the Council on Clinical Cardiology, Council on Cardiovascular Surgery and Anesthesia, and the Quality of Care and Outcomes Research Interdisciplinary Working Group. *Circulation* 2007;**116**:1736–54.

Yagi Y, Clewell DB. Recombination-deficient mutant of *Streptococcus faecalis*. *J Bacteriol* 1980;**143**:966–70.

Yagupsky P, Nolte FS. Quantitative aspects of septicemia. *Clin Microbiol Rev* 1990;**3**:269–79.

AMERICAN SOCIETY FOR MICROBIOLOGY | Infection and Immunity

Antibodies Targeting Hsa and PadA Prevent Platelet Aggregation and Protect Rats against Experimental Endocarditis Induced by *Streptococcus gordonii*

Stefano Mancini, Carmen Menzi, Frank Oechslin, Philippe Moreillon, José Manuel Entenza

Department of Fundamental Microbiology, University of Lausanne, Lausanne, Switzerland

Streptococcus gordonii **and related species of oral viridans group streptococci (VGS) are common etiological agents of infective endocarditis (IE). We explored vaccination as a strategy to prevent VGS-IE, using a novel antigen-presenting system based on non-genetically modified *Lactococcus lactis* displaying vaccinogens on its surface. Hsa and PadA are surface-located *S. gordonii* proteins implicated in platelet adhesion and aggregation, which are key steps in the pathogenesis of IE. This function makes them ideal targets for vaccination against VGS-IE. In the present study, we report the use of nonliving *L. lactis* displaying at its surface the N-terminal region of Hsa or PadA by means of the cell wall binding domain of *Lactobacillus casei* A2 phage lysine LysA2 (Hsa-LysA2 and PadA-LysA2, respectively) and investigation of their ability to elicit antibodies in rats and to protect them from *S. gordonii* experimental IE. Immunized and control animals with catheter-induced sterile aortic valve vegetations were inoculated with 10^6 CFU of *S. gordonii*. The presence of IE was evaluated 24 h later. Immunization of rats with *L. lactis* Hsa-LysA2, *L. lactis* PadA-LysA2, or both protected 6/11 (55%), 6/11 (55%), and 11/12 (91%) animals, respectively, from *S. gordonii* IE ($P < 0.05$ versus controls). Protection correlated with the induction of high levels of functional antibodies against both Hsa and PadA that delayed or totally inhibited platelet aggregation by *S. gordonii*. These results support the value of *L. lactis* as a system for antigen delivery and of Hsa and PadA as promising candidates for a vaccine against VGS-IE.**

The viridans group streptococci (VGS) are commensal bacteria of the human oral cavity but can cause infective endocarditis (IE) when they enter the bloodstream (1). VGS-IE accounts for ca. 20% of IE cases (1) and generally results from cumulative exposure to recurrent bouts of transient low-grade bacteremia, occurring during normal day-to-day activities, including tooth brushing, flossing, and chewing (2–4). Under these circumstances, antibiotic prophylaxis regimens cannot be recommended to prevent VGS-IE. Based upon this assumption, the American Heart Association (AHA) and the European Society of Cardiology (ESC) drastically restricted the use of antibiotic prophylaxis for IE in at-risk patients undergoing dental procedures (5, 6). The British National Institute for Health and Clinical Excellence (NICE) went even further and suggested the total abolition of antibiotic-based prophylaxis (7). However, since the AHA guidelines' revision in 2007, a significant increase in the incidence of VGS-IE has been reported in the United States (8). This suggests that the development of an effective prophylactic strategy against VGS-IE is an unmet medical need.

A number of immunization strategies for the prevention of VGS-IE have been explored in the past and have been shown to protect animal models from IE (9–13). However, no further step has been made toward the development of vaccines against oral streptococci, and no vaccine currently exists against VGS-IE in the market.

The oral VGS bacterium *Streptococcus gordonii* is a major etiological agent of IE (14). *S. gordonii* is well known for its ability to interact with human platelets, a step that is considered crucial for the initiation and progression of IE (15, 16). *S. gordonii* adheres to platelets via the surface-anchored proteins Hsa (hemagglutinin salivary antigen) and PadA (platelet adherence protein A). Hsa mediates the initial interactions with platelets by binding the membrane glycoprotein GPIbα (17–20). The high on-off rate of GPIbα allows rapid loss and formation of new interactions between platelets and the immobilized bacteria, leading to platelets rolling over the microorganisms. This process, which slows down platelets from the high shear stress experienced in the bloodstream, is then followed by the interaction of PadA with the platelet receptor GPIIβIIIα, which promotes firm bacterium-platelet adhesion and ultimately leads to platelet aggregation (21, 22).

Due to their role in platelet aggregation, Hsa and PadA (18, 22) represent intuitively logical candidates for vaccine development against IE induced by VGS. In the present study, we employed a recently developed antigen display system (23) to immunize rats with both adhesins. This system is based on nonliving, non-genetically modified *Lactococcus lactis* cells displaying on the cell wall the functional N-terminal region (directly involved in platelet activation) of Hsa or PadA fused to the C-terminal domain of *Lactobacillus casei* A2 phage lysine (LysA2), which was previously shown to bind to the cell wall of a wide spectrum of lactic acid bacteria (24). The immunizations with *L. lactis* displaying Hsa-LysA2 (*L. lactis* Hsa-LysA2) and *L. lactis* displaying PadA-LysA2 (*L. lactis* PadA-LysA2), individually or after coimmunization,

Received 22 September 2016 **Accepted** 22 September 2016

Accepted manuscript posted online 10 October 2016

Citation Mancini S, Menzi C, Oechslin F, Moreillon P, Entenza JM. 2016. Antibodies targeting Hsa and PadA prevent platelet aggregation and protect rats against experimental endocarditis induced by *Streptococcus gordonii*. Infect Immun 84:3557–3563. doi:10.1128/IAI.00810-16.

Editor: G. H. Palmer, Washington State University

Address correspondence to José Manuel Entenza, jose.entenza@unil.ch.

Supplemental material for this article may be found at http://dx.doi.org/10.1128/IAI.00810-16.

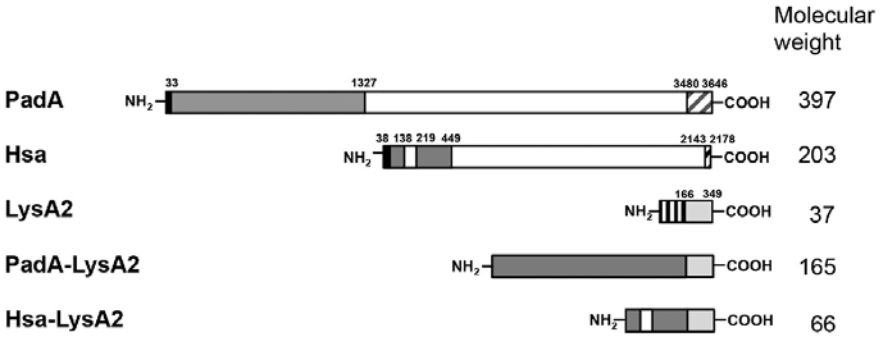

FIG 1 Schematic representations of PadA, Hsa, LysA2, and the chimeric proteins Hsa-LysA2 and PadA-LysA2. PadA is composed of a leader peptide (in black), a unique N-terminal region (in gray) which comprises a von Willebrand factor-A1-like domain, 14 repeat blocks with unknown function (in white), and a C-terminal cell wall anchoring domain (with diagonal lines). The primary sequence of Hsa comprises a leader peptide (in black), two serine-rich regions (in white), one located in the N-terminal region and the other in the C-terminal region (in gray), and a C-terminal cell wall-anchoring domain (with diagonal lines). LysA2 contains an N-terminal catalytic domain (with vertical lines) and a C-terminal cell wall binding domain (in light gray). Molecular weights at right are in thousands.

were evaluated for their ability to induce specific antibodies in rats and to protect against *S. gordonii* experimental IE.

Our results indicate that immunization of rats with *L. lactis* Hsa-LysA2 and/or *L. lactis* PadA-LysA2, individually or together, was effective in inducing functional Hsa- and PadA-specific antibodies that inhibited platelet aggregation and protected against *S. gordonii* experimental IE. Taken together, these results support the suitability of Hsa and PadA as potential candidates for the development of an anti-VGS-IE vaccine.

MATERIALS AND METHODS

Bacterial strains and growth conditions. *L. lactis* (strain MG1363) (25) was grown at 30°C in M17 broth medium (Difco-Becton Dickinson, Sparks, MD) containing 1% glucose (GM17). *S. gordonii* Challis (strain DL1) (19) was grown at 37°C in brain infusion broth (Difco-Becton Dickinson) in the presence of 5% CO_2. *Escherichia coli* DH5α (Invitrogen, Carlsbad, CA) and *E. coli* BL21(DE3)pLysS (24) were grown in Luria-Bertani (LB) broth (Difco-Becton Dickinson).

Construction of the plasmids carrying Hsa-LysA2 and PadA-LysA2 fusion cassettes. Genomic DNA was extracted from *S. gordonii* using a genomic DNA purification kit (Thermo Fisher Scientific, Waltham, MA), according to the manufacturer's instructions. The N-terminal regions coding for amino acids (aa) 39 to 449 of *hsa* and 35 to 1327 of *padA* were PCR amplified from *S. gordonii* genomic DNA using forward primers *hsa*-fw (ATATGGATCCTTTAAGATTAATGAAGGGTGCTG) and *padA*-fw (ATATGGATCCTGATCCTCTGAATATTGAGACG) containing BamHI recognition sites (underlined) and reverse primers *hsa*-rv (TATACGGCCGTACTAATCTGAAGATCTTTAAC) and *padA*-rv (TATACGGCCGCTTCCAAGGTATCAGAAAGTACA) containing EagI recognition sites (underlined). The resulting products of 1,258 bp and 3,901 bp were digested with BamHI and EagI (Promega, Madison, WI) and ligated into the pLysA2 vector, a plasmid containing the gene coding for bacteriophage A2 of *L. casei* (24), previously digested with the same enzymes. The resulting constructs, namely, pHsa-LysA2 and pPadA-LysA2, encoded the N-terminal regions of Hsa and PadA with an N-terminal 6-His tag and Xpress epitope and fused to the cell-binding domain of *L. casei* LysA2 at the C terminus (Fig. 1). The correct insertion of the genes and the absence of mutations were verified by commercial DNA sequencing. Plasmids containing solely the N-terminal regions coding for amino acids 39 to 449 of *hsa* (pHsa) and 35 to 1327 of *padA* (pPadA) were generated using the Q5 site-directed mutagenesis kit (New England BioLabs, Ipswich, MA) according to the manufacturer's instructions. Forward primers *hsa*-fw2 (TAAGCATATTACAAAAATGCC) and *padA*-fw2 (TAAGCATATTACAAAAATGCC) and reverse primers *hsa*-rv2 (CGTACTAATCTGAAGATCTTTAAC) and *padA*-rv2 (TTCCAAGGTATCAGAAAG) were used to delete the LysA2 coding region from pHsa-LysA2 and pPadA-LysA2, respectively, thereby generating pHsa and pPadA. All the plasmids were propagated in *E. coli* DH5α and purified with the Wizard Plus SV Minipreps DNA purification system (Promega), according to the manufacturer's instructions.

Purification of Hsa, PadA, Hsa-LysA2, and PadA-LysA2. Hsa (aa 39 to 449), PadA (aa 35 to 1327), Hsa-LysA2, and PadA-LysA2 were purified as previously described (24). Briefly, *E. coli* BL21(DE3)pLysS containing pHsa, pPadA, pHsa-LysA2, and pPadA-LysA2 was grown aerobically at 37°C in LB containing ampicillin (100 μg/ml) until the mid-exponential phase (optical density at 600 nm [OD_{600}], ~0.5). Then, cells were induced with 1 mM isopropyl-β-D-thiogalactoside (Roche Diagnostics, Basel, Switzerland), and the growth was continued overnight at 18°C. The cells were then harvested by centrifugation, washed with buffer P (100 mM phosphate buffer, pH 5.5) with 5 mM imidazole, and resuspended in 20 ml of the same buffer. Cells were then broken by three passages through a French press at 40 MPa, and cell debris was removed by centrifugation at 4°C. The resulting supernatant was incubated with 0.5 ml nickel-nitrilotriacetic acid (Ni-NTA) agarose (Qiagen, Germantown, MD) for 2 h at 4°C in an end-over-end tube rotator. The suspension was then loaded on a column, and the resin was washed with 10 volumes of buffer P, followed by 10 volumes of the same buffer with 30 mM imidazole. The proteins were eluted with 5 ml buffer P containing 300 mM imidazole. The eluates were analyzed on a 12% acrylamide gel and dialyzed against 100 volumes of phosphate-buffered saline (PBS) twice for 2 h at 4°C. The protein concentrations were determined with the Bio-Rad protein assay, using bovine serum albumin (BSA) as standard.

Binding of Hsa-LysA2 and PadA-LysA2 fusion proteins on the surface of *L. lactis*. *L. lactis* was grown in MG17 until the exponential phase (OD_{600}, ~0.5). Then, cells were harvested by centrifugation, washed two times with PBS, and resuspended in the same buffer to obtain a concentration of 10^9 CFU/ml. Bacteria were then killed by exposure to UV light for 1 h at 1 J/cm^2 (26). UV-induced killing was confirmed by the absence of viable organisms. The cells (100 μl) were then mixed with increasing amounts of Hsa-LysA2 or PadA-LysA2 in order to determine the amounts of proteins necessary for the complete saturation of the *L. lactis* surface and incubated for 1 h at 30°C to promote binding of the proteins. *L. lactis*

cells were also incubated with BSA (control). Cell protein suspensions were then centrifuged, washed with PBS, and resuspended into 100 μl of the same buffer.

Assessment of Hsa-LysA2 and PadA-LysA2 levels on *L. lactis* surface by enzyme-linked immunosorbent assay (ELISA). One hundred microliters of UV-treated *L. lactis* cells (final concentration, 10^8 CFU/ml) preincubated with different amounts of Hsa-LysA2 and PadA-LysA2 was adsorbed on an F96 MaxiSorp microplate (Thermo Fisher Scientific) for 18 h at 4°C. The presence of Hsa-LysA2 and PadA-LysA2 on the surface of immobilized *L. lactis* cells was detected using a mouse anti-Xpress antibody (Invitrogen) and a peroxidase-conjugated goat anti-mouse secondary antibody (Dako, Baar, Switzerland). Fifteen minutes after the addition of the tetramethylbenzidine (TMB) solution (Thermo Fisher Scientific), the reactions were stopped with 2 M H_2SO_4. The absorbance at 450 nm was then measured with the Infinite 200 Pro microplate reader (Tecan, Maennedorf, Switzerland). The assays were carried out in triplicate.

Western blot analysis for the detection of surface-associated Hsa-LysA2 and PadA-LysA2. Twenty microliters of UV-inactivated *L. lactis* used for the immunization studies (see below) was mixed with 10 μl NuPAGE lithium dodecyl sulfate (LDS) sample buffer (4×; Invitrogen) and boiled for 10 min at 99°C. The resulting protein samples together with 1 ng of each purified protein were resolved by 10% SDS-polyacrylamide gel electrophoresis. Western blotting (WB) was performed using a standard procedure (27). Blots were incubated with a 1:1,000 dilution of a mouse anti-Xpress antibody (Invitrogen) and successively with a 1:3,000 dilution of a peroxidase-conjugated goat anti-mouse secondary antibody (Dako). The bands were detected by chemiluminescence with the enhanced chemiluminescence (ECL) Western blotting detection reagents (Amersham Biosciences. Piscataway, NJ).

Animal studies. All animal protocols were reviewed and approved by the Cantonal Committee on Animal Experiments of the State of Vaud, Switzerland (permit number 879.9). A mixture of ketamine (75 mg/kg of body weight) and midazolam (5 mg/kg) anesthetics was administered to the animals before any surgical procedure.

Immunization studies. UV-killed *L. lactis* (10^8 CFU) mixed with 2 μg of Hsa-LysA2 (*L. lactis* Hsa-LysA2) or 5 μg of PadA-LysA2 (*L. lactis* PadA-LysA2), the smallest amounts of proteins sufficient to saturate the *L. lactis* surface (see Results), was used for immunization.

Rats (6-week-old female Wistar rats) were injected subcutaneously with an initial dose of *L. lactis* Hsa-LysA2, *L. lactis* PadA-LysA2, or the combination of the two emulsified with complete Freund's adjuvant (Sigma-Aldrich, Buchs, Switzerland), followed by two booster doses in incomplete Freund's adjuvant (Sigma-Aldrich) at 14-day intervals. Control groups of rats were sham immunized with *L. lactis* plus the adjuvant. Blood samples were collected at days 0 (before immunization) and 45 (at the time of catheter insertion, 14 days after the third immunization dose; see below). Following centrifugation (3,000 rpm for 15 min at 4°C), sera were stored in aliquots at −80°C until use.

Animal model of endocarditis. The production of catheter-induced aortic vegetations and the installation of an intravenous (i.v.) line to deliver the bacterial inocula were performed in rats 2 weeks after the last immunization dose, i.e., on day 45, as described previously (28).

Twenty-four hours later, immunized and control rats were inoculated i.v. by continuous infusion (0.0017 ml/min over 10 h) of 10^6 CFU of *S. gordonii*, to simulate cumulative exposure to low-grade bacteremia (28). Rats were euthanized 24 h after the end of the inoculation. The cardiac vegetations and the spleen were removed, weighed, homogenized, serially diluted, and plated on blood agar plates. Plates were incubated for 48 h at 37°C to determine the number of viable organisms in the tissues.

ELISA for detection of antibodies. The presence of polyclonal antibodies specific for Hsa and PadA in sequentially diluted (from 1:1,000 to 1:100,000) rat sera was determined by ELISA as described above. Binding of antibodies to the immobilized N-terminal regions of Hsa and PadA absorbed for 18 h at 4°C on the microplate was detected using peroxidase-conjugated goat anti-rat secondary antibodies. The reactions were stopped with 2 M H_2SO_4, and the absorbance at 450 nm was measured with Infinite 200 Pro microplate reader (Tecan). The assays were performed in triplicate on two independent occasions.

Characterization of functional antibodies in sera. The presence of functional antibodies was determined by testing the ability of sera from immunized rats to inhibit platelet aggregation by *S. gordonii*.

Platelet-rich plasma (PRP) and platelet-poor plasma (PPP) for platelet aggregation tests were obtained from anticoagulated human blood as described previously (29).

The ability of sera from immunized rats to inhibit *S. gordonii*-induced platelet aggregation was evaluated *in vitro* by conventional light aggregometry as previously described (29). Briefly, 20 μl of *S. gordonii* (final concentration of 1×10^9 CFU/ml in Tyrode's buffer) was preincubated for 1 h at room temperature with 2 μl of control or anti-Hsa-, anti-PadA-, and anti-Hsa- plus anti-PadA-containing sera and then added to 180 μl of PRP in siliconized flat-bottom cuvettes. Sera from sham-immunized rats were used as a control. ADP, a known inducer of platelet aggregation, was used as a positive control. Platelet aggregation was assessed by monitoring light transmission at 37°C with stirring at 120 rpm using a LaBiTec Apact 4004 aggregometer (LaBiTec GmbH, Ahrensburg, Germany). The light transmission of PRP without added bacteria and the light transmission of PPP were defined as 0% and 100% light transmission, respectively. Aggregation was recorded over 20 min. Platelet aggregation was expressed as the interval between the addition of organism-serum samples to the PRP suspension and the onset of aggregation response (lag time) and the number of platelets (percent) that were aggregated in the presence of the bacterium-serum suspension (maximal aggregation). The final values represent results of three independent experiments performed in quadruplicate.

Statistical analysis. Data for antibody titers, platelet aggregation assays, and mean bacterial densities in vegetations and spleens were evaluated by the Student *t* test. The incidences of valve infection were compared by the chi-square test. A value of $P < 0.05$ was considered significant by using two-tailed significance levels. All statistical analyses were performed with the GraphPad Prism 6.0 program (GraphPad, Inc., La Jolla, CA).

RESULTS

Generation of chimeric Hsa-LysA2 and PadA-LysA2. LysA2, the *L. casei* bacteriophage A2 lysine, consists of an N-terminal catalytic domain and a C-terminal cell wall binding domain (CBD), which was previously shown to bind with high affinity to *L. lactis* (23). By virtue of this property, LysA2 CBD was here used to efficiently immobilize Hsa and PadA on the surface of *L. lactis*, which served as an antigen-presenting system. Since Hsa and PadA are large surface-associated proteins composed of 2,178 and 3,646 amino acid residues, respectively, only the functional surface-exposed N-terminal regions were used to generate the fusion proteins. Hsa contains two serine-rich regions (SRs), which are associated with the binding to the sialylated N-terminal region of GPIbα on platelets. SR1 is relatively short (81 amino acid residues) and is located in the N-terminal region between two nonrepetitive regions (NR1 and NR2). In contrast, SR2 is a long serine-rich region containing 113 dodecapeptide repeats, which are comprised between the N-terminal region and the C-terminal cell wall anchoring domain (Fig. 1). Since SR1, NR1, and NR2, but not SR2, were previously shown to be indispensable for the binding to sialoglycoconjugates (18), the N-terminal region spanning SR1, NR1, and NR2 was used to generate Hsa-LysA2. PadA consists of a leader peptide, an N-terminal region comprising a von Willebrand factor-like domain, a long C-terminal domain with 14 repeat blocks of 148 to 152 amino acid residues, and a cell wall anchor domain (Fig. 1). Analogously to Hsa, the N-terminal re-

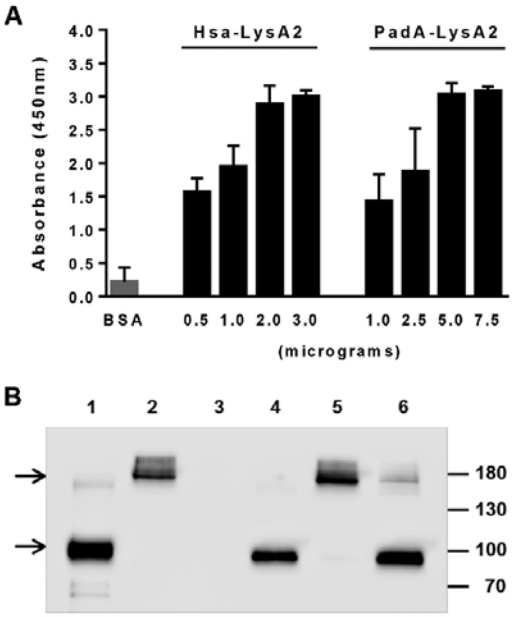

FIG 2 (A) Relative levels of cell wall-associated Hsa-LysA2 and PadA-LysA2. The indicated amounts of Hsa-LysA2 and PadA-LysA2 were incubated with 10^8 CFU of *L. lactis*, and levels of surface-associated proteins were quantified by ELISA. Data were produced from three independent experiments. (B) Detection of Hsa-LysA2 (66 kDa) and PadA-LysA2 (165 kDa) bound to *L. lactis*. Crude extracts of equivalent amounts of *L. lactis* used for the immunization were separated by polyacrylamide gel electrophoresis, followed by Western blotting and development with a monoclonal antibody that recognizes the N-terminal Xpress epitope present on Hsa-LysA2 and PadA-LysA2. Molecular masses in kilodaltons are indicated at the right of the gel. The arrows indicate the bands corresponding to PadA-LysA2 (top) and Hsa-LysA2 (bottom).

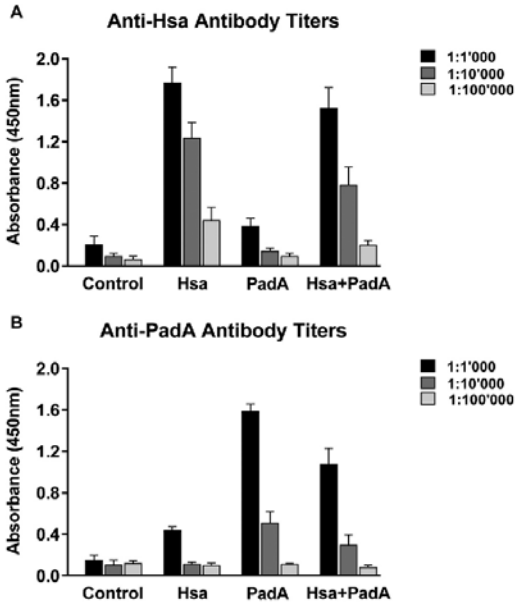

FIG 3 Relative anti-Hsa (A) and anti-PadA (B) antibody levels in the sera of rats immunized with 10^8 CFU of either *L. lactis* (control), *L. lactis* Hsa-LysA2 (Hsa), *L. lactis* PadA-LysA2 (PadA), or the combination of *L. lactis* Hsa-LysA2 and *L. lactis* PadA-LysA2 (Hsa+PadA) as described in Materials and Methods. Antibodies were quantified by ELISA. Data represent the mean ± standard deviation from six samples from six individual rats per group.

gion was used for the generation of PadA-LysA2, as it was shown to be directly involved in the binding to platelets (21).

Binding of surface-saturating levels of Hsa-LysA2 and PadA-LysA2 on *L. lactis*. The ability of the Hsa-LysA2 and PadA-LysA2 fusion proteins to bind to the *L. lactis* cell wall and the optimal protein/cell ratio for antigen presentation were assessed by ELISA and Western blotting (WB). As shown in Fig. 2A, the absorbance increased with the amounts of proteins added to *L. lactis* cells, with maximal signal intensities obtained upon addition of 2 μg of Hsa-LysA2 and 5 μg of PadA-LysA2. Interestingly, further addition of the fusion proteins did not result in increased chemiluminescent signals, suggesting that the binding capacity of the *L. lactis* cells was saturated at those concentrations. Consistently, bands corresponding to Hsa-LysA2 and PadA-LysA2 appeared in *L. lactis* preincubated with 2 μg of Hsa-LysA2 and 5 μg of PadA-LysA2 (Fig. 2B), further corroborating the idea that the chimeric proteins were firmly attached on the cell wall.

Vaccination with *L. lactis* Hsa-LysA2, *L. lactis* PadA-LysA2, and *L. lactis* Hsa-LysA2 plus *L. lactis* PadA-LysA2 efficiently elicited anti-Hsa and anti-PadA antibodies in rats. Animals were immunized with three subcutaneous doses of *L. lactis* Hsa-LysA2, *L. lactis* PadA-LysA2, or the combination of the two bacteria given at intervals of 15 days. Antibody titers of Hsa and PadA in sera were assessed after the third dose. As shown in Fig. 3, sera obtained from rats immunized with *L. lactis* Hsa-LysA2 or *L. lactis* PadA-LysA2 showed an approximately 10- to 15-fold increase in specific antibodies compared to those of control rats and animals before immunization. Coimmunization with *L. lactis* Hsa-LysA2 and *L. lactis* PadA-LysA2 induced antibody levels comparable to those of single-antigen-immunized animals.

Anti-Hsa and anti-PadA antibodies inhibited *S. gordonii*-induced platelet aggregation. As shown in Fig. 4, sera from *L. lactis* Hsa-LysA2- or *L. lactis* PadA-LysA2-immunized animals significantly delayed *S. gordonii*-induced platelet aggregation (lag time of 14.0 ± 1.6 min and 15.0 ± 1.2 min, respectively), compared to sera from sham-immunized rats (lag time of 8.0 ± 0.8 min; $P < 0.0005$). Moreover, upon preincubation with anti-Hsa or anti-PadA, *S. gordonii* exhibited comparable maximum platelet aggregation percentages (64% and 56%, respectively), which were

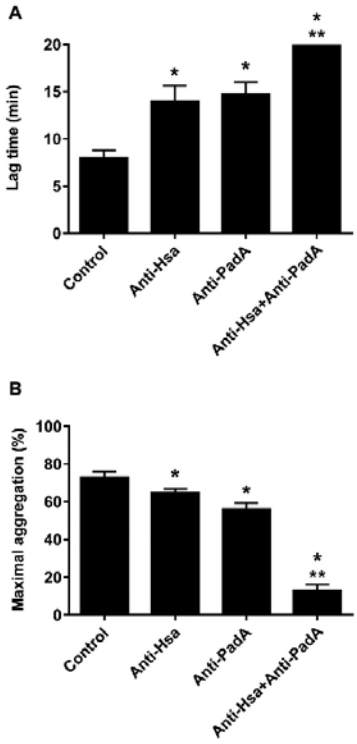

FIG 4 Effects of anti-Hsa, anti-PadA, and control sera on *S. gordonii*-induced platelet aggregation. Sera (10 μl) were preincubated with 10^8 CFU of *S. gordonii* (100 μl), and then platelet aggregability was assessed. Lag time (A) indicates the time between the addition of bacterium-serum mixtures to the PRP suspensions and the onset of aggregation response, and maximal aggregation (B) represents the total number (percent) of aggregated platelets. Results are expressed as the mean ± standard deviation from four samples from four individual rats per group, which were obtained in two independent assays. Lag times of 20 min indicate that there was no aggregation in the time window used to monitor platelet aggregation. *, $P < 0.005$ compared to controls (Student's *t* test); **, $P < 0.001$ compared to anti-Hsa and anti-PadA groups (Student's *t* test).

significantly lower than that induced after the addition of control sera (73%; $P < 0.005$). Remarkably, sera taken from animals coimmunized with *L. lactis* Hsa-LysA2 and *L. lactis* PadA-LysA2 completely prevented *S. gordonii*-induced platelet aggregation (lag time, >20 min; $P < 0.0001$) and reduced maximum aggregation to 13% ($P < 0.0001$).

Vaccination with *L. lactis* Hsa-LysA2/PadA-LysA2 successfully protected rats against *S. gordonii*-induced experimental IE. As shown in Fig. 5, while 14/15 (93%) sham-immunized rats developed *S. gordonii* IE, only 5/11 (45%) animals immunized with *L. lactis* Hsa-LysA2, 5/11 (45%) animals immunized with *L. lactis* PadA-LysA2, and 1/12 (9%) animals coimmunized with *L. lactis* Hsa-LysA2 and *L. lactis* PadA-LysA2 showed infected vegetations ($P < 0.05$). Interestingly, significantly higher levels of protection against *S. gordonii* IE were obtained with coimmunization than in single-immunized groups ($P < 0.05$).

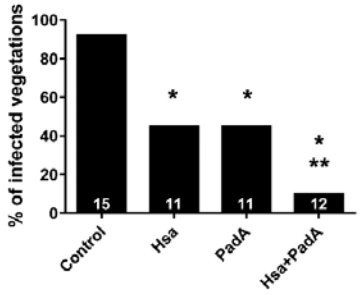

FIG 5 Protective effects of immunization with either *L. lactis* (control), *L. lactis* Hsa-LysA2 (Hsa), *L. lactis* PadA-LysA2 (PadA), or the combination of the two bacteria (Hsa+PadA) against experimental endocarditis induced by *S. gordonii*. Values on the bottom of each column are numbers of animals in each group. *, $P < 0.05$ by chi-square test compared to controls; **, $P < 0.05$ by chi-square test compared to Hsa and PadA groups.

Bacterial counts in vegetations that remained infected were not significantly different between immunized and control rats (6.38 to 7.09 $\log_{10}$ CFU/g).

DISCUSSION

In the present study, we investigated the potential of *L. lactis* displaying *S. gordonii* Hsa or PadA as a vaccine candidate against *S. gordonii* infection in a rat model of IE.

We used for the immunization a recently developed novel display system that allows highly efficient immobilization of antigens on the surface of lactic acid bacteria, such as *L. lactis* (23). This system is based on non-genetically modified *L. lactis* used as a vehicle for antigens bound on the surface by means of a high-affinity cell-binding domain (CBD) from *L. casei* A2 phage lysine LysA2 (24). Such a system offers some advantages over a previously used immunization method based on recombinant *L. lactis* expressing bacterial antigens, such as the *Staphylococcus aureus* clumping factor A (ClfA) or the fibronectin binding protein A (FnbpA) (26). First, it allows use of a non-genetically modified antigen-presenting system. Second, it permits the clustering of antigens on the *L. lactis* cell wall, a feature that increases antigen stimulation of the immune system. Consistent with this notion, while in a pilot study anti-Hsa antibody levels were barely detectable in rat plasma after immunization with recombinant *L. lactis* expressing Hsa (data not shown), vaccination with *L. lactis* with cell wall-saturating amounts of Hsa-LysA2 or PadA-LysA2 fusion proteins triggered production of antibodies against either immunogen with levels approximately 10 to 15 times higher than those found in the sham-immunized rats. Also, whether this strategy is more effective than the vaccination with proteins alone remains to be investigated.

Why then Hsa and PadA? Hsa and PadA were chosen as antigens for two main reasons. First, Hsa is a known virulence factor of *S. gordonii* associated with IE (30). Indeed, deletion of *hsa* was shown to significantly reduce the ability of *S. gordonii* to infect rat aortic valves (30). The role of PadA in IE has not been hitherto analyzed. Second, Hsa and PadA appear to be major factors in triggering *S. gordonii* platelet adhesion and aggregation, which are crucial steps in the pathogenesis of IE (15).

Consistent with this notion, we here showed that *S. gordonii*-

induced platelet aggregation was delayed by anti-Hsa and anti-PadA and, most importantly, completely abolished by the combination of the two. These observations, however, are in contrast with previous results, which showed that concomitant genomic inactivation of *hsa* and *padA* did not have any effect on *S. gordonii*-induced platelet aggregation (21). These contradictory results might be attributed to the cross-reactivity of the anti-Hsa and anti-PadA antibodies with other *S. gordonii* (DL1) adhesins that interact with platelets, such as SspA and SspB (19). In support of this assumption, SspA and SspB sequences exhibit 20% identity to Hsa (see Fig. S1 in the supplemental material). Clearly, this hypothesis requires experimental validation.

The results of the vaccination studies also identified Hsa and PadA as factors primarily responsible for the early steps of IE induced by *S. gordonii*. In fact, rats immunized with Hsa or PadA were significantly protected from *S. gordonii* IE. Most importantly, coimmunization with the two proteins conferred full protection, suggesting that Hsa and PadA act synergistically to promote IE.

Thus, Hsa and PadA represent potential targets for vaccination against *S. gordonii* IE. To be ideal vaccinogens, however, *S. gordonii* Hsa and PadA should afford cross-protection against other VGS. PadA appears to be conserved among viridans streptococci, including *Streptococcus sanguinis* (99% identity), *Streptococcus mitis* (98% identity), *Streptococcus parasanguinis* (68% identity), and *Streptococcus oralis* (66% identity) (see Fig. S2 in the supplemental material). Although less well conserved, *S. gordonii* Hsa homologues can be found in *S. mitis* (83% identity), *Streptococcus sanguis* (named SrpA; 63% identity) (31), *S. gordonii* M99 (named GspB; 40% identity) (17, 32), and *S. oralis* (26% identity) (see Fig. S3). Whether the anti-Hsa and anti-PadA antibodies also cross-react with and block the function of the Hsa- and PadA-like proteins of other VGS is under investigation in our laboratory.

ACKNOWLEDGMENTS

We thank Juan Evaristo Suarez (University of Oviedo, Spain) for providing the pLysA2 vector and Christiane Gerschheimer (Service and Central Laboratory of Hematology, Lausanne University Hospital) for help with aggregometry.

None of the authors has any conflict of interests relevant to this study.

This work was funded by the Swiss National Science Foundation (310030-143799).

FUNDING INFORMATION

This work, including the efforts of Jose M. Entenza, was funded by Swiss National Science Foundation (310030-143799).

REFERENCES

1. Que YA, Moreillon P. 2011. Infective endocarditis. Nat Rev Cardiol 8:322–336. http://dx.doi.org/10.1038/nrcardio.2011.43.
2. Roberts GJ. 1999. Dentists are innocent! "Everyday" bacteremia is the real culprit: a review and assessment of the evidence that dental surgical procedures are a principal cause of bacterial endocarditis in children. Pediatr Cardiol 20:317–325. http://dx.doi.org/10.1007/s002469900477.
3. Forner L, Larsen T, Kilian M, Holmstrup P. 2006. Incidence of bacteremia after chewing, tooth brushing and scaling in individuals with periodontal inflammation. J Clin Periodontol 33:401–407. http://dx.doi.org/10.1111/j.1600-051X.2006.00924.x.
4. Crasta K, Daly CG, Mitchell D, Curtis B, Stewart D, Heitz-Mayfield LJ. 2009. Bacteraemia due to dental flossing. J Clin Periodontol 36:323–332. http://dx.doi.org/10.1111/j.1600-051X.2008.01372.x.
5. Wilson W, Taubert KA, Gewitz M, Lockhart PB, Baddour LM, Levison M, Bolger A, Cabell CH, Takahashi M, Baltimore RS, Newburger JW, Strom BL, Tani LY, Gerber M, Bonow RO, Pallasch T, Shulman ST, Rowley AH, Burns JC, Ferrieri P, Gardner T, Goff D, Durack DT. 2007. Prevention of infective endocarditis. Guidelines from the American Heart Association. A guideline from the American Heart Association Rheumatic Fever, Endocarditis, and Kawasaki Disease Committee, Council on Cardiovascular Disease in the Young, and the Council on Clinical Cardiology, Council on Cardiovascular Surgery and Anesthesia, and the Quality of Care and Outcomes Research Interdisciplinary Working Group. Circulation 116:1736–1754.
6. Habib G, Hoen B, Tornos P, Thuny F, Prendergast B, Vilacosta I, Moreillon P, de Jesus Antunes M, Thilen U, Lekakis J, Lengyel M, Muller L, Naber CK, Nihoyannopoulos P, Moritz A, Zamorano JL, Vahanian A, Auricchio A, Bax J, Ceconi C, Dean V, Filippatos G, Funck-Brentano C, Hobbs R, Kearney P, McDonagh T, McGregor K, Popescu BA, Reiner Z, Sechtem U, Sirnes PA, Tendera M, Vardas P, Widimsky P. 2009. Guidelines on the prevention, diagnosis, and treatment of infective endocarditis (new version 2009): the Task Force on the Prevention, Diagnosis, and Treatment of Infective Endocarditis of the European Society of Cardiology (ESC). Eur Heart J 30:2369–2413. http://dx.doi.org/10.1093/eurheartj/ehp285.
7. Richey R, Wray D, Stokes T, Guideline Development Group. 2008. Prophylaxis against infective endocarditis: summary of NICE guidance. BMJ 336:770–771. http://dx.doi.org/10.1136/bmj.39510.423148.AD.
8. Pant S, Patel NJ, Deshmukh A, Golwala H, Patel N, Badheka A, Hirsch GA, Mehta JL. 2015. Trends in infective endocarditis incidence, microbiology, and valve replacement in the United States from 2000 to 2011. J Am Coll Cardiol 65:2070–2076. http://dx.doi.org/10.1016/j.jacc.2015.03.518.
9. Durack DT, Gilliland BC, Petersdorf RG. 1978. Effect of immunization on susceptibility to experimental *Streptococcus mutans* and *Streptococcus sanguis* endocarditis. Infect Immun 22:52–56.
10. Scheld WM, Thomas JH, Sande MA. 1979. Influence of preformed antibody on experimental *Streptococcus sanguis* endocarditis. Infect Immun 25:781–785.
11. van de Rijn I. 1985. Role of culture conditions and immunization in experimental nutritionally variant streptococcal endocarditis. Infect Immun 50:641–646.
12. Viscount HB, Munro CL, Burnette-Curley D, Peterson DL, Macrina FL. 1997. Immunization with FimA protects against *Streptococcus parasanguis* endocarditis in rats. Infect Immun 65:994–1002.
13. Kitten T, Munro CL, Wang A, Macrina FL. 2002. Vaccination with FimA from *Streptococcus parasanguis* protects rats from endocarditis caused by other viridans streptococci. Infect Immun 70:422–425. http://dx.doi.org/10.1128/IAI.70.1.422-425.2002.
14. Douglas CW, Heath J, Hampton KK, Preston FE. 1993. Identity of viridans streptococci isolated from cases of infective endocarditis. J Med Microbiol 39:179–182. http://dx.doi.org/10.1099/00222615-39-3-179.
15. Moreillon P, Que YA, Bayer AS. 2002. Pathogenesis of streptococcal and staphylococcal endocarditis. Infect Dis Clin North Am 16:297–318. http://dx.doi.org/10.1016/S0891-5520(01)00009-5.
16. Kerrigan SW, Cox D. 2010. Platelet-bacterial interactions. Cell Mol Life Sci 67:513–523. http://dx.doi.org/10.1007/s00018-009-0207-z.
17. Bensing BA, Lopez JA, Sullam PM. 2004. The Streptococcus gordonii surface proteins GspB and Hsa mediate binding to sialylated carbohydrate epitopes on the platelet membrane glycoprotein Ibalpha. Infect Immun 72:6528–6537. http://dx.doi.org/10.1128/IAI.72.11.6528-6537.2004.
18. Takahashi Y, Yajima A, Cisar JO, Konishi K. 2004. Functional analysis of the *Streptococcus gordonii* DL1 sialic acid-binding adhesin and its essential role in bacterial binding to platelets. Infect Immun 72:3876–3882. http://dx.doi.org/10.1128/IAI.72.7.3876-3882.2004.
19. Jakubovics NS, Kerrigan SW, Nobbs AH, Stromberg N, van Dolleweerd CJ, Cox DM, Kelly CG, Jenkinson HF. 2005. Functions of cell surface-anchored antigen I/II family and Hsa polypeptides in interactions of *Streptococcus gordonii* with host receptors. Infect Immun 73:6629–6638. http://dx.doi.org/10.1128/IAI.73.10.6629-6638.2005.
20. Kerrigan SW, Jakubovics NS, Keane C, Maguire P, Wynne K, Jenkinson HF, Cox D. 2007. Role of *Streptococcus gordonii* surface proteins SspA/SspB and Hsa in platelet function. Infect Immun 75:5740–5747. http://dx.doi.org/10.1128/IAI.00909-07.
21. Petersen HJ, Keane C, Jenkinson HF, Vickerman MM, Jesionowski A, Waterhouse JC, Cox D, Kerrigan SW. 2010. Human platelets recognize a novel surface protein, PadA, on Streptococcus gordonii through a unique interaction involving fibrinogen receptor GPIIbIIIa. Infect Immun 78:413–422. http://dx.doi.org/10.1128/IAI.00664-09.

22. Keane C, Petersen HJ, Tilley DO, Haworth J, Cox D, Jenkinson HF, Kerrigan SW. 2013. Multiple sites on *Streptococcus gordonii* surface protein PadA bind to platelet GPIIbIIIa. Thromb Haemost 110:1278–1287. http://dx.doi.org/10.1160/TH13-07-0580.
23. Ribelles P, Benbouziane B, Langella P, Suarez JE, Bermudez-Humaran LG. 2013. Protection against human papillomavirus type 16-induced tumors in mice using non-genetically modified lactic acid bacteria displaying E7 antigen at its surface. Appl Microbiol Biotechnol 97:1231–1239. http://dx.doi.org/10.1007/s00253-012-4575-1.
24. Ribelles P, Rodriguez I, Suarez JE. 2012. LysA2, the *Lactobacillus casei* bacteriophage A2 lysin is an endopeptidase active on a wide spectrum of lactic acid bacteria. Appl Microbiol Biotechnol 94:101–110. http://dx.doi.org/10.1007/s00253-011-3588-5.
25. Que YA, Haefliger JA, Francioli P, Moreillon P. 2000. Expression of *Staphylococcus aureus* clumping factor A in *Lactococcus lactis* subsp. *cremoris* using a new shuttle vector. Infect Immun 68:3516–3522. http://dx.doi.org/10.1128/IAI.68.6.3516-3522.2000.
26. Veloso TR, Mancini S, Giddey M, Vouillamoz J, Que YA, Moreillon P, Entenza JM. 2015. Vaccination against *Staphylococcus aureus* experimental endocarditis using recombinant *Lactococcus lactis* expressing ClfA or FnbpA. Vaccine 33:3512–3517. http://dx.doi.org/10.1016/j.vaccine.2015.05.060.
27. Towbin H, Staehelin T, Gordon J. 1979. Electrophoretic transfer of proteins from polyacrylamide gels to nitrocellulose sheets: procedure and some applications. Proc Natl Acad Sci U S A 76:4350–4354. http://dx.doi.org/10.1073/pnas.76.9.4350.
28. Veloso TR, Amiguet M, Rousson V, Giddey M, Vouillamoz J, Moreillon P, Entenza JM. 2011. Induction of experimental endocarditis by continuous low-grade bacteremia mimicking spontaneous bacteremia in humans. Infect Immun 79:2006–2011. http://dx.doi.org/10.1128/IAI.01208-10.
29. Veloso TR, Que YA, Chaouch A, Giddey M, Vouillamoz J, Rousson V, Moreillon P, Entenza JM. 2015. Prophylaxis of experimental endocarditis with antiplatelet and antithrombin agents: a role for long-term prevention of infective endocarditis in humans? J Infect Dis 211:72–79. http://dx.doi.org/10.1093/infdis/jiu426.
30. Takahashi Y, Takashima E, Shimazu K, Yagishita H, Aoba T, Konishi K. 2006. Contribution of sialic acid-binding adhesin to pathogenesis of experimental endocarditis caused by *Streptococcus gordonii* DL1. Infect Immun 74:740–743. http://dx.doi.org/10.1128/IAI.74.1.740-743.2006.
31. Plummer C, Wu H, Kerrigan SW, Meade G, Cox D, Ian Douglas CW. 2005. A serine-rich glycoprotein of *Streptococcus sanguis* mediates adhesion to platelets via GPIb. Br J Haematol 129:101–109. http://dx.doi.org/10.1111/j.1365-2141.2005.05421.x.
32. Xiong YQ, Bensing BA, Bayer AS, Chambers HF, Sullam PM. 2008. Role of the serine-rich surface glycoprotein GspB of *Streptococcus gordonii* in the pathogenesis of infective endocarditis. Microb Pathog 45:297–301. http://dx.doi.org/10.1016/j.micpath.2008.06.004.